



Pressure effects on neurons: investigations into the pathogenesis of glaucoma.

Author:

Agar, Ashish

Publication Date:

2006

DOI:

<https://doi.org/10.26190/unsworks/17653>

License:

<https://creativecommons.org/licenses/by-nc-nd/3.0/au/>

Link to license to see what you are allowed to do with this resource.

Downloaded from <http://hdl.handle.net/1959.4/31548> in <https://unsworks.unsw.edu.au> on 2024-04-28

*Pressure Effects on Neurons:
Investigations into the
Pathogenesis of Glaucoma*

A thesis submitted for the requirement of the degree of Doctor of Philosophy

University of New South Wales

Ashish Agar MB.BS, FRANZCO

Department of Ophthalmology, Prince of Wales Hospital

&

Cell Biology Laboratory, Anatomy, School of Medical Sciences

University of New South Wales

December 2006

DEDICATION

To my beloved daughter

Saranya Radha Agar

Who makes everything worthwhile

ACKNOWLEDGEMENTS

An endeavour such as this is invariably the result of many people's help, without which this research would not have been possible. I would like to thank my supervisors, Professor Minas Coroneo and Dr Mark Hill, for their unfailing guidance, support and seemingly endless patience. Professor Coroneo's unfathomable faith in me has allowed me to pursue a career in both clinical and academic ophthalmology, and he remains an inspiration and fount of knowledge in both. Dr Hill taught me about life in the lab, persistently steering every step of the research process. Both of my supervisors have kept the flame of pure research alive, which is no mean feat in today's academic climate.

In the Cell Biology Lab several colleagues helped in the practical realities of cell culture work. Dr Stephanie Watson helped develop the model we used so successfully, as well as showing me how to dissect neonatal rat eyes well before I got near any of my patients' eyes! Dr Melissa Broe showed me the ropes in my first year, and taught me that match-making rats is not as easy as it looks. Moya Seeto, our research assistant kept the lab running for which we were always grateful. The late Aunt Beverly Hill mothered all of the lab crew and was never without a joke and a smile, let alone an encyclopedic grasp of MS Word. Her loss was keenly felt. Certain sections of this project were the result of vital input and work with co-researchers. Dr Sonia Yip was instrumental in the PC12 experiments, and likewise Dr Shaojuan Li in the differentiated RGC-5 work.

In our university Anatomy department Rob Wadley and I spent countless hours trying to decipher the LSC, and our pioneering use of this technology in Australia would have been impossible without his efforts. Paul Halasz always seemed to be able to turn my digital blob of a cell on the microscope screen into a biological work of art!

Beyond our faculty I would like to thank several people for their generous and freely given assistance. Dr Raj Devashayan and Professor Frank Billson of the Lions NSW Eye Bank allowed us access to human donor tissue, and Professor Tuch at Prince of Wales Hospital and Dr Nathan Sachdev did so for our human fetal eye work. Professor R Frost of the university's Department of Mechanical Engineering kindly constructed our pressure chambers, and Professor Mick Perry of Physiology helped with the pressurising device and gas sampling.

My last acknowledgements are the most important of all, for they encompass far more than a research project. My family has been behind every fruitful endeavour of my life and this was no exception. My father, Professor N.S Agar, a distinguished scientist in his own right, has always been my inspiration. Playing in his lab as children made science come alive and instilled a respect for knowledge which his children have inherited. Of far greater impact however has been the nurturing received, and the lessons of life which sustain me still. My mother, a teacher, gave all of this a context and provided the emotional reserves to keep me going through a demanding (albeit self-inflicted!) career. I hope to one day be able to repay the eternal debt I owe my parents, and shall strive to reflect their faith in me. My little sister has taught me much about how to actually write a thesis, and in her guidance on life has displayed wisdom far beyond her years.

My wife, Meera, has been with me throughout the post-graduate process, enduring the disruptions of my late nights and weekends spent in the lab waiting for an experiment to finish. Her patience has been invaluable and her advice equally so, as I tried to navigate the dual hospital and lab roles often simultaneously. Thank you for all your support and those memorable years.

Finally, to the most valuable team member of all. To my daughter Saranya Radha all my efforts are ultimately dedicated. She has been the light of my life since she graced us with her presence, and I feel that no-one has sacrificed more than she did for me. Of course at this tender age of five years she may not be aware of this yet, but whatever time I spent elsewhere seemed but an interlude to being with her. If research teaches one anything, I hope it is the value of searching for the truth, and the dedication required to achieve this. For my little one then, I wish her the chance to lead such a life of discovery and opportunity as I have had, and to be able to follow her mind wherever it may lead.

DECLARATION

Statement of Originality

‘I hereby declare that this submission is my own work and to the best of my knowledge it contains no materials previously published or written by another person, or substantial proportions of material which have been accepted for the award of any other degree or diploma at UNSW or any other educational institution, except where due acknowledgement is made in the thesis. Any contribution made to the research by others, with whom I have worked at UNSW or elsewhere, is explicitly acknowledged in the thesis. I also declare that the intellectual content of this thesis is the product of my own work, except to the extent that assistance from others in the project’s design and conception or in style, presentation and linguistic expression is acknowledged.’

Signed

Dated

PUBLICATIONS

(Arising from work presented in this thesis)

Papers

- Agar, A., S. S. Yip, et al. (2000). "Pressure related apoptosis in neuronal cell lines." J Neurosci Res **60**(4): 495-503. (Results in Chapter Five, also see Appendices).
- Agar, A., S. Li, et al. (2006). "Retinal ganglion cell line apoptosis induced by hydrostatic pressure." Brain Res **1086**(1): 191-200. (Results in Chapter Six, also see Appendices).

Presentations

- Agar, A., M. Hill, et al. (1999). "Pressure induced apoptosis in neurons." Invest Ophthalmol Vis Sci **40**(4): S265 [ARVO abstract].
- Agar, A., S. S. Yip, et al. (2000). "Pressure induced apoptosis in an RGC neuronal cell line." Invest Ophthalmol Vis Sci **41**(4): S4378 [ARVO abstract].
- Coroneo, M., A. Agar, et al. (2000). "Differentiated neuronal apoptosis following elevated hydrostatic pressure." Invest Ophthalmol Vis Sci **41**(4): S4379 [ARVO abstract].
- Agar, A., N. J. Agarwal, et al. (2001). "Retinal Ganglion Cell line apoptosis in a hydrostatic pressure model." Invest Ophthalmol & Vis Sci **42**(4): S139 [ARVO Abstract].
- Coroneo, M., A. Agar, et al. (2001). "Pressure related apoptosis in human and neuronal cell lines." Invest Ophthalmol & Vis Sci **42**(4): S129 [ARVO Abstract].
- Agar, A., S. Li, et al. (2002). "In-vitro pressure induced apoptosis in RGC line shows graded response to simulated Acute, Chronic Glaucoma & normal pressure." Invest Ophthalmol Vis Sci **43**(4): S4060 [ARVO abstract].

Grants Received

- Ophthalmic Research Institute of Australia. "The Effects of Pressure on Retinal Ganglion Cell Survival In Vitro", 2000.
- Ophthalmic Research Institute of Australia. "The Response of a Novel Retinal Ganglion Cell Line to Elevated Pressure in an In Vitro Model for Glaucoma", 2001.

ABSTRACT

Cellular responses to changes in pressure are implicated in numerous disease processes. In glaucoma apoptosis of retinal ganglion cells (RGCs) is associated with elevated intra-ocular pressure (IOP), however the exact cellular basis of this link remains unclear. This research aimed to examine the direct response of neuronal cells to elevated hydrostatic pressure in terms of apoptosis.

We developed an in vitro model consisting of a pressure chamber to adjust ambient hydrostatic pressure, a source of neuronal cells and methods to measure apoptosis in these cells. The neural cells examined were primary retinal cultures, four neuronal cell lines (B35, PC12, C17, NT2), and the RGC-5 cell line.

Pressure conditions selected were within physiological limits; 100 mmHg above atmospheric pressure (as seen clinically in severe acute glaucoma) and extended in RGC-5 neurons to 30 mmHg (chronic glaucoma) and 15 mmHg (normal IOP). Apoptosis was detected by cell morphology and specific immunochemical markers: TUNEL and Annexin V. Caspase-3 activation, a known pathway of apoptosis, was also investigated in RGC-5 neurons. These fluorescent markers were detected and quantified by automated Laser Scanning Cytometry. Negative controls were treated identically except for the application of pressure, while positive controls were generated by treatment with a known apoptotic stimulus.

The results showed that neurons responded to elevated hydrostatic pressure directly and that an apoptotic process was induced. There was a greater level of apoptosis in pressurised cells compared to the negative controls. This apoptotic effect at high pressures was seen in primary rat retinal cultures and in both undifferentiated (B35, C17, NT2, RGC-5) and differentiated (PC12, RGC-5) neuronal cell lines. RGC-5 neurons showed a graded response, proportionate to the level of pressure elevation, representative of the severity of analogous clinical settings (acute, chronic glaucoma & normal). RGC-5 neurons also showed increased activation of Caspase-3. Thus this pathway may play a role in pressure induced apoptosis.

Our findings indicate that pressure alone may act as a stimulus for apoptosis in neuronal cells. We suggest the possibility of novel mechanisms of pressure related mechanotransduction and cell death, relevant to the pathogenesis of glaucoma.

CONTENTS

<i>Chapter One</i>	<i>I</i>
<i>Review of Literature</i>	<i>I</i>
1.1 Glaucoma	2
1.1.1 Ocular anatomy and physiology	3
1.1.2 Classification	9
1.1.3 Epidemiology	11
1.1.4 Clinical presentation	12
1.1.4.1 Optic disc appearance	14
1.1.4.2 Visual field changes	18
1.1.4.3 Intraocular pressure	19
1.1.5 Understanding glaucoma	22
1.2 Retinal ganglion cell death in glaucoma	23
1.2.1 Cell death	23
1.2.1.1 Necrosis	25
1.2.1.2 Apoptosis	25
1.2.2 The process of apoptosis	27
1.2.2.1 Apoptotic stimuli	27
1.2.2.2 Apoptotic mechanisms	29
1.2.3 Detecting apoptosis	31
1.2.3.1 Immunofluorescent analysis	31
1.2.3.2 Apoptosis vs Necrosis	33
1.2.4 Apoptosis in glaucoma	36
1.2.4.1 Animal studies	37
1.2.4.2 Human studies	38

1.3 Pathogenesis of glaucoma	40
1.3.1 Historical perspective	40
1.3.2 Conventional theories	41
1.3.2.1 Mechanical theory	42
1.3.2.2 Vascular theory	44
1.3.2.3 Excitotoxicity theory	45
1.3.3 Critique of conventional theories	47
1.3.3.1 Critique of mechanical theory	48
1.3.3.2 Critique of vascular theory	50
1.3.3.3 Critique of excitotoxicity	51
1.3.4 Toward a new paradigm	52
1.4 Pressure effects on cells	54
1.4.1 Historical perspective	55
1.4.2 Types of pressure effects	56
1.4.2.1 Cell growth and proliferation	56
1.4.2.2 Cell morphology	57
1.4.2.3 Protein synthesis	58
1.4.2.4 Cell activity	60
1.4.3 Pressure and apoptosis	61
1.4.3.1 General cell types	62
1.4.3.2 Ocular cells	63
1.4.4 Cells sensing pressure	64
1.4.4.1 Mechanotransduction	64
1.4.4.2 Mechanosensitive channels	68
1.5 Hypothesis and Aims	69

<i>Chapter Two</i>	<i>71</i>
<i>Materials and Methods</i>	<i>71</i>
2.1 Introduction	72
2.2 Materials	73
2.3 Pressurisation system	75
2.3.1 Apparatus development	75
2.3.2 Evaluation of the pressure apparatus	77
2.3.3 Experimental design	78
2.3.3.1 Positive control group	79
2.3.3.2 Pressure group	79
2.3.3.3 Negative control group	80
2.3.3.4 Analysis	80
2.3.4 Primary retinal culture	81
2.3.4.1 Neonatal rat retinal culture	81
2.3.4.2 Human retinal culture	83
2.3.4.3 RGC identification	83
2.3.5 Neuronal cell lines	84
2.3.6 Retinal ganglion cell line	85
2.4 Apoptosis detection	86
2.4.1 Immunofluorescent markers of apoptosis	86
2.4.1.1 Early apoptosis marker	86
2.4.1.2 Late apoptosis marker	87
2.4.2 Morphological analyses of apoptosis	87
2.4.3 Quantitative analysis of immunofluorescent markers	88
2.4.3.1 Manual cell counts	88
2.4.3.2 Laser scanning cytometry	89
2.4.3.3 Statistical Analysis	91
2.4.4 Activated caspase-3 assay	95

<i>Chapter Three</i> -----	<i>96</i>
<i>Study of Pressure System</i> -----	<i>96</i>
3.1 Introduction _____	97
3.2 Results _____	98
3.2.1 Pressure testing _____	98
3.2.2 Gas effect _____	98
3.3 Discussion _____	103
 <i>Chapter Four</i> -----	 <i>105</i>
<i>Study of Primary Retinal Cultures</i> -----	<i>105</i>
4.1 Introduction _____	106
4.2 Results _____	108
4.2.1 Morphological examination _____	110
4.2.2 Quantitative analysis _____	114
4.3 Discussion _____	119
 <i>Chapter Five</i> -----	 <i>124</i>
<i>Study of Neuronal Cell Lines</i> -----	<i>124</i>
5.1 Introduction _____	125
5.2 Results _____	127
5.2.1 Morphological examination _____	127

5.2.2 Quantitative analysis	140
5.2.2.1 B35 cell line	141
5.2.2.2 C17 cell line	146
5.2.2.3 NT2 Cell line	146
5.2.2.4 PC12 cell line	149
5.3 Discussion	154
<i>Chapter Six</i>	<i>164</i>
<i>Study of Retinal Ganglion Cell Line</i>	<i>164</i>
6.1 Introduction	165
6.2 Results: Pressure response	167
6.2.1 Morphological examination	167
6.2.2 Quantitative analysis	176
6.3 Results: Activated caspase-3	184
6.3.1 Morphological examination	184
6.3.2 Quantitative analysis	187
6.4 Discussion	189
<i>Chapter Seven</i>	<i>206</i>
<i>General Discussion</i>	<i>206</i>
<i>References</i>	<i>224</i>
<i>Appendices</i>	<i>256</i>

FIGURES and TABLES

Chapter One - Review of Literature

<i>Figure 1-1 Structure of the retina.....</i>	<i>5</i>
<i>Figure 1-2 (A) Structure of the optic nerve and (B) Clinical view of the optic disc</i>	<i>6</i>
<i>Figure 1-3 Anatomy and physiology of the angle of the eye</i>	<i>8</i>
<i>Figure 1-4 (A) Retinotopicity and (B) Pathology of optic disc cupping</i>	<i>16</i>
<i>Figure 1-5 Progression of (A) Optic disc cupping and (B) Visual fields in glaucoma..</i>	<i>17</i>
<i>Figure 1-6 Modes of cell death.....</i>	<i>24</i>
<i>Figure 1-7 Overview of apoptotic pathways</i>	<i>30</i>
<i>Table 1-1 Morphological criteria for identification of apoptosis and necrosis.....</i>	<i>35</i>
<i>Figure 1-8 Schematic diagram of the components of mechanotransduction</i>	<i>66</i>
<i>Table 1-1 Morphological criteria for identification of apoptosis and necrosis.....</i>	<i>35</i>

Chapter Two - Materials and Methods

<i>Table 2-1 Sources of chemicals.....</i>	<i>73</i>
<i>Figure 2-1 (A) Design of pressure system and (B) Photo of pressure chambers</i>	<i>76</i>
<i>Figure 2-2 Laser Scanning Cytometer</i>	<i>92</i>
<i>Figure 2-3 LSC scan.....</i>	<i>93</i>

Chapter Three - Study of Pressure System

<i>Table 3-1 Assessment of pressure apparatus for gas effect.....</i>	<i>102</i>
<i>Figure 3-1 Analysis of gas effect in pressure chamber: pH.....</i>	<i>99</i>
<i>Figure 3-2 Analysis of gas effect in pressure chamber: pO₂.....</i>	<i>100</i>
<i>Figure 3-3 Analysis of gas effect in pressure chamber: pCO₂.....</i>	<i>101</i>

Chapter Four - Study of Primary Retinal Cultures

<i>Table 4-1 Summary of experiments on neonatal rat retinal cultures</i>	109
<i>Figure 4-1 Morphology of rat retinal culture: general</i>	111
<i>Figure 4-2 Morphology of rat retinal culture: cell types</i>	112
<i>Figure 4-3 Morphology of rat retinal culture: TUNEL assay</i>	113
<i>Figure 4-4 Survival assay of rat retinal cultures</i>	115
<i>Figure 4-5 Rat retinal culture: Quantitative analysis of TUNEL assay (GMP)</i>	117
<i>Figure 4-6 Rat retinal culture: Quantitative analysis of TUNEL assay (GI)</i>	118

Chapter Five - Study of Neuronal Cell Lines

<i>Figure 5-1 Morphology of B35 cells</i>	128
<i>Figure 5-2 Morphology of C17 and NT2 cells</i>	129
<i>Figure 5-3 Morphology of undifferentiated & differentiated PC12 cells</i>	130
<i>Figure 5-4 Morphology of B35 cells: Pressure experiment</i>	133
<i>Figure 5-5 Morphology of B35 cells: TUNEL assay</i>	134
<i>Figure 5-6 Morphology of B35 cells: Annexin V assay</i>	136
<i>Figure 5-7 Morphology of PC12 cells: TUNEL assay</i>	137
<i>Figure 5-8 Morphology of differentiated PC12 cells: TUNEL assay</i>	138
<i>Figure 5-9 Morphology of apoptotic differentiated PC12 cells (Nomarski image)</i>	139
<i>Figure 5-10 B35: Quantitative analysis of TUNEL assay (GI) timecourse</i>	142
<i>Figure 5-11 B35: Quantitative analysis of TUNEL assay (GMP) 2 hrs</i>	143
<i>Figure 5-12 B35: Quantitative analysis of TUNEL assay (GI) 2 hrs</i>	144
<i>Figure 5-13 B35: Quantitative analysis of Annexin V (GI) timecourse</i>	145
<i>Figure 5-14 C17: Quantitative analysis of TUNEL assay (%) timecourse</i>	147
<i>Figure 5-15 NT2: Quantitative analysis of TUNEL assay (%) timecourse</i>	148

<i>Figure 5-16 Differentiated PC12:</i>	
<i>Quantitative analysis of TUNEL assay (GI) timecourse.....</i>	<i>150</i>
<i>Figure 5-17 Differentiated PC12:</i>	
<i>Quantitative analysis of TUNEL assay (GMP) 24 hrs</i>	<i>151</i>
<i>Figure 5-18 Differentiated PC12:</i>	
<i>Quantitative analysis of TUNEL assay (GI) 24 hrs</i>	<i>152</i>
<i>Figure 5-19 Differentiated PC12:</i>	
<i>Quantitative analysis for TUNEL (%) timecourse</i>	<i>153</i>

Chapter Six - Study of Retinal Ganglion Cell Line

<i>Figure 6-1 Morphology of undifferentiated & differentiated RGC-5 cells</i>	<i>168</i>
<i>Figure 6-2 Morphology of RGC-5 cells: TUNEL assay (30 mmHg)</i>	<i>170</i>
<i>Figure 6-3 Morphology of RGC-5 cells: TUNEL assay (100 mmHg)</i>	<i>172</i>
<i>Figure 6-4 Morphology of differentiated RGC-5 cells: TUNEL assay (100mmHg)</i>	<i>173</i>
<i>Figure 6-5 Morphology of RGC-5 cells: Annexin V assay (100 mmHg)</i>	<i>175</i>
<i>Figure 6-6 RGC-5: Quantitative analysis of TUNEL assay (% , 100 mmHg)</i>	<i>178</i>
<i>Figure 6-7 RGC-5: Quantitative analysis of TUNEL assay (% , 30 mmHg)</i>	<i>179</i>
<i>Figure 6-8 RGC-5: Quantitative analysis of TUNEL assay (% , 15 mmHg)</i>	<i>180</i>
<i>Figure 6-9 RGC-5: Quantitative analysis of Annexin V assay (% , 100 mmHg)</i>	<i>182</i>
<i>Figure 6-10 Differentiated RGC-5:</i>	
<i>Quantitative analysis of TUNEL assay- (%) timecourse (100 mmHg) ...</i>	<i>183</i>
<i>Figure 6-11 Morphology of RGC-5 cells: cleaved caspase-3 assay (Low power)</i>	<i>185</i>
<i>Figure 6-12 Morphology of RGC-5 cells: cleaved caspase-3 assay (High power)</i>	<i>186</i>
<i>Figure 6-13 RGC-5:</i>	
<i>Quantitative analysis of cleaved caspase-3 assay (%) (100 mmHg)</i>	<i>188</i>

Chapter One

Review of Literature

1

1.1 Glaucoma

The word ‘glaucoma’ is derived from the ancient Greek ‘glaukos’ (γλαυκωσ) meaning a blue-green hue. Hippocrates used the term around 400 BC to describe the blindness of old age associated with a bluish glazed appearance of the pupil (Blodi 2000). This was most likely a reference to the appearance of the eye of a person with the disease glaucoma. The swollen cornea would appear cloudy, or perhaps a rapidly developing lens opacity was seen, both of which may be caused by the chronically increased intra-ocular pressure of glaucoma (Mantzioris 2006).

Glaucoma is a major cause of blindness worldwide, and this loss of vision cannot be reversed. The mechanisms of how this disease affects the eye, its *pathogenesis*, is central to understanding glaucoma. Ultimately this allows for the investigation of new treatment options for patients suffering from this debilitating condition. However even today the pathogenesis of glaucoma is not fully explained, with many unanswered questions remaining (Levin 2005; Casson 2006; Tan, Kalapesi et al. 2006).

In basic terms glaucoma is thought of as “...the presence of ocular tissue damage apparently related at least partially to the pressure of the fluid in the eye (intraocular pressure)...” (Spaeth 1995). The damaged tissue referred to is the optic nerve, hence glaucoma can be considered as a form of optic neuropathy (Osborne, Wood et al. 1999). There are however many other disorders which damage this vital neural pathway and hence are also classified as optic neuropathies (Levin and Gordon 2002). These encompass the full breadth of pathological aetiologies, including congenital, ischaemic, infective, inflammatory, compressive, and toxic optic neuropathies (Hedges, Friedman et al. 2000). What then distinguishes glaucomatous optic neuropathy?

Before this can be addressed it is important to understand that in ophthalmology 'glaucoma' refers to a range of diseases which fall under this broad term, and currently there are over 60 types known (Morrison and Pollack 2003). These vary in their pathophysiology and clinical presentation, hence there is no single definition which can encompass all aspects of glaucoma (Kanski 2003). However some key features are common to these disorders: the death of retinal ganglion cells (RGCs) associated with certain risk factors, principal among them being intra-ocular pressure (IOP) (Quigley 1999). Thus glaucoma has the following characteristics (Palmberg and Wiggs 1999):

- i. The progressive loss of retinal ganglion cells of the optic nerve which results in
- ii. A characteristic appearance of the optic disc and
- iii. A specific pattern of corresponding visual field loss
- iv. Most frequently associated with increased intra-ocular pressure

With our ever increasing understanding of glaucoma the definition of the disease will continue to evolve. In order to understand the implications of this definition, a brief review of the underlying structures and processes involved follows.

1.1.1 Ocular anatomy and physiology

The visual system consists of the eye or globe which is connected by the optic nerve to the brain. The globe is housed within its own bony cavity within the skull, the orbit. The eye itself is a balloon-like structure with a spherical wall and a central cavity. This wall consists of a strong structural outer coat comprising the white sclera which is continuous anteriorly with the transparent cornea. Lining the interior of the sclera behind the level of the iris is the uvea. This is a layer of pigmented tissue which consists of the muscular iris in front, inserting into the secretory ciliary body, which merges then into the vascular choroid. The innermost lining is the neural retina, comprising the

photoreceptors and neurons subserving the detection of light (Vaughan, Asbury et al. 1992; Forrester, Dick et al. 1996; Kanski 2003).

Light travels through transparent optical media, entering through the cornea and travelling via the pupil (formed by the iris) to be transmitted through the lens and then focussed on to the retina. The retina is an extremely complex neural tissue with a unique layered architecture which allows initial processing of visual information (Fig. 1-1). Retinal photoreceptors are capable of being stimulated by a single photon of light. This signal is conveyed by second order sensory neurons, the bipolar cells, and may be modulated by a complex network of associated neurons also within the retina (Cohen 1992). These include amacrine cells, horizontal cells, and glial Muller cells. The visual stimulus is then transmitted by a third order sensory neuron, the retinal ganglion cells (RGC) (Vaughan, Asbury et al. 1992; Forrester, Dick et al. 1996).

The cell bodies of RGCs comprise a distinct layer in the retina, the ganglion cell layer (Fig. 1-1). From this layer RGC axons emerge to form the innermost retinal sub-layer, the nerve fibre layer (NFL) in which they course toward the central optic nerve head, the clinically visible portion of this nerve at the back of the eye. Anatomically this is a distinct region where RGC axons exit the globe via perforations in the scleral wall of the eye to form the optic nerve (Fig. 1-2A). These unmyelinated axons turn sharply at the margin of the nerve into tiny apertures created by collagenous beams which criss-cross the scleral defect. This meshwork is a specialised section of the sclera called the lamina cribrosa. It represents a relative weakness in an otherwise strong ocular wall, and is crucial to the formation of the optic nerve and to the clinical definition of glaucoma (Anderson and Quigley 1999; Morrison and Pollack 2003; Shields 1992). This optic disc, as it is referred to clinically, is the most distinct feature visible in the fundus of the eye as seen in Fig. 1-2B (Spalton, Hitchings et al. 2005).

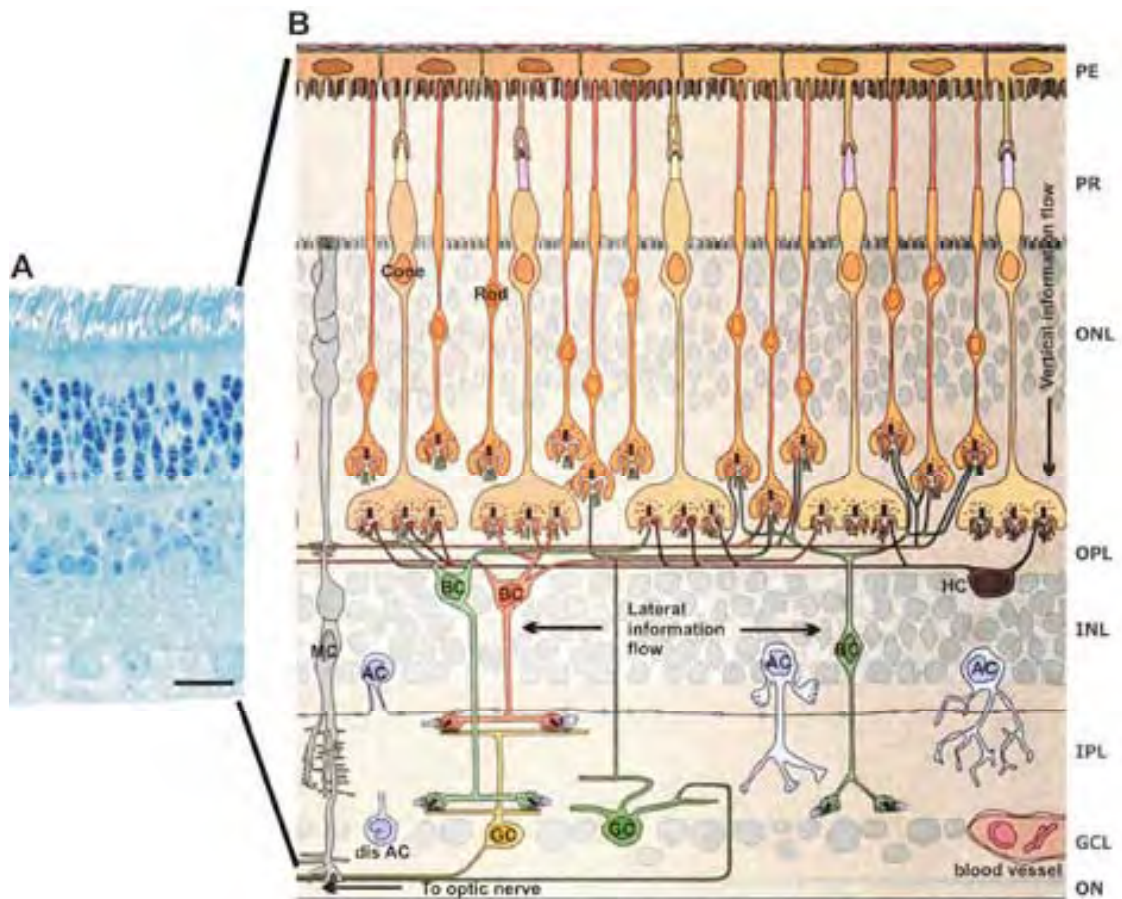
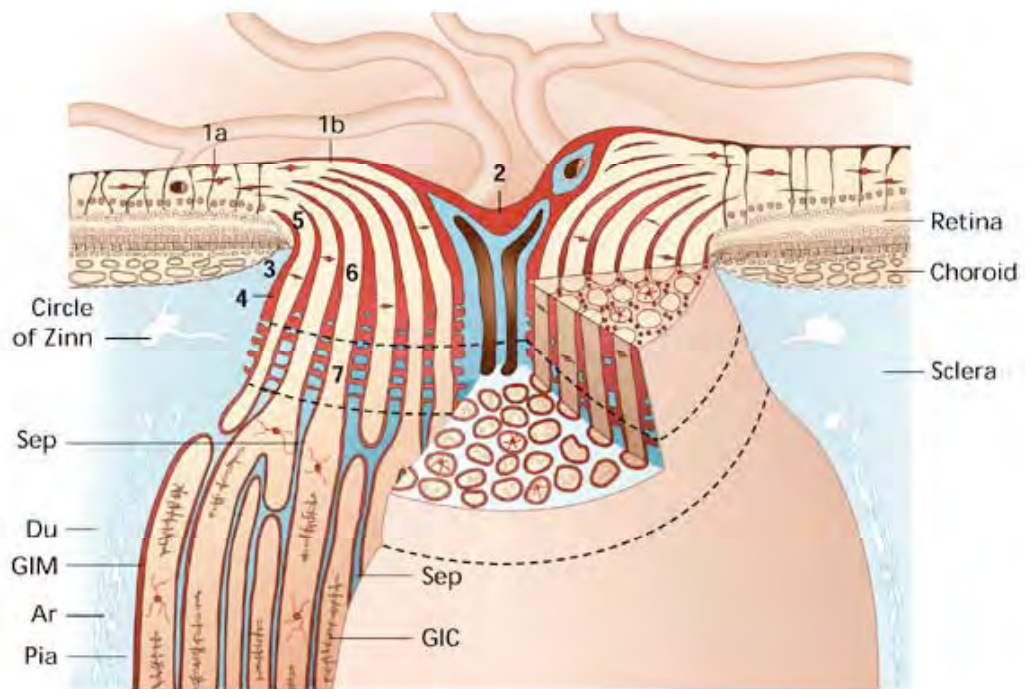


Figure 1-1 Structure of the retina

A. Histological section of the retina, expanded into diagram **B.** showing cellular components and connections. Layers from above: PE= pigment epithelium, PR= photoreceptors (cones and rods), ONL= outer nuclear layer, OPL= outer plexiform layer, INL= inner nuclear layer, IPL= inner plexiform layer, GCL= (retinal) ganglion cell layer, ON=optic nerve or 'NFL' nerve fibre layer, comprising RGC axons. Cell types shown: AC= amacrine cells, BC= bipolar cells, GC=(retinal) ganglion cells, HC=horizontal cells, MC= Muller (glial) cells. (From: Anatomy 2006)



A



B

Figure 1-2 (A) Structure of the optic nerve and (B) Clinical view of the optic disc

A. Anatomy of the optic nerve head. 1-6 are subregions of the pre-laminar section of the optic nerve; 7 is the lamellar region formed by a meshwork of scleral derived collagen (light blue) dividing the component RGC axons into bundles or **Septae**, posterior to which is the retro-laminar myelinated portion of the optic nerve with coverings of **Dura**, **Pia** and **Arachnoid**. (From: Fantes and Anderson 2000)

B. View of the normal optic disc 'en face' with retinal blood vessels arising from the centre of the optic nerve head. Physiological 'cup' seen as pale area in the middle of the disc, and striations of the nerve fibres are just visible as they radiate toward the nerve from the surface of the retina. (Photograph by author)

The optic nerve is the second of the cranial nerves but is actually an extension of the central nervous system, connecting to the brain where higher order processing of visual information occurs. This nerve consists of the axons of all RGCs, approximately 1.1 million in each retina (Bron, Tripathi et al. 1997; Spalton, Hitchings et al. 2005). The optic nerve has three sections defined by its relationship to the lamina cribrosa (Fig. 1-2A). The pre-laminar segment comprises the axons at the margins of the lamina, heaping up as they approach the sharp turn into the meshwork. The intra-laminar section of the optic nerve corresponds to its formation as a more distinct anatomical entity as it transits through the lamina cribrosa. Beyond this the RGC axons become myelinated and the nerve thus increases in thickness. In this post-laminar section it acquires the full complement of coverings- namely the layered dura mater, the cerebrospinal fluid filled arachnoid and the fine pia- that are the signature of the central nervous system (Bron, Tripathi et al. 1997; Anderson and Quigley 1999).

At the optic nerve head these axons converge from all areas of the retina in an ordered fashion such that each part of the retina is represented by a well defined section of the optic nerve margin, and then of the nerve itself. This remarkable preservation of spatial co-ordinates on the retina, known as retinotopicity, continues throughout the visual pathway into the brain itself (Cohen 1992). It is the basis for the processing of visual stimuli to generate a representative view of the visual world.

The lens and iris divide the interior of the globe into an anterior chamber, filled with clear water-like aqueous humor and a much larger posterior cavity containing a clear jelly-like substance, the vitreous. Aqueous humor is secreted by the ciliary body and circulates through the anterior chamber before being drained through a fine network of collagenous and endothelial beams which rings the outer circumference of the chamber, known as the trabecular meshwork. Anatomically this is located at the junction of the

cornea and the iris/ciliary body complex, a region known as the angle (Fig. 1-3). From the meshwork the aqueous collects in a circular channel, Schlemm's canal, before being drained through the episcleral venous system (Cantor, Berlin et al. 2000; Rhee 2003). In addition to this 'conventional' route of aqueous outflow, a small percentage (~10%) exits through interstitial spaces of the uvea. This 'uveoscleral' flow travels directly through the ciliary body and into the vascular choroid, to be drained by the venous system here (Forrester, Dick et al. 1996; Cantor, Berlin et al. 2000).

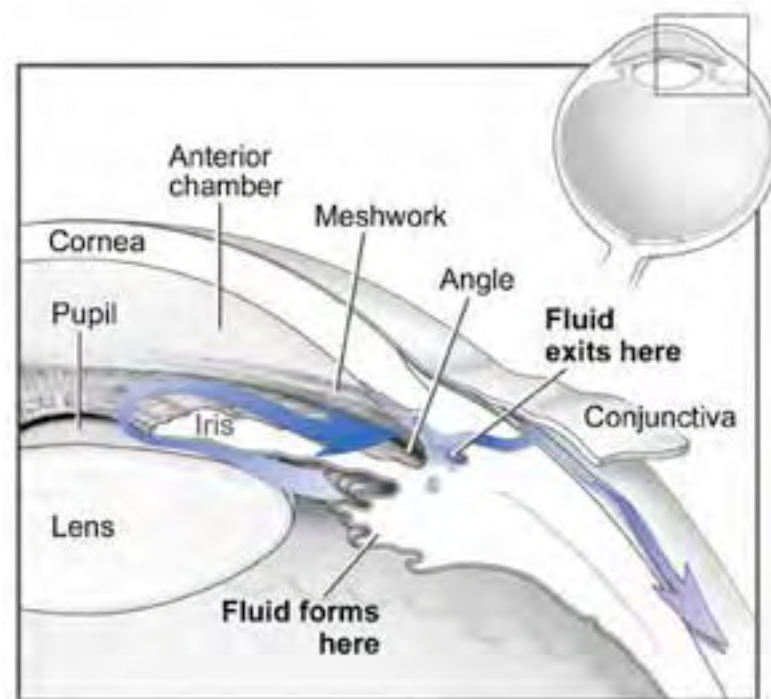


Figure 1-3 Anatomy and physiology of the angle of the eye

Aqueous **fluid** is secreted by the ciliary body and flows around the **iris** through the **anterior chamber** to exit via the **angle**, where the trabecular **meshwork** is situated. From here aqueous drains into the episcleral venous system just beneath the **conjunctiva**. (From: NEI Health Information, 2006)

Intraocular pressure is the hydrostatic pressure within the closed cavity of the globe, by virtue of which the eye is maintained in an anatomically and physiologically functional state. In effect, it is what keeps the eye inflated to just the right level so that it can continue to function (Anderson 1995). IOP is determined by the equilibrium between production and drainage of aqueous humour. The balance is thus between the rate of aqueous secretion by the ciliary body and its outflow through the trabecular meshwork in the angle of the anterior chamber (Hart 1992). The formation of aqueous is a physiological process determined by the active transport of solutes and osmotic gradients across a double layered ciliary epithelium, and is influenced by sympathetic tone. It is however relatively unaffected by hydrostatic pressure (Anderson 1995).

In contrast the outflow of aqueous by conventional and uveoscleral pathways is a passive process and largely dependant on hydrostatic pressure. Specifically it is determined by the pressure gradient between IOP and the pressure in the episcleral vein compartments into which aqueous drains, and by the resistance to flow between these two compartments (Hart 1992). The causes of high pressure within the eye are principally related to problems with the outflow of aqueous rather than production, and this forms the basis for the classification of the major types of glaucoma.

1.1.2 Classification

There are various schemes for the classification of types of glaucoma, and in clinical practice a specific case may require a combination of diagnostic categories to accurately describe it (Bathija, Gupta et al. 1998). In the first instance glaucoma may be classed by its age of onset and thus be **congenital** or **acquired**. Each type may also be labelled by the rapidity of onset of pressure elevation or of symptoms as **acute** or **chronic** glaucoma. Glaucoma may also be described by the presence or absence of associated

factors contributing to the pressure rise. **Primary** glaucoma has elevated IOP not associated with any other ocular disorder, while **secondary** glaucoma results from a separate recognisable eye disease which is responsible for initiating the pressure rise, such as inflammation, tumours or vascular anomalies (Kanski 2003).

The most important and widely used classification is that based on the mechanism of hydrostatic pressure elevation. Since elevated IOP is a result of impaired aqueous outflow through the anterior chamber angle, these diagnostic types of glaucoma are described by clinicians according to the mechanism of outflow obstruction (Anderson 1995). These may be grouped by the status of the angle as **open angle** or **closed angle** glaucoma. Closed angle glaucoma involves obstruction of aqueous outflow by the peripheral iris. This can be due to an anatomical predisposition (the commonest variety) or as a result of secondary forces closing an otherwise normal angle, for example severe inflammation causing fibrovascular contraction of the trabeculum (Palmberg and Wiggs 1999). By far the most common form of glaucoma is a chronic form known as primary open angle glaucoma. This is of slow onset with an open anterior chamber angle. The mechanism of IOP elevation is however unknown or idiopathic, hence its classification as a primary disease (Palmberg and Wiggs 1999; Rosenberg and Krupin 1999).

Two other types of glaucoma are worth noting. **Normal tension** glaucoma is a primary open angle glaucoma associated with IOPs that are not significantly elevated, but are causative nonetheless (Hitchings 1999). **Ocular hypertension** is present where IOPs are notably raised but there is no evidence of glaucomatous optic nerve damage (ie. normal disc appearance and visual fields) (Rhee 2003). It may be a 'pre-glaucoma' state in some respects as there is a higher likelihood of developing glaucoma, and above a certain level of IOP this has been shown to necessitate treatment before waiting for damage to occur (Kass, Heuer et al. 2002).

All these types of IOP related eye diseases have common characteristics which are unique to glaucoma. These are most evident in the clinical appearance of this condition. Though the various types can present differently and show great disparity in many aspects, the hallmarks of a glaucomatous eye described in Section 1.1.4 form the defining features of this disorder.

1.1.3 Epidemiology

Glaucoma is an important disease of the eye which can lead to irreversible blindness. It is a major cause of loss of vision worldwide, and is increasingly being recognised as a major public health problem. Estimates at the end of the last century of the number of people in the world affected by glaucoma were 67 million, with 6.7 million bilaterally blind as a result (Quigley 1996). The WHO ranks glaucoma as the second biggest cause of blindness globally, after cataract and ahead of macular degeneration (Thylefors, Negrel et al. 1995). The UN's health body calculated that 12% of the world's blindness was due to glaucoma, making it the single most important cause of irreversible blindness (Foster and Resnikoff 2005). Understandably the worldwide program to address blindness, 'Vision 2020' has made the management of this disease a priority (WHO 2004).

In Australia the number of affected people is estimated to be at least 300,000 (Glaucoma-Australia 2006). Here it is the leading preventable cause of blindness and second only to macular degeneration in terms of total blindness (Access-Economics 2004). In 2004 glaucoma was responsible for 14% of blindness, greater than that from cataract (12%) which is the typical pattern in developed nations where cataract surgery is readily accessible. Nonetheless even in Australia it is believed that the true number of glaucoma patients is twice these reported levels, as half of the glaucoma is undiagnosed

(Access-Economics 2004; Wong, Keeffe et al. 2004).

In terms of the overall population it is estimated that in Australia one person in 11 will develop glaucoma if they live long enough (Access-Economics 2004). The most common form of glaucoma in Australia is primary open angle glaucoma, responsible for 90% of glaucoma cases (Morgan 1995; Mukesh, McCarty et al. 2002). The Blue Mountains Eye Study found the prevalence of this type of glaucoma in the susceptible population (over 49 years of age) to be 2.4% (Mitchell, Smith et al. 1996). Different studies report varied prevalence of glaucoma around the world. The Beaver Dam study described rates of 2.1%, and the increasing prevalence with age confirmed with a rate of 4.7% in those over 75 years (Klein, Klein et al. 1992). Ethnicity is a known risk factor and African-Americans have a glaucoma prevalence around four-times greater than Caucasians as reported by the Baltimore Eye Study (Tielsch, Sommer et al. 1991).

The economic burden of glaucoma is also substantial. The cost of glaucoma in the United States has been calculated at \$2.5 billion annually (Brubaker 1996). In Australia glaucoma costs \$144 million in direct health care and \$254 million in indirect care costs (Access-Economics 2004). The number of people affected and the related socioeconomic impact are expected to steadily increase as the population ages and glaucoma detection improves (Quigley and Broman 2006). It is estimated that by 2020 the economic impact of glaucoma in Australia will be in the order of \$500 million per annum (Access-Economics 2004).

1.1.4 Clinical presentation

One important feature of glaucoma is that, unlike many other leading causes of visual loss, that which is caused by glaucoma cannot be restored. Cataracts are by far the major cause of blindness, however they are readily treated with surgery to remove

the opacified lens (Frick and Foster 2003). Glaucomatous visual loss, on the other hand, can only be stabilised at best by treatment to reduce pressure within the eye. In spite of this a degree of progressive deterioration can still occur. Thus the effect of this disease even with the best medical attention is not able to be reversed (Quigley 1999).

Further the presentation of glaucoma is notoriously insidious. The majority of cases, viz. of primary open angle glaucoma, have no symptoms until very advanced stages when considerable vision has already been lost. This is due to the slow, chronic and painless nature of the disease (Anderson 1995). Also important is the type of visual loss that glaucoma causes- a gradual shrinking of peripheral vision which is difficult to notice until very late. Glaucoma results in a reduction of the total area of vision, the visual field, which begins at the edges and if untreated can progress to tunnel vision where only central vision remains (Walsh 1996). In advanced cases this too is affected and total blindness ensues. Coupled with the irreversible nature of these changes, this means that when an undiagnosed patient first becomes aware of the symptoms of glaucoma, significant and permanent damage has already occurred (Spaeth 1995).

As a result the emphasis in glaucoma is very much on the prevention of visual loss. Public education and awareness, population screening and early diagnosis are the most important agents in preventing glaucoma blindness (Flanagan 1998). Only then can an understanding of the disease, and the promise of better treatment, help preserve vision and avoid blindness.

Currently the evaluation of a patient suspected of having glaucoma includes several components such as the patient's presentation, the presence or absence of risk factors (age, race, family history, high myopia or hyperopia, diabetes) and the clinical examination (Rhee 2003). The clinical features described below are the hallmarks of glaucoma, defining the disease condition. They also serve to distinguish this optic

neuropathy from other conditions which affect RGCs and the optic nerve (Burgoyne, Crawford Downs et al. 2005). In ophthalmic practice they are used to diagnose the disease, monitor its progression and ultimately guide the treatment of glaucoma. These features are the optic disc appearance, visual field changes, and intraocular pressure.

1.1.4.1 Optic disc appearance

Changes in the appearance of the visible portion of the optic nerve, or optic disc as it is referred to clinically, have been noted in glaucoma for over a century. Indeed the first report of this appeared soon after the development of the ophthalmoscope by Helmholtz in 1850 (Duke-Elder 1941). Today theories on its development may vary, but there is agreement that this is a reliable indicator of optic nerve disease specifically due to glaucoma (Quigley and Green 1979; Pedut-Kloizman and Schuman 1999).

Optic disc damage is superimposed upon the normal physiological appearance of this most anterior segment of the optic nerve (Fig. 1-2B). A 'normal' disc consists peripherally of a neuroretinal rim of RGC axons of the retinal nerve fibre layer (NFL). This appears as an orange or pink, often raised area of tissue at the perimeter of the disc. Central to this is the optic cup, a pale depression which is not occupied by neural tissue. The pallor is due to the lack of NFL and also the absence of glial tissue, exposing the white sclerally derived lamina cribrosa (Anderson 1995). In a stereoscopic view the borders may be seen three-dimensionally to appreciate the depth of this physiological cup, and a guide to the boundary between the coloured rim and the pale central cup is the bending of blood vessels coursing over the NFL rim (Cantor, Berlin et al. 2000).

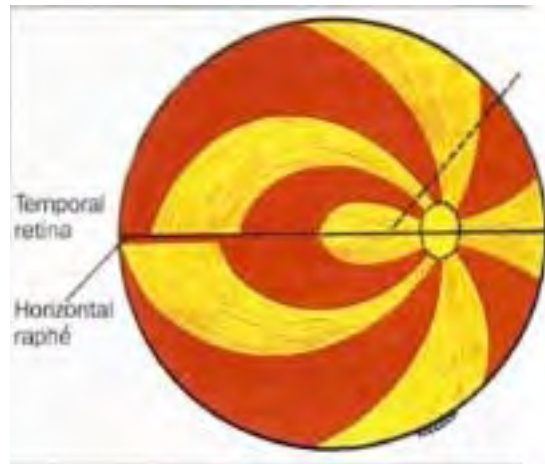
In the eye of a patient with glaucoma the cup assumes a more prominent appearance and the rim a lesser one. The loss of RGCs is reflected in a loss of their axons, the number of which passing through the lamina cribrosa is reduced. As a result there is

diminution of the NFL and the thickness of the neuroretinal rim is correspondingly reduced (Pedut-Kloizman and Schuman 1999). The effect of this loss of neural tissue forming the optic nerve head is to change the relative proportions of neural and structural elements of the optic disc, and this is clearly visible (Ernest and Potts 1971).

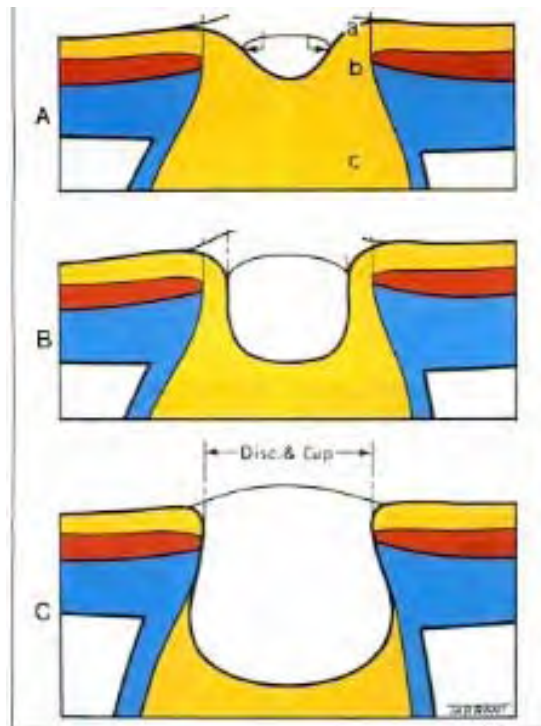
The most striking change is an increase in the size of the cup over time. The diameter of this central pale region grows as a fraction of the total disc diameter as more RGCs and their axons are lost, thinning the neural component of the disc as seen schematically in Fig. 1-4B (Drance 1995). This is shown in the progressive increase in cupping of the disc in a glaucoma patient's eye as depicted in Fig. 1-5A.

Even more significant than simply an enlarged cup though is the outward bowing or excavation of the lamina cribrosa which accompanies the cupping (Quigley 1995). In a three-dimensional view the excavation in an advanced case of glaucoma is dramatic, with a very clear appreciation of a hollowing out of the optic disc. This reflects the collapse of this crucial support structure as well as the loss of axonal tissue which once provided the bulk of its tissue (Burgoyne, Crawford Downs et al. 2005).

Other less consistent features of a glaucomatous disc are Drance splinter haemorrhages, atrophy of the surrounding retinal and even subretinal tissue (peripapillary atrophy), and actual defects in the NFL visible with a red-free illumination (Pedut-Kloizman and Schuman 1999). Always associated with an increased optic disc cupping however is the thinning of the neuroretinal rim, reflecting as it does the health of RGCs and the NFL. Certain regions of the rim are known to be attenuated earlier in glaucoma than other regions, and the appearance of the rim alone can suggest the severity of the disease (Cantor, Berlin et al. 2000). It is the areas of this marginal rim that correspond to particular areas of the retina, so thinning of specific sections can give clues as to the presence of changes in the visual field.



A



B

Figure 1-4 (A) Retinotopicity and (B) Pathology of optic disc cupping

A. Retinotopicity of RGC axons. The axons form the nerve fibre layer (NFL) which courses towards and forms the optic nerve. View of retina showing surface topography of the NFL, with a horizontal ‘raphe’ dividing axons from upper and lower hemispheres. Dotted line indicates axons from central macula. Note uppermost and lowest areas of retina curve to reach the optic nerve at its vertical poles, the most susceptible in glaucomatous RGC loss. Damage to these RGC-NFL fibres explain the ‘arcuate’ distribution of corresponding visual field defects in early glaucoma.

B. Pathology of optic disc cupping. Normal cross section of nerve (A) shows thick neuroretinal rim (yellow) formed by RGC axons. Glaucoma causes loss of RGCs and their axons, thinning the rim (B) until in end-stage disease little remains (C). This loss of RGCs results in corresponding visual field loss. (A & B: From: Kanski, J. 2003).

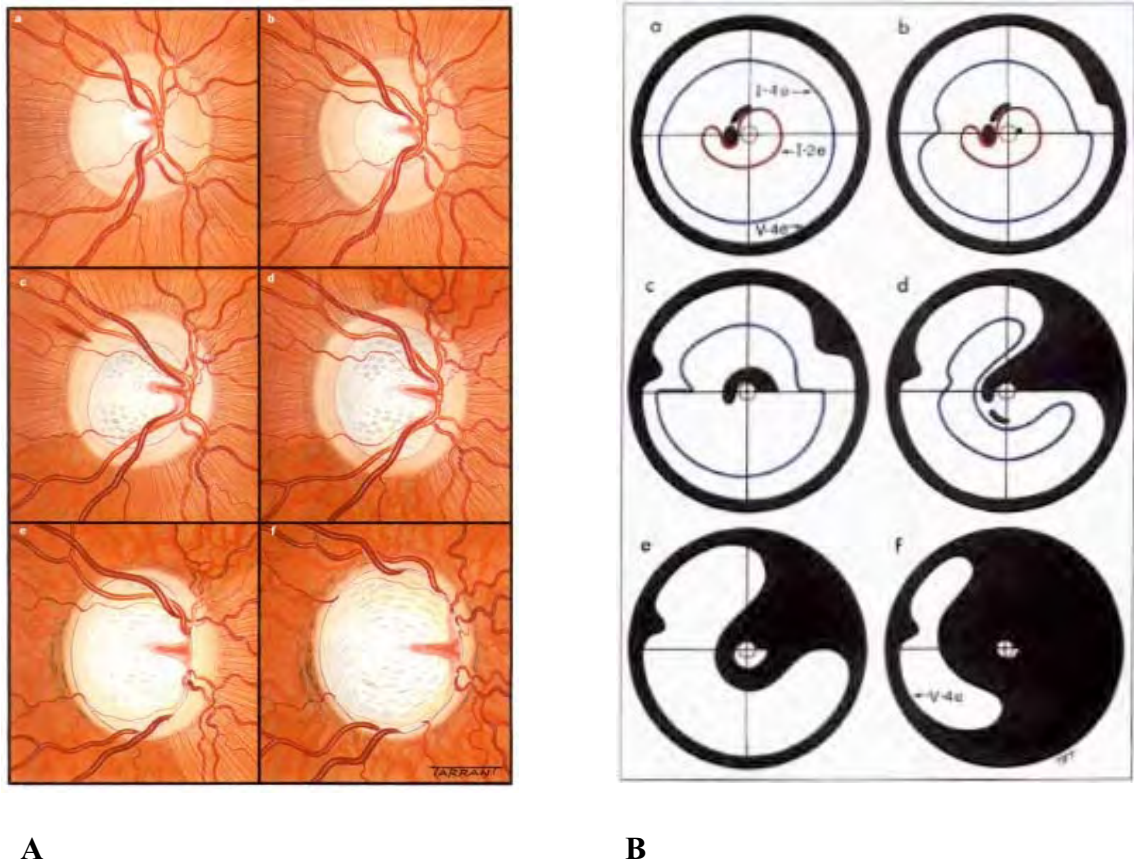


Figure 1-5 Progression of (A) Optic disc cupping and (B) Visual fields in glaucoma

A. Optic disc cupping. Serial illustrations of the optic disc showing changes seen in advancing glaucoma. Progressive increase in optic disc cupping seen, from (a) ‘normal’ physiological cupping with healthy neuroretinal rim (pinkish surround of pale central cup) to end-stage glaucoma with little residual neuroretinal rim (f).

B. Visual fields. Perimetric measurements of a glaucoma patient showing changes with advancing glaucoma. Blackened region represents lost areas of vision, or ‘visual field defects’. In early glaucoma they are just detectable as a central arc above the physiological blind spot (a). This progresses to a classic arcuate defect, (c) which enlarges until only an island of central vision remains, (e) and then continuing peripheral loss, (f). Changes correspond to the progressive optic disc cupping seen in A.

(From: Kanski, J. 2003)

1.1.4.2 Visual field changes

The loss of RGCs in glaucoma is reflected ultimately in the appearance of the optic disc and in the neuroretinal rim in particular. The damaged RGCs may remain in a compromised state for some time before eventually disappearing altogether, and this has functional implications for vision that may be present even before the anatomical changes are detected (Katz, Tielsch et al. 1995).

Many aspects of visual function are affected in glaucoma, but the most specific and sensitive is the change in peripheral vision. Importantly from a patient's perspective these usually go unnoticed until a major proportion of the RGC population has been lost, mainly because of the distribution of these neurons (Weiner, Ripkin et al. 1998). Further, the commonest type of glaucoma, primary open angle with a moderate chronic increase in IOP, involves a slow and painless loss of vision over many years.

As described earlier the spatial distribution of RGCs is preserved in the architecture of the optic disc and further beyond in the visual pathway by virtue of retinotopicity. RGC axons converging on the optic disc follow a rigidly defined pattern that reflects their retinal point of origin. Thus the NFL from a particular part of the retina, which serves an RGC population for a defined area of vision, is located in a defined part of the neuroretinal rim (Fig. 1-4A) (Cantor, Berlin et al. 2000). It follows that the loss of a given part of the optic disc rim, reflecting a particular NFL region and thus the loss of defined ganglion cells, will result in impaired function for a corresponding area of vision. This is the basis for the clinical assessment of visual field testing which demonstrates the visual implications of optic disc changes in glaucoma (Walsh 1996).

The term visual field refers to the total spatial area of visual perception, the dimensions of which are defined by the extent of peripheral vision. In glaucoma the loss

of RGCs is not random but follows a characteristic pattern. This is demonstrated in the anatomical appearance of the optic disc and also in the region of visual field served by the lost RGCs. In the clinical setting the standard test to recognise the presence of glaucomatous damage is called a visual field test or perimetry, developed by Goldmann over 50 year ago (Werner 1999). This test determines the ability to perceive visual stimuli at various locations within the visual field. Most contemporary testing is computerised and generates a 'map' of the area of vision with indicators of any points where the field is deficient (Katz, Tielsch et al. 1995). Representative visual fields are shown in Fig. 1-5B. They show evidence of glaucoma with a distribution of field loss in an arcuate pattern which corresponds to RGC loss that can only be explained by segmental loss of a defined part of the optic disc rim, and hence is unique to glaucoma.

1.1.4.3 Intraocular pressure

Several risk factors are known to be associated with the development of glaucoma. They include familial or hereditary glaucoma (Craig, Baird et al. 2001; Hewitt, Craig et al. 2006), demographic factors such as age and race, ocular conditions altering the anatomy of the eye such as high myopia, and systemic diseases with manifestations in the eye such as diabetes (Fraser and Wormald 1999). The presence of an elevated hydrostatic pressure within the eye however remains the single most frequent and important association of glaucoma (Armaly, Krueger et al. 1980; Caprioli 1995). It is a causative factor in virtually all types of glaucoma. The evidence for this is now overwhelming, from epidemiological studies to laboratory in vivo animal experiments (Quigley 1999). Some of the main bodies of evidence are presented below.

i. Epidemiological data

Large scale studies have demonstrated the association between IOP and the presence

of glaucomatous optic disc changes and/or visual field changes (Fraser and Wormald 1999). The Baltimore Eye Survey for example found the prevalence of primary open angle glaucoma increased with increasing IOP (Sommer, Tielsch et al. 1991). The relative risk of glaucoma rises with IOP above a certain level, as does its probability (Jay and Murdoch 1993). In studies where IOP is excluded from the definition of glaucoma, it is still related strongly to the risk of developing the disease (Wormald, Basauri et al. 1994) (Sommer, Tielsch et al. 1991).

ii. Clinical treatment data

The mainstay of glaucoma treatment has been to lower the IOP by pharmacological agents, laser or using surgical procedures to slow the progression of visual field loss (Shields 1992; Rait 2000). Treatment studies have consistently shown a dose-response relationship between IOP and the progression of visual field loss (Odberg 1993; Higginbotham, Gordon et al. 2004) . This is irrespective of how the lowering is achieved (Tuulonen, Koponen et al. 1989; Uusitalo and Palkama 1989; Migdal, Gregory et al. 1994). If an individual has glaucoma, the eye with the highest IOP tends to lose field more quickly, even if both IOPs are relatively low to begin with (Dielemans, de Jong et al. 1996).

iii. Animal laboratory data

Experimentally induced elevation of IOP in vivo produces glaucomatous changes in the optic discs of animals. Indeed this is the established model for studying glaucoma in numerous animal species. These studies have successfully induced glaucoma in several animal models, such as mice, rats, rabbits, cats and monkeys (Johansson 1983; Quigley, Nickells et al. 1995; Shareef, Garcia-Valenzuela et al. 1995; Janssen, Naskar et al. 1996; Adachi, Takahashi et al. 1996; Morgan, Uchida et al. 2000).

The range of IOP elevations varies with the type of glaucoma. Angle closure glaucoma is the most severe and acute form, comprising more than 10% in some ethnic groups (Congdon, Quigley et al. 1996), and often presents with very high IOPs well over 50 mmHg and up to 100 mmHg (Coleman and Trokel 1969; Aung, Ang et al. 2001). Primary open angle glaucoma, the most frequent form, is typically associated with pressures up to 30 mm Hg (Anderson 1977; Sommer 1989).

Conventionally the concept of a 'normal' and thus of an elevated IOP is based largely on epidemiological studies (Hollows 1966; Hollows and Graham 1966). Mean IOP in whole populations has been measured at 15 ± 2.5 mmHg (Colton and Ederer 1980). By assuming a Gaussian distribution an 'abnormally high' IOP was thus defined as greater than two standard deviations from the mean, which was >21 mmHg (Smith and Doyle 1999). The definition of 'normal' IOP has been problematic however and it is now accepted that such a neat distribution of pressures is inaccurate, implying that no cutoff exists for an arbitrary definition of 'normal' vs 'abnormal' IOP (Fraser and Wormald 1999).

Another impetus behind this revision has been the increasing recognition of what is termed normal tension glaucoma. In these patients classic glaucomatous optic nerve damage is seen at pressures less than the so-called normal levels of 15 mmHg (Hitchings 1999). This was thought to be in a small proportion of glaucoma cases but it is now known that in some demographics, such as in Japan, this type of glaucoma is much more prevalent (Tang, Toda et al. 2003). Significantly though its treatment remains the same as for any other glaucoma, and lowering the IOP is the only means to retard RGC loss (Bhandari, Crabb et al. 1997).

The concept of what level of elevated IOP defines glaucoma has shifted over time. Previously the disease was considered in terms of an IOP being above a certain range.

Diagnostic screening in its simplest form was based on an IOP value below which glaucoma was presumed to be unlikely, such as 21 mmHg (Duke-Elder 1941). This thinking has evolved to one where currently the IOP elevation responsible for glaucomatous damage is a function of the individual rather than a population. Thus each eye has its own maximal IOP above which the RGC-optic nerve complex is susceptible to glaucomatous damage (Caprioli 1995).

1.1.5 Understanding glaucoma

Glaucoma results in the loss of RGCs, the key neuron serving the eye which forms the optic nerve. This is the basic and undisputed pathology of this disease (Quigley 1995). What is less clear is how and why this occurs. The current concepts of glaucoma pathogenesis are reviewed below in Section 1.3. However despite decades of theorising, clinical observation and scientific research the exact nature of how glaucoma damages these vital cells remains to be fully explained (Weinreb 2001). There are enough ‘unknowns’ in this field to continue to stimulate ongoing research efforts from a variety of perspectives, all aimed at answering this crucial question (Casson 2006).

One of the drivers behind this global research endeavour is our inability to cure this condition. Glaucoma can be controlled in the majority of cases, but even the most optimistic assessment would not consider this to be an alleviation of the disease (Blodi 2000). The clearest evidence for this is the need for lifelong treatment and monitoring. This is a chronic disease with a start date for treatment but never a conclusion (Plitz-Seymour and Walker 1999). Continual monitoring and adjustment of treatment regimes are essential in managing glaucoma, and without this the risk of progression of the disease is unacceptably high (Rait 2000). Further, in a proportion of glaucoma patients

maximal treatment is unable to retard the deterioration in vision (Higginbotham and Lee 1994). Even those in whom therapy is thought to be successful, it is not uncommon for some degree of progressive visual loss, albeit minor, to continue regardless.

The optimal management of this debilitating disease thus remains a hot topic. Central to our efforts to achieve this is our understanding of the nature of glaucoma, and in particular how the pathology of ocular damage occurs. This then is the context in which the research reported in this thesis has been undertaken.

1.2 Retinal ganglion cell death in glaucoma

The underlying pathology of glaucoma is the loss of RGCs related to raised IOP. Hence in order to examine the pathogenic processes responsible for this end result, it is necessary to consider how this cell death occurs. This has become increasingly relevant with the discovery that cell death is not a simple degenerative phenomenon, and that specific cellular processes can regulate its initiation and progress.

1.2.1 Cell death

Cell death is a fundamental biological process, and may be defined as the irreversible loss of vital cellular structure and function (Buja, Eigenbrodt et al. 1993). As a specific area of study however it has only been of relatively recent significance. This may in part be attributed to the historical relegation of cell death to a simple degenerative process due to injury, dating from the time of the great pathologist Virchow in the 1850s (Wyllie, Kerr et al. 1980).

The development of modern research techniques such as molecular biology has led to the realisation that there is more than one type of cell death, and that ‘normal cell

death' can involve active self-destruction rather than passive degeneration. The term **apoptosis** was coined by Australian pathologist J.F. Kerr and his colleague A.H. Wyllie to describe this active form of cell death (Kerr, Wyllie et al. 1972). Apoptosis is now recognised to have a crucial role in normal development as well as homeostasis and pathogenesis in all higher organisms (Wilson 1999). Necrosis is the term used to describe the traditionally known mode of cell death. There are thus two distinct fundamental modes of cell death, necrosis and apoptosis, summarised in Fig. 1-6.

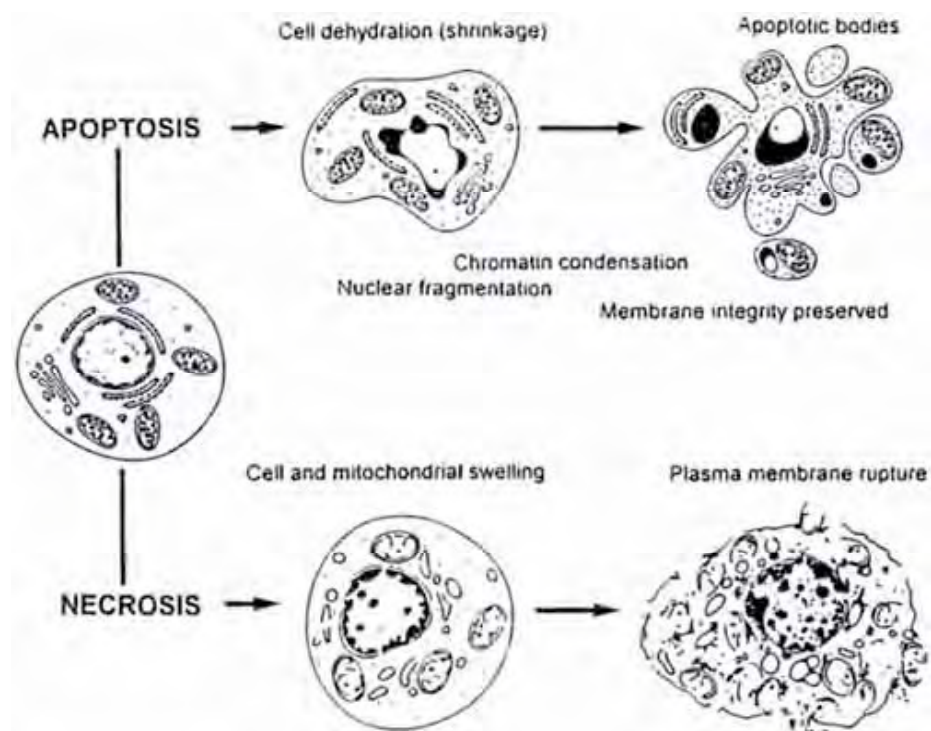


Figure 1-6 Modes of cell death

Diagram showing the two principle forms of cell death and the morphological characteristics of each. Apoptosis is marked by shrinkage of the cytoplasm and nucleus (pyknosis). Nuclear changes also include fragmentation of the DNA and chromatin condensation. The membrane retains its integrity but undergoes blebbing, which then leads to the formation of discrete 'apoptotic bodies' which are ultimately phagocytosed by other cells. Necrosis by contrast involves swelling of the cytoplasm and nucleus, including mitochondria, and eventual rupture of the cell membrane with an inflammatory process resulting. (From: Chinese University of Hong Kong 2006).

1.2.1.1 Necrosis

Necrosis is a passive, catabolic and degenerative process (Darzynkiewicz, Juan et al. 1997). Necrosis generally represents a cell's response to gross injury and triggers an inflammatory reaction which can result in scar formation. In macroscopic pathology two forms are recognised representing the spectrum of necrosis. Coagulative necrosis results from denaturation and coagulation of cellular proteins and develops in response to severe injuries, such as hypoxia, ischaemia, infections and trauma (Farber 1982). Colliquative necrosis by contrast is marked by rapid liquefaction of necrotic tissue which is lacking in protein and/or has excessive hydrolytic enzyme activity, such as in abscess formation (Buja, Eigenbrodt et al. 1993).

Morphologically necrosis is marked early by mitochondrial swelling with subsequent plasma membrane rupture and release of the cytoplasm contents, including proteolytic enzymes capable of damaging surrounding cells and tissue (Majno and Joris 1995). Cellular fragmentation is a late phase and is the result of activation and release of the cell's own lysosomes and enzymes (autolysis), and is also due to the actions of inflammatory cells invading the necrotic tissue (heterolysis) (Searle, Kerr et al. 1982). The nucleus undergoes karyolysis, a process of slow dissolution, and DNA degradation. This degradation is not however extensive and the resultant fragments are of variable length with no particular electrophoretic pattern (Wyllie, Arends et al. 1992).

1.2.1.2 Apoptosis

The word apoptosis is derived from the Greek *apo-* (away) and *ptosis-* (fall) meaning "to fall away", describing the morphological finding of single cells dying and being lost, resembling dead leaves falling off a tree (Kerr, Wyllie et al. 1972). This description refers to the apoptotic trait of cell death that affects individual cells rather

than contiguous groups or whole tissues as is the case in necrosis. The key to this is the capacity for cells to initiate their own destruction, a phenomenon which has been compared to 'cell suicide', with the analogy for necrosis then being 'cell murder' (Majno and Joris 1995). Apoptosis is thus an active and controlled physiological mode of cell death (Nicholson 2001).

Morphologically apoptosis is characterised by the condensation of the cell with intact organelles, so that the cell shrinks and becomes rounded (Wyllie, Kerr et al. 1980). The nucleus demonstrates condensation of the nuclear chromatin, a process called pyknosis. The nuclear envelope disintegrates and its proteins undergo proteolytic degradation followed by nuclear fragmentation or karyorrhexis. Nuclear fragments are extensive and of defined length which can be characterised by gel electrophoresis (Wyllie, Arends et al. 1992). Together with cytoplasm components are packaged and enveloped in the plasma membrane, forming membrane protruberances or blebs which separate as membrane-bound globules and the cell thus fragments into these apoptotic bodies (Fig. 1- 6) (Darzynkiewicz, Juan et al. 1997).

In vivo these apoptotic bodies can be phagocytosed by macrophages, but generally are phagocytosed by surrounding resident cells which are stimulated to become surrogate cells (Nickells and Zack 1996). As the dying cell shrinks and fragments the place it once occupied is filled by surrounding cells or by extracellular material. Thus in apoptosis the macroscopic appearance of the organ or tissue is generally unaffected. This entire process occurs without triggering an inflammatory reaction in the tissue (Wyllie 1992). Cell death in a growing number of diseases is believed to occur by apoptosis (Nicholson 2000). This is the case in glaucoma, where RGCs are lost by this form of cell death (Nickells 1996; Morrison and Pollack 2003).

1.2.2 The process of apoptosis

Perhaps the most striking feature of apoptosis is the finding that this is a cell-autonomous event that is genetically controlled by the dying cell (Nickells 1999). Apoptosis is often referred to as 'programmed cell death' to reflect this concept (Ben-Sasson, Sherman et al. 1995). The cell designs and executes its own program for its demise as well as the disposal of its constituents. There is a multi-step mechanism which regulates the cell's capacity to respond to various stimuli and which can trigger the initiation of apoptosis. A cell once triggered activates a series of molecular events which ultimately lead to its disintegration (Vaux and Strasser 1996). The genes and molecular pathways involved have been the subject of intense research, and increasingly the complexity of this system is now becoming apparent (Oltvai and Korsmeyer 1994; Sakurai, Itoh et al. 2005).

1.2.2.1 Apoptotic stimuli

There exist a wide variety of triggers of apoptosis, both specific stimuli and defined conditions, which are now known to activate cells to become apoptotic. Indeed the discovery of these diverse stimuli has linked apoptosis to many physiological and medical conditions, and has been an impetus for the study of this process as well as the ongoing search for more stimuli (Darzynkiewicz, Juan et al. 1997; Elinder, Akanda et al. 2005). Broadly the stimuli may be considered in terms of the following three broad groupings (Nickells and Zack 1996).

(i) Abnormality or injury to the cell

These are exogenous as well as naturally occurring endogenous factors. Exogenous stimuli include ischaemia, irradiation, toxins and pressure (McHugh and Turina 2006; Galea, Armstrong et al. 1999). More 'internal' factors relate to the physiological role of

apoptosis in multicellular tissue development, the maintenance of homeostasis and aging of the cell or senescence (Wyllie, Kerr et al. 1980). Neoplastic transformation is a pathological situation where apoptosis has been implicated as the means of eliminating cancerous cells (Isaacs 1993). The common feature of these factors is damage to the cell's DNA, as in radiation injury, or damage to cellular proteins, causing accumulation of denatured protein or enzyme derangements (Nickells and Zack 1996).

(ii) Withdrawal of trophic factors

External growth factors are a requirement for survival in many cell types. These molecules are typically short polypeptides which normally interact with surface receptors. This activates a cascade of molecular events that controls various vital cell functions (Schlessinger and Ullrich 1992). Defined trophic factors include certain cytokines, neurotrophins, and fibroblast growth factor. Removal of these factors from the environment has been shown to lead to the death of these 'dependant' cells by apoptosis (Zhao and Barnstable 1996; Cohen, Bray et al. 1994). This has also been described in laboratory tissue cultures of RGCs (Raju, Rao et al. 1994).

(iii) External activators

These exogenous agents are molecules that are believed to have evolved a specific ability to stimulate apoptosis in certain conditions. In nature this encompasses infective agents such as viruses, cell to cell interactions and hormones such as glucocorticoids (Nickells and Zack 1996). A common example of this form of apoptotic stimulation is seen in the role of such factors in the immune system (Linette and Korsmeyer 1994). Here agents like cytokines (eg. Tumor Necrosis Factor 'TNF') and interferons can trigger a cell to 'self-destruct'. The activity of these factors is mediated through target cell membrane receptors, such as the Fas or APO-1 receptor of lymphoid cells which is involved in apoptotic regulation of lymphocyte homeostasis (Cleveland and Ihle 1995).

1.2.2.2 Apoptotic mechanisms

After a cell has been stimulated by an apoptotic stimulus and is thus destined for this mode of cell death, a complex series of molecular events is activated. These biochemical cascades are the means by which the program for cell death is executed (Wilson 1999). Unravelling these mechanisms is a continually evolving process which has been made possible by many advances in molecular biology (McHugh and Turina 2006). The current knowledge regarding the mechanisms is expanding annually and is now so complex that a detailed analysis is beyond the scope of this treatise. Hence a simplified pathway for apoptosis is described below (Nickells 1999).

An apoptotic stimulus is translated to the cellular machinery by mechanisms that are not fully understood. The resulting classic 'first event' is typically the onset of cellular damage, which may be DNA or protein degradation. This initial damage is detected by a sensor protein which activates the tumour suppression protein p53. This protein has several functions including blocking the cell cycle and activating parts of the cell death machinery (Nork, Poulsen et al. 1997; Aloyz, Bamji et al. 1998). It also has a role in regulating apoptosis by controlling the expression of the bcl-2 family of genes. Specifically p53 upregulates the expression of bax which is pro-apoptotic and down regulates its antagonist bcl-2 gene, which is antiapoptotic (Boise, Gonzalez-Garcia et al. 1993; Cuende, Ales-Martinez et al. 1993; Yin and Schimke 1996). Their protein products affect the release of cytochrome c from mitochondria, and this in turn activates a family of proteases. These cysteine proteases are called caspases and are responsible for digesting the cell's contents and the gradual disintegration of the cell (Vaux and Strasser 1996).

The process of apoptosis then has several components to its regulatory system. There are at least two distinct checkpoints, one controlled by the bcl-2/bax protein

family and the other by the caspase effectors of proteolysis. This system interacts with the machinery that regulates cell proliferation and DNA repair via several oncogenes including p53 (Oltvai and Korsmeyer 1994). This has implications for the cell cycle and differentiation, and also suggests the possibility of modulating apoptosis (Darzynkiewicz 1995). Fig. 1-7 gives an overview of the mechanisms of apoptosis.

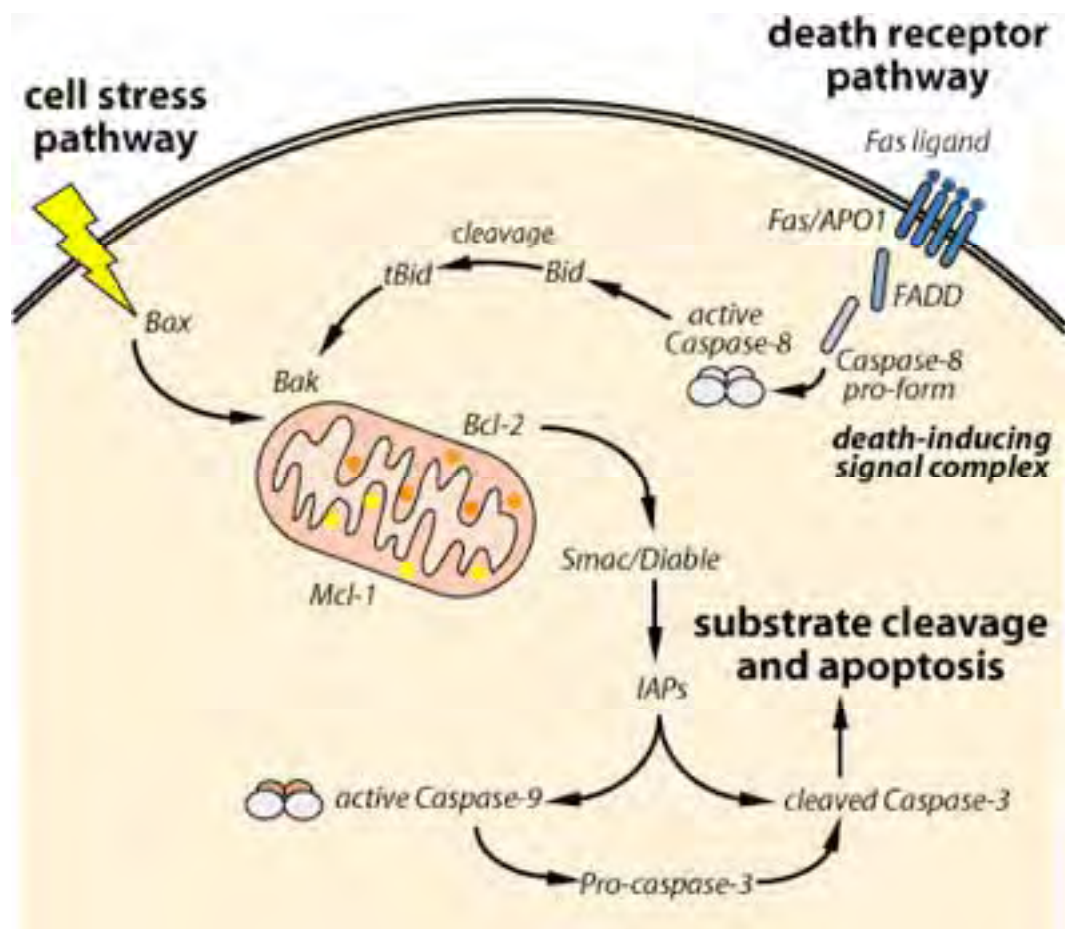


Figure 1-7 Overview of apoptotic pathways

Diagram of some of the principal intracellular pathways implicated in the mechanism of apoptosis. Apoptotic stimuli via stressors or specific receptor activation lead to a series of molecular events involving the bcl/bax family of anti- and pro-apoptotic proteins and the caspase protease cascade, in particular via caspase-3 activation. (From: Yau 2006)

1.2.3 Detecting apoptosis

The identification of apoptotic cells is central to any study of disease where cell death is thought to occur by this process. The methods for detection of such cells have been developed in parallel with the increased interest in this type of cell death, and is now a research area in its own right. The pioneering studies of Kerr and Wyllie that first noted apoptosis relied on the morphology of affected cell, whose microscopic appearance was indeed the inspiration behind the term apoptosis (Kerr, Wyllie et al. 1972). The features have been described in detail in Section 1.2.1.2. Briefly the cell shrinks initially and then becomes progressively rounded. Blebbing of the membrane is seen which proceeds to the formation of apoptotic bodies. The nuclear chromatin shows areas of condensation and eventually the whole nucleus condenses (pyknosis), before fragmenting and disintegrating (karyorrhexis) (Wyllie, Kerr et al. 1980). In neuronal cells apoptosis also demonstrates a retraction and loss of processes as the cell shrinks (Buja, Eigenbrodt et al. 1993). In adherent in vitro cultures this is also manifest ultimately as detachment from the substrate, as dead end-stage cells lift off and float freely in the culture medium (Akaike, Adachi et al. 1998).

1.2.3.1 Immunofluorescent analysis

The classical features of apoptosis are readily identifiable with light microscopy. However such an examination is labour intensive and quite subjective in nature. Remembering that apoptosis is by definition cell autonomous and multi-focal, it can be particularly difficult to distinguish an apoptotic cell from a non-apoptotic neighbour which may look very similar, particularly in the early stages of the process (Darzynkiewicz, Bedner et al. 1998). The advent of techniques derived from molecular biology however has seen an explosion in additional tools to 'see' the apoptotic cell

(Castedo, Ferri et al. 2002). The most widespread tool is by marking the apoptotic cell so that it can be readily distinguished from non-apoptotic cells (Ecker and Steiner 2004). Fluorescent dyes are used to label antibodies directed against specific apoptotic events, and are combined with fluorescent microscopy to enable immunofluorescent morphological analysis. This technique enhances morphological assessment but importantly also enables quantitative automated cellular analysis, or cytometry, of apoptotic cells (Juan and Darzynkiewicz 1998).

The DNA in condensed chromatin exhibits hyperchromasia, staining strongly with fluorescent or light absorbing dyes (Darzynkiewicz, Juan et al. 1997). The most established immunofluorescent markers make use of even more specific changes in apoptotic nuclei. Activation of endonucleases leads to preferential cleaving of DNA at the internucleosomal sections in a characteristic event of apoptosis (Wyllie, Arends et al. 1992). These products of DNA degradation are sections of defined base-pair lengths and thus generate a characteristic 'ladder' pattern in agarose gel electrophoresis (Gong, Traganos et al. 1994). Indeed these 50-kb and 300-kb DNA fragments are considered to be a hallmark of apoptosis (Arends, Morris et al. 1990; Compton 1992).

This DNA ladder formation can be identified without having to extract the DNA for electrophoresis by using an immunofluorescent label for the DNA fragments. This common method of apoptosis detection is based on in situ antibody labelling of the DNA strand breaks with biotin linked deoxynucleotides in a reaction catalysed by terminal deoxynucleotidyl transferase (TdT). An antibody linked to a fluorescent molecule such as fluorescein is then used to visualise these strand breaks. The procedure is called **TdT-mediated dUTP biotin Nick End Labelling** or the **TUNEL** method (Ben-Sasson, Sherman et al. 1995). This technique is regarded as the most specific in terms of positive labelling of apoptotic cells, and is now an established tool

(Darzynkiewicz, Juan et al. 1997; Tatton, Tezel et al. 2001; Ecker and Steiner 2004).

Membrane changes in apoptosis can also be used to identify affected cells. Viable cells have been known to maintain an asymmetric distribution of phospholipids between their inner and outer membranes (Bretscher 1972). Plasma membrane asymmetry has been found to be lost in apoptotic cells, even before disruption of the membrane integrity. One of the translocated phospholipids is phosphatidyl serine, which becomes exposed on the external surface of apoptotic cells possibly as a tag for specific recognition by macrophages and thus eventual phagocytosis (Fadok, Voelker et al. 1992). This externalisation can be labelled with a phosphatidyl serine binding protein, Annexin V, linked to a fluorescent marker (van Engeland, Ramaekers et al. 1996).

TUNEL and Annexin V are two of many markers available today. These markers are particularly useful as they cover the spectrum of apoptotic stages and also rely on different cell sites. The membrane changes have been observed to be one of the earlier changes in apoptosis (Castedo, Hirsch et al. 1996). TUNEL strand breaks by contrast appear to represent a relatively late stage in apoptosis with DNA already having been subject to endonuclease activation and fragmented as a result. Direct comparison of these two immuno-assays has confirmed this, with membrane asymmetry initiated at a time following the initial caspase activation but preceding the nuclear condensation and degradation stage (Naito, Nagashima et al. 1997; van Engeland, Nieland et al. 1998).

1.2.3.2 Apoptosis vs Necrosis

Identifying one form of cell death by necessity requires exclusion of the other. There are significant differences in the defining features of the two main modes of cell death. On the macroscopic level apoptotic tissue can appear normal with no evident abnormality, quite unlike the gross pathological changes of necrosis exemplified by the

coagulative and colliquative forms. Less dramatic are the microscopic differences in cellular morphologies (Fig. 1-6). The morphological criteria for apoptosis and necrosis are summarised in Table 1.1.

In general it can be seen that some criteria are diametrically different for the two forms of cell death, and so differentiating one from the other can be straightforward. For example the shrunken apoptotic cell compared to the swollen necrotic one, or the plasma membrane rupture in necrosis as distinct from the intact but blebbed apoptotic membrane. Other criteria however are more subtle, such as the nuclear chromatin condensation and the mitochondrial changes (Majno and Joris 1995).

Specific immunofluorescent markers are one solution, with a high degree of specificity in their detection of apoptosis. A simpler method is by the use of vital dye staining. This is based on the dye exclusion principle where an intact cell membrane is able to prevent the permealisation of a cell by a specific dye, such as propidium iodide (PI) or Hoechst blue, but a compromised cell membrane is not intact and hence allows the dye to enter the cell. Apoptotic cells maintain the integrity of their cell membranes and so do not stain with vital dyes, whereas necrotic cells with their ruptured membranes are easily distinguished by colouration by the dye, (which may also be fluorescent, eg. PI).

Table 1-1 Morphological criteria for identification of apoptosis and necrosis

<i>Apoptosis</i>	<i>Necrosis</i>
<i>Reduced cell size, rounded shape</i>	<i>Cell and nuclear swelling</i>
<i>Loss of cell processes</i>	
<i>Plasma membrane blebbing</i>	<i>Plasma membrane rupture</i>
<i>Nuclear chromatin condensation 'pyknosis'</i>	<i>Patchy chromatin condensation</i>
<i>Loss of nuclear structural features</i>	
<i>Nuclear fragmentation 'karyorrhexis'</i>	<i>DNA dissolution 'karyolysis'</i>
<i>Presence of apoptotic bodies</i>	
<i>Dilatation of the endoplasmic reticulum</i>	<i>Cytoplasm vacuolation</i>
<i>Relatively unchanged organelles</i>	<i>Mitochondrial swelling</i>
<i>Phagocytosis of cell remains (in vivo)</i>	<i>Attraction of inflammatory cells (in vivo)</i>
<i>Detachment from substrate at terminal stage (in vitro)</i>	

(Adapted from Darzynkiewicz, Bedner et al. 1998)

There can still be confounders, though strategies for circumventing these have also been developed. For example occasional DNA strand breaks in necrotic cells are detectable with TUNEL, but these are several orders of magnitude less than the staining in apoptotic nuclei (Ben-Sasson, Sherman et al. 1995; Darzynkiewicz 1998). Atypical presentations of cells for both apoptosis and necrosis have been described, and the possibility of mistaken detection can never be totally excluded.

Thus the aim of any apoptotic bioassay should be to minimise any errors in identifying apoptosis and therefore optimise its detection. Reliance on only one method of detection can magnify any confounders, and it is now acknowledged that apoptosis can be identified with better assurance when more than one technique is used (Nickells and Zack 1996). Cell morphology remains the gold standard and should always be assessed (Wyllie, Kerr et al. 1980). Use of immunofluorescent markers improves morphological inspection and detects specific biomolecular changes, and adds the possibility of objective cytometry (Darzynkiewicz and Bedner 2000). The combination of multiple methods enhances accurate apoptosis detection compared to any one method on its own (Li, Melamed et al. 1996; Darzynkiewicz, Bedner et al. 1998).

1.2.4 Apoptosis in glaucoma

The awareness that cell death is a far more sophisticated phenomenon than had been believed previously, and that techniques are available to study apoptosis at a cellular level, has spurred the development of a whole new field of cell biology. The search for apoptosis in disease led to the discovery that it was the key mode of cell loss in a host of pathologies (Majno and Joris 1995; Darzynkiewicz, Juan et al. 1997; Ecker and Steiner 2004). Among these are a spectrum of eye diseases such as certain corneal dystrophies (Helena, Baerveldt et al. 1998; Wilson and Kim 1998), cataract (Li, Kuszak et al. 1995;

Spector, Wang et al. 1995), and retinal degeneration (Adler 1996; Travis 1998). RGC loss in ocular pathology has also been demonstrated to be associated with apoptosis. This is not unexpected, since RGC apoptosis is known to be a feature of normal retinal development (Ilschner and Waring 1992). In fact the loss of RGCs is an essential element of the development of the retina, with a substantial reduction in numbers in late embryogenesis (Perry, Henderson et al. 1983; Forrester, Dick et al. 1996). It is pertinent to note that there is no evidence for the death of RGCs by necrosis in either clinical or experimental glaucoma (Osborne, Wood et al. 1999). The evidence for RGC loss in glaucoma occurring by apoptosis is based on experimental *in vivo* models of glaucoma and studies on human glaucoma patients (Nickells 1996; Quigley 1999). A brief description of these animal and human studies now follows.

1.2.4.1 Animal studies

Morphological changes of apoptosis were first noted in primate models of experimental glaucoma (Quigley and Addicks 1980). Glaucoma was induced by the elevation of IOP and damage to the RGC layer of monkey retinas ascertained. This damage was seen as pyknotic nuclei and the shrinkage of cells which then disappeared in a multi-focal fashion without any remnant. Subsequent work utilised electron microscopy for enhanced morphological assessment, combined with immunofluorescent TUNEL staining for nuclear signs of apoptosis. These observations confirmed that RGC loss was due to apoptosis (Quigley, Nickells et al. 1995).

These findings have been replicated in other species where IOP has been raised to simulate glaucoma *in vivo*. Rat models of glaucoma are among the most widely used. Apoptotic morphology including RGC shrinkage and nuclear condensation along with phagocytosis by other cells has been reported in induced glaucoma in rats (Buchi 1992).

In other experiments on rats where IOP was elevated for prolonged periods apoptosis was found by TUNEL marker staining (Shareef, Garcia-Valenzuela et al. 1995; Laquis, Chaudhary et al. 1998). RGC apoptosis in similar models of experimental glaucoma continues to be documented by several laboratories around the world in rats (Garcia-Valenzuela, Shareef et al. 1995; Kanamori, Nakamura et al. 2004; Kim and Park 2005) Oka, Tamada et al. 2006) and in mice (Zhou, Li et al. 2005; Harada, Nakamura et al. 2006).

Another method of simulating glaucomatous optic neuropathy in vivo is directed to the optic nerve itself with transection of the nerve. These models have also shown RGC death by apoptosis. The study into primates also used this method and confirmed TUNEL positive apoptosis in RGCs following axotomy (Quigley, Nickells et al. 1995). Similar observations have also been made in rabbits (Quigley, Nickells et al. 1995) and in rats (Berkelaar, Clarke et al. 1994; Garcia-Valenzuela, Gorczyca et al. 1994; Levkovitch-Verbin, Dardik et al. 2006; Levkovitch-Verbin, Kalev-Landoy et al. 2006).

1.2.4.2 Human studies

Research into the mechanism of RGC death in patients with glaucoma has been carried in order to define this process and possibly confirm the results of animal experiments. Thus special attention has been paid to the presence of apoptosis. Though clearly reliant on surgically removed or post-mortem eyes, the identification of apoptosis nonetheless is based on the same criteria as in laboratory studies. Interestingly different types of human glaucoma have been investigated to try to determine any variations in the pathological processes.

The first report of apoptosis in human glaucoma was by Kerrigan et al. who studied donated eyes from 17 patients with documented primary open angle glaucoma as well

as eyes from 21 matched control subjects that were disease free (Kerrigan, Zack et al. 1997). They found apoptosis by TUNEL marker analysis to detect DNA fragmentation in glaucomatous eyes at over 15 times the frequency of control eyes, suggesting apoptosis as a mechanism of cell death. Another study examined eyes from patients with secondary glaucoma, and found apoptosis by TUNEL as well as by morphological criteria (Okisaka, Murakami et al. 1997). These researchers also noted the presence of apoptosis in RGCs as a result of ageing, with tissue from a 95 year old patient confirming the role of senescence as a stimulus for apoptosis. Another type of glaucoma, normal tension or 'low-pressure' glaucoma has also been studied. RGC apoptosis was detected by combining morphology and immunofluorescent staining for DNA strand breaks (similar to the TUNEL method) (Tatton, Tezel et al. 2001). TUNEL labelling has also been reported in the retina of a patient with anterior ischaemic neuropathy, indicating that apoptosis may be the mechanism of cell death in optic neuropathies other than glaucoma (Levin and Louhab 1996).

Subsequent research has not only provided further evidence for the apoptosis of RGCs in human glaucoma, but is now increasing our knowledge of this process by investigating specific aspects of apoptosis. For example genetic aspects have been studied by examining mitochondrial function in RGC apoptosis (Abu-Amero, Morales et al. 2006). The apoptosis regulatory protein p53 has been analysed in open angle and normal tension glaucoma (Dimasi, Hewitt et al. 2005). As the pathways of apoptosis have been better defined more regulatory genes and proteins have been identified, and these have been studied in combined epidemiological and genetic studies (Ressiniotis, Griffiths et al. 2005). Novel stimuli of RGC apoptosis implicated in glaucoma, such as heat shock protein hsp27, have been studied in human retinae (Tezel and Wax 2000).

One of the most innovative approaches to studying RGC apoptosis that holds great promise for human glaucoma research is the development of real-time imaging of nerve cell apoptosis *in vivo*. This is a confocal laser-scanning ophthalmoscope based technique which can visualise single RGCs in the retina and has already shown apoptosis in primate models of neurodegenerative retinal disease (Cordeiro, Guo et al. 2004). The potential for imaging patients for apoptosis may provide an unprecedented link between a basic science investigation and its clinical application. The study of the mechanism of cell death in human glaucoma provides novel avenues for understanding different aspects of its pathogenesis (Nickells 1999; Kuehn, Fingert et al. 2005).

1.3 Pathogenesis of glaucoma

The understanding of the mode of the origin and development of a disease is termed its pathogenesis (Critchley 1984). The pathogenesis of glaucoma then must explain the mechanism of RGC loss. Specifically it seeks to explore how elevated hydrostatic pressure in the eye, the major risk factor, damages RGCs and leads to their apoptosis (Palmberg and Wiggs 1999).

1.3.1 Historical perspective

The concept of what causes glaucoma has changed dramatically over the ages. In antiquity ‘glaukosis’ was used to describe the appearance of an eye which had a bluish hue, but this was not specific to the condition we now call glaucoma. It also applied to cataract, and indeed it was assumed that glaucoma and cataract were identical (Blodi 2000). The first association with a rise in eye pressure was made in the Arabian writings “Book of Hippocratic treatment” of At-Tabari in the 10th century AD (Mantzioris 2006).

In Europe it was not until the 17th century that the first clear recognition of increased ‘eye tension’ was made in the first book of ophthalmology written in English by Bannister in 1622. This was not stressed as a key feature of the disease however until the 19th century (Mantzioris 2006).

In 1823 Guthrie noted hardness of the eye as a characteristic of a disease he called ‘glaucoma’, and McKenzie first wrote in his classic textbook of 1835 of raised tension as being the essential feature of the disease in both acute and chronic forms (Mantzioris 2006). Only with the invention of the ophthalmoscope by Helmholtz in 1850 was it at last possible to observe the changes in the optic disc associated with glaucoma (Duke-Elder 1941). The term pressure excavation was coined by von Graefe, and the hypothesis of glaucoma as an optic nerve disease developed by pathologic examinations of Muller (Blodi 2000).

The final unifying concept was made by Donders in 1862 when he described an incapacitating increased eye tension devoid of inflammation as ‘Simple Glaucoma’, what we now call common primary open angle glaucoma (Mantzioris 2006). The last century has seen further refinement in the understanding of this condition culminating in Drance’s description of glaucoma as a disease of the optic nerve (ie. an optic neuropathy) caused by numerous risk factors, principally elevated IOP (Drance 1973).

1.3.2 Conventional theories

There are two principal theories that have been promulgated and have formed the basis of much of the discussion regarding glaucoma pathogenesis: the mechanical theory of axonal injury and the vascular theory of optic nerve head ischaemia. The concept of excitotoxicity has also gained credence as a potential mechanism.

1.3.2.1 Mechanical theory

According to this theory a pressure-related injury damages RGC axons at the level of the optic nerve head. The axons are effectively compressed by the collagenous cross beams of the lamina cribrosa resulting in the blockage of axoplasmic transport and the subsequent death of the RGC (Quigley, Flower et al. 1980). This concept is based on this perceived site of RGC damage, and is supported by clinical observation as well as extensive experimental work.

At the outset it is important to recall that one of the few absolute features of glaucoma, and hence a defining hallmark of the disease, is the excavation of the optic nerve head. This has long suggested an insult to the RGC axons, which make up the bulk of the optic nerve as a whole, and of the optic nerve head in particular. The first experimental support for the idea that the axon is the site of injury came from Anderson studying a primate model of glaucoma (Anderson and Hendrickson 1974). They demonstrated blockage of retrograde (toward the cell body) axonal transport in RGCs at the level of the sclera in the optic nerve head using radioactive probes. Subsequent research refined the site of transport interruption to the collagenous cross beams of the lamina cribrosa (Quigley and Anderson 1977; Quigley and Addicks 1980).

The disruption to RGC axons is thought to be mediated by the anatomical peculiarities of this specialised region of the optic nerve. In this theory then pressure elevation induces backward bowing of the lamina cribrosa resulting in mis-alignment of the holes through which RGC axons pass (Quigley and Addicks 1981). As a result transiting axons are literally pinched off and axoplasmic flow is blocked (Minckler, Bunt et al. 1977). The deformation of collagen beams can be attributed to their microanatomy, including local variations in elasticity and collagen subtypes (Morrison

1995). The characteristic excavation of the optic nerve head is also thought to relate to the details of the structure of this region, including connective tissue components (Quigley 1995; Bellezza, Hart et al. 2000).

Supporting this concept of axonal compression is the observation that larger diameter pores in the upper and lower poles of the optic nerve head may correspond to weaker lamina cribrosa support for axons and hence greater vulnerability to misalignment (Quigley and Addicks 1981). This correlates with the clinical finding that these regions of the optic disc are the most common sites of NFL loss and corresponding visual field defects (Smith and Doyle 1999).

In this paradigm RGCs are lost due to an obstruction to transport along the axon. The axoplasmic flow that results in this cell death is retrograde, from the peripheral terminals of the optic nerve located in the lateral geniculate region of the brain toward the cell body. Such a blockade has been shown in other nerves in animal models to block the return of trophic factors to the cell body and thus stimulate the cell into apoptosis (Palmberg and Wiggs 1999). This retrograde neuronal degeneration has been demonstrated in animal models of glaucoma too, similarly attributed to the cell body being deprived of 'target-derived' trophic factors (Rudzinski, Wong et al. 2004). Transection of the optic nerve for example has resulted in dramatic losses of RGCs in the retinae of cats (Silveira, Russelakis-Carneiro et al. 1994), rats (Berkelaar, Clarke et al. 1994; Garcia-Valenzuela, Gorczyca et al. 1994; Levkovitch-Verbin, Kalev-Landoy et al. 2006) and mice (Bonfanti, Strettoi et al. 1996). Animal models of glaucoma using elevated IOP have also shown retrograde RGC loss (Minckler, Bunt et al. 1977; Burke, Cottee et al. 1986; Li, Schlamp et al. 1999).

As a corollary to the induction of apoptosis by trophic factor withdrawal there is experimental data to suggest that this effect can be at least partially prevented by the

administering these factors onto the retina via the vitreous cavity. Large doses of putative trophic factors have been injected intra-vitreally in animal glaucoma models and found to mitigate the effects of axonal transport interruption. Tested factors include fibroblast growth factor (Sievers, Hausmann et al. 1987), nerve growth factor (Carmignoto, Maffei et al. 1989) and brain derived growth factor (Pease, McKinnon et al. 2000).

1.3.2.2 Vascular theory

This theory maintains that in glaucoma the optic nerve head undergoes a chronic ischaemic injury. Raised IOP interferes with the blood supply of this region and as a result RGCs suffer hypoxic damage which can act as an apoptotic stimulus in its own right (Palmberg and Wiggs 1999). Evidence for this mechanism again derives from clinical observations and experimental research.

Alterations in the blood flow of the optic nerve head in glaucoma patients have been reported by several workers (Chung, Harris et al. 1999; Flammer and Orgul 1998; Prunte, Orgul et al. 1998; Plange, Kaup et al. 2004). Interestingly clinical studies also provide substantial evidence of retinal blood flow abnormalities in the eyes of persons with glaucoma (Wolf, Arend et al. 1995; Arend, Plange et al. 2004; Huber, Plange et al. 2004). In addition some types of glaucoma, most notably normal tension glaucoma, have an association with systemic conditions which impair blood flow (Hitchings 1999). These include nocturnal hypotension, Raynaud's disease and migraine, the latter two being marked by vasoconstriction of blood vessels. These suggest the possibility of vascular incompetence affecting RGCs (Osborne, Ugarte et al. 1999).

Aspects of the optic disc appearance in normal tension glaucoma have also lent support to the vascular theory. The occurrence of scleral crescents adjacent to the optic disc have been noted to be four times more likely in patients with normal tension

glaucoma, and twice as frequent in those with primary open angle glaucoma, than in matched controls (Buus and Anderson 1989). These crescents are areas of retinal and choroidal atrophy and represent enlarged versions of an otherwise normal defect in the blood-retinal barrier. This would allow normally confined vasoactive agents to travel from the blood to RGCs in the adjacent optic nerve head.

Thus substances such as noradrenaline and angiotensin could reach receptors on pericytes and capillaries of the optic nerve head, which is not the case elsewhere in the retina (Anderson 1996). This is supported by the observation that the addition of angiotensin can augment axonal transport blockade in an animal model of glaucoma (Sossi and Anderson 1983). Angiotensin delivered directly to the vitreous of the animal model also results in vasoconstriction of retinal blood vessels and alters pericyte autoregulation (Matsugi, Chen et al. 1997).

Other corroborative data comes from animal models where the blood supply of the optic nerve head is deliberately compromised. These ischaemic models of experimental glaucoma have been shown to induce RGC loss similar to that in other animal models such as optic nerve transection. These studies have been performed in primates (Levy and Adams 1975), rabbits (Kaskel, Valenzuela et al. 1976) and extensively in rats (Adachi, Takahashi et al. 1996; Selles-Navarro, Villegas-Perez et al. 1996; Geyer, Almog et al. 1995; Kuroiwa, Katai et al. 1998; Crisanti, Laplace et al. 2006).

1.3.2.3 Excitotoxicity theory

Excitotoxicity describes a process of neuronal death due to the prolonged or excessive activation of receptors for excitatory amino acids neurotransmitters (Olney and Sharpe 1969). This was originally found in brain lesions and has been shown to play a role in the pathogenesis of neurological disease (Doble 1999). Excitotoxicity has

since been demonstrated in neurons in the retina, and there is evidence that excessive extracellular levels of the neurotransmitter glutamate are toxic to RGCs (Casson 2006).

Glutamate is the major excitatory neurotransmitter in the central nervous system and is normally present in the retina. Elevated levels are thought to injure neurons by overstimulation of membrane bound receptors, such as the N-methyl-D-aspartate (NMDA) glutamate receptor. This generates a cascade of events involving Ca^{++} channels, resulting in the influx of this ubiquitous intracellular messenger and elevated levels within the cell, which in turn induces apoptosis (Sucher, Lipton et al. 1997). Another proposed consequence of this ionic imbalance is disturbance of the intracellular redox system. This results in the release of nitric oxide (NO) which acts as a free radical and combines with reactive oxygen species (ROS) causing oxidative damage to the cell. This is also a trigger for apoptosis (Maher and Hanneken 2005).

Glutamate levels were first reported to be elevated in the vitreous of eyes from both clinical and experimental glaucoma (Dreyer, Zurakowski et al. 1996; Vorwerk, Lipton et al. 1996), and this subsequently led to the development of the excitotoxicity theory (Dreyer 1998). Experimental ischaemic injury to the optic nerve and the retina was known to be attenuated by glutamate receptor blockade (Lam, Siew et al. 1997; Lam, Siew et al. 1997). Thus glutamate toxicity was seen to complement the vascular theory based on ischaemia (Casson 2006).

Excitotoxicity has also been proposed as an explanation for another experimental finding from animal models of glaucoma. Secondary degeneration refers to the delayed loss of RGCs after optic nerve crush injury (Yoles, Muller et al. 1997). This is especially evident following partial transection of the optic nerve, where RGCs that are outside the region of axotomy subsequently die (Levkovitch-Verbin, Quigley et al. 2003). The release of excitatory neurotransmitters by injured RGCs or the activation of

related biochemical cascades appears to be responsible for this delayed apoptosis. This is supported by studies indicating that RGC loss is reduced by glutamate NMDA receptor antagonists (Yoles, Muller et al. 1997; Yoles, Wheeler et al. 1999).

Further evidence has been obtained from other work carried out to attenuate experimental glaucoma using NMDA receptor blockers. The well studied agent MK-801 has proven effective in combating glutamate toxicity in primates (Hare, WoldeMussie et al. 2004) and in rat models (el-Asrar, Morse et al. 1992; Lam, Siew et al. 1997). These results have led to the study of agents with potential clinical application, most notably the NMDA receptor antagonist, Memantine, which is currently in clinical trials (Levin 1999; Casson 2006). The intent of such therapy is to prevent the apoptosis of neurons that have escaped the initial apoptotic stimulus, an approach known as neuroprotection (Kuehn, Fingert et al. 2005; Levin 2005).

1.3.3 Critique of conventional theories

The mechanical and vascular theories have competed for supremacy for almost 150 years (Casson 2006), at times polarising the debate and generating passionate arguments amongst their respective proponents (Drance 1995). Excitotoxicity has added to the discussion in the last decade, and these theories continue to dominate the field and research efforts, even in the age of molecular biology. Despite this the pathogenesis of glaucoma remains unclear and controversial (Osborne, Wood et al. 1999; Palmberg and Wiggs 1999; Burgoyne, Crawford Downs et al. 2005; Casson 2006). The precise nature of these mechanisms is undetermined, and observational findings have not been fully explained for any of the theories. There is a sizable quantum of clinical and experimental work that provides evidence that appears to contradict these conventional approaches to glaucoma pathogenesis. This work is summarised below.

1.3.3.1 Critique of mechanical theory

The mechanical theory is in many respects the most established, with a clear anatomical basis that correlates well with clinical findings and has extensive research support (Quigley 1999). Nevertheless there are inconsistencies in this theory that have emerged. These extend to the anatomical basis for the concept, centred on the lamina cribrosa as the cause for axonal compression.

In a series of studies Radius used a monkey model of experimental glaucoma with increased IOP and transmission electron microscopy to examine the interruption of axonal transport in the optic nerve (Radius 1981). He found diffuse involvement of affected RGC axons across an axonal bundle, with centrally placed axons as susceptible as peripheral ones. This contradicted the association of blockage with crosswise oriented beams of the lamina cribrosa, and "...fails to support the notion that blocked axonal transport with elevated pressure is produced by kinking of axons at the lamina cribrosa..." (Radius 1981). A cat model for glaucoma with even higher IOPs was subsequently studied, measuring the dimensions of axonal pores within the lamina cribrosa and associated axonal transport interruption assessed by radioactive labels. Once again there was no correlation between the location of the axonal blockage and any anatomical measurements (Radius 1982).

Anatomical inconsistencies are also raised by clinical observations. Pathological studies have shown that the lamina cribrosa becomes increasingly rigid with age as collagen cross-linking strengthens the cross beams (Anderson and Quigley 1999). This should make them less susceptible to the deformation that is characteristic of a glaucomatous optic disc, and hence to the misalignment of the pores thought to kink the axons. However it is well known that age is a significant risk factor for the development of glaucoma, and that the young optic nerve head is far less likely to have optic nerve

damage due to pressure (Drance 1995). This would appear contrary to the proposal that the earliest affected region of the optic disc, the vertical poles, are susceptible due to weaker support in the optic nerve head for axons (Palmberg and Wiggs 1999).

There are also questions surrounding the loss of trophic factors, a key tenet of the mechanical theory. Much of the experimental data supporting this is derived from indirect evidence from exogenous administration of growth factors in in vitro models (McCaffery, Bennett et al. 1982; Cohen, Bray et al. 1994; Meyer-Franke, Kaplan et al. 1995). Experiments involving even the most dramatic form of axonal transport interruption, transection of the optic nerve, suggests that this is not fully responsible for RGC apoptosis. In a rat model RGC apoptosis was assessed morphologically following optic nerve axotomy and also following a reversible transport block induced by local anaesthetic (Fagiolini, Caleo et al. 1997). The pharmacologic blockage induced significantly less apoptosis compared to physical transection, suggesting factors other than trophic supply may be involved in glaucomatous RGC injury. Other research indicates that chronic partial physiologic obstruction to axoplasmic flow is present at normal IOPs in a range of mammals, from rats to humans, and is not associated with any anatomical abnormality of the lamina cribrosa (Hollander, Makarov et al. 1995).

Johansson also contradicts the mechanical theory in an elegant study where he controlled for any contribution of axonal kinking (Johansson 1983). Inbred hooded rats were used in an animal model of glaucoma in which their optic nerve heads were first studied by electron microscopy. This revealed a lamina cribrosa comprised of single complete collagenous sheet, thus minimising axonal compression by the misalignment of holes in a multilayered lamina cribrosa. Experimental glaucoma was then induced by increasing the IOP, and retinal levels measured of a retrograde dye injected into the lateral geniculate body (the terminus of the optic nerve). At increases of IOP of 35 mm

Hg to 50 mmHg retrograde transport of the dye was inhibited in a pressure dependant manner (Johansson 1983). The axonal compromise was thus independent of any mechanical effect, and this was later confirmed in further in vivo work (Johansson 1988).

1.3.3.2 Critique of vascular theory

The role of ischaemia in the pathogenesis of glaucoma is grounded in both clinical and experimental research. Once again however observations reported in the literature appear to contradict this hypothesis.

Anatomic features of the optic nerve head have been considered in relation to the potential for vascular insufficiency to cause pressure induced RGC loss. In parallel with mechanical studies on the lamina cribrosa, there have been studies on the distribution of optic nerve fibre loss within the axonal bundles (Minckler 1986). They indicated that RGC loss occurred initially furthest from the capillaries and attendant blood supply of the optic nerve, which runs contrary to an ischaemic mechanism of injury. This lack of correlation between the loss of RGC axons and the loss of capillary blood vessels in glaucoma has been commented on extensively (Quigley 1999). In both human and experimental primate models of glaucoma, for example, the number of capillaries affected by reduced perfusion is only in proportion to the RGC loss and has not been shown to precede it, raising the possibility that this is an effect of glaucoma rather than a cause of it (Quigley, Hohman et al. 1984).

Experimental models of glaucoma have also suggested a lesser role for vascular factors. In primate models of glaucoma with elevated IOP in both acute and chronic settings the delivery of diffusible molecules and metabolic nutrition was assessed (Quigley, Hohman et al. 1985). No decrease in these markers of vascular function was

seen in chronic pressure elevation, and in the acute simulated glaucoma impairment was only observed with very high IOPs over 75 mmHg. Other studies in similar primate models raised IOP with the production of typical glaucomatous RGC loss, but without any detectable alteration in blood flow, even at the level of the neuronal bundle (Sperber and Bill 1985).

The study by Johansson referred to in the last section also examined the vascular theory (Johansson 1983). The globe-optic nerve complex was excised from anaesthetised rats and then promptly subject to IOP elevation *in vitro* to simulate glaucoma. Retrograde dye labelling of RGCs was again used to assess the viability of RGCs at increase pressure. The results showed an inhibition of axoplasmic transport that varied in a dose-dependant manner with the magnitude of IOP elevation. Since the glaucoma had been induced effectively in an organ culture, the contribution of the optic nerve head circulation was insignificant and the vascular mechanism excluded from the induced RGC loss.

1.3.3.3 Critique of excitotoxicity

The newest of the prevailing theories has its basis in the biomolecular physiology of neurons. It also provides complementary support for the vascular theory as the dispersal of neurotransmitters is circulation dependant. Further, this concept has already resulted in the development of potential novel therapies for glaucoma in the form of neuroprotectants. There are however discordant notes with respect to this approach.

The evidence for excitotoxicity as a mechanism for RGC death in glaucoma remains circumstantial and speculative (Casson 2006). The findings of increased levels of the neurotransmitter glutamate has been difficult to corroborate in the eyes of glaucoma patients (Honkanen, Baruah et al. 2003) and in animal models (Wamsley, Gabelt et al.

2005). The precise molecular mechanisms which would mediate glutamate toxicity remain unclear (Quigley 1999). In the context of secondary degeneration, for example, exactly how neurotransmitter release would come to affect non-contiguous axons in the optic nerve post injury is unknown (Levkovitch-Verbin, Quigley et al. 2003).

Another key concern is raised by the very agents being studied for their potential neuroprotective properties. Glutamate receptors like the NMDA receptors are the proposed vector for the success of MK-801 and similar antagonists in attenuating the RGC loss attributed to excitotoxicity. However there is no evidence for the existence of NMDA receptors at the level of the axons in the optic nerve head, the presumed site of injury (Casson 2006). Thus the means whereby glutamate toxicity causes RGC death remains a mystery.

1.3.4 Toward a new paradigm

The understanding of how and why glaucoma occurs thus continues to be the subject of debate. The concepts being assessed are not static but rather have evolved over time and doubtless shall continue to do so. Given the depth of evidence for several competing theories, what then do we make of its pathogenesis? How do we reconcile apparently contradictory observations?

In many areas of medicine, causation and effect is increasingly recognised as more complex than previously thought. Once simple and isolated ideas of disease aetiology are being supplanted as knowledge of a pathological condition grows by concepts that embrace multiple factors (Kasper 2006). Glaucoma is no exception. The answer to what constitutes glaucoma pathogenesis can lie in several areas, such that no single hypothesis can explain the totality of the disease (Brubaker 1996; Nickells 1996;

Kuehn, Fingert et al. 2005).

Concepts of glaucoma pathogenesis are now emerging that seek to provide a framework for such multiple pathophysiologies in glaucoma. One of the most interesting of these is based on a bio-engineering approach, using sophisticated computer modelling of the optic nerve head to analyse the effects of hydrostatic pressure (Bellezza, Hart et al. 2000). What has emerged is a proposed new paradigm which addresses the principal theories of pathogenesis and analyses them by biomechanical principles in concert with physiology and microanatomy. For instance, the clinical appearance of optic disc excavation, a hallmark defining characteristic of glaucoma, may not reflect the mechanism of injury (Burgoyne, Crawford Downs et al. 2005). Rather this can be shown to be the result of the relative involvement of separate but related components of the optic nerve head, such as the neural, connective tissue and even the age of these elements. Inherent in this pioneering approach is the acceptance of plural complementary theories in glaucoma pathogenesis.

The implications of this are profound. The site of injury in glaucoma was considered the unique province of one theory or another, located at the lamina cribrosa in the mechanical theory, or deriving from the blood vessels in the vascular theory. The contradictions in the literature outlined in the preceding critiques could be explained by accepting that elements of more than one mechanism apply. Further, the real possibility of other sites of RGC damage would be equally valid conjectures in view of discrepancies in the conventional theories (Nickells 1996; Casson 2006).

There is evidence that retinal photoreceptors may be susceptible to pressure related injury (Wyganski, Desatnik et al. 1995; Nork, Ver Hoeve et al. 2000; Nork 2000). Separate pathophysiologies may be relevant in the RGC target region of the brain, the lateral geniculate nucleus (Gupta and Yucel 2001; Yucel, Zhang et al. 2001). These

suggest that glaucoma may be more than just a disease of the white matter which is the conventional thinking, and may affect cell bodies. Substantial evidence from the vascular theory indicating abnormal blood flow in the retina is another interesting finding, which implies that the RGCs may also be primarily affected at the level of the cell body (Casson 2006). Further, Johansson's elegant experiments clearly points to a non-vascular and non-axonal kinking component to RGC injury, and a more directly mediated mechanism of pressure related damage was suggested (Johansson 1983; Johansson 1988). Indeed, the inability to fully explain glaucoma suggests that all aspects of pressure related injury are worthy of exploration, and the possibility for glaucoma pathogenesis to involve the cell body needs to be considered (Nickells 1996) (Casson 2006).

1.4 Pressure effects on cells

Pressure is a crucial component of the cellular environment. At the most fundamental level, it is the physical quantity controlling the mean distance between molecules, and hence knowledge of its role is central to our understanding of cell biology (Takano, Takano et al. 1997; Ashcroft 2000). Pressure has a major impact on cell function and viability. This is self-evident in pathologies that are the result of this variable exceeding physiologically safe limits, which can be grouped under the term 'baropathies' (Kalapesi, Coroneo et al. 2005). Glaucoma is a classic example of such a pressure related disorder.

Mechanical forces that can affect cells, be they in isolation or as part of a tissue, can present in several forms. These can be externally applied forces, such as compression,

torsion, vibration, tensile shear and stress and hydrostatic pressure, or arise from within the cell as osmotic pressure and swelling (Tan, Kalapesi et al. 2006). In the context of glaucoma the pressure is mediated through a liquid medium, viz. aqueous and vitreous, and is hence termed hydrostatic pressure (Critchley 1984). Hydrostatic pressure has been the subject of considerable study into the interaction between this key element of the environment and living organisms (Landau 1965; Somero 1991).

1.4.1 Historical perspective

The study of the relationship of pressure to biological systems dates from early work into deep sea life. Depths of 1000 m or more are thought to apply to over 90% of the ocean floor, which translates to hydrostatic pressures of over 100 atmospheres (atm). One atm is defined as the pressure at sea level and equals 760 mmHg, so this depth equates to 7.6×10^4 mmHg. Studies undertaken during the period of deep sea exploration of the 19th century discovered living organisms at 6000 m (4.5×10^5 mmHg) ((Ashcroft 2000). In the 1970s micro-organisms were found in the deepest part of the ocean floor, the Mariana Trench in the Pacific, at 11000 m or over 1100 atm (Yayanos, Dietz et al. 1981).

The discovery of complete ecosystems surviving at hydrostatic pressures previously believed to be incompatible with life stimulated intense scientific interest. A new classification of organisms termed baroduric or barophilic emerged to describe these lifeforms, and research into pressure effects in biology was dominated by work into deep sea bacteria (Zobell and Morita 1957; Somero 1991; Takami, Inoue et al. 1997). Laboratory studies into the effects of hydrostatic pressure also began with the investigation of micro-organisms. These studies established that various aspects of cellular physiology were susceptible to pressure, including protein function (Johnson

and Wright 1946), enzyme activity (Holyoke and Johnson 1951) and the biosynthesis of macromolecules (Landau 1967; Scheck and Landau 1982). Morphological alterations have also been noted (Zobell and Oppenheimer 1950) Landau 1965) as have changes in cell division (Zimmerman, Landau et al. 1957) and growth (Strehler and Johnson 1954; McMahon and Landau 1983).

1.4.2 Types of pressure effects

Current knowledge of the impact of pressure on cells extends to biomedical research in many animal species and in man. The breadth of cellular processes that respond to pressure includes most aspects of cell form and function, and many have been characterised from in vitro studies. Baropathies studied include hypertension, cardiac failure, renal disease, prostate hyperplasia and bone and cartilage deformation (Harris, Haralson et al. 1992; Urban 1994; Hegarty, Watson et al. 2002). The effects of pressure on cell biology are summarised below.

1.4.2.1 Cell growth and proliferation

Hydrostatic pressure has been shown to directly affect several cell types. Research into *E.Coli* subjected to elevated pressure in vitro found changes related to the phase of the cell cycle, and also implications for cell death (Manas and Mackey 2004). In studies into the pathogenesis of renal hypertension human glomerular mesangial cell cultures were subjected to increased pressures of 50 mmHg in an in vitro pressure chamber model (Mattana and Singhal 1995). Cell proliferation was inhibited but with increased synthesis of cell matrix. Another report suggests changes in DNA synthesis, and similar proliferative inhibition (Mertens, Espenkott et al. 1998).

Rat vascular endothelial cells have been studied in relation to systemic hypertension in a similar model. In contrast to mesangial cells increased hydrostatic pressures of

between 40 mmHg to 120 mmHg was shown to enhance proliferation (Sumpio, Widmann et al. 1994). In terms of neuronal tissue, astrocytoma cells exposed to hydrostatic pressures of 60 mmHg to 120 mmHg responded with increased DNA synthesis and proliferation (Oishi, Uezono et al. 1998).

In many cell types the growth and division of cells has also been demonstrated to be influenced by other forms of mechanical stimuli in vitro. Shear stress applied to vascular endothelial cells results in a transient increase in early growth response in mRNA expression and thus increased proliferation (Chiu, Wung et al. 1999). In stretched myoblast cells DNA content is increased, a response which was independent of levels of growth factors and so attributable to stretch alone (Vandeburgh, Hatfaludy et al. 1989). Proliferation was found to be increased in response to cyclical stretch in rat aortic smooth muscle cells (Standley, Obards et al. 1999) and in glomerular mesangial cells (Harris, Haralson et al. 1992). Laboratory models of benign prostatic hypertension looking at both stromal and epithelial cells also suggest enhanced proliferation (Hegarty, Watson et al. 2004). Cartilage and disc tissue growth has similarly been increased after pressure (Urban 1994).

1.4.2.2 Cell morphology

Elevated pressure alters morphology in different ways according to the type of cell (Manas and Mackey 2004; Landau and McAlear 1961), often reflecting their embryological layer of origin (Hegarty, Watson et al. 2004). Hydrostatic pressure applied to human chondrocyte cultures causes rounding of cells and disruption of cytoskeletal elements (Haskin, Athanasiou et al. 1993). Endothelial cells in pressure chamber models exhibit elongation in a dose dependant fashion and redistribute their actin filaments (Ives, Eskin et al. 1986; Sumpio, Widmann et al. 1994).

In response to flow induced shear stress aortic endothelial cells also elongate, and in addition align their long axes and microtubules perpendicular to the direction of flow (Ives, Eskin et al. 1986). This reorientation to flow stress is also seen in other vascular elements such as aortic smooth muscle cells (Dartsch and Hammerle 1986), and cardiac myocytes (Terracio, Miller et al. 1988). Stromal cells from patients with prostatic hyperplasia show smooth muscle like contractility (Hegarty, Watson et al. 2004). Chondrocytes reorganised stress fibres and the appearance of the Golgi apparatus altered was after hydrostatic pressure elevation (Parkkinen, Lammi et al. 1995).

Studies into carpal tunnel syndrome simulating the compression experienced by the median nerve have been reported. Pressures of just 30 mmHg on rabbit vagus nerves have been demonstrated to disperse Nissl substance in the cytoplasm and reduce the nuclear volume (Dahlin, Nordborg et al. 1987). There was also an inhibition of axonal transport. This is significant as these were changes in the nerve cell body as a result of axonal compression, not dissimilar to the mechanical theory in glaucoma but manifesting much more proximally.

Morphological changes from hydrostatic pressure in the eye have also been reported. Porcine trabecular meshwork cells were subjected to 15 mmHg to 50 mmHg in a pressure chamber. Cell elongation, reduction of intercellular spaces and a doubling in contractility was found (Qian, Tripathi et al. 1999).

1.4.2.3 *Protein synthesis*

Protein synthesis is a useful indicator of cell function as the products can be measured and variations due to particular stimuli quantified. Research into micro-organisms has shown that hydrostatic pressure has differential effects on some of the processes involved in the biosynthesis of macromolecules (Schwarz and Landau 1972).

In the bacterium *E.Coli* for example pressure reduces nucleic acid synthesis and the incorporation of certain amino acids into protein (Landau 1966), as well as affecting protein translation (Landau 1967; McMahon and Landau 1983).

Studies on rat arteries subjected to hydrostatic pressures of 90 mmHg to 120 mmHg found induction of *c-fos* proto-oncogene expression and rRNA production (Allen, Liang et al. 1996). Similar results were obtained with human saphenous veins (Galea, Armstrong et al. 1999). Renal mesangial cells showed increased synthesis of collagen and cell matrix proteins in pressure chamber models (Mertens, Espenkott et al. 1998; Mattana and Singhal 1995). Prostatic epithelial cells increase the production of TGF- β in response to stretch (Hegarty, Watson et al. 2002).

Cartilage responds to hydrostatic pressure elevation by the synthesis of heat shock protein which may help repair damaged cytoskeleton (Haskin, Athanasiou et al. 1993). The synthesis of proteoglycans is enhanced by compression of chondrocytes while some production of other proteins is inhibited at high pressures (Urban 1994). These cells also show increased collagen synthesis from work into post-operative human tissue explants (Smith, Rusk et al. 1996). After a compressive load cycle osteoblasts produce more prostaglandin (Somjen, Binderman et al. 1980) and new bone formation increases (Skerry, Bitensky et al. 1988).

Trabecular meshwork cells from the human eye respond to cyclic mechanical stretch by increasing the production of prostaglandin (Matsuo, Uchida et al. 1996) as well as that of matrix metalloproteinase (MMP) (Okada, Matsuo et al. 1998) and myocillin (Tamm, Russell et al. 1999). A similar stimulus applied to rat retinal pigment epithelium culture demonstrated increased expression and secretion of vascular endothelial growth factor (VEGF) (Seko, Fujikura et al. 1999). Human lamina cribrosa cells subject to hydrostatic pressure elevation modulate synthesis and secretion of

collagen matrix macromolecules (Yang, Neufeld et al. 1993). In cultures of human optic nerve head astrocytes hydrostatic pressure increased the synthesis of fibrillin (Pena, Mello et al. 2000) and elastin (Pena, Agapova et al. 2001; Hernandez, Pena et al. 2000).

1.4.2.4 Cell activity

Cellular functions vary with cell type and the physiological mechanisms that mediate these activities are also responsive to pressure changes. Cardiac myocytes in patients with heart failure associated with chronic pressure overload have been found to have increased intracellular Ca^{++} levels which may mediate the cellular damage (Bing 1994). These muscle cells also respond to hydrostatic pressure by displaying increased excitability and a prolongation of their refractory period. Experiments with high hydrostatic pressures showed altered membrane permeability in human erythrocytes (Hall and Ellory 1986).

Membrane changes are also seen in chondrocytes after pressure stimuli, with hyperpolarisation and the activation of Ca^{++} dependant K^{+} channels (Wright, Jobanputra et al. 1996). Another study on chondrocytes showed inhibition of membrane transport after pressure, along with reduced cell exocytosis (Urban 1994). The most dramatic membrane sensitivity to pressure is seen in cells whose activity is highly dependant on this structure, namely neurons.

Studies have been undertaken into the electrophysiology of neural cells in the in vitro setting of elevated hydrostatic pressure. Work on rat hippocampal slices subject to hydrostatic pressure elevations found reduced conductance of ion channels and electrical activity (Southan and Wann 1996). Lowered calcium currents have also been reported from chromaffin cells (Heinemann, Conti et al. 1987), and in the brain (Gilman, Kumaroo et al. 1986). Reduced neurotransmitter release due to hydrostatic

pressure elevation has been found in spinal cord neurons (Gilman, Colton et al. 1987) and in cerebral cortical neurons (Gilman, Colton et al. 1986). Delayed cell injury with reduced resting membrane potential an hour after a stretch stimulus has been shown in rat neural cultures (McKinney, Willoughby et al. 1996).

Pressure related changes have also been demonstrated to affect neuronal transmission. Research has been carried out into carpal tunnel syndrome in humans, where the hydrostatic compartment pressure was artificially increased, and the median nerve responses then measured. At pressures of 40 mmHg to 50 mmHg a reduction in the amplitude of the action potential was noted, and motor and sensory responses cut by up to 40%. Pressures over 60 mmHg saw an even more rapid decline in action potentials, especially for sensory responses (Gelberman, Szabo et al. 1983). Subsequent functional studies in patients matched these findings to a corresponding loss of function (Goodman, Steadman et al. 2001).

There are limited in vitro studies on pressure related activity of ocular tissue. The exception is work on human trabecular meshwork cells. Hydrostatic pressure elevations in pressure chamber models have been reported (Matsuo 2000) (Matsuo, Uchida et al. 1996). Reports indicate that increased intracellular Ca^{++} at only 25 mmHg, and increased NO production between 30 mmHg to 50 mmHg, well within the range of most types of glaucoma.

1.4.3 Pressure and apoptosis

It is apparent from the studies reported above that pressure at levels within physiological limits is capable of damaging cells and hence is implicated in disease. It stands to reason then that cell death may be yet another effect of pressure, and that this death may occur by apoptosis. There is a growing body of evidence that pressure can

indeed directly mediate apoptosis. This work is reviewed below.

1.4.3.1 General cell types

Research into pressure mediated apoptosis has been carried out in several different cell types in numerous pathological conditions. Work in the field of high blood pressure has naturally looked at the response of vascular cells to hydrostatic pressure elevation. Human saphenous veins subject to pressures of 350 mmHg have demonstrated apoptosis by the TUNEL method (Galea, Armstrong et al. 1999). Rat cardiac myocytes have also shown apoptosis in models of pressure overload heart failure by TUNEL and by upregulation of pro-apoptotic bcl-2 family proteins (Teiger, Than et al. 1996; Condorelli, Morisco et al. 1999). These findings have also been made in patients with cardiac failure (Bing 1994; Williams 1999). One study has reported elevated plasma levels of the apoptosis inducer Fas ligand protein in patients (Nishigaki, Minatoguchi et al. 1997).

Glomerular mesangial cell cultures in studies of hypertensive renal disease have also demonstrated hydrostatic pressure related apoptosis (Mertens, Espenkott et al. 1998). In studies into pulmonary hypertension in rabbits lung endothelial cells were subjected to increased hydrostatic pressures. They revealed a pressure dependant rate of apoptosis and a parallel reduction in anti-apoptotic bcl-2 expression (Gotoh, Kambara et al. 2000). Very high pressures have been used in a range of mammalian cell lines and found to induce apoptosis in vitro (Frey, Franz et al. 2004).

Relatively few studies have been reported on apoptosis in neurons. Post mortem work into the brains of high intracranial pressure injury caused by cerebral edema has shown extensive apoptosis (Runnerstam, Bao et al. 2001). 'High pressure neurological syndrome' has also been investigated in animals. The post mortem examination of rats

subjected to very high pressure of several atmospheres showed morphological changes of apoptosis, especially in dopaminergic neurons of the cerebrum and the brainstem (Mennel, Stumm et al. 1997).

Perhaps the most dramatic evidence for pressure induced apoptosis comes from studies that were designed specifically to look for this phenomenon. Using a sophisticated high pressure chamber apparatus, human lymphoblast cultures were subjected to hydrostatic pressures in excess of 50 mega pascals (3.7×10^5 mmHg) (Takano, Takano et al. 1997). Apoptosis as demonstrated by morphology and by TUNEL staining increased in a dose-dependant manner. There was also an effect on the growth of the cultures with an increase in the S-phase of the growth cycle. This model has been subsequently used in erythroblast cultures with similar results. In these experiments gel electrophoresis and flow cytometry of immunofluorescent labels was performed in addition to the morphological changes to confirm the presence of apoptosis (Take, Yamaguchi et al. 2001).

1.4.3.2 Ocular cells

In view of the significance of pressure as a causal factor in major pathology in the eye there is surprisingly little research into its direct relationship with cell death. A study with SY5Y human neuroblastoma cell cultures and chick retinal cultures used a cone and plate viscometer to subject cells to shear stress. Along with increased NO production, about 30% of the cells were found to be apoptotic by TUNEL assay (Edwards, Chiou et al. 1998).

At the time of commencing the work reported in this thesis there were no published studies looking at hydrostatic pressure and its direct impact on neurons of any kind, let alone those affected by increased pressure in the eye of glaucoma patients.

The research described in this thesis attempts to address this issue.

1.4.4 Cells sensing pressure

Clearly pressure as a physical variable can have profound effects on cells. This includes the capacity to induce the ultimate outcome, namely cell death. Medical and in vivo research into this phenomenon has been reinforced by the extensive in vitro studies described in the previous section. There is thus clear evidence that cells can respond to pressure directly. In order for this response to occur the cell must therefore be able to detect mechanical changes in the environment, and signal responses to this change.

1.4.4.1 Mechanotransduction

The processes that mediate sensitivity to mechanical forces are common to many different types of cells. Indeed they are preserved across different species, from single cell micro-organisms to man, and may even have played a role in the evolution of life from its marine origins (Somero 1991; Ko and McCulloch 2000). The process by which an individual cell perceives a physical force and converts the physical signal into a biological one is termed mechanotransduction (Ingber 1997). The mechanisms that underlie mechanotransduction have been described and some of them are now characterised at the molecular level.

Several components of the cell have been implicated in mechanotransduction. The plasma membrane is the interface between the cell interior and external environment and maintains this difference. It is a fluid and continuous lipid bilayer held which encapsulates the cell and is relatively impermeable to water soluble molecules. Embedded within the membrane or spanning its structure are myriad proteins which are crucial to cellular processes. Membrane channels dictate ion and molecular transport into and out of the cell. Receptors transduce chemical signals and enzymes catalyse

intracellular reactions. Membrane bound proteins are also responsible for linking it to the environment, including the extracellular matrix, and to adjacent cells (Ingber 1997; Tan, Kalapesi et al. 2006).

Equally important are the internal links to the cytoskeleton mediated by proteins called integrins. As eukaryotic cells are without rigid walls the plasma membrane, and indeed the cell itself, is supported by an internal structure that constitutes the cytoskeleton. This elaborate structure resists membrane deformation and provides scaffolding for linking and tethering intracellular proteins and organelles. The principal component of the cytoskeleton is the protein actin, which forms filaments whose organisation can be studied to give clues to cell growth, development and function (Hill and Gunning 1995; Broe 1997; Hill and Walsh 1997). These components of the mechanical sensation apparatus are illustrated in Fig. 1-8.

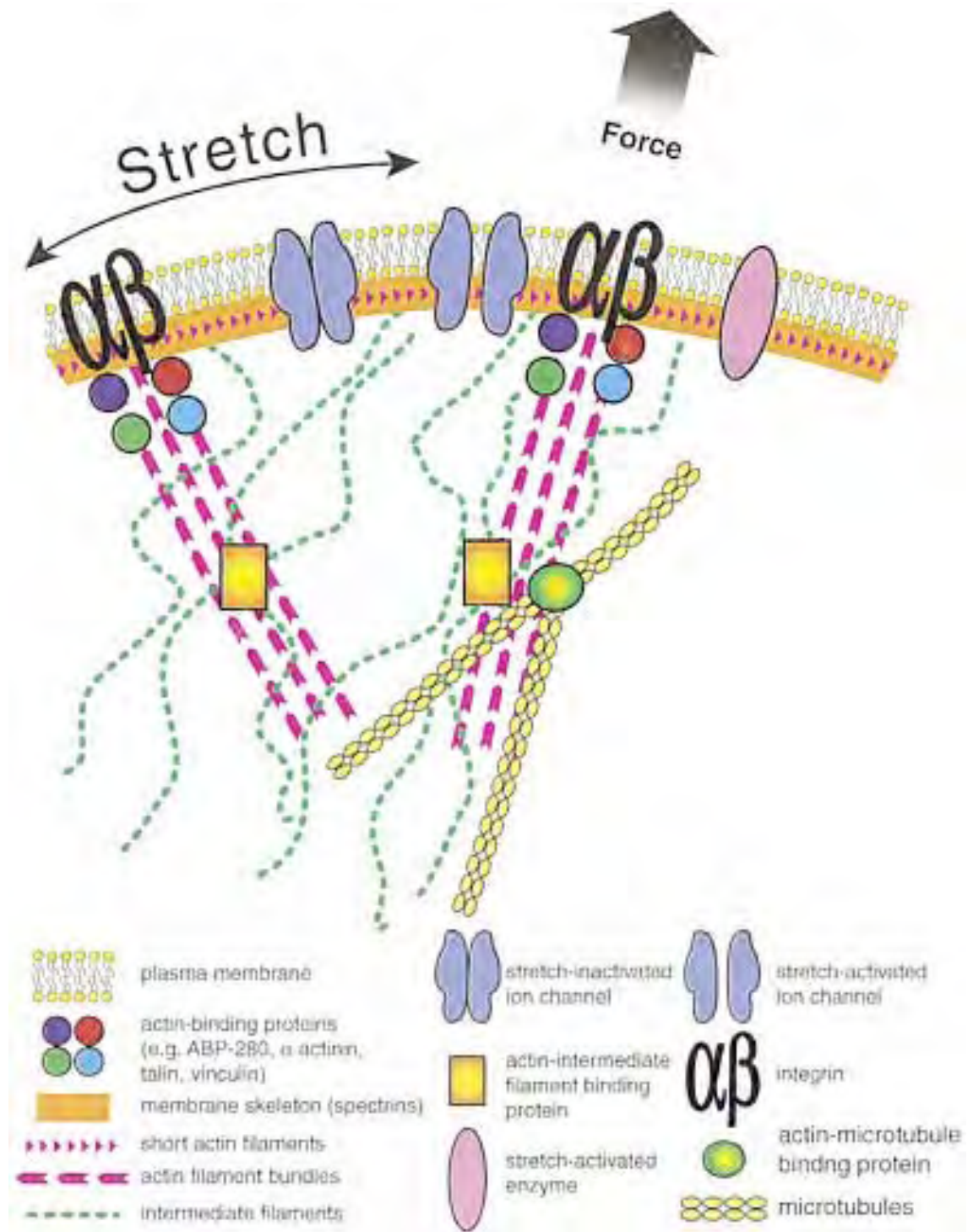


Figure 1-8 Schematic diagram of the components of mechanotransduction
 (From: Ko and McCulloch, 2000)

Each of these components- the extracellular milieu, the cell membrane, associated proteins including channels, integrins and the cytoskeleton- have a role in mechanotransduction. Understanding the interplay of this complex arrangement has been daunting. Principles of architecture and engineering design have been used to formulate a model that integrates these disparate elements and has successfully explained many of their interactions. Tensegrity architecture depends on the integrity of each element to place the surrounding structure under tension and thereby create an internal 'pre-stress'. This is a structural system of self-stabilisation which is in fact the basis for the way the body is constructed, from insects to humans (Ingber 1997; Chen and Ingber 1999; Galli, Guizzardi et al. 2005).

Sophisticated computer models, such as the optic nerve head finite element model, have further refined these principles to a molecular level and allowed a novel explanation of biological systems from a new perspective (Burgoyne, Crawford Downs et al. 2005). More significantly, experimental findings from tensegrity models have been replicated in biological systems in vitro (Stamenovic, Mijailovich et al. 2003).

The 'hard-wiring' of cell components such as membrane integrins and the cytoskeleton, as suggested by tensegrity, offers an explanation of how mechanical stresses can be transferred from the cell surface well into its depths. Paths for molecular changes in a cells as a result of physical stress have been mapped out. These show how other factors such as signal transduction and enzyme activity may also be involved. The current model of tensegrity demonstrates that living cells and indeed nuclei are literally built to sense and respond immediately to mechanical stress, including hydrostatic pressure (Ingber 1997; Wang, Naruse et al. 2001; Wendling, CaNadas et al. 2002; Canadas, Wendling-Mansuy et al. 2006).

1.4.4.2 Mechanosensitive channels

The most recently defined and extensively studied mechanosensitive structures are the membrane channels which respond to applied physical stress. These are of particular interest as they offer a potential mechanism for many pressure related responses of cells. These mechanosensitive channels respond to applied pressure in a definable way, either opening or closing as a response (Sackin 1995). In humans they have been found in vascular endothelia, renal cells, myocytes and in the peripheral nervous system (Kalapesi, Coroneo et al. 2005).

The mechanosensitive channels include both stretch-activated and stretch inactivated channels, and may be permeable to anions such as Cl^- or cations like Ca^{++} and K^+ (Morris 1990) These ions can mediate the transduction of pressure stimuli, and much of the evidence for this is based on in-vitro patch clamping experiments (Wright, Jobanputra et al. 1996). Excessive K^+ efflux may serve as a trigger for apoptosis, and intracellular levels have been noted to decrease early in apoptosis prior to cell fragmentation (Barbiero, Munaron et al. 1995; Krick, Platoshyn et al. 2001). Thus mechanotransduction of pressure stimuli via a stretch activated K channel could potentially trigger apoptosis.

Recently a class of mechanosensitive channels have been characterised that are found only in neuronal systems. These stretch-activated membrane channels with weak inwardly rectifying conductance are known as TREK and TRAAK (Maingret, Patel et al. 1999). They have been identified in the brain, spinal cord and retina (Patel, Honore et al. 1998; Popp, Hoyer et al. 1993; (Kalapesi, Tan et al. 2005). TRAAK channels have been shown to respond to hydrostatic pressure, and at levels of 25 mmHg to 30 mmHg (Maingret, Fosset et al. 1999). This is interesting in the context of glaucoma, where this is the same range of IOP associated with the bulk of chronic glaucoma (Rhee 2003).

1.5 Hypothesis and Aims

It is evident from the review of literature presented above that the question of glaucoma pathogenesis remains unanswered. However some salient points emerge from this review, viz.:

- (1) elevated IOP is the most frequent and important association of glaucoma
- (2) this elevated hydrostatic pressure results in the loss of RGCs
- (3) the loss of RGCs is mediated by apoptotic processes
- (4) other cells are able to respond directly to pressure, including by undergoing apoptosis

Although some postulated molecular mechanisms may potentially explain such a direct effect, the link between raised IOP and the subsequent induction of apoptosis in the RGC has not yet been established. Our work presented in this thesis is based on a novel approach to this area of glaucoma pathogenesis. We hypothesised that RGC apoptosis is the result of a direct response of neuronal cells to raised hydrostatic pressure independent of any other factor. The aim of our research was therefore to test this hypothesis. To our knowledge a study of this nature was not reported prior to undertaking the present work.

In endeavouring to investigate this relationship between a stimulus and a response at the cellular level, all other variables had to be controlled. This can be accomplished in the biological sciences *in vitro*. Thus our work required the development of an *in vitro* model of glaucoma. Since the interest is in the response of single cells, this dictates a tissue culture approach. The form of tissue culture most amenable to isolated cell studies is cell culture (Freshney 1994).

Our work was therefore planned to achieve the following objectives:

- (1) To devise a pressure chamber system to apply and adjust hydrostatic pressure over and above atmospheric pressure.
- (2) To establish cell cultures to be tested in this system. The cell cultures investigated were of the same type as are affected in glaucoma, ie. a neuronal cell, ideally retinal in origin and preferably a RGC.
- (3) To select the conditions within the pressure chamber such that the hydrostatic pressures to which the cell cultures were to be exposed were within physiological limits, and for a duration sufficient to induce a measurable response in cells without being detrimental to the entire cell population in culture.
- (4) To develop and refine the techniques to measure this response, specifically in terms of apoptosis; ie. identifying the apoptotic cells by traditional morphology and quantifying the extent of this apoptosis by modern immunofluorescent labelling and automated cytometry.

We were able to develop an *in vitro* model which enabled us to achieve these stated objectives. The results presented in this thesis provide evidence that elevated hydrostatic pressure induces apoptosis *directly* in primary retinal cultures, neuronal cell lines, and RGC-5 neurons. We now suggest the possibility of a novel relationship linking pressure and apoptosis directly that may complement known factors in the pathogenesis of glaucoma.

Chapter Two

Materials and Methods

2

2.1 Introduction

The primary aim of the experiments undertaken in this study was to examine the effect of a single physical factor, pressure, on apoptosis in neurons and thereby enhance our understanding of the pathogenesis of glaucoma.

To achieve this objective it was imperative to design an *in vitro* model. This system consisted of three principal components: (i) a means to apply and adjust hydrostatic pressure in a consistent manner with minimal or no impact on other related physical variables, (ii) the cells to which the stimulus was to be applied and the response measured, and (iii) a method to measure the response of these cells to pressure, specifically in terms of apoptosis; this entailed the development of a bioassay for the detection of apoptosis.

The first stage in undertaking these studies was therefore to develop and validate a pressurisation system. In an *in vitro* setting neurons can be studied using cell culture. The target cell in glaucoma is the RGC, however this is not easily grown in laboratory conditions. Thus the next step involved primary retinal cultures, with identifiable RGC neurons, obtained directly from mammalian eyes. Subsequently more established neuronal cell lines were used to refine the cellular analysis in a more consistent and reproducible manner. This led to the establishment of a reliable and repeatable bioassay. Finally these stages were combined in work with the recently developed RGC-5 cell line, which enabled us to study the effects of pressure on the target cell in glaucoma.

2.2 Materials

The following chemicals and materials used in this research were obtained from the companies or individuals listed in Table 2-1.

Table 2-1 Sources of chemicals

Company	Chemicals
BOC gases (Sydney, NSW, Australia)	5% CO ₂ & air gas mix
Boehringer Ingelheim (Sydney, NSW, Australia)	Triton-X 100
Calbiochem (San Diego, CA, USA)	Soybean trypsin inhibitor, normal goat serum, normal rabbit serum, horse serum
Cell Signalling (Danvers, MA, USA)	cleaved Caspase-3
Gibco BRL (Gaithersburg, MD, USA)	Dulbecco's modified essential medium (DMEM), fetal bovine serum (FBS), fetal calf serum (FCS), glutamine, Hanks balanced salt solution (HBSS), Neurobasal/B27 supplement medium, Opti-modified essential medium (Opti-MEM), phosphate buffered saline (PBS), sodium citrate buffer, trypsin
Molecular Probes (Eugene, OR, USA)	antifade, Thy1.1 rat primary antibody, rhodamine anti-mouse secondary antibody
Professor I Hendrey (John Curtin School of Medical Research, Australian National University, Canberra)	nerve growth factor (NGF)
Promega (Madison, WI, USA)	binding buffer, equilibration buffer, DNase, TdT-mediated dUTP biotin Nick End Labelling (TUNEL),
Sigma (St Louis, MO, USA)	di-butryl cyclic Adenosine Mono Phosphate (cAMP), paraformaldehyde (PFA), penicillin-streptomycin, poly-L-lysine, succinyl concanavalin A
Zymed (San Francisco, CA, USA)	Annexin V- FITC, Cy-3 anti-rabbit secondary & FITC anti-rabbit secondary antibody, propidium iodide (PI)

The following instruments used in this research were obtained from the companies listed in Table 2-2.

Table 2-2 Sources of scientific instruments

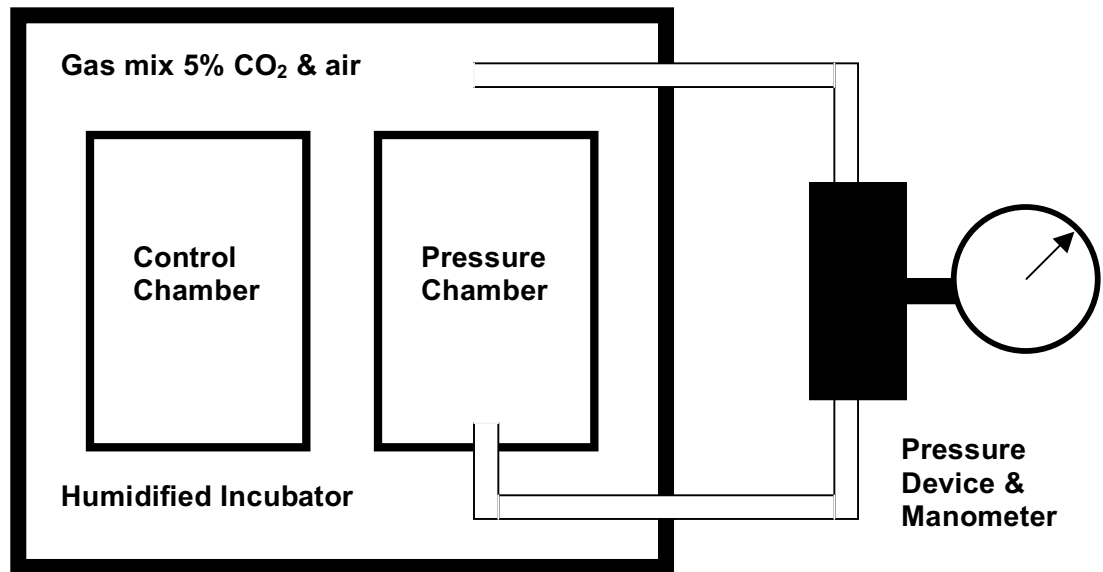
Company	Scientific Instrument
Accoson (London, UK)	Mercury manometer
Beckman Coulter (Fullerton, CA, USA)	Centrifuge Model TJ
BOC gases (Sydney, NSW, Australia)	Low pressure regulator
Compucyte (Cambridge, MA, USA)	Laser Scanning Cytometer (LSC)
Email (Sydney, NSW, Australia)	Biological safety cabinet: Class II Laminar flow hood
Nuaire (Plymouth, MN, USA)	4500E humidified incubator
National Institute of Health (Bethesda, MD, USA)	NIH Image ver 1.61
Olympus (Tokyo, Japan)	Dissecting microscope, IX-70 light microscope, GB200 laser scanning microscope (LSM)
Radiometer (Villeurbane Cedex, France)	Stat gas analyzer ABL 725

2.3 Pressurisation system

2.3.1 Apparatus development

The basic design of the pressure apparatus was based on a combination of features of a well established pressure chambers used in other fields of biomedical research (Sumpio, Widmann et al. 1994; Mattana and Singhal 1995), illustrated in Fig. 2-1A. These features are particularly applicable to cell culture work as the culture conditions are maintained during the pressurisation process. A rectangular plexiglass pressure chamber measuring 80 x 190 x 215 mm externally was constructed with a resealable lid (Fig. 2-1B). The internal dimensions (40 x 145 x 120mm) allowed a standard 24 well culture plate to be enclosed. The lid is secured by stainless steel clamps which attach to the long sides of the chamber. A rubber O-ring seal is situated in a groove within the thickness of the walls, and combined with vacuum grease enable an airtight seal to be created. Two ports were built in to the chamber, to allow access for pressurising the gas mixture and pressure release, and monitoring of the pressure levels. Duplicate chambers were constructed by the Department of Mechanical Engineering at the University of New South Wales (UNSW) with the kind assistance of Professor R Frost.

Both pressure chambers were kept inside an electronically controlled incubator. The same incubator was used for the cell cultures. The incubator had a water reservoir to maintain a humidified atmosphere and was set at 37⁰C. The other components, the pressurising and monitoring apparatus, were located outside the incubator and connected by tubing through a small sealable port built into the incubator wall. A Mercury manometer was connected directly to the pressure chamber to provide continuous real time monitoring of pressure.



A



B

Figure 2-1 (A) Design of pressure system and (B) Photo of pressure chambers

A. Design of pressure system. Schematic diagram of our system for pressurising neurons *in vitro*. Pressure chambers are situated within a humidified incubator which contains an electronically controlled gas mix of 5% CO₂ and air used for cell culture. An external pressure device uses the same gas mix to elevate the pressure within one of the chambers, containing a 24-well plate with cells, forming the ‘Pressure’ group. The companion chamber is not connected to the pressurising device, so the cell culture within forms the negative ‘Control’ group.

B. Photograph of the pressure chambers used in this study. The chamber on the left was for for pressurisation of cultures (pressure group) and the chamber on the right was the control chamber (negative control group). The same incubator was used for growth and maintenance of the cell cultures (note that their 24-well plates also seen here). Also seen are the connections to the externally placed manometer and pressurising apparatus.

The pressure chamber was initially designed to be connected to a low pressure regulator which in turn was attached to a gas cylinder containing a gas mix of 95% air, 5% CO₂. This is the same composition as that used in the incubator. However the possibility of unmeasurable discrepancies between the cylinder and incubator gas mixtures could not have been excluded. Hence the design was further refined, consistent with guiding principles of simplicity and transparency. The gas mix used in pressurisation was now sourced from within the incubator itself (Fig. 2-1). This was done via the manometer which was attached to a compression and deflation pressurising device based on sphygmomanometry. We could thus elevate and adjust the chamber pressure with the added benefits of greater precision and finer control than the regulator. The cell culture media transmitted the applied gas pressure into hydrostatic pressure upon the plated cells. All absolute measurements were made with atmospheric pressure (760 mmHg) calibrated to zero mmHg.

2.3.2 Evaluation of the pressure apparatus

The pressure apparatus was first evaluated to ensure that an enclosed system was created with no potential for leakage of pressurised gases. The pressure chamber and attachments were tested by immersion in a large water bath with all seals closed, and the air within pressurised to 200 mmHg. Any defects in the seals or tubing were readily identified and repaired to ensure an airtight system. The procedure was repeated with the apparatus set up in situ within the incubator and with external ancillary components connected outside it. The desired gas mix was successfully pressurized to a constant ambient pressure ranging from 0-200 mmHg (over and above atmospheric pressure). Compression and decompression was attained over 30 seconds.

The final validation of the model was to investigate the potential for a gas effect. Due to the intimate relationship between pressure and the relative composition of gases and liquids in their respective physical states, the possibility exists that elevated pressure could alter gas exchange. In the context of a cell culture which depends on a defined gas mix and liquid media for viability, and which is being subjected to elevated hydrostatic pressure, this is an important confounder. If present to any significant extent this would make any results open to question, as they may then be attributable to varied gas effect rather than varied pressure (Sumpio, Widmann et al. 1994; Kosnosky, Tripathi et al. 1995).

To assess this phenomenon culture media was sampled from the wells of a 24-well culture plate placed within the pressure chamber (pressure group), and simultaneously from an identical culture plate kept inside the control chamber (negative control group). Sampling was done at zero hr (before pressurisation), at 2 hrs (immediately after pressure conditions of 100 mmHg for 2 hrs) and again at 4 hrs (a further 2 hrs after pressurisation ceased and normal atmospheric conditions restored). Culture media samples were then analysed for pH, pO₂ and pCO₂ by a stat gas analyser. Results of this validation process are described in Chapter 3.

2.3.3 Experimental design

All cell cultures were grown as adherent monolayers on glass coverslips placed in 24-well plates with 300µl of culture media. Each experiment comprised three culture groups: a positive control to confirm apoptosis detection, a pressure group subjected to experimental conditions of increased ambient hydrostatic pressure, and a negative control consisting of cells not exposed to the increased pressure. For each experimental run cell cultures were from the same plating, and experiments were conducted on the

three groups simultaneously. Just prior to each run all coverslips were examined by phase light microscopy to ensure cells were viable and of correct density, excluding coverslips with confluent cultures or low densities. For each experimental category and timepoint coverslips were matched for equal densities to allow meaningful comparisons to be made.

2.3.3.1 Positive control group

A maximum apoptosis control for the cell culture was established in each experiment by treatment with ethanol, a known stimulator of apoptosis (De, Boyadjieva et al. 1994; Oberdoerster, Kamer et al. 1998; Mizushima, Tsutsumi et al. 1999). This enabled validation of the various methods used in apoptosis detection in each experiment. DNase was also used as the inducer of apoptosis in some cultures (Wang, Lin-Shiau et al. 2000; Lechardeur, Xu et al. 2004). In differentiated PC12 neurons, for example, ethanol leads to excessive cell loss by detachment. Hence the positive control culture in PC12 experiments was treated with DNase for 25 minutes at room temperature to induce apoptosis (Shiokawa, Kobayashi et al. 2002).

2.3.3.2 Pressure group

Cultures were analysed before any pressure conditions (zero hr timepoint) by removal of selected coverslips. The culture dishes were then placed within the pressure chamber and the incubating gas mix was pressurised. The cultures were exposed to elevated ambient hydrostatic pressure, over and above atmospheric, for a defined period of time (2 hrs). The pressure conditions were then restored to atmospheric and the culture dishes removed from the chamber. Coverslips were removed for immediate analysis (2 hrs timepoint), and at serial timepoints (4 hrs, 6 hrs, 20 hrs or 24 hrs after time zero).

Pressure elevations were selected to represent the range of IOPs seen in clinical glaucoma. We chose 100 mmHg, the maximal observed IOP in the condition of acute glaucoma, and later included 30 mmHg, associated with chronic glaucoma, and 15 mmHg for 'normal' IOP.

2.3.3.3 *Negative control group*

Negative controls were included in all experiments with cells treated similarly to the pressure group. Culture plates were placed within identical pressure chambers at the same time for the same experimental period. However the gas mix was not pressurized, so these neurons were not subjected to elevated pressure conditions. Analysis in this negative control group was carried out simultaneously with the corresponding pressure group. The first analysis thus was at timepoint zero (before experimental conditions of pressurisation in pressure cultures). Culture dishes were removed from the chamber when conditions were restored to atmospheric in the companion pressurised chamber (ie after 2 hrs) and coverslips removed for analysis. Subsequent analysis was then carried out at serial timepoints (4 hrs, 6 hrs, 20 hrs or 24 hrs after time zero).

2.3.3.4 *Analysis*

Cell cultures were examined on a regular basis for morphology. Conventional light microscopy of live cells was the mainstay for ongoing assessment of cell viability and measuring the success or otherwise of a given culture. Once cultures were established, fluorescent labels could then be applied to highlight morphological features of the cells, which were imaged in colour with laser scanning microscopy. Pictures of cells depicted in this study thus comprise both light and laser scanning microscope images.

Following the experimental conditions described above coverslips were removed immediately for analysis. Cells were stained live or fixed for examination by treatment

with 4% w/v paraformaldehyde (PFA) in phosphate buffered saline (PBS) pH 7.5 for 10 min, and coverslips then mounted in antifade for further analysis. Morphological examination was by microscopy and quantitative assessment was performed by automated cytometry.

All experiments used duplicate coverslips which enhanced reliability while still allowing immunofluorochemistry to be conducted without delay. As the timepoints needed to be synchronised simultaneously across all three culture groups (pressure group, positive and negative controls), the technical practicalities of immediately staining multiple coverslips limited their number to duplicates.

2.3.4 Primary retinal culture

2.3.4.1 Neonatal rat retinal culture

All work on animals in these experiments was conducted in accordance with guidelines of the UNSW Animal Care & Ethics Committee under ethics approval (AEC No. 1997/101). Animal tissue was obtained from the Charles River strain of Sprague-Dawley rat (Animal Breeding and Holding Unit, UNSW). This strain is well documented in terms of neural development and has the added advantage of large litter sizes, minimising the number of adult rats required as breeding pairs. The tissue culture techniques for rat retinal cultures have been well reported (Takahashi, Lam et al. 1992) (Cohen, Bray et al. 1994; Nichol, Everett et al. 1994; Zhao and Barnstable 1996). We used a method described by Nichol et al (Nichol, Schulz et al. 1995).

(i) Tissue Collection

Post-natal 1-2 day old rat pups were sacrificed by decapitation and eyes immediately removed by enucleation. The eyes were immersed in Hanks Balanced Salt Solution

(HBSS). Retinae were removed by blunt dissection in HBSS using a dissecting microscope under sterile conditions. Once collected the retinae were dissociated in a test tube containing a solution of 0.05% Trypsin in 10 ml HBSS, and incubated in a 37^o C water bath for 15-20 min. The test tube was then removed and centrifuged at 500 RPM for 30 sec forming a tissue pellet. The supernatant was carefully aspirated and the pellet resuspended in 0.004% DNase and 0.025% soybean trypsin inhibitor in 10ml HBSS for 1 min to inactivate the trypsin and stop enzymatic dissociation. This process of pellet formation and resuspension in this inactivating solution was repeated. After a final pellet formation the supernatant was replaced with PC12 conditioned medium (grown from PC12 cell line within our Cell Biology Laboratory) and followed by gentle trituration by bulb pipette to completely dissociate the cells mechanically. The dissociated cells were diluted in culture media (see below) to give a final concentration of approximately 10,000 cells/sq.cm or 5×10^6 cells per ml.

(ii) Culturing

Retinal cell culturing was done in 24-well tissue culture plates which were prepared one to two days prior to use. Glass coverslips (12mm diameter) were autoclaved and then placed at the bottom of each well. A substrate for cell adherence was created on each coverslip by adding 0.5 ml of 80 µg/ml poly-L-lysine for 1 hr before being aspirated. This work was carried out in a Biological Safety Laminar Flow hood and the plates were left to dry in this overnight.

Cells were plated onto the pre-prepared coverslips in 300 µl culture media and grown in optimal conditions. Early work used 50% PC12 conditioned media and 50% Dulbecco's Modified Eagle's Medium (DMEM) supplemented with 10% Fetal Calf Serum (FCS). To the DMEM had been added penicillin-streptomycin 0.05%. Later retinal cultures used a defined media of Neurobasal with B27 supplement (Brewer

1995) with added glutamine (2 mM) and penicillin-streptomycin (0.05%). Cells were grown in a humidified incubator at 37⁰ C with 5% CO₂ and air.

2.3.4.2 Human retinal culture

All work on human ocular tissue was conducted in accordance with the guidelines of the UNSW Committee on Experimental Procedures Involving Human Subjects and ethics approval was obtained for the use of fetal eyes (CEPIHS No. 99243). Human ocular tissue was obtained only after informed consent from the legal guardian. Fetal tissue was obtained by kind arrangement from an established research program of Professor Tuch, Department of Endocrinology, Prince of Wales Hospital, UNSW in collaboration with the Royal Hospital for Women, Sydney.

The culture techniques for human tissue were very similar to those we had used in neonatal rats, with only minor modifications in the culture media. Tissue collection was carried out in a manner similar to that described above for rat eyes. The fetal eyes were of similar size and thus dissection protocols were unchanged.

Dissociation of retinal cells was completed as described previously, and cell densities comparable to the rat tissue achieved. Culture media comprised serum free Neurobasal medium with B27 supplement 0.05% penicillin-streptomycin and 2mM glutamine. Cultures were seeded onto poly-L-lysine coated coverslips in 24-well plates and maintained at 37⁰ C supplemented with 5% CO₂ and air in the humidified incubator.

2.3.4.3 RGC identification

RGCs can be identified by the use of specific immunofluorescent markers, such as Thy1.1, a plasma membrane glycoprotein which in the mammalian retina is considered to be exclusive to RGCs (Beale and Osborne 1982). In all cultures morphological and immunofluorescent analyses were conducted to confirm the presence of RGCs.

Dendritic processes, especially axon formation, are more pronounced in RGCs. The soma of these neurons are larger than other retinal cells, and in mixed retinal cultures only RGCs have cell body diameters over $\sim 12 \mu\text{m}$ (Guenther, Schmid et al. 1994). Coverslips were examined live with phase contrast microscopy and NIH Image (ver 1.61) software for characteristic morphological features.

Cell culture coverslips were fixed with 4% PFA and washed with PBS. The culture was incubated for 90 min with 1:100 dilution of Thy 1.1 primary antibody in PBS containing 10% normal goat serum to block non-specific staining. The coverslips were washed, exposed to a fluorescent secondary antibody, rhodamine conjugated anti-mouse, washed and mounted on glass slides with antifade. Negative controls were treated identically except for the use of Thy 1.1. Slides were examined with a confocal laser scanning microscope.

2.3.5 Neuronal cell lines

As with primary cultures, clonal cell lines in these experiments were also grown as monolayers on a coverslip based substrate. Neurons were plated at similar densities to primary cultures, viz. ~ 2.5 million cells per ml, onto poly-L-lysine coated glass coverslips in 24-well culture dishes. They were grown in 300 μL of growth media per well, and incubated at 37°C in 5% CO₂ and air.

The cell line cultures used were the B35, C17, NT2 and PC12 lines. The rat B35 cell line was grown in DMEM supplemented with 10% FCS and 1% penicillin-streptomycin (Schubert, Heinemann et al. 1974). The mouse C17 line was grown in DMEM with 10% FCS (Weinstein, Shelanski et al. 1990). The NT2 cell line, derived from human primary cultures, was grown in a culture media of Opti Modified Eagle's Medium (Opti-MEM) supplemented with 10% FCS (Younkin, Tang et al. 1993). The PC12 line,

derived from rat pheochromocytoma cells, is one of the most established clonal lines in use (Greene and Tischler 1976; Greene, Sobeih et al. 1991). PC12 cultures were grown in DMEM with 5% FCS and 10% horse serum.

Since these neuronal cell lines may not be post-mitotic and continue to proliferate, we also used a differentiated neuronal line. PC12 cells were differentiated to produce neurons that had exited the cell cycle (Gunning, Landreth et al. 1981). Differentiation was induced by treatment of undifferentiated PC12 cultures in DMEM with 1% horse serum supplemented with 1 mM di butyryl cAMP and 50 ng/mL NGF for 3 days (Michel, Vyas et al. 1995).

2.3.6 Retinal ganglion cell line

The RGC-5 cell line was developed from primary rat retinal cultures by Professor N Agarwal's team in Fort Worth, Texas, and has numerous characteristics of retinal ganglion cells (Krishnamoorthy, Agarwal et al. 2001). This line was kindly donated to our laboratory for the research described herein.

RGC-5 cell cultures were grown in DMEM supplemented with 10% heat inactivated fetal bovine serum and 100 U/ml of penicillin and 100 µg/ml of streptomycin. These neurons were plated at densities of ~5 million cells/ml or 10,000/sq.cm onto poly-L-lysine coated glass coverslips in 24-well culture dishes. Cultures were grown in 300 µL of growth media per well, and incubated at 37° C in 5% CO₂ and air.

Differentiated RGC-5 cultures were prepared after cells had adhered to coverslips by substituting growth media for serum-free DMEM for 24 hrs. After this period of serum starvation they were cultured in DMEM with 5% fetal calf serum and 1% penicillin/streptomycin. This was supplemented with succinyl concanavalin A and cells maintained in this media for six days.

2.4 Apoptosis detection

Apoptosis in the cultured cells was detected by a combination of classical morphological changes along with immunocytochemistry of specific molecular features of apoptosis. Fluorescent markers of both early and late cell death were used. These markers and the morphological changes of apoptosis were then examined with microscopy and automated Laser Scanning Cytometry. Finally cleaved Caspase-3 was also detected by an immunofluorescent technique.

2.4.1 Immunofluorescent markers of apoptosis

2.4.1.1 Early apoptosis marker

The externalisation of phosphatidylserine residues to the outer cell membrane is one of the first processes in apoptosis (van Engeland, Nieland et al. 1998). This can be detected by the Annexin V phospholipid binding protein. We used a commercial kit (Zymed) with a fluorescein isothiocyanate (FITC) label for identifying early apoptosis.

Staining was performed on live cells by pre-treatment with PBS followed by application of Binding Buffer. The coverslips were then incubated with Annexin V-FITC (1:20 stock) for 10 min at room temperature before being washed in buffer. They were incubated with red Propidium Iodide (PI) stain (1:20 stock) for 10 min before being washed and mounted with antifade. Counterstaining live cells with PI enables necrotic cells to be distinguished by the dye exclusion principle. Negative controls for staining were also included with no Annexin V application. Positive controls were treated with 5% ethanol, a well established inducer of apoptosis; these served as the third experimental group.

2.4.1.2 *Late apoptosis marker*

Apoptosis is also characterised by endonuclease activation leading to DNA fragmentation into segments. This is a late stage of apoptosis that can be labelled by immunofluorescent markers. This apoptosis detection was done by the established TUNEL assay (Ben-Sasson, Sherman et al. 1995). We chose a direct binding FITC-conjugated dUTP as the green fluorochrome with a red PI counterstain to enable visualisation of viable and necrotic cells. For this we used a commercially available kit (Promega).

The staining procedure followed the protocol sheet supplied with the kit. Coverslips were fixed with 4% PFA and washed with PBS. They were pretreated with 0.2% Triton X-100 solution in PBS for 5 min on ice to permeabilise cells, washed in PBS, and then covered with equilibration buffer for 10 min at room temperature. Excess buffer was removed from the coverslips and the cells incubated with dUTP nucleotide label and Terminal Transferase (TdT) at 37⁰ C in a humidified chamber in the dark for 90 min. All subsequent steps were also protected from direct light. Coverslips were washed with sodium citrate buffer then with PBS, before PI counterstaining for 10 min. Finally coverslips were mounted with antifade on glass slides. Negative controls for the staining procedure were included with coverslips treated without the TdT enzyme. Positive controls subjected to treatment with known apoptosis inducers (ethanol 5% or DNase) were included as the third experimental group.

2.4.2 **Morphological analyses of apoptosis**

Morphologically apoptosis is characterised by progressive condensation of the cytoplasm and nucleus, followed by fragmentation and phagocytosis. In neurons there is also seen a withdrawal of cell processes and a "blebbing" or "budding" of the cell

membrane (Majno and Joris 1995). Neurons were examined for these features of apoptosis and to allow identification of necrotic cells. Adherent live cells were visualized initially by phase contrast microscopy with a Olympus IX-70 light microscope and NIH Image (ver 1.61) software. Visualisation of Annexin V and TUNEL apoptosis markers was performed with a confocal Laser Scanning Microscope (LSM) and high resolution digital images taken.

Laser scanning cytometry (LSC) was used to perform concurrent assessment of both morphology and objective marker data, due to its ability to visualise scanned cells with a co-mounted fluorescent microscope (Fig. 2-3). Morphological inspection was done both in real time as the laser scan is performed (a LSC image via the 'Scan data' feature) and later after the scan for additional image analysis. The latter was made possible by the LSC recording of the spatial X-Y co-ordinates of each cell, so that an individual neuron can be relocated (via the 'compusort' feature) for visualisation in greater detail via the integrated fluorescent microscope. The position was recorded and since LSC image resolution is limited the confocal LSM was used to digitally image the cell.

2.4.3 Quantitative analysis of immunofluorescent markers

2.4.3.1 Manual cell counts

Neurons stained for immunofluorescent markers were imaged on confocal LSM for features of apoptosis. In general apoptotic cells had significantly increased fluorescent marker staining of the relevant cellular anatomy. Once specific characteristics of apoptosis had been identified, and just as importantly the contrasting characteristics of non-apoptotic cells determined, visual analysis could be reliably performed. For example, TUNEL positive cells should demonstrate FITC fluorescent nuclei in contrast

to non-apoptotic cells with little or no such staining characteristics.

Manual cell counts were done at a fixed microscope objective magnification (usually X20 or X40 depending on fluorescent features). The coverslip was scanned vertically in columns one field width apart, and one field of view at a time. Every 5th field was analysed for the number of positive apoptotic cells which was noted with a cell counter.

2.4.3.2 Laser scanning cytometry

Quantitative assessment of immunofluorescent markers was done by LSC (Fig. 2-2). This is a unique tool for this purpose as it combines the microscope based study of adherent cells, such as neurons, with the automated analysis once restricted to flow cytometry (Kamentsky, Burger et al. 1997). The LSC has been demonstrated to be an accurate tool for the detection of apoptosis using both markers employed in this study (Darzynkiewicz 1998; Schutte, Nuydens et al. 1998). Cytometric parameters of the fluorescent apoptosis markers were measured by the instrument. These included the intensity of the fluorescent signal, its distribution and overall characteristics such as the size and area of the scanned cell.

FITC was the hapten label in both Annexin and TUNEL assays, which was used in conjunction with a red PI counterstain. The LSC Argon laser and appropriate sensors were selected for the green FITC fluorochrome to detect and measure this marker (note that red PI intensity was not always measured). The laser was set to 488 nm and sensors to wavelengths of 530 nm for FITC and 600 nm for PI measurements.

FITC label intensity was measured and cell values determined for two LSC parameters, Green Max Pixel (GMP) and Green Integral (GI). GMP is the fluorescence peak reflecting the highest value within a cell. Hyperchromicity of DNA in condensed

chromatin of apoptotic cells can be recognised by high GMP values with the nuclear TUNEL assay (Li and Darzynkiewicz 1995). Membrane bound Annexin V label also gives high readings for apoptotic cells, as other cells do not stain or do so at a significantly lower intensity. The sum of the signal value for all pixels over threshold for a scanned cell is given as the GI. This measure of total fluorescence is similarly indicative of the degree of labeling (Darzynkiewicz, Bedner et al. 1998).

For each scan a population of single neurons was selected for analysis. The LSC determines the size of all scanned objects by the number of pixels over threshold, or the 'fluorescent area'. Visual inspection of cells during scanning allowed exclusion of debris and cell clumps on the basis of size. Appropriate area limits were then set to select or gate the target group of single cells, seen within the coloured rectangular region in the representative data scattergrams of LSC data output (Fig. 2-3).

At each timepoint in each experiment duplicate coverslips were stained for immunofluorescent markers. Neurons on the coverslips were scanned in each of four equal sized quadrants thus for each coverslip 4 sets of LSC measurements were made, one per quadrant. Cells were visualized during scanning to validate the predominantly single cell population and marker staining. TUNEL positive neurons with FITC positive nuclei, and Annexin positive neurons with FITC positive membranes were identified and appropriate LSC sensor settings derived to optimise their detection. Data was collected for both intensity parameters (GMP, GI) as well as the cell's fluorescent area. PI sensors were also optimised to detect all cells and select for the desired population.

Absolute measured values were recorded by the LSC and data analysed as the average for the gated single cell population. This data was also used to determine the proportion of the total selected cell population that was marker positive. Normalised data of pooled results were obtained by comparison of individual absolute

measurements with the averaged positive control (maximal apoptosis) value for that experiment. Data could thus be expressed as a ratio of the positive control. Quantitative data on TUNEL and Annexin V are expressed as direct readings of marker intensity for the given parameter in Chapters 4 and 5. The analysis protocol was refined during the course of this work, so that it was then possible to express quantitative marker data for GI in terms of apoptotic cells as a percentage of the whole cell population. The results presented in the latter sections of Chapter 5 and those in Chapter 6 are thus given in this format.

2.4.3.3 Statistical Analysis

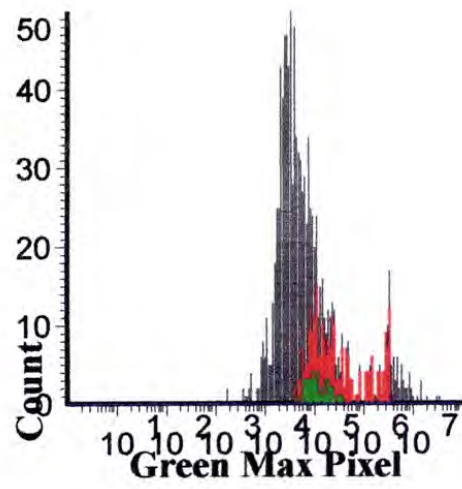
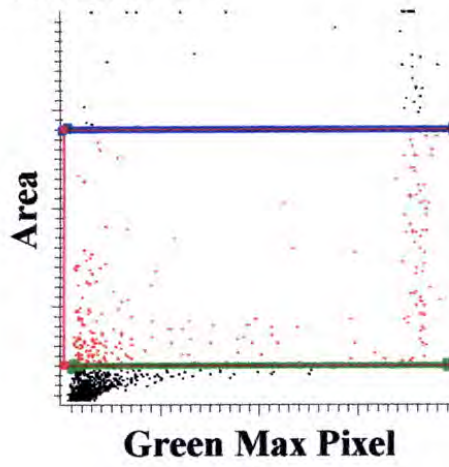
Raw data was entered into Microsoft Excel spreadsheets and tabulated. Our aim in selecting a statistical method was based on ensuring reliability while also maximising reproducibility across related experiments. We thus chose to limit data analyses to the comparison of two sample groups only, obviating the need for multivariate statistical tools such as ANOVA. To optimise the robustness of paired comparisons the ideal method would be parametric. However sample sizes could potentially be small so first we needed to determine whether the measured variables followed a normal distribution, and thus be amenable to a parametric tool. Hence non-parametric (Wilcoxon Signed Rank test) and parametric (Students paired t-test) analyses were done on the same data from initial experiments. Comparisons of the two, including of p-values for statistical significance, revealed similar results. Thus an assumption regarding a parametric distribution of the experimental variable was valid, so subsequent and final data analyses were then carried out universally by Students paired t-tests. Results of quantitative data presented herein are of variance statistically analyzed using Student's paired t-test, and presented as the mean \pm Standard Error of Mean (SEM).



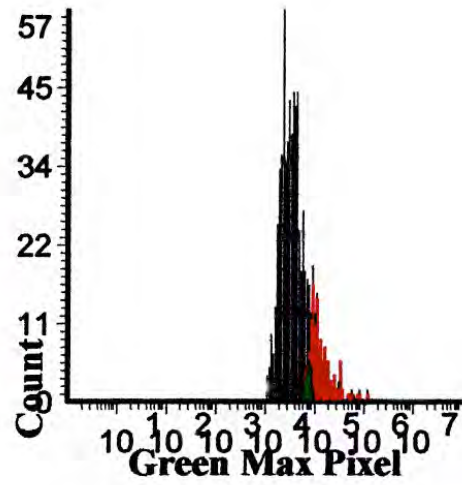
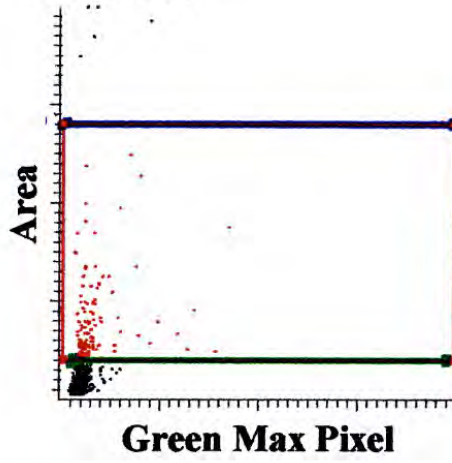
Figure 2-2 Laser Scanning Cytometer

Photograph of the Laser Scanning Cytometer (LSC) used in this study. Lasers are in the unit at the left which is integrated with the fluorescent microscope in the centre. Slides of adherent cells are viewed with the microscope as for conventional imaging. Laser scanning is then performed in the same location without disturbing the slide. Instrument settings and scanned data as well as images are managed via the computer monitor on the right. The representative monitor display shows the LSC's ability to concurrently visualise scanned cells and record automated cytometry data from the same material, a unique feature of this technology. (CAF, Cellular Analysis Facility, UNSW).

Ethanol



Control



Pressure

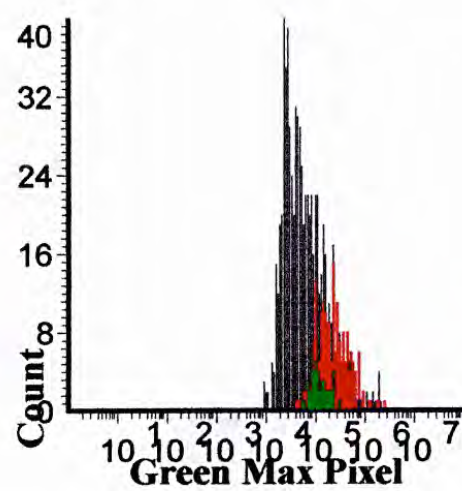
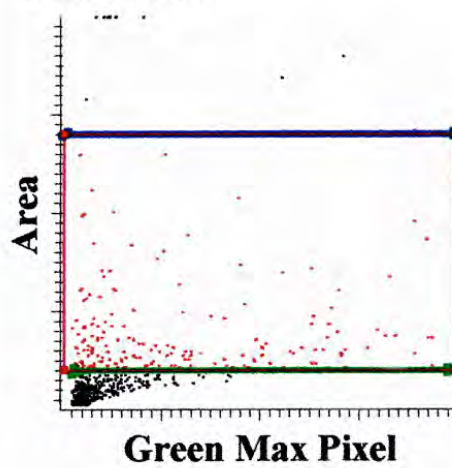


Figure 2-3 LSC scan

Figure 2-3 Legend for LSC scan

Typical quantitative TUNEL data from LSC analysis of B35 cultures following ethanol, control or pressure treatment (100 mmHg). Single scan for green dUTP-FITC fluorochrome is shown as displayed by LSC software. Scattergrams (left column) show **Green Max Pixel** (peak TUNEL label intensity of cell) plotted against **Area** (fluorescent area of scanned cell). Boxed area in graph includes only single cells (coloured red), and excludes cell clumps and debris (black). Scattergram data reflected in adjacent histogram (right column; note arbitrary '**Count**' scale is set by LSC software). Colours correspond to scattergram with red region lying within selected box. High apoptosis in positive control cultures, (ie. **ethanol** treated) is shown by high fluorescent signal (red peak shifted right). Corresponding scattergram also shows strongly fluorescent cells at right within boxed region. This pattern is seen to a lesser degree in **pressure** treated cells, but is negligible in negative **control** cells.

2.4.4 Activated caspase-3 assay

One of the key executors of apoptosis is the caspase cascade, and the caspase-3 component has been implicated in high pressure induced apoptosis in haemopoietic cells (Take, Yamaguchi et al. 2001). Specifically caspase-3 activation is thought to be partially or totally responsible for the proteolytic cleavage of many key proteins which are implicated in apoptosis, including poly (ADP-ribose) polymerase (PARP) (Nicholson, Ali et al. 1995). Activated caspase-3 can be detected by antibodies to the cleaved (active) state. We selected a commercial kit for cleaved caspase-3 for immunofluorescent detection of this apoptotic pathway (Cell Signalling).

Neurons on coverslips were fixed by 4% PFA and washed with PBS. Cells were blocked in 5% normal rabbit serum in PBS/0.3% Triton X-100 for 60 min. After a PBS wash they were incubated with primary cleaved caspase-3 antibody (1:100 stock in PBS/Triton) at 4⁰ C in a humidified chamber overnight. Coverslips were rinsed in PBS and incubated with FITC or Cy3 secondary anti-rabbit antibodies (1:50 stock in PBS/Triton) at room temperature in the dark for 120 min. All subsequent steps were undertaken without direct light exposure. After rinsing in high salt PBS (0.4M NaCl) coverslips were mounted with antifade onto glass slides. FITC coverslips were counterstained with PI (1:20 stock) for 10 min prior to mounting. Analysis was performed for morphology and marker staining as per techniques described above.

Chapter Three

Study of Pressure System

3

3.1 Introduction

In vitro systems for subjecting biological tissues to variable pressure conditions have been used for some years. One of the first reported studies directly linking pressure and apoptosis used a sophisticated design capable of attaining very high pressures, and the subsequent effects on haemopoietic cells (Takano, Takano et al. 1997). Using an optical liquid high-pressure apparatus these cells were exposed to over 85 Mega Pascals, or 600,000 mmHg over and above atmospheric pressure. This range is beyond physiologically relevant levels, especially considering baropathies like glaucoma, where RGC death occurs at between 10 to 100 mmHg (Caprioli 1995; Aung, Ang et al. 2001).

Neuronal cultures from rat brains have been exposed to 50 millisecond pressure pulses of gas applied to modified cell culture wells with deformable silastic membrane bottoms (McKinney, Willoughby et al. 1996). Oscillatory pressures have also been applied to non-neuronal tissues (Parkkinen, Ikonen et al. 1993) (Seko, Fujikura et al. 1999). These transient pressure conditions however do not reflect the pathological processes of diseases like glaucoma where the application of pressure is much more subtle and dependant on constant rather than rapidly varying levels of pressure.

The most physiologically relevant in vitro model for varying pressure conditions in a range and manner consistent with the pathogenesis of glaucoma is a pressure chamber with consistently variable hydrostatic pressure stable over time. Such an in vitro model is well established in other areas of research, with several analogous apparatuses achieving constant pressures in the range of 0-250 mmHg for durations of hours (Sumpio, Widmann et al. 1994; Mattana and Singhal 1995). We developed such a pressure chamber apparatus and used this in the studies reported in this thesis.

3.2 Results

3.2.1 Pressure testing

The apparatus was successfully demonstrated in water bath testing for airtightness to maintain a pressure of over 100 mmHg for several hours. Testing the apparatus in situ within the pressure chamber and connected to external components confirmed the water bath findings. The pressure within the chamber was determined to be consistently within 2 mmHg of the initial target pressure, even at the upper ranges of 100–200 mmHg. From time to time when connections experienced fatigue from repeated experiments this airtight quality deteriorated and the pressure holding ability was more variable. Maintenance was carried out (repeat testing as described in Chapter 2), and repair or replacement of faulty components undertaken, around every 6 months.

3.2.2 Gas effect

Sampling of culture media prior to and immediately following pressurisation was undertaken for primary rat retinal cultures and the B35 cell line. Six B35 experiments were undertaken for the gas effect. Specimens were taken from control (C) and pressurised (P) groups at three serial timepoints; (i) prior to any experimental conditions (t0), (ii) after 2 hrs of 100 mmHg pressurisation (C2, P2), and (iii) a further 2 hrs after pressure had been normalised to 0 mmHg (C4,P4). Data for pH, pO₂ and pCO₂ were analysed for timepoints in both pressure and control groups (Figs. 3-1 to 3-3).

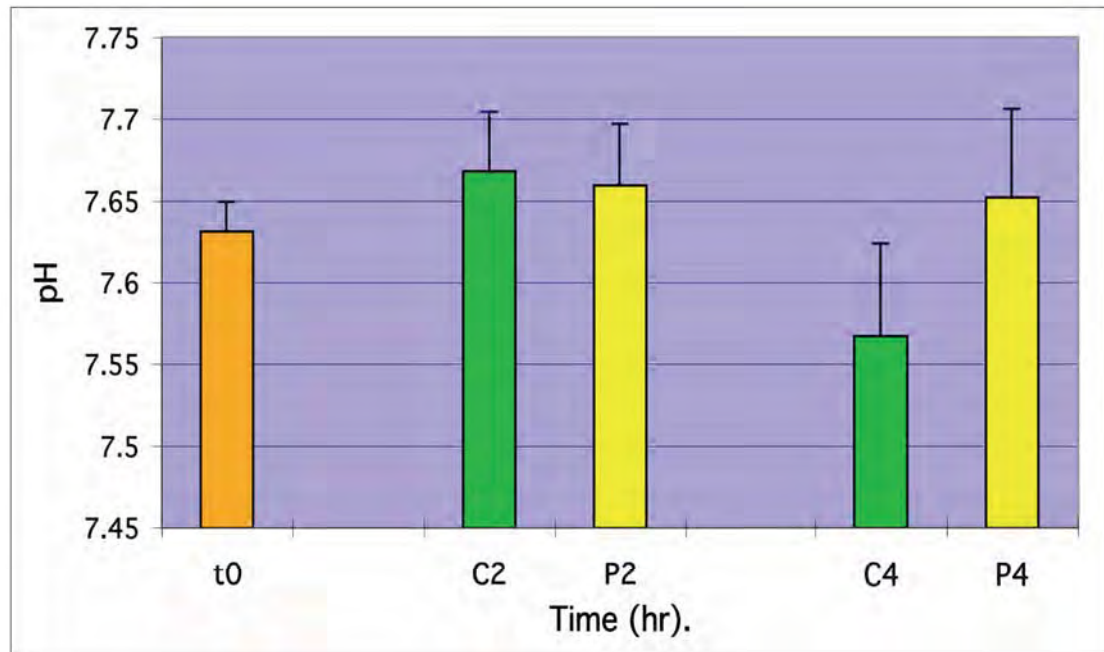


Figure 3-1 Analysis of gas effect in pressure chamber: pH

Graph of culture samples analysed for pH at sequential timepoints for Control (C) and Pressure (P) groups. pH values at C2, P2 timepoint (immediately after pressure conditions of 100 mmHg for 2 hrs) are close to pre-experiment levels and to each other. Statistical analysis of both 2 hrs and 4 hrs timepoints failed to show any significant difference between the negative control and pressure group samples ($p > 0.4$, $n = 6$, mean \pm SEM). Thus the results suggest that pressure conditions in the experimental apparatus had no effect on pH.

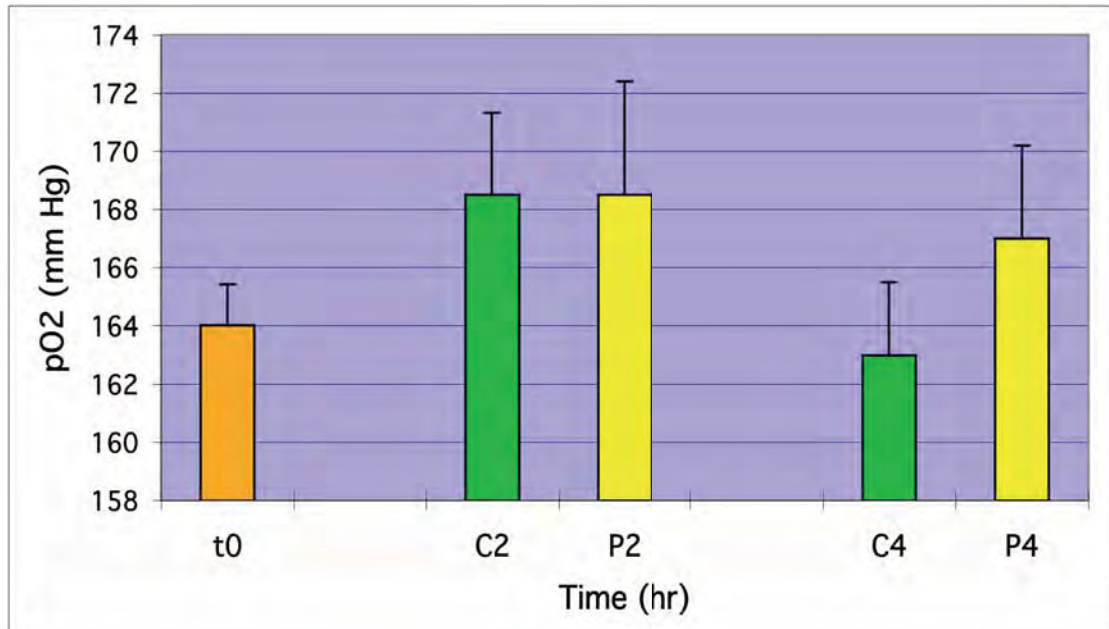


Figure 3-2 Analysis of gas effect in pressure chamber: pO₂

Graph of culture samples analysed for pO₂ at sequential timepoints for Control (C) and Pressure (P) groups. Statistical analysis of both 2 hrs and 4 hrs timepoints failed to show any significant difference between the negative control and pressure group samples ($p > 0.5$, $n = 6$, mean \pm SEM). The results suggest that pressure conditions in the experimental apparatus had no effect on pO₂ composition.

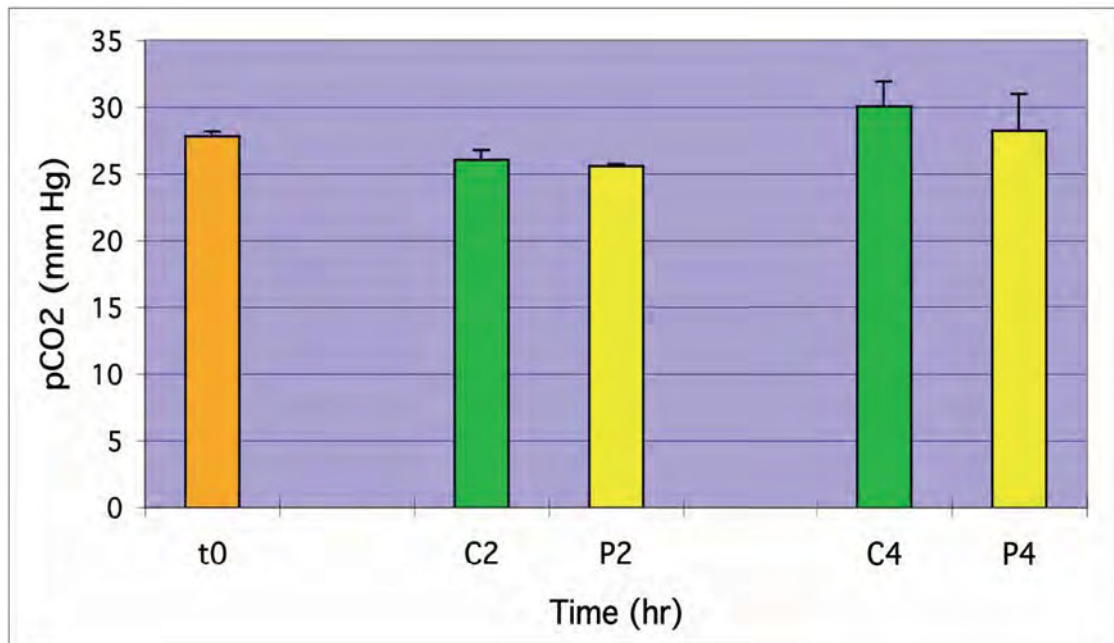


Figure 3-3 Analysis of gas effect in pressure chamber: pCO₂

Graph of culture samples analysed for pCO₂ at sequential timepoints for Control (C) and Pressure (P) groups. Statistical analysis of both 2 hrs and 4 hrs timepoints failed to show any significant difference between the negative control and pressure group samples ($p > 0.1$, $n = 6$, mean \pm SEM). These results suggest that pressure conditions in the experimental apparatus had no effect on pCO₂ composition.

Two key points emerge from the data presented in Figs. 3-1 to 3-3. Firstly there were no significant changes in the three parameters pH, pO₂ and pCO₂ at all three timepoints in either the 100 mmHg pressure application (P) or the unpressurised control (C) group. Secondly and more importantly all the parameters were also unchanged after cultures were subjected to the experimental conditions of 100 mmHg for 2 hrs.

Data were most consistent for the 2 hrs timepoint (C2, P2). Later timepoints showed the same pattern in pressure and control groups though the variations were inconsistent. Further statistical analysis was therefore done on this more reliable 2 hrs timepoint data, and these results are summarised in Table 3-1.

Table 3-1. Assessment of pressure apparatus for gas effect

Treatment	Control	Control	Pressure
Time (hr)	t0	t2	t2
pH	7.63 ± 0.02	7.67 ± 0.04	7.66 ± 0.04
pCO ₂ (mmHg)	27.8 ± 0.4	26.1 ± 1.0	25.6 ± 0.4
pO ₂ (mmHg)	164 ± 1.4	168.5 ± 2.8	168.5 ± 3.8

This table shows pH, pCO₂ and pO₂ measurements at time zero (initial or 'atmospheric' measurements, t0) and at 2 hrs (t2) in the 'pressure' group (cultures exposed to conditions of 100 mmHg for 2 hrs) and in the unpressurised 'control' group. Statistical analysis of the data showed no significant difference between t0 and t2 for pH, pCO₂ and pO₂ measurements for control or pressure groups. Likewise the difference between the t2 control and t2 pressure group was not significant (n=6 in all cases).

3.3 Discussion

We designed a system based on pressure chambers which offered several advantages. The relative simplicity of the design ensured a more transparent process with fewer elements that may have affected the experiment or gone undetected. As a result we were able to control and minimise potentially confounding variables, as there were no hidden ‘black boxes’ to complicate the setup. This enhanced our ability to troubleshoot the system as the apparatus was refined.

The ability of the apparatus to maintain desired pressure levels of ~100 mmHg is consistent with the range of pressures used in this pressure chamber model by its earlier proponents, who also achieved constant pressures in the range of 0-250 mmHg for durations of hours (Sumpio, Widmann et al. 1994; Mattana and Singhal 1995).

Measures of gas effect parameters showed that the elevated pressure conditions of 100 mmHg did not significantly alter the composition of culture media compared to non-pressurised controls. Further there was no statistical change in the absolute values compared to initial readings. This was the case for both pO₂ and pCO₂, as well as for pH. These data were most reliable at the 2 hrs timepoint reflecting the nature of culture media immediately after pressurisation (Figs. 3-1 to 3-3). This period is important in assessing a potential gas effect as it is close to the altered pressure environment being studied.

Relative variability at later timepoints applied both to absolute values of the parameters and the comparisons to each other. One likely explanation for these differences or inconsistencies may be the changing nature of the culture populations. In primary retinal cultures there is a mix of neuronal and non-neuronal cells, and the

survival of these decreases dramatically over the experimental period (see Fig. 4-5). The B35 cell line remains proliferative and with prolonged time the potential for varying cell numbers increases. Thus for this proliferative cell line culture the nature of the culture varies over time. This would affect culture media composition as nutrient and O₂ uptake changed. Ultimately the reliability of the experiment is also questioned at these points as the consistency in cell numbers between wells is lost. This is highlighted in the next chapters with consistently reliable bioassay data confined to the earliest timepoints in these cultures.

This pressure model has previously been found to have a negligible impact on gas relationships of culture media, and thus has become well established in exposing cell cultures to elevated pressure regimes. Our findings compare favourably with previous studies using similar pressure chamber models in other cell systems. A variety of cell cultures have been subjected to conditions of raised pressure (from 40 mmHg to over 100 mmHg) for a range of durations (1 hr to 1 week), (Kosnosky, Tripathi et al. 1995; Qian, Tripathi et al. 1999). Relatively small variations in pH, pCO₂ and pO₂ have been noted with extended durations of pressures applied, for 24 hrs or longer, however these were not considered to have affected the viability of cells (Sumpio, Widmann et al. 1994). Mattana and Singhal (1995) using mesangial cells found small but statistically significant changes in pCO₂ and pH but none in pO₂. A series of experiments were then run with culture media adjusted to various pH levels to assess the impact of this effect on cell viability. No significant effect on the cells was found.

In summary our results suggest that the pressure conditions used (100 mmHg for 2 hrs) in the present studies did not induce any significant gas effect that might invalidate experimental results. The system could thus be used to study the effects of hydrostatic pressure on cell cultures.

Chapter Four

Study of Primary Retinal Cultures

4

4.1 Introduction

Tissue culture is a research tool for studying animal cells free of systemic influences, and is now over a century old (Kevles and Geison 1995). The principal advantage of this technique is the ability to control the physical environment. Elements of the cellular milieu including pressure can be controlled very precisely as an independent experimental variable. Organ and primary explant cultures were the first types of tissue culture developed (McGehee Harvey 1975). They retain much of the architecture of the original tissue and hence the capacity to study one component in isolation, such as neurons, is naturally limited. These types of cultures are not readily segmented into experimental subgroups and thus require fresh tissue for every experiment. It follows that for the purposes of a bioassay reproducibility is difficult to ensure (Freshney 1994).

Cell culture is the most recent method of initiating a culture and overcomes many of these limitations while retaining the benefits of tissue culture (Schaeffer 1979). The tissue from a primary explant is dispersed into a cell suspension which could then be cultured as an adherent monolayer on a solid substrate in culture medium (Freshney 2001). Primary retinal culture then involves dissection of retinal tissue from mammalian eyes and then deriving a cell culture directly from this primary explant.

Retinal cultures have been successfully established from several avian and mammalian species. Many of the dissection techniques we used in this study were based on work done on chick embryo eyes, which are relatively large and easy to separate (Finlay, Wilkinson et al. 1996). Much of the work relating to ocular diseases has focussed on mouse and rat models, as with many areas of medicine (Seigel and Notter

1992; Otori, Wei et al. 1998). Human adult retinal cultures have been described only in a few studies. Basic culture techniques have been very similar to generic methods used in rat retinal cultures, with only minor differences in the culture media (Picaud, Hicks et al. 1998; Hu and Ritch 1997). No published work on retinal cultures from human fetal tissue was available at the time we began these experiments, hence techniques were extrapolated from the neonatal rat and the adult human studies alluded to above.

The optimisation of growth conditions to ensure survival is a key concern of cell culture. This is even moreso with neuronal cells which are more difficult to successfully establish and maintain than other cell types (Sheedlo and Turner 1996; Brewer 1995). Part of the reason lies in the need for a substrate for these cells to attach to and grow on (Brewer, Deshmane et al. 1998). Once this has been addressed the main interest then turns to the nature of the culture media, and this is where much of the research focus has been. Serum supplementation has been the mainstay for most media. However it is intrinsically variable and may contain undefined elements (Honn, Singley et al. 1975). Increasingly the aim is to develop media with known constituents, so-called 'defined media'. This process necessitates the trial of different factors that may encourage survival of the cells (Brewer 1995; Cohen, Bray et al. 1994; Raju, Rao et al. 1994). Hence the establishment of a primary culture involves an extensive investigation into the potential variations in all stages of technique to ensure optimal growth conditions and reproducible cultures.

For experiments described in this chapter primary retinal cultures were established from Sprague-Dawley rats. The adults were mated at regular intervals and monitored for the birth of neonates. Donated tissue was used to establish human retinal cultures.

4.2 Results

In total 25 experimental runs were performed on neonatal rat eyes with 6 to 10 eyes per experiment (Table 4-1). The rats were aged between 1 to 2 days postnatal (P1– P2). In three experiments the age was not known precisely but was no later than 4 days (P4).

The initial experiments were designed to develop and refine the culture techniques. Once these techniques were established the growth conditions of cultures were optimised by trialling serum-based and then defined serum-free culture media. Morphological and survival assays were conducted to confirm the nature of the retinal cultures and their viability. Finally pressure experiments were undertaken exposing retinal cultures to conditions of elevated ambient hydrostatic pressure of 100 mmHg over and above atmospheric. Three of 25 experiments had to be abandoned due to either dissociation error, microbial contamination or technical errors in immunochemistry (Table 4-1).

In addition, three separate experiments with human fetal retinal cultures using a single pair of eyes in each experiment were also performed. Cultures were established with the techniques that we had developed in our rat primary retinal culture experiments. Viability was similar to that observed with neonatal rat eyes, however the relatively smaller tissue size and lower total cell numbers made quantitation difficult.

Table 4-1 Summary of experiments on neonatal rat retinal cultures

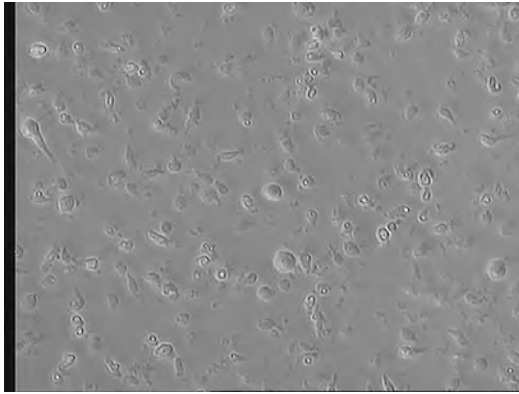
Exp No.	Age.days	n Eyes	Comment
1	P1	10	Dissection techniques trialled
2	P1	8	Dissection refined
3	P2	4	Dissociation techniques trialled
4	P1	8	Dissociation error: culture abandoned
5	<P4	6	Dissociation refined
6	P1-2	8	Culture techniques trialled
7	P1	8	DMEM F10 + PC12 conditioned media
8	<P4	6	Microbial contamination: abandoned
9	P2	6	DMEM F10 + PC12 conditioned media
10	P1	6	DMEM F10 + PC12 conditioned media
11	P1-2	6	RGC marker immunofluorescence
12	P1	6	Defined Neurobasal-B27 media
13	P1-2	6	RGC marker & survival assay
14	<P4	8	Defined Neurobasal-B27 media
15	P1	8	Defined Neurobasal-B27 media
16	P1	8	Survival assay
17	<P4	6	RGC marker assay, Annexin V assay
18	P1	6	Survival assay
19	P1	6	Survival assay, Annexin V assay
20	P1	6	Pressure run: Trial Annexin V Flow Cytometry
21	P1	8	Pressure run, TUNEL assay: Staining error: abandoned
22	P2	6	Pressure run, TUNEL assay
23	P1	6	Pressure run, TUNEL assay
24	P2	8	Pressure run, TUNEL assay
25	P1	8	Pressure run, TUNEL assay

4.2.1 Morphological examination

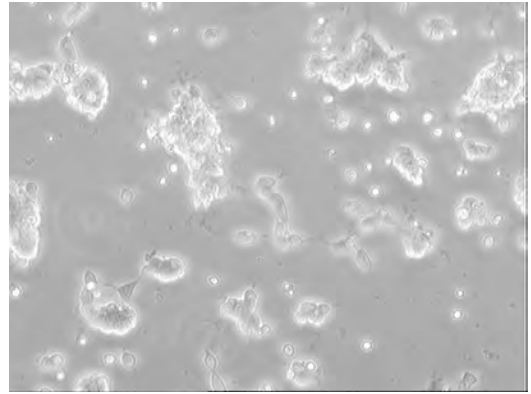
Retinal cultures from neonatal rats and human fetuses were examined by phase microscopy to assess cell viability and the general health of retinal cultures. All cultures displayed adherent cells to varying degrees with non-viable cells easily discerned as detached and floating freely in the culture media. The integrity of the cell membrane was another indicator of cell survival, as was the absence of vacuolation. Growth was evident from spreading of the soma and the proliferation of processes (Fig. 4-1).

Examination of cultures revealed scattered round neurons and glial cells. Representative pictures taken with the light microscope are shown in Figs. 4-1 and 4-2. Glial cells were noted by their fibroblast-like appearance with elongated flattened soma with no neurites (Fig. 4-2C). Neurons by contrast had more rounded cell bodies and dendrite formation, particularly after they had become more established on their substrates, usually after 4-6hr, as seen in Fig. 4-1. By several days of culture extensive neural networks were seen (Fig. 4-1E, F). Subgroups of retinal neurons were occasionally discernible. Photoreceptors had small cell bodies with fine dendrites. Amacrine and horizontal-like cells for example had intermediate sized soma, often stellate, with larger dendrites (Figs. 4-2D, E). Bipolar-like cells showed long neurites extending from the rounded soma (Figs. 4-2B, E). Morphologically RGCs were identified by their extensive neurites and the largest cell bodies (Fig. 4-2B).

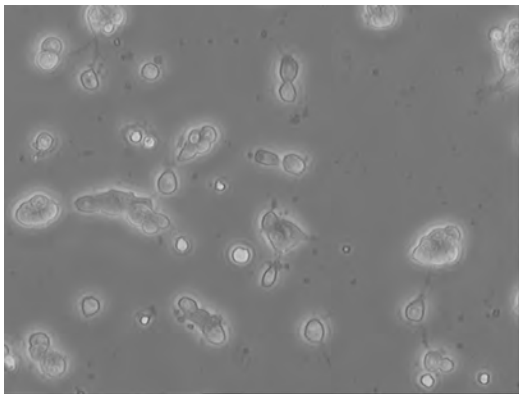
Immunocytochemistry of rat and human retinal cultures with Thy1.1 fluorescent labelling also assisted in identification of RGCs. The rhodamine secondary antibody was examined with LSM and the characteristically large cell soma and the extended ramification of the dendritic tree were noted.



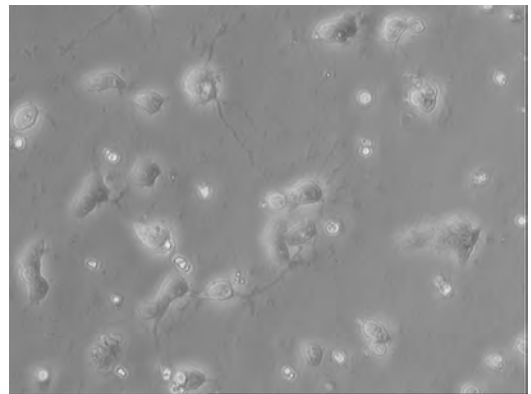
A. Cells at 6 hrs after plating (10x)
(10x magnification)



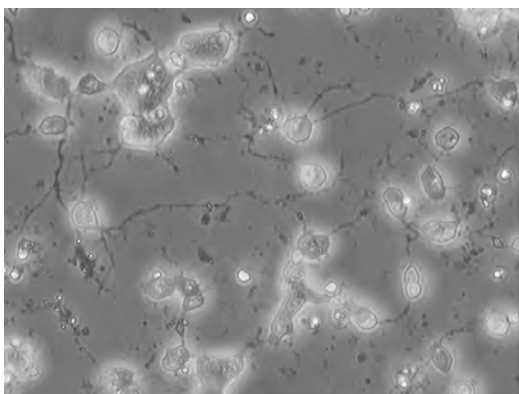
B. Cells at 18 hrs (20x)



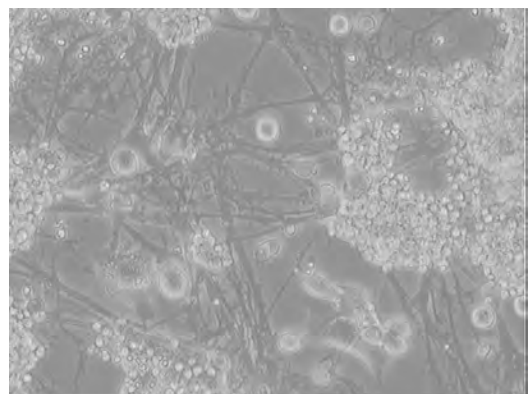
C. Cells at 18 hrs (30x)



D. Cells at 68 hrs (30x)

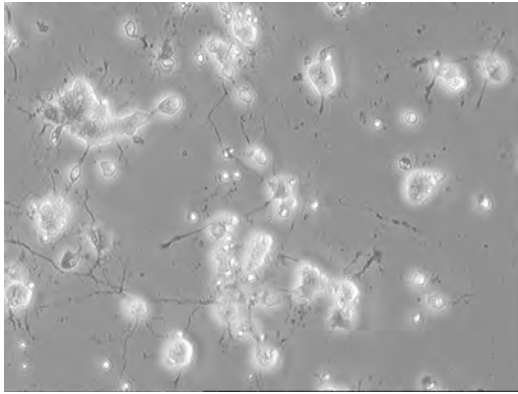


E. Cells at 144 hrs (30x)

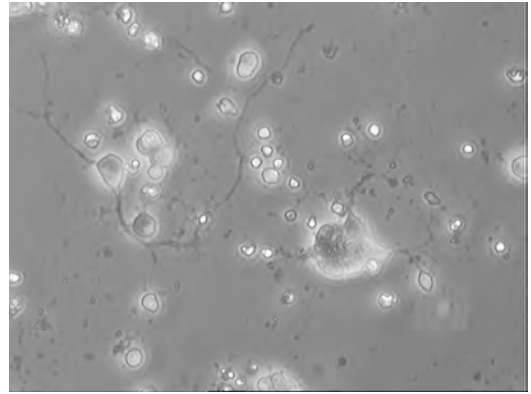


F. Cells at 198 hrs (20x)

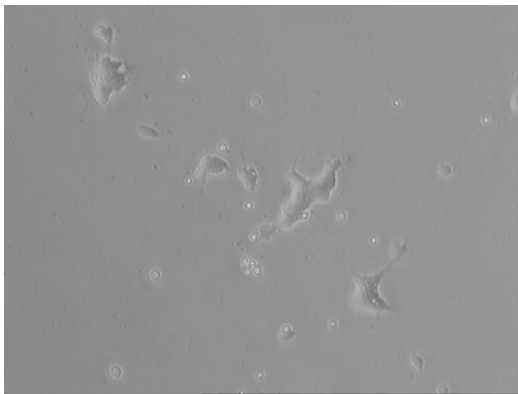
Figure 4-1 Morphology of rat retinal culture: general



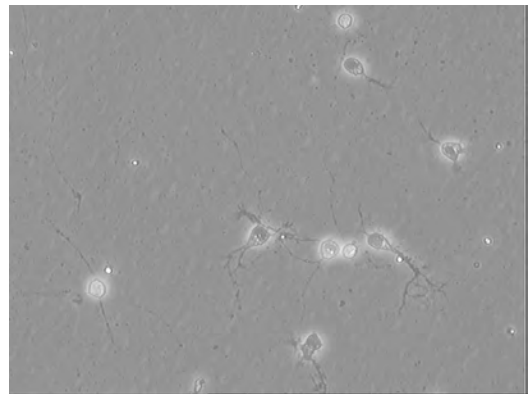
A. Mixed retinal cell types (20x)



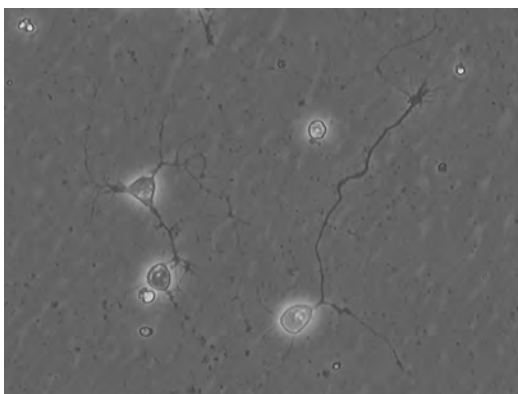
B. Bipolar-like (left) and RGC-like (right) cells (30x)



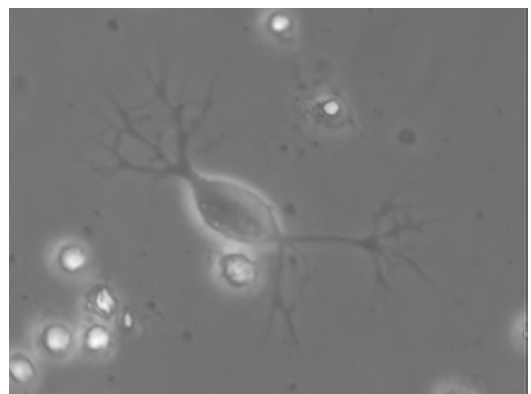
C. Glial cells (20x)



D. Amacrine-like cells (20x)



E. Amacrine-like (left) and Bipolar-like (right) cells (20x)



F. Horizontal-like cell (60x)

Figure 4-2 Morphology of rat retinal culture: cell types

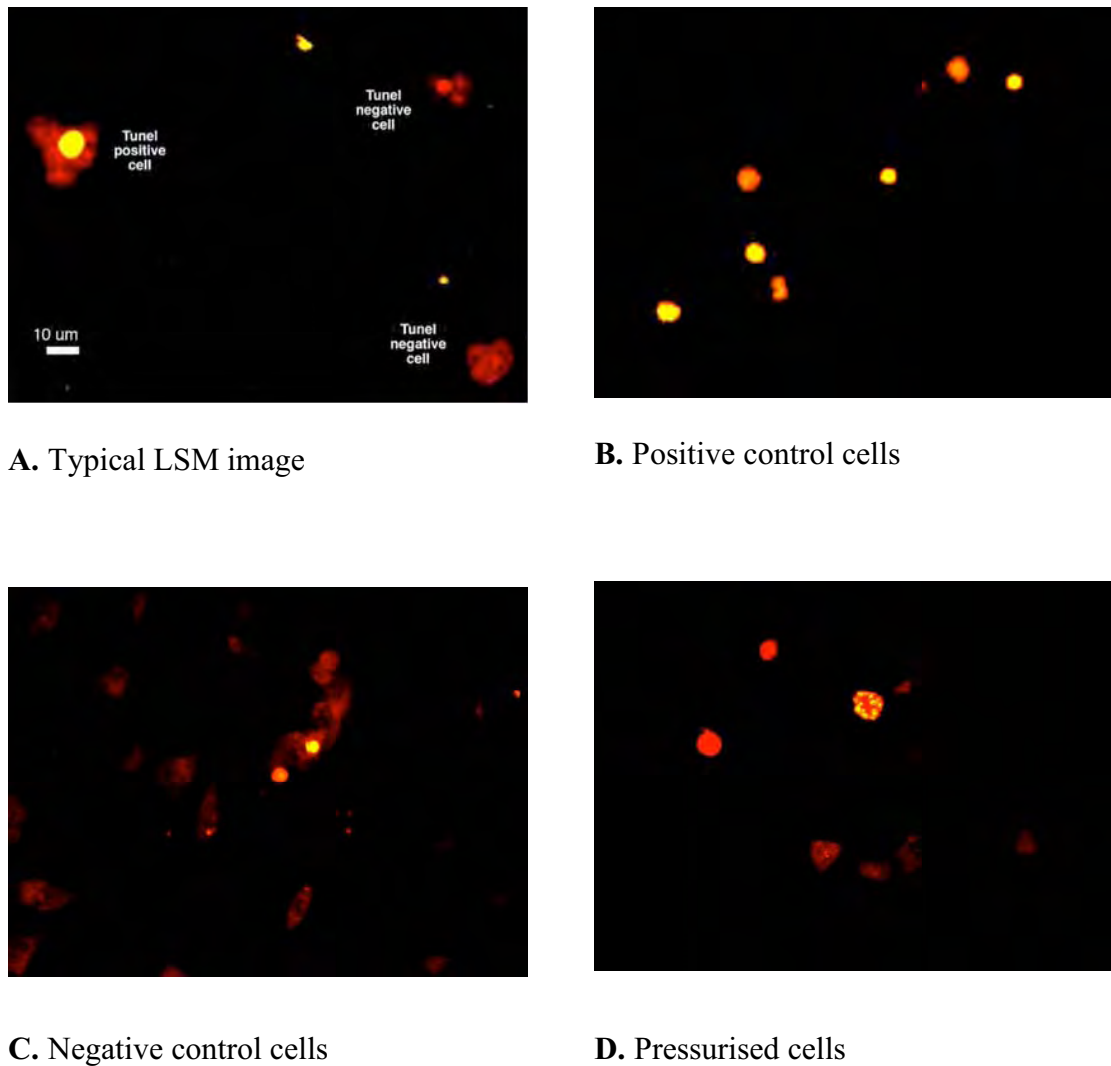


Figure 4-3 Morphology of rat retinal culture: TUNEL assay

Laser scanning microscope (LSM) images of rat retinal culture subjected to experimental protocol. Scale bar (A) equals 10 μm . **A.** Image showing typical staining of cells. TUNEL positive nuclei stain yellow, while negative nuclei do not. **B.** All positive control (ethanol treated) cells show apoptotic morphology (pyknotic cells devoid of processes) and frequent TUNEL positive staining. **C.** Negative control cells show normal morphology and infrequent apoptosis by morphology or TUNEL positive staining. **D.** Cells subjected to 100 mmHg pressure conditions demonstrate greater levels of apoptosis (a higher proportion of apoptotic cells by morphology, and more intense TUNEL positive nuclear staining) than in negative controls (C), but less than in positive control cultures (B).

Pressure experiments on rat retinal cultures were assessed for apoptosis by immunofluorescent markers Annexin V and TUNEL (Fig. 4-3). Vital dye exclusion with PI confirmed the absence of significant necrosis. Morphologically characteristics of apoptosis were seen on LSC and then imaged at higher resolution by LSM. These included the loss of processes, shrinkage of the cell body, membrane blebbing, and nuclear pyknosis. In addition specific apoptosis marker staining was noted in apoptotic cells corresponding to the label distribution, viz membrane bound for Annexin V and nuclear for TUNEL. The positive control (ethanol treated) cultures displayed the most intensely staining apoptotic cells, with lesser signs in pressurised cells and the least in negative control cultures.

4.2.2 Quantitative analysis

Rat retinal cultures were assayed live with immunofluorescent stains for PI vital dye exclusion and Annexin V for apoptosis marking. Manual cell counts were taken with the LSM, which enabled quantification of survival curves. The median counts for the four survival assays are graphed in Figure 4-4. Early cell counts (12 hrs) show that almost two-thirds of adherent cells were viable. This decreased dramatically and by 48 hrs only one third of the original numbers remained. Across the range of experiments the curves repeated the drop off in viable cells but varied considerably by 24 hrs and at the later timepoints, with some cultures managing only 15% survival by 48 hrs.

The RGC component of retinal cultures was assessed with Thy1.1 antibody immunofluorescence. Manual cell counts were taken of Thy1.1 positive RGCs and total cell numbers on the LSM. The average RGC proportion was about 4% of all cells.

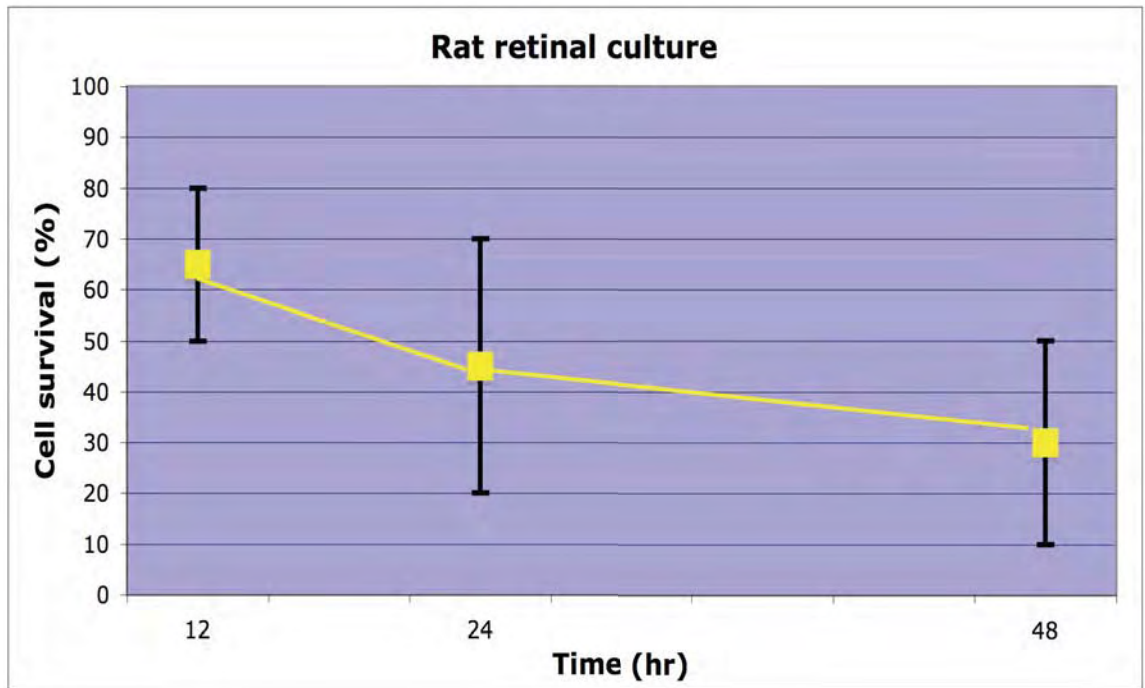


Figure 4-4 Survival assay of rat retinal cultures

Graph showing survival of mixed retinal culture cells over time. Yellow markers represent median values of manual cell count and black error bars are the range of counts for assays (n=4).

A trial of assaying retinal cells after pressure experimentation by flow cytometry was then undertaken (experiment 20 in Table 4-1). These were stained by immunocytochemistry live for Annexin V apoptosis marker. The sample preparation is dependant on cells being resuspended in media to enable the flow cytometry. This disrupted the adherent neurons to a large extent, such that the data generated were meaningless with almost no reliable cell signal measured and no pattern discernible.

In the last four pressure experiments on rat retinal cultures (Table 4-1) cells were assayed for apoptosis with the TUNEL immunofluorescent marker. Quantitative analysis was performed with LSC and marker intensity for both parameters of Green Max Pixel (GMP) and Green Integral (GI) was assessed. These results are graphed in Figs. 4-5 and 4-6.

It is evident from these figures that the known apoptotic stimulus ethanol (E) induced a high level of apoptosis. Staining intensity for these positive control cultures was markedly higher for both LSC parameters of GMP and GI. This confirmed the bioassay's ability to detect this mode of cell death. At each timepoint (2 hrs, 6 hrs and 24 hrs) the level of apoptosis of retinal cultures subjected to 100 mmHg for 2 hrs (P) is greater than the matched negative control (C). This was statistically significant ($p < 0.05$) at 6 hrs and 24 hrs for both GMP (Fig. 4-5), and GI (Fig. 4-6). These results thus suggest that the hydrostatic pressure elevation was associated with induced apoptosis in these primary rat retinal cultures.

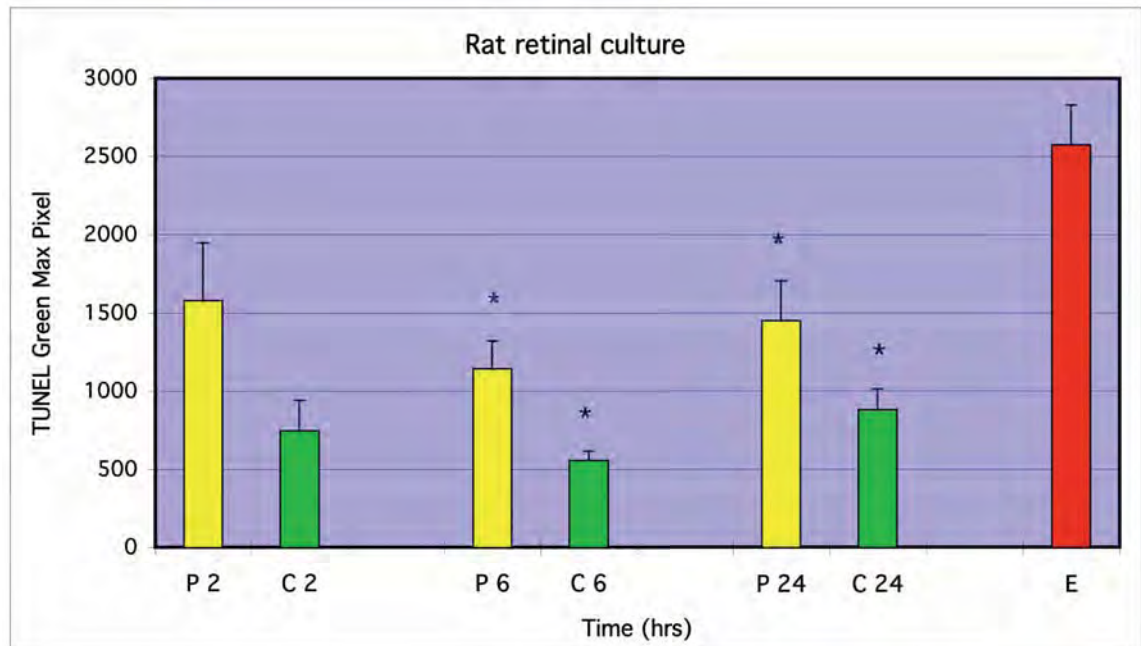


Figure 4-5 Rat retinal culture: Quantitative analysis of TUNEL assay (GMP)

Rat retinal culture following pressure conditions of 100 mmHg for 2 hrs. TUNEL assay for this immunofluorescent marker of apoptosis, whose intensity was measured by LSC for the Green Max Pixel (GMP) parameter (numerical intensity values set by LSC). Positive ethanol control (E) confirms highly induced apoptosis. Cultures exposed to pressure (P) show greater levels of GMP staining compared to unpressurised negative controls at all three timepoints. However the results were significant at 6 hrs and 24 hrs ($p < 0.05$, $n=4$; mean \pm SEM).

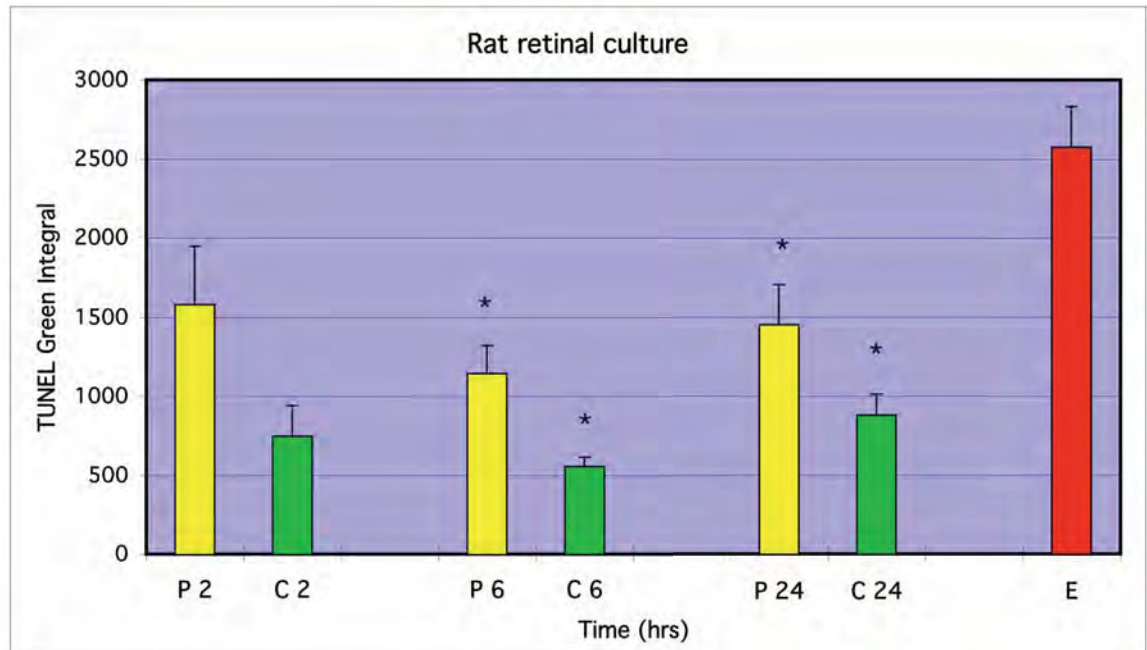


Figure 4-6 Rat retinal culture: Quantitative analysis of TUNEL assay (GI)

Rat retinal culture exposed to pressure of 100 mmHg for 2 hrs. TUNEL assay for this immunofluorescent marker of apoptosis, whose intensity was measured by LSC for the Green Max Pixel (GMP) parameter (numerical intensity values set by LSC). Positive ethanol control (E) confirms highly induced apoptosis. Cultures exposed to pressure (P) show greater levels of GI staining compared to unpressurised negative controls at all three timepoints. However the results were significant at 6 hrs and 24 hrs ($p < 0.05$, $n = 4$; mean \pm SEM).

4.3 Discussion

During the initial phase of these experiments we developed the culture techniques that would optimise the cell survival and yield reproducible results. This methodology was then continued and subject to ongoing refinement as problems were identified or improvements trialled. The first step was the dissection of ocular tissue which was facilitated by the use of a dissecting microscope with a 10x magnification objective. Refinements included immersing the eyes in culture media to minimise tissue disruption and prevent retinæ from drying out.

Dissociation of the retinal tissue is a balancing act between achieving an ideally single cell suspension without destroying too many valuable cells in the process. We used enzymatic methods, using Trypsin and DNase, for the most part supplemented by trituration to physically dissociate any residual clumps at the end. This also needed some modification, in particular the need to minimise cell damage by mechanical dissociation by reducing the intensity and vigour of trituration. These phases of the culturing process were successfully developed within the first five experiments.

In vitro work on animal tissue is in the first instance invariably preoccupied with trying to maximise the survival of the extracted tissue in an artificial setting. Cell culture takes this concern to a higher level as the laboratory must attempt to reproduce the in vivo environment. The major emphasis in establishing the cultures then was on maximising the survival of retinal cells. Adherence was a crucial starting point as survival assays with PI staining of early runs suggested a minimum of 2 hrs was required to allow a reasonable number of cells to attach to coverslips. The coating substrate was changed from rat tail Collagen Type 1 to Poly-L-Lysine with improved

cell retention and reduced variability in substrate adherence, as has been the experience of others (Raju, Rao et al. 1994; Brewer, Deshmane et al. 1998).

As mentioned earlier, the greatest impact on optimising cell culture viability is from the culture media. Retinal cultures were first grown in media based on DMEM supplemented with FCS and PC12 conditioned media, broadly similar in composition, and similar to Nichol's technique (Nichol, Everett et al. 1994). Initial results were encouraging with some viable cells and occasional prolonged survival. However microbial contamination and extreme variability in survival led to the trialling of 'defined media' - the Neurobasal/B27 based media.

This media demonstrated greater consistency in culture viability and was used in the remainder of experiments (experiments 12-25, Table 4-1). The improved survival reflects the work of GJ Brewer, who developed the B27 supplement (Brewer, Torricelli et al. 1993). They offer several reasons why this combination may be more useful than DMEM for neuronal cultures in particular. Neurobasal contains less NaCl and NaHCO₃ lowering osmolality and thus reducing glial proliferation. It has additional amino acids and the B27 supplement has 20 further ingredients including vitamin E, antioxidants, insulin and transferrin (Brewer 1995). The serum free nature of this medium may also help explain greater consistency in cultures, compared to the earlier cultures with the inherent variability of fetal calf serum.

A host of other factors have been suggested as enhancing the survival of retinal cultures, and RGCs in particular. These include brain derived neurotrophic factor from astrocyte conditioned medium (Castillo, del Cerro et al. 1994), neurotrophins-4/5 in adult retinal explants (Cohen, Bray et al. 1994) and target derived trophic factor from retinal glial conditioned medium (Raju, Rao et al. 1994). These are however dependant on the generation of additional primary cultures thus adding another level of both

complexity and potential variability to the culture model.

The human fetal retinal cultures appear to have grown favourably in this defined media. Interestingly the published studies involving adult human retinal cultures used serum supplementation of DMEM media (Hu and Ritch 1997; Picaud, Hicks et al. 1998). The scarcity of this tissue pre-empted the investigation of alternative or supplemental media compositions for optimising culture conditions. Related to this low tissue supply was the smaller size of samples, namely a single pair of eyes at a time, and hence of total retinal cell numbers. The potential for survival and other quantitative assays, including of pressure conditions, was thus limited.

Survival rates of rat retinal cultures in our experiments (Fig. 4-4) were comparable to those of others using similar methods. Attrition rates of 50% by 24 hrs, with survival rates of 25% by 48 hrs have been reported in such cultures (Takahashi, Lam et al. 1992), while another study suggests even lower rates of 10% survival by 24 hrs (Nichol, Everett et al. 1994). The composition of these mixed retinal cultures with respect to RGCs in our study was also similar to other research, with RGC proportions of 7% reported (Castillo, del Cerro et al. 1994). Our results suggest that the viability of established retinal cultures and the RGC population grown therein were similar to reported work, though the marked variability in survival was also comparable.

Morphological analysis reflected the expected mix of glial and neuronal cells. Specific characteristics of neurons such as neurite formation were readily seen (Fig. 4-1). Although cultures were by nature variable in exact composition from one coverslip to the next, it was possible to broadly delineate subgroups of retinal neurons such as horizontal and amacrine cells and photoreceptors (Fig. 4-2) (Picaud, Hicks et al. 1998).

Rat retinal cultures subjected to pressure conditions demonstrated morphological features of apoptosis such as cell shrinkage and loss of processes. In addition specific apoptosis markers corroborated the presence of morphological characteristics with positive immunofluorescence in affected cells. The LSC was found to be a particularly useful research tool by enabling automated cytometry and concurrent fluorescent microscopy of cells of interest (Bedner, Li et al. 1999; Juan and Darzynkiewicz 1998).

Known apoptosis induction by ethanol was also demonstrated reliably and at consistently high levels. TUNEL immunofluorescent marker labelling was measured by LSC for two parameters of fluorescent intensity, Green Max Pixel (GMP) and Green Integral (GI). Both of these have been demonstrated to be reliable indicators of apoptosis with the TUNEL apoptosis assay (Darzynkiewicz 1998). Figs. 4-5 and 4-6 illustrate that for both GMP and GI the maximal levels of ethanol induced apoptosis were almost twice the intensity of the highest values seen in any experimental culture. This correlates well with morphological analysis of retinal cultures, where subjectively the fluorescence of labelled cells was much greater with the ethanol treatment.

Quantitative pressure data for the rat retinal cultures demonstrated a definite increase in measurable apoptosis after the experimental conditions of 100 mmHg ambient hydrostatic pressure over and above atmospheric pressure for a duration of 2 hrs. This was true for both intensity parameters of TUNEL measured by LSC, namely GMP and GI. Absolute values for fluorescent marker labelling were consistently higher in pressurised cultures (P) than corresponding negative controls (C) at all timepoints after the application of pressure (Figs. 4-5 and 4-6). However this difference was not of statistical significance until the later timepoints. The initial timepoint of 2 hrs was taken immediately after termination of experimental pressure conditions (ie. restoration of pressure to atmospheric conditions). No induced apoptosis of significance was recorded

at this timepoint. It was not until at least 6hr after pressure conditions were applied that the recorded data reached this level of statistical significance ($p < 0.5$, $n=4$). This was noted in both GMP and GI analyses (Figs. 4-5, 4-6). TUNEL intensity values also varied between timepoints, with high initial readings but trending higher over time. The data clearly suggest the presence of apoptosis induced by our experimental conditions of 100mmHg for 2 hrs.

These results suggest that the sensitivity of cells in the rat retinal cultures to the experimental stimulus varies with time. A temporal relationship may be due to several factors, including the type of the cells in culture, their numbers and changes in this over time. For cells still able to proliferate, such as glial cells, the stage of the cell cycle is also relevant. The mixed nature of the retinal cultures implies that several types of cells, neuronal and non-neuronal, are present in every culture and every coverslip. The relative contributions of these subpopulations to any observed effect is difficult to assess. The survival data suggest that there was a decline in total numbers, further complicating the picture.

Ultimately then although an apoptotic effect on rat retinal cultures was demonstrated further interpretation of this was complicated by the multiple variables described above. These confounders also have implications for the experimental model. The primary retinal cultures were generated successfully and provided excellent morphological data as well as developing a competent algorithm for LSC analysis. However the variable survival and cell types made it difficult to achieve the consistent reproducibility needed to enhance the bioassay. This is dependant on predictable and uniform characteristics of the biological material being studied. In order to achieve this in our in vitro system an alternate form of tissue culture was required. This then is the subject of the investigations described in the next chapter.

Chapter Five

Study of Neuronal Cell Lines

5

5.1 Introduction

Cell proliferation is often found within primary cultures, including explants, and this makes the propagation of cell lines a possibility. Subculturing of a primary culture into fresh vessels constitutes a 'passage', and the resulting daughter cultures are termed 'cell lines' (Kevles and Geison 1995). Continuously replicatable cell lines can be derived by treatment such as transfection with a defined viral vector to induce phenotypic change, or 'transformation', to a clonal state. The principal features of a cell line are an implied increase in population over several generations, uniformity of cell lineage and characteristics consistent for the lifespan of the cell (Freshney 1994).

The ability to propagate uniform cell cultures repeatedly with reproducible properties confers several advantages to cell lines. For bioassays they offer consistent features of quantitation, characterisation and replicate sampling. Cell lines that have neuronal characterization are monolayer cultures that need to be propagated adherent to a substrate in order to survive. Many established continuous cell lines have been characterised for neuronal properties that have made them useful tools in research (Mills, Wang et al. 1995; Wainer, Kwon et al. 1997).

The studies reported in this chapter were carried out on four different cell lines. The first was the neuroblastoma cell line B35 derived from the rat central nervous system (Schubert, Heinemann et al. 1974; Schubert 1974). The second was the C17 cell line derived from mouse cerebellum (Weinstein, Shelanski et al. 1990). Next was the human cell line NT2, a neuronally committed teratocarcinoma cell line (Hsu and Everett 2001). Among neuronal characteristics displayed are glutamate receptor expression (Younkin, Tang et al. 1993) and neurotransmitter excitotoxicity (Lockhart, Warner et al. 2002).

These three cell lines are capable of continuous replication and have many neuronal characteristics. However they may not be post-mitotic and thus continue to proliferate. This can be problematic in a bioassay where analysis of later timepoints can be affected by population variation. Further the differentiation of a neuron to a post-mitotic state implies a further level of cell maturation with altered characteristics worthy of study.

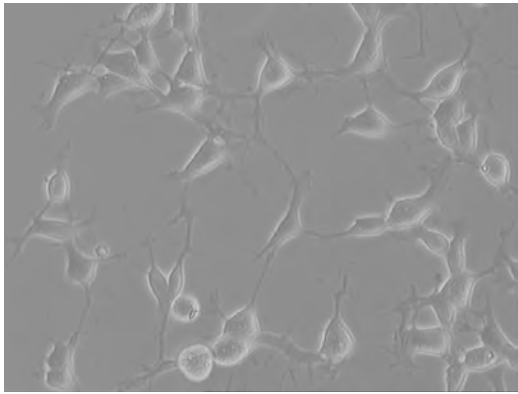
To address these issues a cell line capable of differentiation was selected. Thus the fourth cell line used was PC12, derived from rat pheochromocytoma cells and one of the most established clonal lines in use (Greene and Tischler 1976; Greene, Sobeih et al. 1991). Treatment in vitro with cyclic adenosine mono phosphate (cAMP) and nerve growth factor (NGF) produces neurons that have exited the cell cycle (Gunning, Landreth et al. 1981; Michel, Vyas et al. 1995). PC12 cultures have been used widely for the study of neuronal differentiation and function. They offer the advantage of being modifiable between a replicating state and one which is non-dividing as well as neuronally differentiated (Young, Gunning et al. 1983). Further the cell line possesses the differentiated properties of an identifiable specific subclass within the whole neuronal phenotype (Greene and Tischler 1982). Hence the PC12 cell line was included in the present studies.

All these cell lines were subjected to 100 mmHg for 2 hrs, assayed at different time intervals from 2 hrs to 24 hrs and examined for morphological and quantitative evidence of apoptosis. The methods used for these assays have been described in Chapter 2.

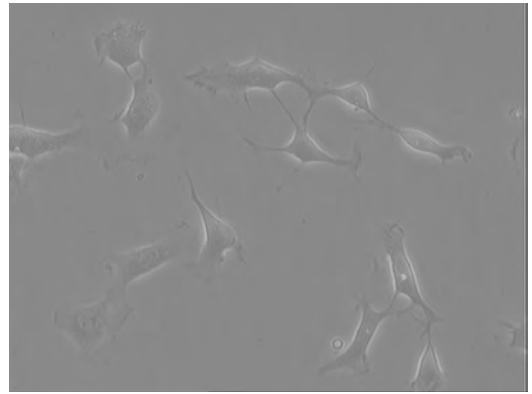
5.2 Results

5.2.1 Morphological examination

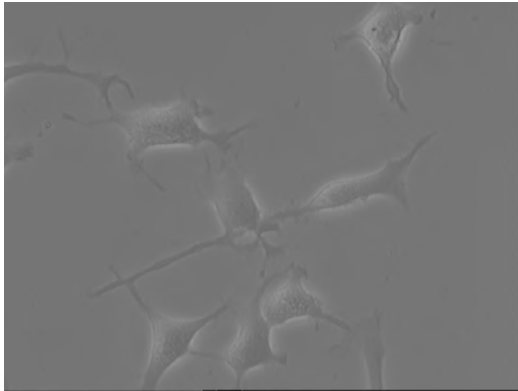
The microscope images of cell lines studied are depicted in Figs. 5-1 to 5-3. Phase light microscopy confirmed cell viability and optimal culture conditions. Similar to retinal cultures, viable cells were adherent with intact cell membranes and were non-vacuolated. Different cell lines had characteristic morphologies which varied slightly, however individual cells in a given line showed marked uniformity, a feature of cell lines in general. Neurons also displayed vigorous process formation which varied according to specific cell line characteristics. For example NT2 cell neurites were broad (Fig. 5-2) whereas PC12 neurons displayed fine dendrites (Fig. 5-3). B35 and C17 neurites were intermediate in size (Fig. 5-1, 5-2). PC12 differentiated neurons had slightly increased cell surface areas, compared with rounded undifferentiated PC12 cells (Fig. 5-3). Differentiated PC12 neurons also showed prolific dendrite formation with distinct ramifications and at times extensive growth (Figs. 5-3).



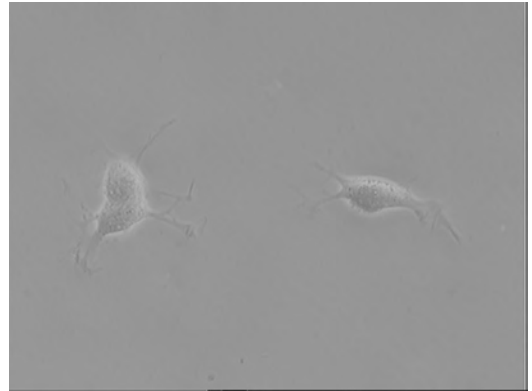
A. (20x)



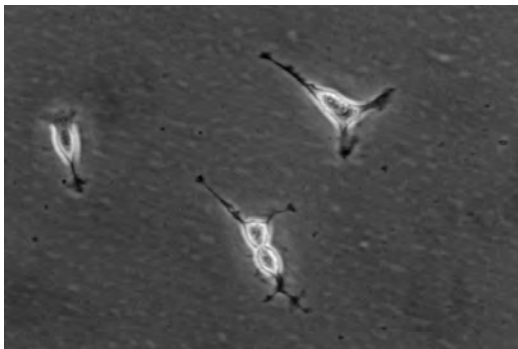
B. (20x)



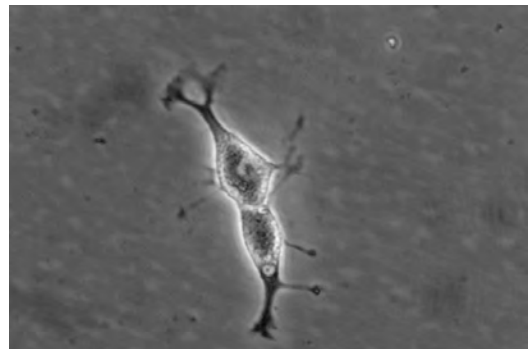
C. (30x)



D. (30x)

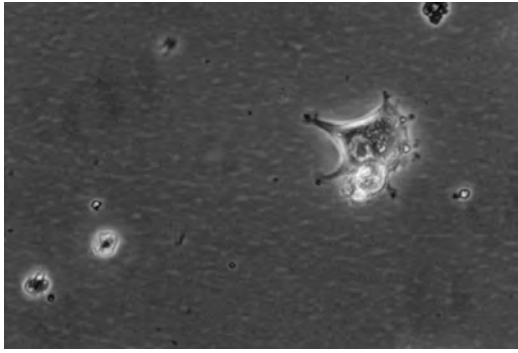


E. (30x)

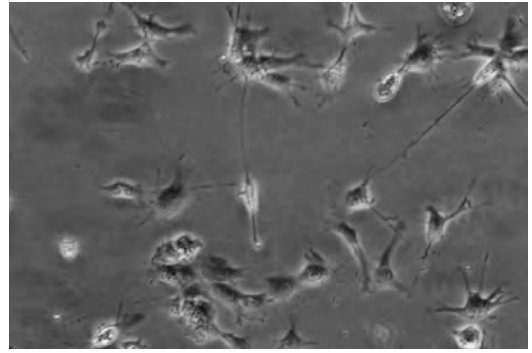


F. (40x)

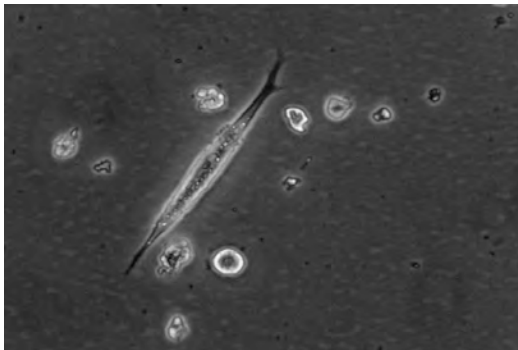
Figure 5-1 Morphology of B35 cells



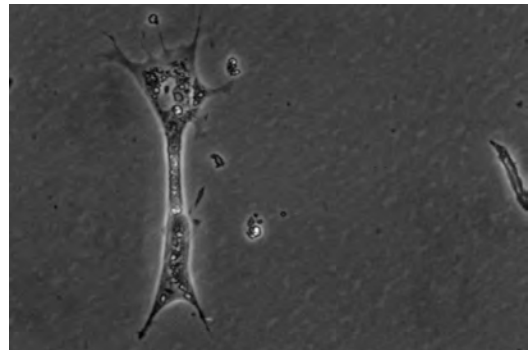
A. C17 cells (40x)



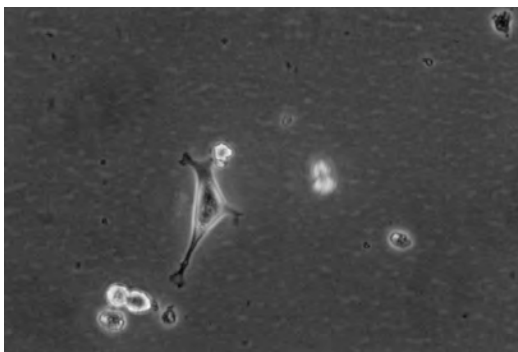
B. NT2 cells (20x)



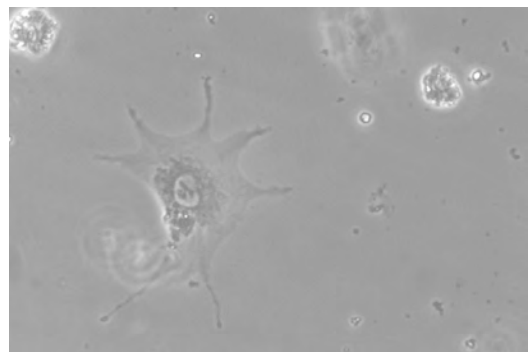
C. C17 cells (40x)



D. NT2 cells (40x)

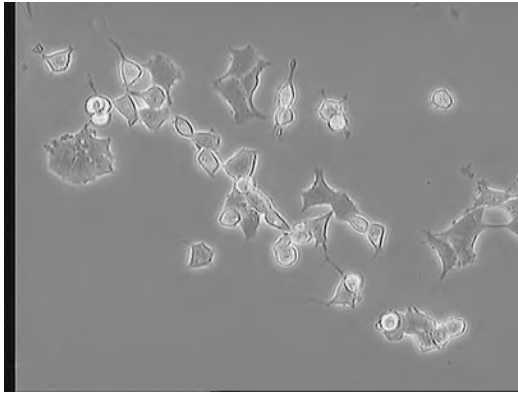


E. C17 cells (40x)

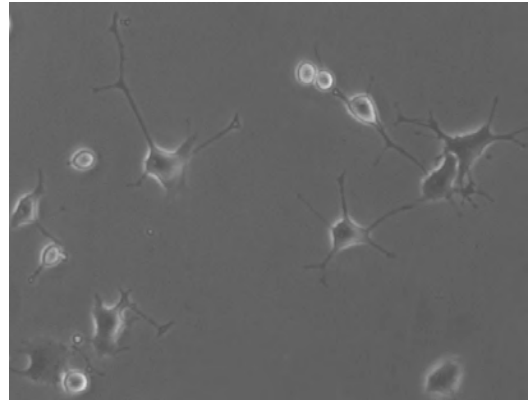


F. NT2 cells (40x)

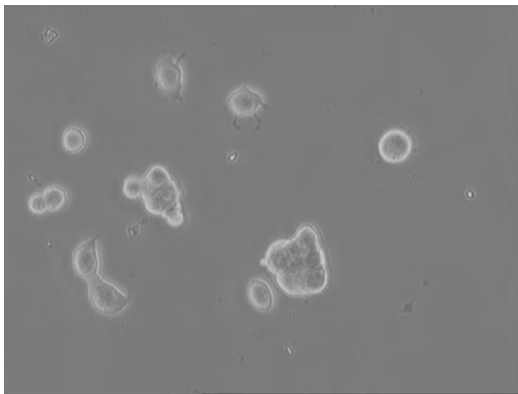
Figure 5-2 Morphology of C17 and NT2 cells



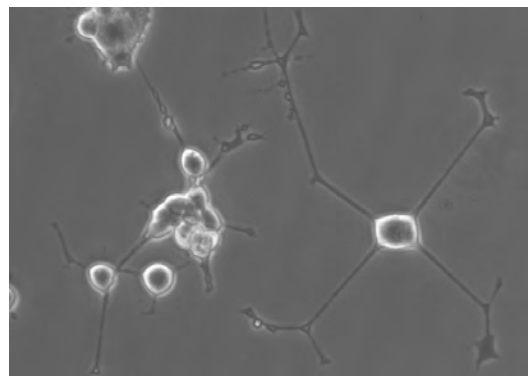
A. PC12 undifferentiated (20x)



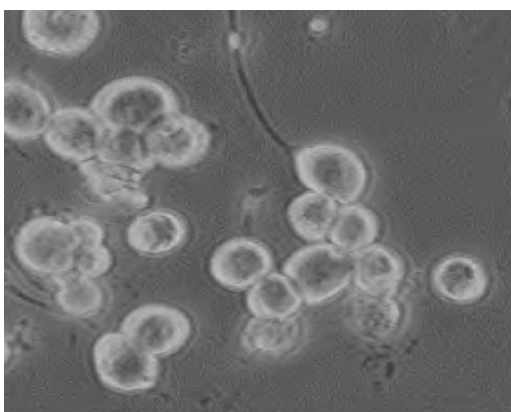
B. PC12 differentiated (20x)



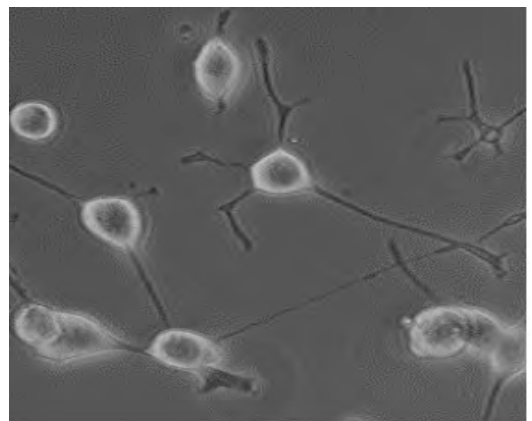
C. PC12 undifferentiated (20x)



D. PC12 differentiated (20x)



E. PC12 undifferentiated (40x)



F. PC12 differentiated (40x)

Figure 5-3 Morphology of undifferentiated & differentiated PC12 cells

Morphological analysis of the various cell line cultures subjected to pressure conditions was carried out for features of apoptosis after immunofluorescent labelling for markers Annexin V and TUNEL (Figs. 5-4 to 5-9). Staining of live cells with Annexin V and PI counterstain confirmed that the necrosis was insignificant in the populations studied by PI dye exclusion. Morphological features examined in randomly selected fields for necrotic features included swelling of both soma and nucleus, plasma membrane rupture, vacuolation and karyolysis. Confocal fluorescent LSM imaging allowed concomitant examination of both morphology and fluorochrome molecular marker. The LSM and the co-mounted fluorescent microscope of the LSC were used to examine these fluorescent markers. Digital images were taken with the higher resolution of the LSM.

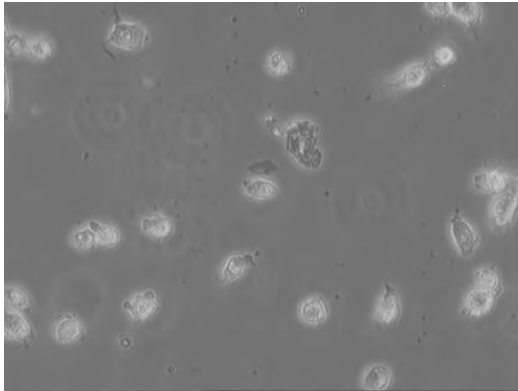
Positive control cultures treated with ethanol or DNase clearly demonstrated apoptotic characteristics consistently across all cell lines. Neurons lost their processes and their cell bodies constricted. The membranes showed scattered 'bumps' representing apoptotic blebbing (Figs. 5-4 to 5-9). This was especially evident with membrane-bound Annexin V staining (Fig. 5-6). Nuclear changes included pyknosis-shrinkage and condensation of the nuclei. TUNEL apoptosis marker staining demonstrated this most clearly. The localisation of the FITC fluorescence was seen in the nucleus, and the intensity of the staining reflected the positive finding of the nuclear fragmentation detected by this method (Figs. 5-5, 5-7 to 5-9). This intensity on morphological analysis also correlated with quantitative intensity parameters for the marker by LSC cytometry. The LSC thus confirmed the association of visual features of apoptosis with positive labeling in individual cells.

Negative control cultures (ie. not exposed to pressure conditions) showed little or no evidence of apoptosis. By far the majority of neurons in all lines showed normal

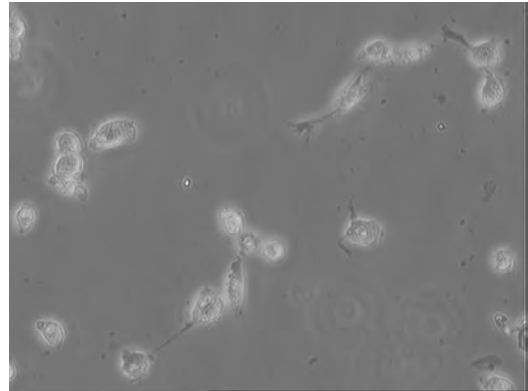
morphology of large bodied cells with processes and no membrane changes. Nuclei were not condensed and TUNEL-FITC staining was not prominent. Apoptotic cells were seen but their incidence was markedly lower. These features are seen in Figs. 5-4 to 5-8.

Cell line cultures subjected to the experimental conditions of pressure showed morphological evidence of apoptosis. The main difference in comparison to the control groups was in the frequency of apoptotic cells. These were seen in most fields and often several were evident in each field. By contrast the negative control cultures showed apoptosis only occasionally, with most fields showing none. Intensity of marker staining appeared to be intermediary in the pressure group compared to the positive and negative control cells. However this was a qualitative determination and hence it was harder to make definitive comparisons of this feature based on morphology alone. These findings applied to all cell lines (Figs. 5-5 to 5-8). Subjectively later timepoints also showed the same general pattern.

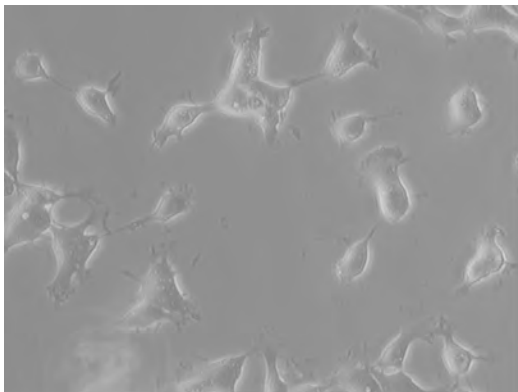
The overall impression after morphological assessment then was that the incidence and level of apoptosis in cultures exposed to pressure conditions was intermediary, less than in positive control cultures but more than in negative controls (non-pressurised neurons). This is highlighted in Figs. 5-5 to 5-8 which are montages of neurons from B35 and PC12 cultures. Each set comprises representative images from positive, negative and pressure culture groups from a single experiment assayed by TUNEL staining. Fig. 5-9 in addition includes Nomarski imaging of pressurised neurons showing details of the morphological changes described above.



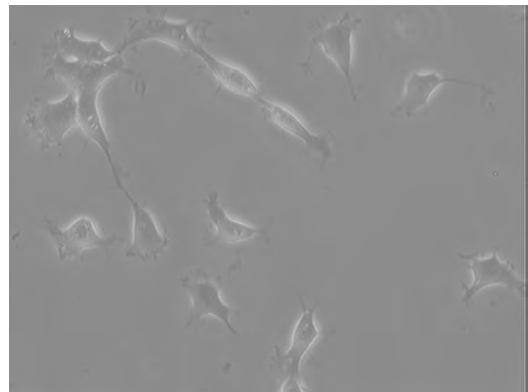
A. B35 positive control cells



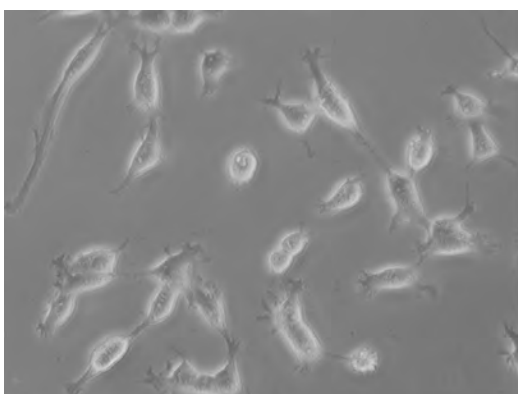
B. B35 positive control cells



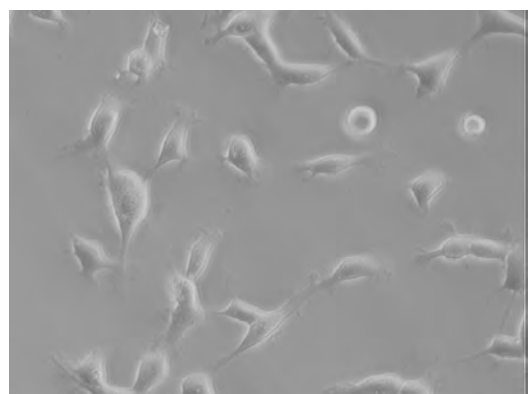
C. B35 negative control cells



D. B35 negative control cells



E. B35 pressurised cells



F. B35 pressurised cells

Figure 5-4 Morphology of B35 cells: Pressure experiment

Note apoptotic morphology (loss of processes, pyknosis, membrane blebbing) in positive controls (**A,B**). Negative controls show normal morphology (**C,D**), while several pressurised cells also show features of apoptosis (**E,F**). (20x)

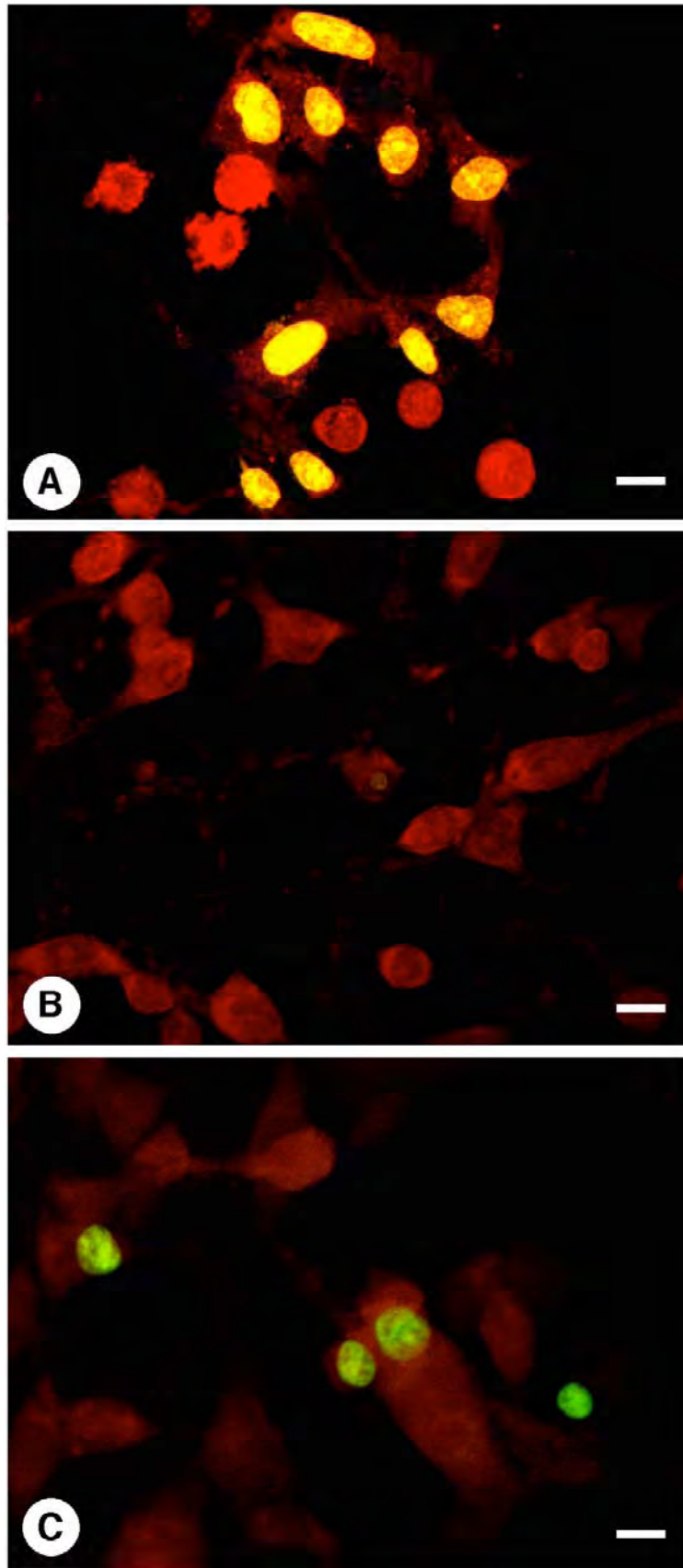


Figure 5-5 Morphology of B35 cells: TUNEL assay

Figure 5-5 Legend: Morphology of B35 neurons: TUNEL assay

A. Positive control neurons

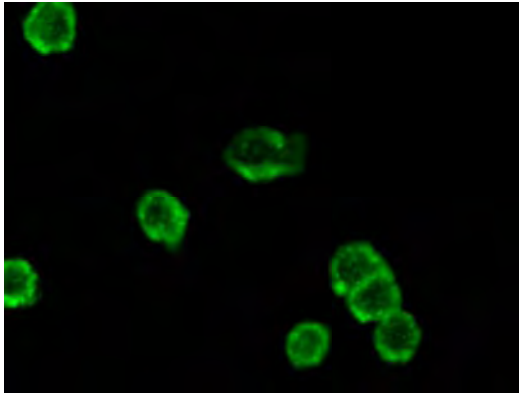
Immunofluorescent images of cultured B35 neurons treated with 5% Ethanol, a known stimulus of apoptosis, for 2 hrs. Cells stained with TUNEL assay for DNA fragmentation (green FITC fluorochrome). Counterstain with Propidium Iodide (red). Ethanol treatment gave maximal fluorochrome signal strength, with intense green and red signals appearing as yellow. Neurons show high level of apoptosis, with strongly positive nuclei for TUNEL marker, and chromatin condensation also evident in some nuclei. Remainder of cells in late stage apoptosis show morphological features of shrunken cell body, loss of processes and membrane blebs, but no longer showing nuclear changes as detected by TUNEL. Viewed with Laser Scanning Microscope (Olympus GB200). Scale Bar = 10 μ m.

B. Negative Control neurons

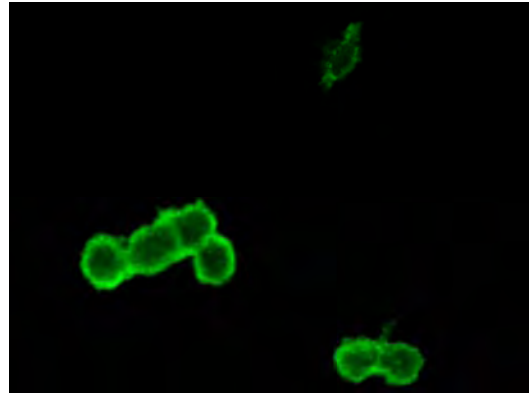
Cultured B35 neurons maintained in pressure chamber for 2 hrs but not subjected to altered pressure conditions. TUNEL assay and Propidium Iodide staining. Neurons show generally normal morphology and little or no nuclear staining for DNA fragmentation. Note centrally located cell showing weakly TUNEL positive nucleus.

C. Neurons subjected to pressure conditions

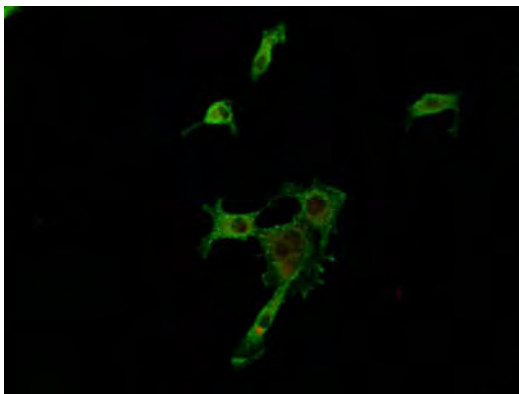
Cultures of B35 neuronal cell line following experimental conditions of elevated ambient hydrostatic pressure (100 mmHg for 2 hrs). Cells assayed with TUNEL (green) and counterstained with Propidium Iodide (red). Compared to negative controls (B) the neurons in this group showed increased levels of DNA fragmentation and some chromatin condensation as detected by fluorescent label.



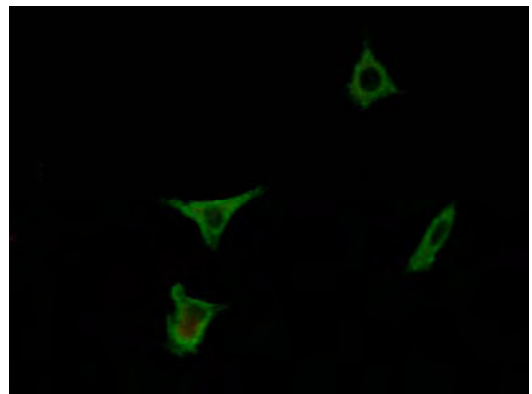
A. B35 positive control cells (40x)



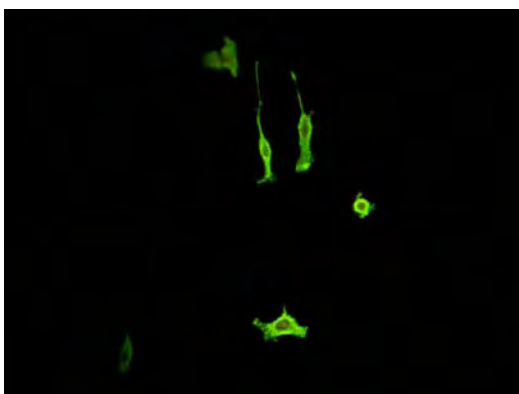
B. B35 positive control cells (40x)



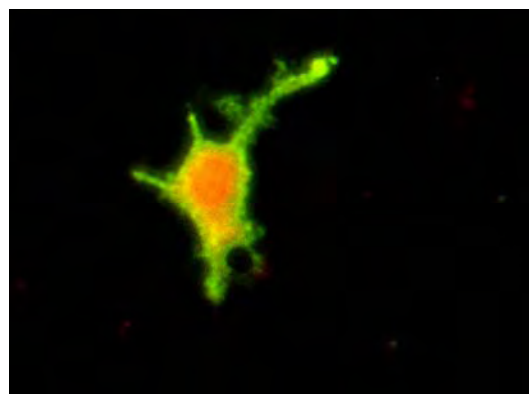
C. B35 negative control cells (20x)



D. B35 negative control cells (20x)



E. B35 pressurised cells (10x)



F. B35 pressurised cell (60x)

Figure 5-6 Morphology of B35 cells: Annexin V assay

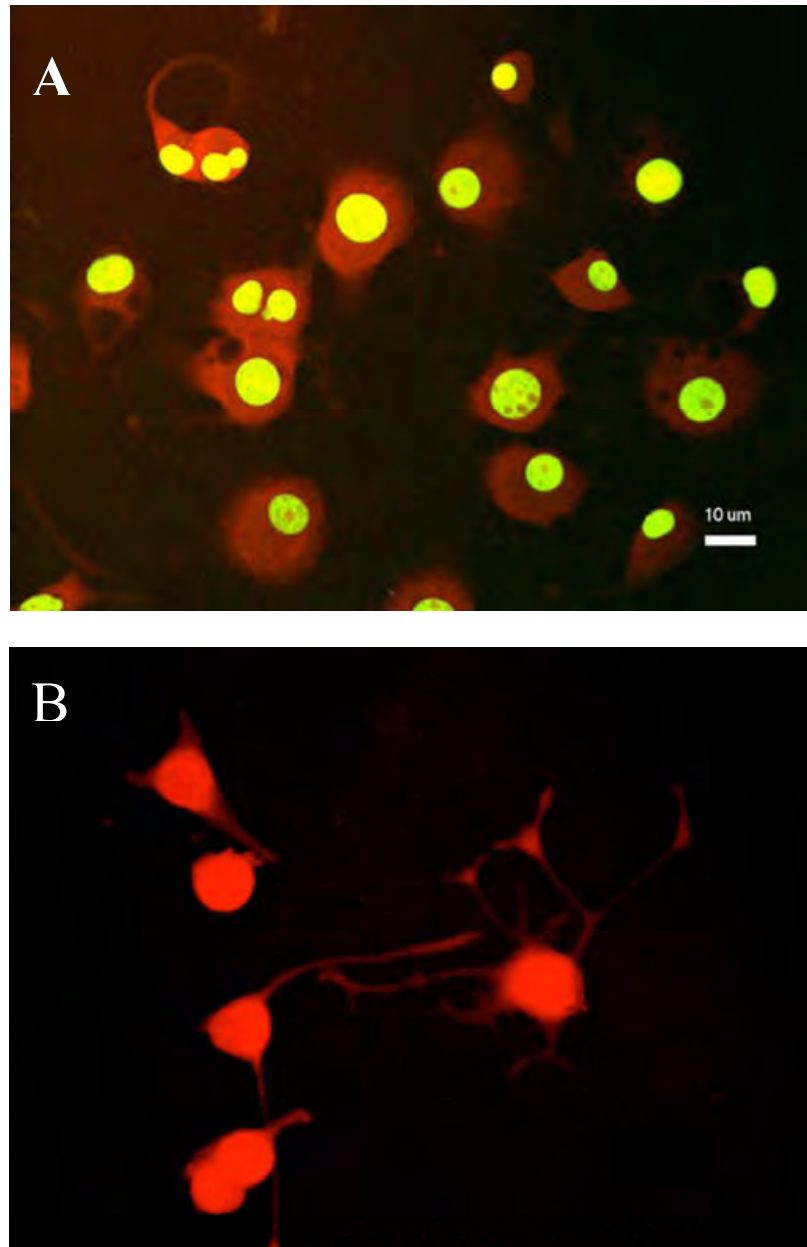
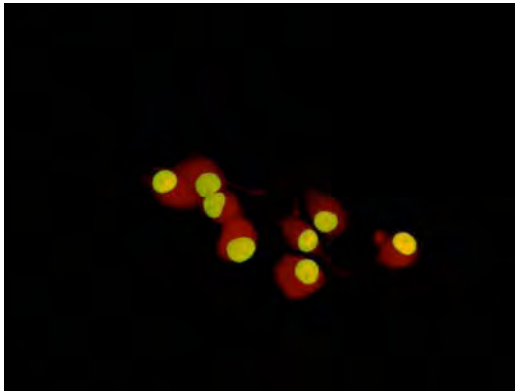
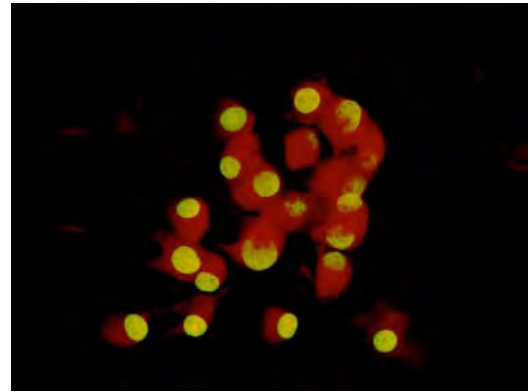


Figure 5-7 Morphology of PC12 cells: TUNEL assay

A. Differentiated PC12 neurons treated with DNase (positive control). TUNEL assay with FITC positive nuclei (yellow/green). Note widespread apoptosis (by positive nuclei and apoptotic morphology). **B.** Culture of differentiated PC12 neurons maintained in pressure apparatus at ambient pressure only (negative controls). TUNEL assay showing lack of detected apoptosis features. Scale Bar = 10 μm .



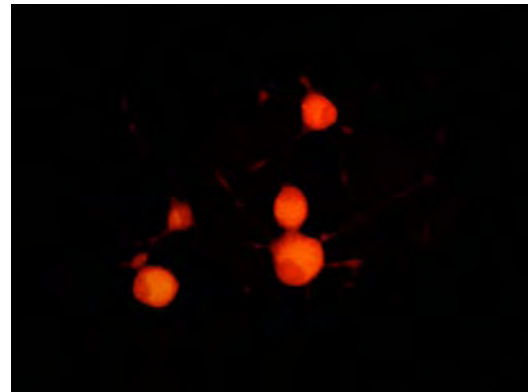
A. PC12 positive control cells (20x)



B. PC12 positive control cells (20x)



C. PC12 negative control cells (20x)



D. PC12 negative control cells (20x)

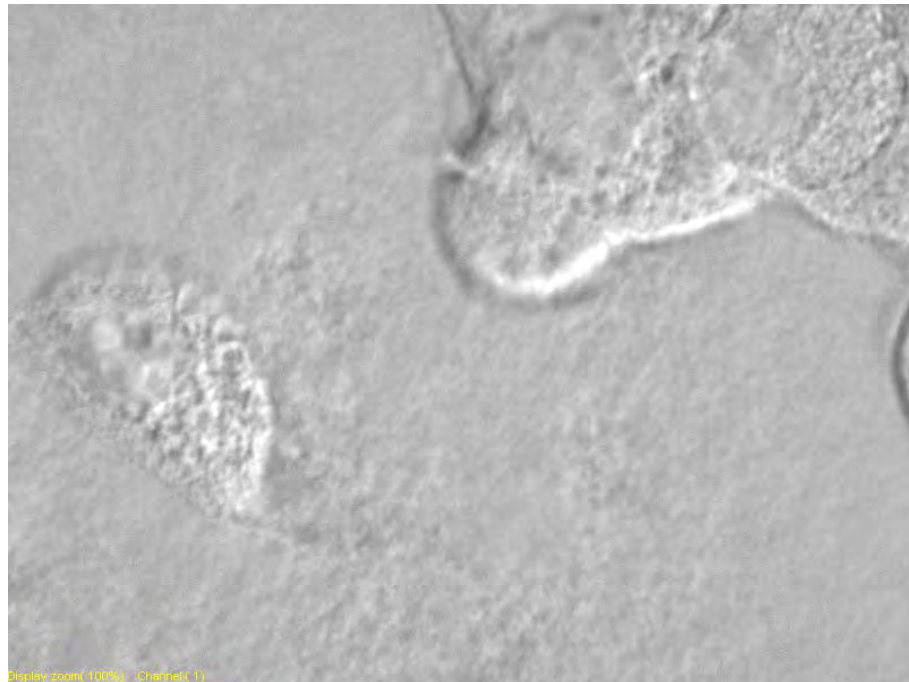


E. PC12 pressurised cells (20x)

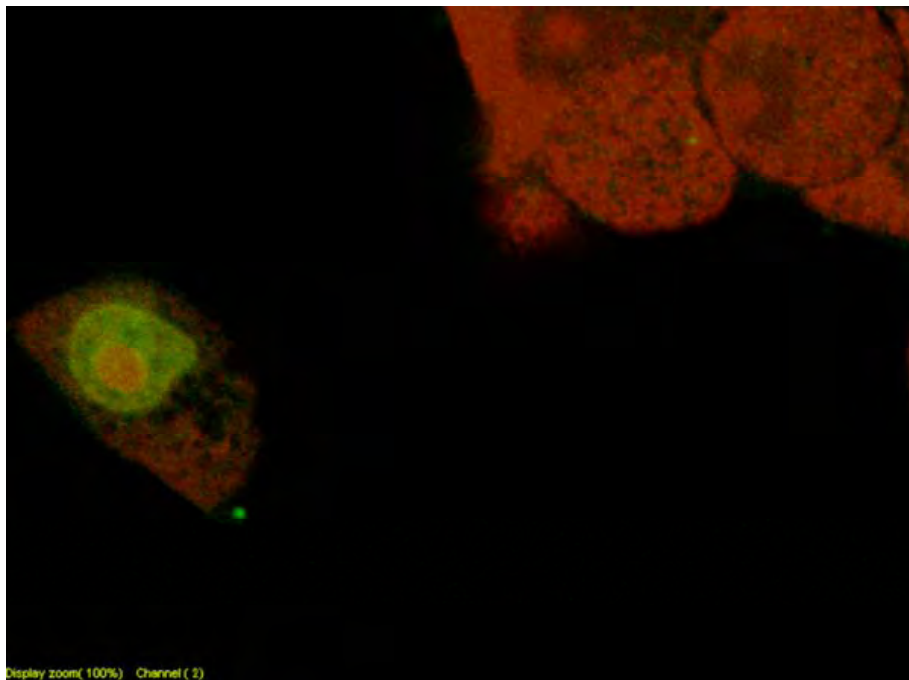


F. PC12 pressurised cells (20x)

Figure 5-8 Morphology of differentiated PC12 cells: TUNEL assay



A



B

Figure 5-9 Morphology of apoptotic differentiated PC12 cells (Nomarski image)

A. Nomarski image showing surface morphology. Apoptotic cell at lower left with pyknosis, membrane blebbing and vacuolated surface.

B. Combined Nomarski and TUNEL assay image. Positive TUNEL nucleus stains green in lower apoptotic PC12 neuron.

5.2.2 Quantitative analysis

Cell line cultures were stained with immunofluorescent markers of apoptosis and assayed by LSC. Quantitative measurements of marker intensity were made for LSC parameters of GMP and GI. GI data was also obtained for the positively staining apoptotic proportion of the total cell population from C17 work onwards.

All experiments in all cell lines confirmed the very high levels of apoptosis from the known apoptosis stimuli in the positive control cultures. The intensity parameters showed both Annexin V and TUNEL marker staining in these cultures to be between two to four times that of the negative control levels, and up to twice the levels measured in pressurised cultures. The proportion of the total cell population measured to be apoptotic was much greater in the positive controls and by a similar order of magnitude. Different cell lines showed slight variations in their sensitivity to the known stimuli of ethanol or DNase but nonetheless reflected this general trend.

All experimental pressure group cultures were subjected to elevated hydrostatic pressure conditions of 100 mmHg for 2 hrs. The first measurements were done on negative control (C) and pressure (P) cells taken immediately after the pressurisation (C2, P2). After normalisation of pressure additional measurements were made in some experiments for timecourse data at 4 hrs (C4, P4) or 6 hrs (C6, P6) and 20 hrs (C20, P20) or 24 hrs (C24, P24) after the initiation of the 2 hrs pressure conditions. Data shown is the mean value for the scanned population of single cells.

5.2.2.1 B35 cell line

Experiments were performed for the TUNEL bioassay for GMP and GI. The data presented was normalised against the positive control (ethanol treated). Fig. 5-10 illustrates this for three timecourse experiments with 2 hrs, 6 hrs and 20 hrs timepoints. This graph shows that at each timepoint there was relatively higher marker staining intensity (ie. a greater level of apoptosis) in pressurised neurons compared to controls. It was statistically significant ($p < 0.05$) at the 2 hrs timepoint, ie. immediately after the cessation of pressure conditions. Later timepoints showed a similar trend but with greater variability, such that no statistically significant differences were present at 6 hrs or 20 hrs.

Subsequent quantitative analysis was therefore focussed on this 2 hrs timepoint. The B35 data was pooled for all TUNEL experiments and normalised as previously described. This data is shown in Fig. 5-11 for GMP and Fig. 5-12 for GI. B35 neurons subjected to pressure conditions showed increased apoptotic marker intensity compared to controls. This result was significant at this 2 hrs timepoint for both parameters GMP ($p < 0.05$) and GI ($p < 0.006$).

Quantitative data for a single B35 run using Annexin V also showed similar results; neurons subjected to pressure conditions had greater values for Annexin V staining compared with negative controls (Fig. 5-13). This difference was significant at 2 hrs ($p < 0.05$) and also at 20 hrs ($p < 0.05$). The intensity levels were also increased at the later timepoints, for both pressure and negative control neurons. Staining intensity data was similarly greater in positive controls than in the other two groups.

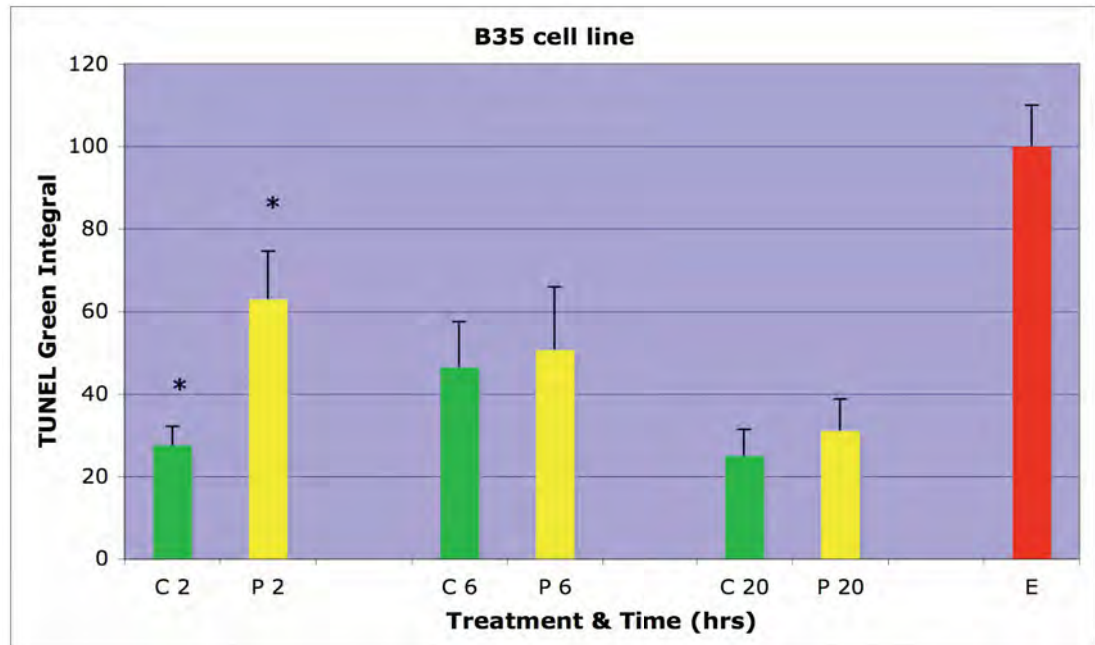


Figure 5-10 B35: Quantitative analysis of TUNEL assay (GI) timecourse

LSC data for TUNEL apoptosis marker over time for B35 neurons following control (C), pressure (P) and ethanol (E) treatment. Greater TUNEL labeling of neurons subjected to pressure conditions in comparison to control B35 neurons was significant at 2 hrs (C2, P2), ($p < 0.05$, $n = 8$, mean \pm SEM). Note that intensity measurements are always higher in the pressure group than in the comparable controls, but at later timepoints this was not statistically significant.

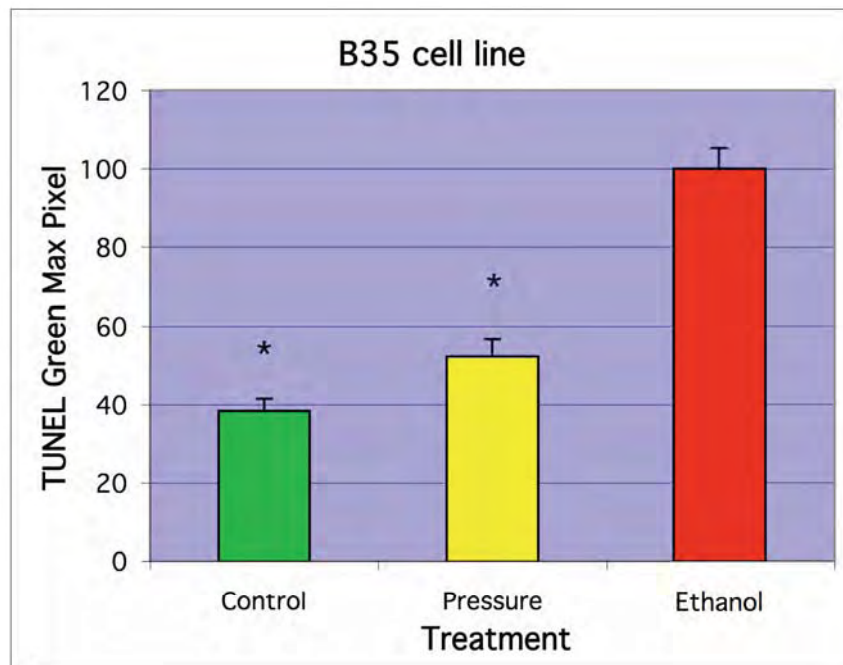


Figure 5-11 B35: Quantitative analysis of TUNEL assay (GMP) 2 hrs

Apoptosis in B35 neurons after 2 hrs as measured by TUNEL using the LSC. An increase in apoptosis in neuronal cultures subjected to elevated pressure relative to control neurons is seen. Data is shown for quantitative fluorescence of Green Max Pixel normalised to the average value for positive (Ethanol) control. The difference between pressure and negative control B35 cultures was significant ($p < 0.05$, $n = 24$, mean \pm SEM).

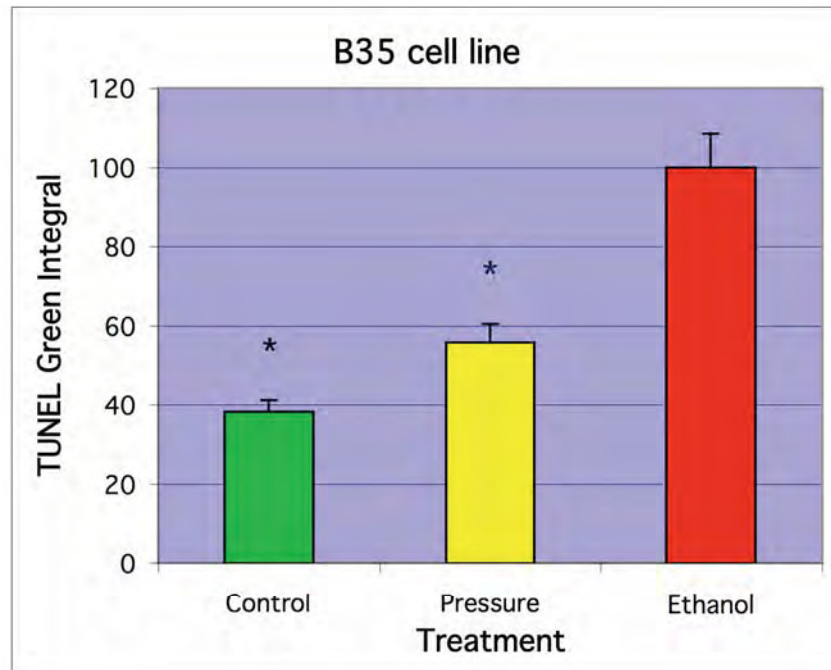


Figure 5-12 B35: Quantitative analysis of TUNEL assay (GI) 2 hrs

Apoptosis in B35 neurons after 2 hrs as measured by TUNEL using the LSC. An increase in apoptosis in neuronal cultures subjected to elevated pressure relative to control neurons is seen. Data is shown for quantitative fluorescence of Green Integral normalised to the average value for positive (Ethanol) control. The difference between pressure and negative control B35 cultures was significant ($p < 0.006$, $n = 24$, mean \pm SEM).

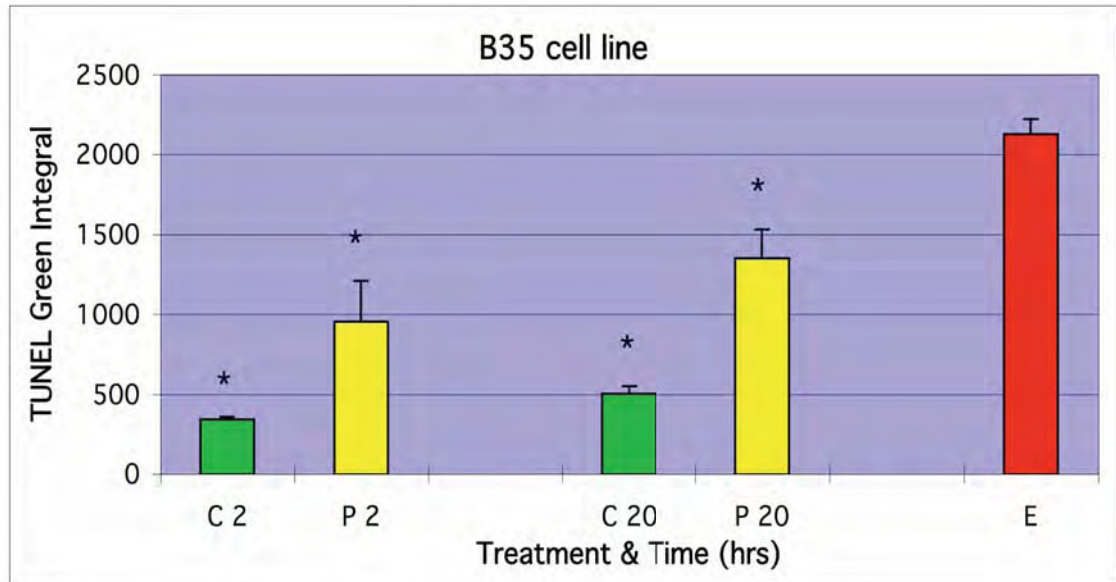


Figure 5-13 B35: Quantitative analysis of Annexin V (GI) timecourse

Annexin V apoptosis marker results for B35 cell line subjected to experimental protocols and assayed at 2 hrs and 20 hrs. Data are from a single run for LSC parameter Green Integral, a measure of Annexin V labelling intensity. (E) represents positive control culture (5% ethanol treatment for 2 hrs). Pressure group (P) exposed to 100 mmHg for 2 hrs. Negative control cultures (C) were not pressurised. The difference between pressure and negative control B35 cultures was significant at 2 hrs ($p < 0.05$) and also at 20 hrs ($p < 0.05$, $n=4$, mean \pm SEM).

5.2.2.2 C17 cell line

Three experiments were conducted on the C17 cell line with LSC data for GI shown at sequential timepoints. (Note that from this time onward the refined analysis of quantitative data allowed us to express LSC intensity for GI measurements in terms of apoptotic cells as a percentage of the total cell population, as described in Chapter 2.) Fig. 5-14 graphs the GI positive apoptotic neurons as a proportion of the total cell population, normalised to the maximal induced apoptosis of DNase positive controls. Neurons in the pressurised group had a greater percentage of apoptotic cell compared to negative controls at the early timepoints. This was statistically significant at 2 hrs ($p < 0.01$) and also at 4 hrs ($p < 0.05$). Later timepoints did not replicate this effect.

5.2.2.3 NT2 Cell line

A series of three experiments were also carried out with NT2 cell line cultures and assayed for TUNEL. This data is graphed for the GI positive proportion of apoptotic cells in Fig. 5-15. Significantly higher apoptosis was found in neurons subjected to pressure conditions compared to negative controls at 2 hrs ($p < 0.006$) and also at the 4 hrs timepoint ($p < 0.005$). Once again later timepoints showed no statistically significant differences.

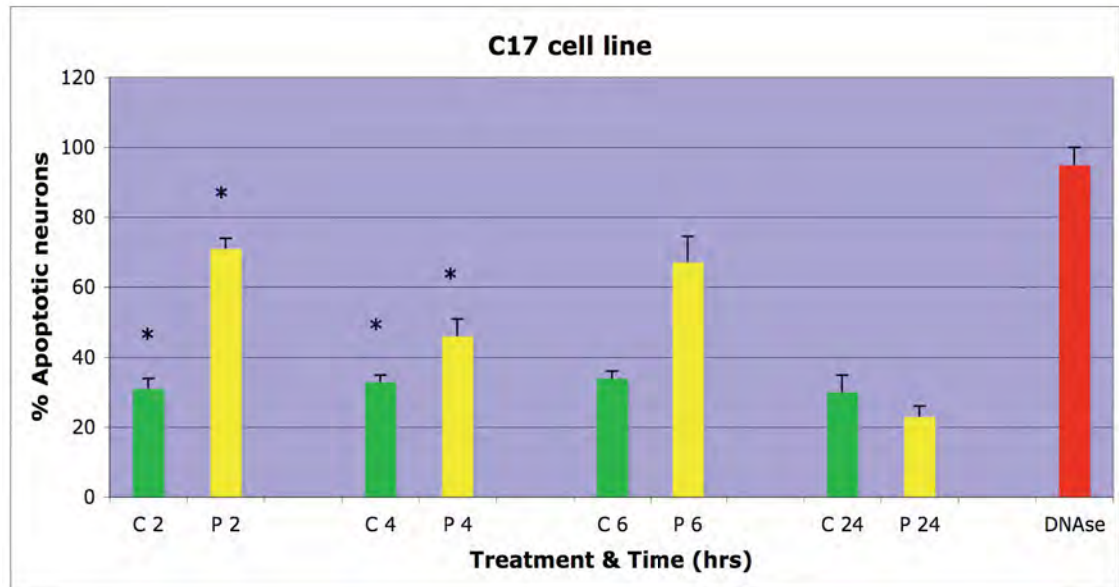


Figure 5-14 C17: Quantitative analysis of TUNEL assay (%) timecourse

TUNEL apoptosis marker results for C17 cell line subjected to experimental protocols and assayed at 2 hrs, 4 hrs, 6 hrs and 24 hrs. Data are for the LSC parameter GI positive proportion of the total neuronal population expressed as the percentage of apoptotic cells. Measurements are pooled for three experiments and are graphed normalised to average positive control culture (DNase). Pressure group neurons (P) exposed to pressure conditions of 100 mmHg for 2 hrs. Negative control cultures (C) not pressurised. The difference between pressure and negative control C17 cultures was significant at 2 hrs ($p < 0.01$) and 4 hrs ($p < 0.05$) ($n=6$, mean \pm SEM).

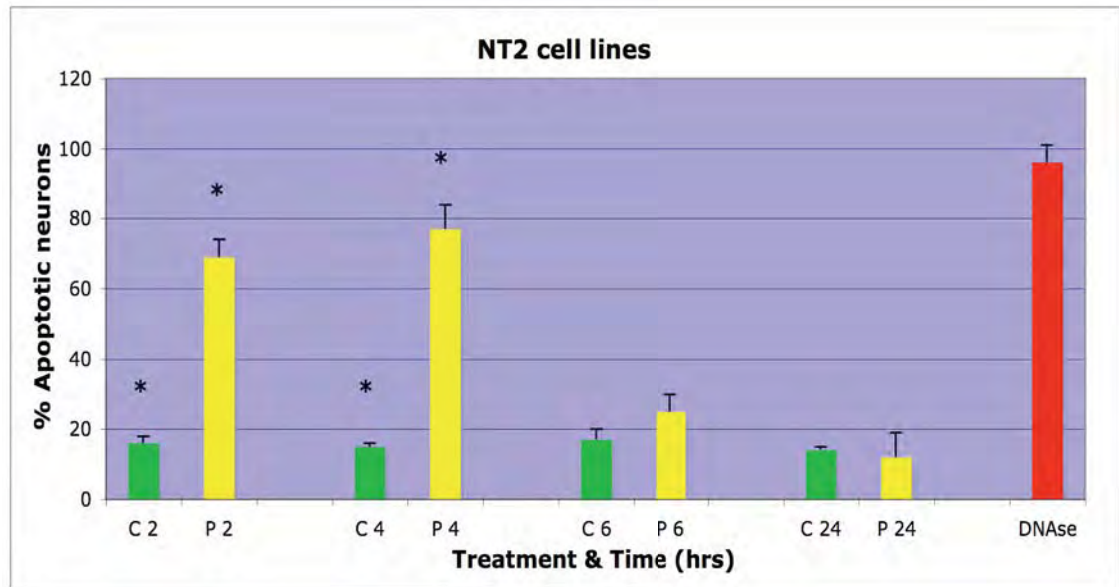


Figure 5-15 NT2: Quantitative analysis of TUNEL assay (%) timecourse

TUNEL apoptosis marker results for NT2 cell line subjected to experimental protocols and assayed at 2 hrs, 4hrs, 6 hrs and 24 hrs. Data are for the GI positive proportion of the total neuronal population expressed as the percentage of apoptotic cells. Measurements are pooled for three experiments and are graphed normalised to average positive control culture (DNase). Pressure group neurons (P) exposed to pressure conditions of 100 mmHg for 2 hrs. Negative control cultures (C) not pressurised. The difference between pressure and negative control NT2 cultures was significant at 2 hrs ($p < 0.006$) and 4 hrs ($p < 0.005$) ($n = 8$, mean \pm SEM).

5.2.2.4 PC12 cell line

In addition to the work on undifferentiated cell lines described above experiments were also carried out on differentiated PC12 neurons. Results for these post-mitotic neurons also showed increased apoptosis following elevated pressure conditions. Fig. 5-16 shows representative GI TUNEL data for one such PC12 run normalised against the maximal apoptosis control of DNase treatment. Though the apoptosis marker intensities for neurons subjected to pressure conditions were higher than comparable controls at all timepoints, the difference was statistically significant only at 24 hrs ($p < 0.02$). When TUNEL data for all PC12 experiments at 24 hrs was pooled and normalised to the positive DNase control the effect was again statistically significant ($p < 0.05$). This difference in 24 hrs data was found for both GMP (Fig. 5-17) and GI (Fig. 5-18), confirming greater levels of apoptosis in pressure treated neurons compared to controls.

Pooled data from an additional three experiments is presented in Fig. 5-19 as the apoptotic proportion of the total neuronal population. The figure shows that this percentage was significantly ($p < 0.02$) greater at 24 hrs after application of pressure conditions compared to corresponding negative controls. The data therefore shows that in the differentiated PC12 neurons significant differences in induced apoptosis were evident only at the latest timepoints and not at the earliest 2 hrs assay. This is in contrast to the findings from the undifferentiated cell lines described earlier.

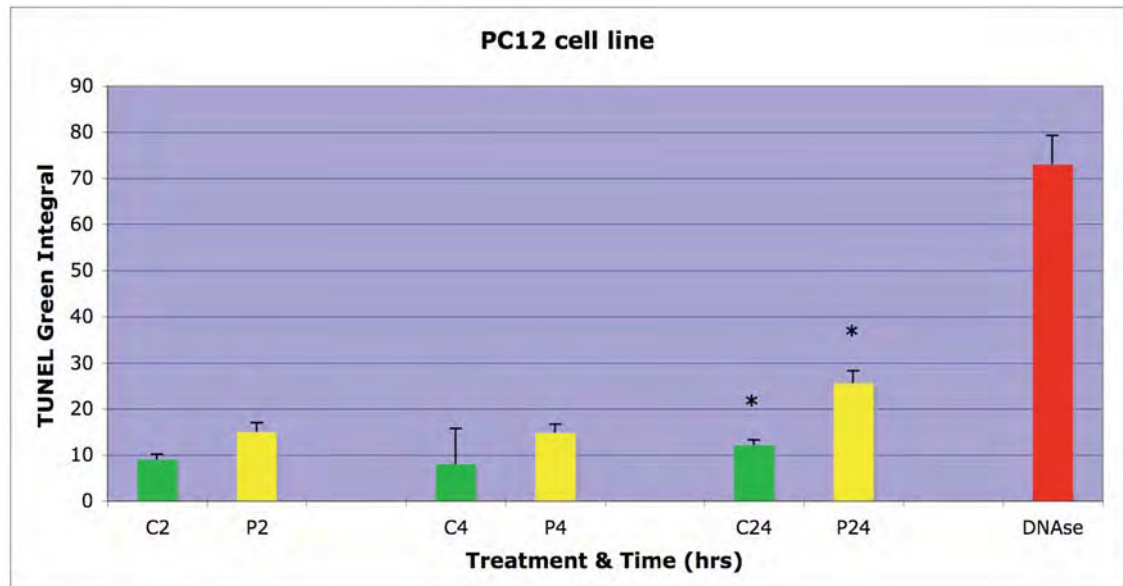


Figure 5-16 Differentiated PC12: Quantitative analysis of TUNEL assay (GI) timecourse

TUNEL apoptosis marker results for differentiated PC12 cell line subjected to experimental protocols and assayed at 2 hrs, 4 hrs and 24 hrs. Data are for LSC parameter Green Integral. Pressure group neurons (P) exposed to pressure conditions of 100 mm Hg for 2 hrs. Negative control cultures (C) were not pressurised. The difference between pressure and negative control PC12 neuron cultures was significant at 24 hrs ($p < 0.05$, $n = 4$, mean \pm SEM).

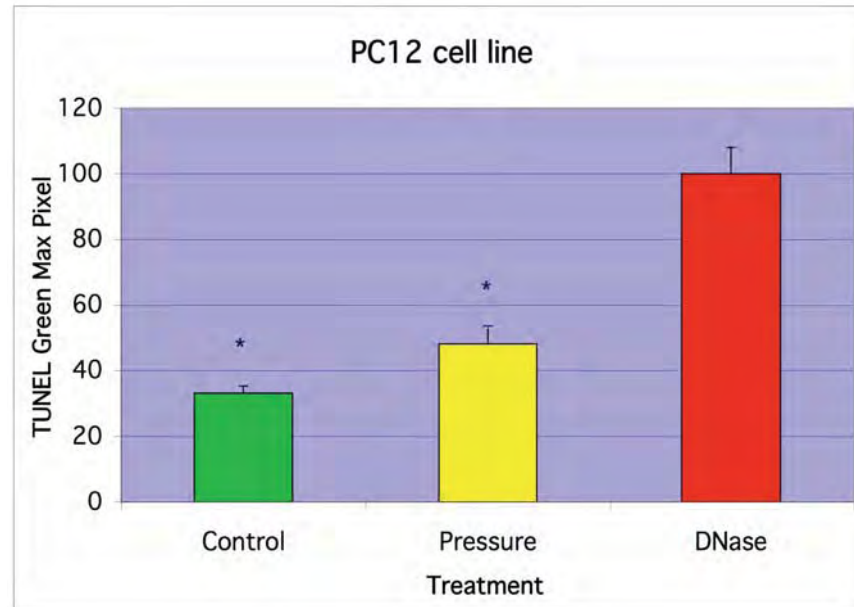


Figure 5-17 Differentiated PC12: Quantitative analysis of TUNEL assay (GMP) 24 hrs

TUNEL apoptosis marker results for differentiated PC12 cell line subjected to experimental protocols and assayed at 24 hrs. Data are for LSC parameter Green Max Pixel (GMP), a measure of TUNEL labelling intensity. GMP measurements are pooled and graphed normalised to average positive control culture (DNase). Pressure group neurons (P) exposed to pressure conditions of 100 mmHg for 2 hrs. Negative control cultures (C) not pressurised. The difference between pressure and negative control PC12 neuron cultures was significant ($p < 0.05$, $n = 11$, mean \pm SEM).

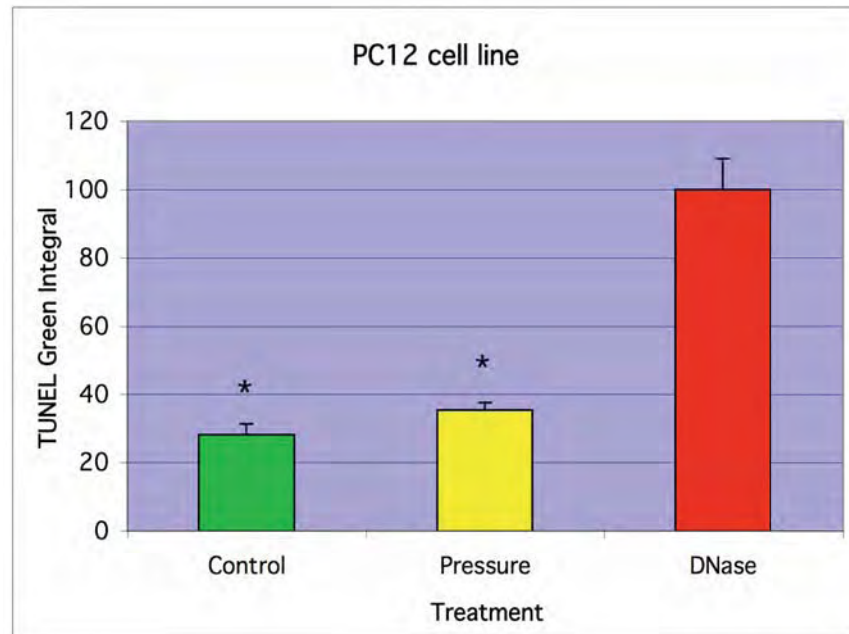


Figure 5-18 Differentiated PC12: Quantitative analysis of TUNEL assay (GI) 24 hrs

TUNEL apoptosis marker results for differentiated PC12 cell line subject to experimental protocols and assayed at 24 hrs. Data are for LSC parameter Green Integral (GI). Measurements are pooled and are graphed normalised to average positive control culture (E: ethanol). Pressure group neurons (P) exposed to pressure conditions of 100 mmHg for 2 hrs. Negative control cultures (C) not pressurised. The difference between pressure and negative control PC12 cultures was significant ($p < 0.05$, $n = 11$, mean \pm SEM).

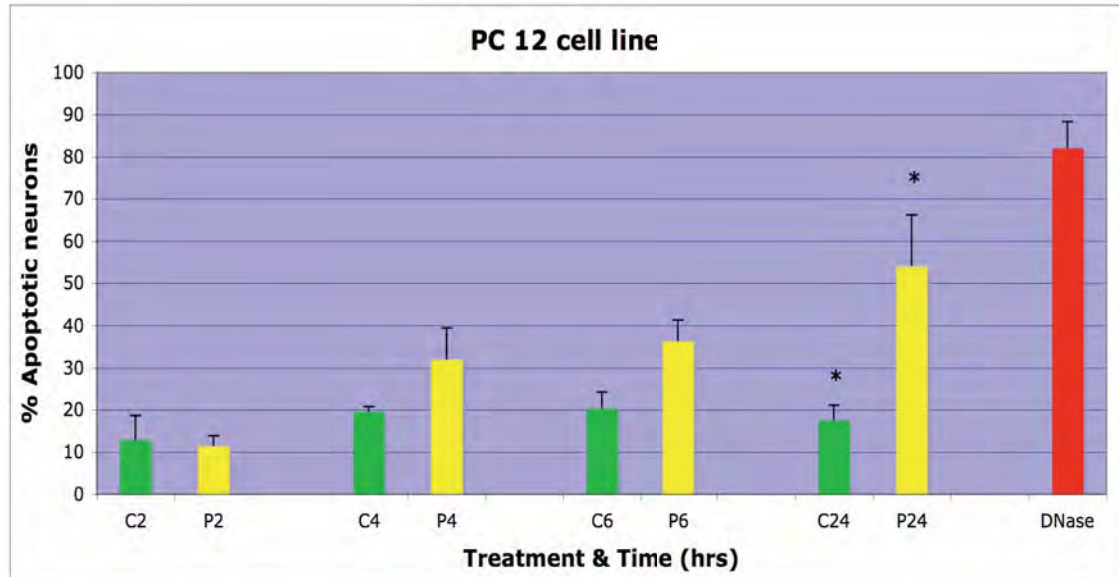


Figure 5-19 Differentiated PC12: Quantitative analysis for TUNEL (%) timecourse

TUNEL apoptosis marker results for differentiated PC12 cell line subjected to experimental protocols and assayed at 2 hrs, 4 hrs, 6 hrs and 24 hrs. Data are for the GI positive proportion of the total neuronal population expressed as the percentage of apoptotic cells. Measurements are pooled and graphed normalised to average positive control culture (DNase). Pressure group neurons (P) exposed to pressure conditions of 100 mmHg for 2 hrs. Negative control cultures (C) not pressurised. The difference between pressure and negative control PC12 neuron cultures was significant at 24 hrs ($p < 0.02$) ($n=7$, mean \pm SEM).

5.3 Discussion

Cell cultures were introduced for the investigation of biological systems over 25 years ago (Kevles and Geison 1995). The technique has since been improved and refined to the extent that currently it is possible to grow almost any cell, including stem cells, *in vitro*. Various cell lines are available to study different aspects of neuronal morphology, growth and cell death (Mills, Wang et al. 1995).

We used four different cell lines to examine the effect of elevated hydrostatic pressure on neurons to better understand the pathogenesis of glaucoma. These cell lines had defined neuronal characteristics and included rat and human derivatives as well as mitotic and post-mitotic cells. In parallel with the studies presented in the preceding chapter we had to refine our experimental techniques to optimise the bioassay; that is, to minimise the variability of cultures and enhance their reproducibility. This was particularly so with quantitative analysis using the LSC.

Over the course of these experiments, particularly the numerous initial runs on B35 cell lines, many of the analytical nuances were refined as familiarity and expertise with the LSC increased. Among these was the observation that variability in marker intensity was still a concern with the GMP, but less so with GI. Hence subsequent studies concentrated on this GI parameter as it was found to be more reliable.

A further development was the ability to perform two-pass laser scans simultaneously. This enabled numerical data to be obtained for the whole neuron population by lasers set to the red PI and area criteria, as well as for the apoptotic population with separate laser settings for the green FITC apoptosis marker. As a result later analyses included data for the apoptotic percentage of the total cell population.

The morphology of the cell lines under discussion revealed common neuronal characteristics. The cells were dependant on adherence to the poly-L-lysine coated coverslip not only to survive but also to develop these features. Once established they readily grew neural processes, generally in the form of dendrites. The quality of these processes was one of the distinguishing features of the cell line. For example, broad NT2 neurites were seen (Fig. 5-2) in contrast to fine PC12 processes (Fig. 5-3). B35 cultures displayed dendrites that were intermediate in morphology between the NT2 and PC12 cells (Fig. 5-1). The characteristics were consistent with those described for the cell lines by other researchers (Schubert, Heinemann et al. 1974; Hsu and Everett 2001; Greene and Tischler 1976). The morphology of the cell was uniform throughout the cell culture of a particular cell line, and was maintained for the life of the culture as well as in subsequent passages. This is in keeping with the traits of cell lines in general, and is a defining property of an established cell line (Freshney 1994).

Consistent and uniform morphology within a single culture enabled direct comparisons to be made between different experimental groups. Thus a specific cell line subject to positive control treatment, for example, could be expected to demonstrate the same types of apoptotic changes in any coverslip from any experiment. This indeed was found to be the case, as exemplified in the similar appearance of B35 cells in positive control cultures from separate experiments seen in Fig. 5-4. The same principle held for all cell lines studied, as well as for negative control and pressure cultures.

This was not the case with the primary mixed retinal cultures described in the previous chapter where a variety of cell types with differing morphology was present in each culture and indeed in each coverslip (Figs. 4-1 and 4-2). Further the proportions of these differing cells, including non-neuronal glia, also varied. Though the features of apoptosis were still seen in those culture groups, the ability to compare corresponding

cultures was limited by this inherent variability. Thus for the purposes of the bioassay used in this study this homogeneity of cell line morphology was an important development, so that definitive conclusions could be drawn based upon the morphological analysis of cell cultures.

Morphological indicators of apoptosis were evident across all cell lines, and the features discussed below are applicable to each individual line with little variation between different types. Apoptosis was most pronounced in the cultures treated with known stimuli of apoptosis, the positive control groups of either ethanol or DNase treatment. This was evident even by light microscopy, as seen in the B35 cells in Fig. 5-4. Immunofluorescent marker labelling however enhanced many of these changes in neuronal morphology. TUNEL staining allowed not only positive nuclei to be readily ascertained but also provided evidence of other nuclear changes. Condensation of the DNA within an apoptotic nucleus increases the concentration and thus intensity of this fluorescent marker (Li and Darzynkiewicz 1995). This is evident in Fig. 5-5A which shows positive B35 nuclei with pockets of intense staining within the nuclei themselves. Another apoptotic nuclear change is pyknosis, with shrinkage and condensation of the entire nucleus. Once again the TUNEL fluorescence highlights this change as seen in Fig. 5-7A where smaller nuclei are present in some of the apoptotic PC12 neurons.

Membrane alterations in apoptotic neurons were also apparent. Blebbing of affected cells was often associated with cell shrinkage as a whole, as seen in positive control B35 neurons in Fig. 5-5A. Nomarski imaging of differentiated PC12 neurons in Fig. 5-9 provides another perspective of this change, with the membrane morphology clearly seen in the isolated apoptotic cell, this time from a culture subject to the experimental pressure conditions. Labelling with Annexin V allowed apoptotic cells with changes of phosphatidyl externalisation to be visualised. As this is a membrane bound alteration the

apoptotic cell shows immunofluorescence localised to this part of the cell. Cells positive for apoptosis then are identified by intense staining of the cell wall (van Engeland, Nieland et al. 1998). This was seen in B35 neurons assayed for this marker, as represented in Fig. 5-6. Since this is an early marker of apoptosis it is often seen without the later features of process loss, cell shrinkage and nuclear condensation. Thus the pressurised cells in Fig. 5-6 still have neurites and are relatively normal in morphologic appearance, while clearly staining positive for the Annexin V apoptosis marker. Positive controls by contrast were already in advanced stages of apoptosis.

The frequency of apoptotic changes in a cell line culture varied with the experimental protocol. The vast majority of neurons examined in positive control cultures were noticeably apoptotic. Neurons displayed a range of the apoptotic characteristics described above, and this was the case for both TUNEL and Annexin V staining. Some cells showed many features, but almost all cells showed some demonstrable characteristic of apoptosis. Figs. 5-5A, 5-6A,B, 5-7A, 5-8A,B and 5-9 illustrate this finding. By contrast negative control cultures, not exposed to elevated pressure conditions, showed apoptosis only occasionally. Most microscope fields were notable for their absence of apoptotic morphology, and immunofluorescent marker staining was similarly sporadic. This is seen clearly in the unremarkable morphology of most neurons in Figs. 5-5B, 5-6C,D, 5-7B and 5-8C, D.

Neuronal cell line cultures exposed to increased hydrostatic pressure of 100 mmHg for 2 hrs were noted to have levels of apoptosis intermediary between these companion experimental groups. The incidence of cells with morphologic features of apoptosis was higher than in corresponding negative controls, with most microscope fields showing at least one apoptotic cell. However apoptosis was not seen in the majority of cells as was the case in positive controls. This is illustrated in Figs. 5-4 to 5-6 for B35 neurons and

Fig. 5-8 for differentiated PC12 neurons. With relatively fewer positive cells by TUNEL or Annexin V staining and morphology, it follows that the occurrence of clearly positive neurons was less common in these pressurised cultures. Further the relative intensity of even clearly fluorescence positive cells was subjectively less than, for example, that seen in the positive control panels described above for B35 or PC12 cultures (Figs. 5-5, 5-6 and 5-8). However these were subjective judgements. In order to assess exactly how much less this marker intensity in pressurised cultures was, and it's comparison to negative controls, it was necessary to proceed to quantitative analysis.

The results presented in Figs. 5-10 to 5-19 provide evidence that our assay techniques using morphology and apoptotic markers all indicated that cell death following experimental pressure conditions occurred by apoptosis. Results for positive control cells subjected to a known stimulus show much greater labeling for TUNEL (ethanol or DNase) and Annexin V (ethanol). Combined with morphological findings, they suggest that the experimental protocol was able to detect apoptotic neurons. We detected a background level of apoptosis occurring in negative control neurons. It would be expected that this would apply to all experimental groups equally, as the cells used in each cell line were identical and from the same populations.

With respect to morphological examination the LSC enabled validation of fluorescent marker intensity data with the distribution of the marker within individual cells. During cytometry the scanned cells are concurrently imaged and the position of selected cells, such as those with strong marker labelling, can be recorded in x-y spatial co-ordinates. This information is then used to re-locate these cells while viewing directly through the co-mounted scanning microscope. This is a unique features of the LSC and one that has made it especially useful in the study of neurons and other adherent cells (Bedner, Li et al. 1999).

In the present work this technique confirmed the morphological attributes of neurons that appeared to be apoptotic by cytometric data alone. TUNEL positive nuclei on initial scans were found to have appropriate nuclear staining when visualised directly. Nuclear condensations seen as pinpoint areas of high intensity within a nucleus on the scan was another aspect of apoptotic morphology seen in detail with the microscope. Similarly Annexin V membrane labelling alluded to in scans was then also highlighted by fluorescent microscopy. Further the visual inspection revealed other apoptotic features not as readily apparent with marker cytometry, such as loss of processes and membrane blebs, which were below the relatively low resolution of the LSC scans. This study then also established the Laser Scanning Cytometer as an efficient bioassay tool for apoptosis in neurons.

The analysis of apoptosis by LSC demonstrated a differential level of apoptosis induction by various treatments. These findings were common to all the four cell lines studied. Morphological results provided clear evidence for apoptosis, which was noted at very high levels in terms of marker labelling and the apoptotic population. How successfully these subjective observations were in predicting this result was verified in the quantitative analysis.

Positive control cultures repeatedly demonstrated intensities of fluorescent marker staining far in excess of those seen in the other two culture groups, both within the same experiment and between different experiments. This was seen for example clearly in the pooled data for the largest number of studies of a single cell line, namely for B35 neurons. Figs. 5-11 and 5-12 show the averaged data of 24 measurements in seven experiments. The TUNEL intensity for both GMP and GI LSC parameters in positive controls was almost twice that of the pressure group. In PC12 experiments the equivalent pooled data showed a similar magnitude of induced apoptosis by DNase

(Figs. 5-17 and 5-18). This maximal apoptosis in positive control cultures was also demonstrated in terms of the apoptotic proportion of the total population, with typically over 90% of scanned cells positive for TUNEL apoptosis. This analysis was performed in the C17 cell line (Fig. 5-14), NT2 cells (Fig. 5-15) and PC12 cultures (Fig. 5-19), all with very similar results. The Annexin V assay for B35 neurons also showed markedly higher apoptosis marker labelling in the positive control cultures, as seen in Fig. 5-13. The induction of apoptosis by known stimulators was thus successful in verifying the bioassay's ability to detect this method of cell death.

The maximal apoptosis induction by known stimuli was thus seen in all cell lines. However there were variations in sensitivity of the various neuronal types to the pressure stimulus. Compared to the just described positive control groups showing maximal apoptosis, the level of induced apoptosis in pressure groups varied from ~50% in B35 cells (Fig. 5-11, 5-12) and PC12 cells (Fig. 5-17, 5-18) to ~75% in cultures of C17 (Fig. 5-14) and NT2 (Fig.5-15). Across all experiments nonetheless morphology and quantitative data were supportive of the assertion that maximal apoptosis was certainly induced and reliably measured. It would be expected that differing cell lines have differing sensitivities to apoptotic stimuli, in parallel with their dissimilar sources of origin and unique phenotypes, and this may explain these observed variations (Wainer, Kwon et al. 1997).

Data for all cell lines showed that increased TUNEL labeling was significantly greater in neuronal cultures subject to elevated hydrostatic pressure compared to negative controls. The results for the Annexin V assay (Fig. 5-13) confirms the TUNEL data with greater apoptosis in pressure treated cells. TUNEL data from the undifferentiated cell lines B35, C17 and NT2 (the 'B35 group') show that there was a significant increase at the 2 hrs timepoint, i.e. immediately after application of pressure

conditions. All these cell lines within this B35 group were found to have remarkably consistent results at this 2 hrs timepoint, with a significant increase in apoptosis in all experiments and by analysis of all intensity data. The results for later timepoints were more varied and hence inconclusive.

The early induction of significantly higher apoptosis by elevated pressure conditions in these undifferentiated neurons was consistent for all three cell lines B35, C17 and NT2. These findings for B35 experiments are highlighted in the pooled TUNEL data for the 2 hrs timepoint only, shown in Figs. 5-11 for GMP and 5-12 for GI intensity. The cultures undergoing pressure treatment had significantly ($p < 0.05$) higher apoptosis marker labelling compared to corresponding unpressurised negative controls. C17 experiments showed a similarly statistically significant difference at this 2 hrs timepoint for the apoptotic proportion of the total neuronal population ($p < 0.01$) (Fig. 5-14). The NT2 cultures were also found to have increased apoptosis at the 2hr timepoint ($p < 0.006$) (Fig. 5-15). Pressure induced apoptosis was significantly higher at the 4 hrs timepoints in pressurised cells compared to negative controls in both C17 and NT2 cell lines. Later timepoints in all these undifferentiated cell lines (B35, C17, NT2) failed to show any significant rise in induction of apoptosis. The only exception to this was the data from one single run in B35 cells assayed for Annexin V (Fig. 5-13).

The above findings were in contrast to the LSC data from the experiments on the differentiated PC12 cell line. These neurons when subjected to pressure conditions of 100 mmHg were also found to have significantly increased TUNEL apoptosis labeling compared to controls, but the results were significant only 24 hrs after the initiation of pressure treatment (Figs. 5-16 to 5-19). Values of TUNEL labeling GI intensity in early (4 hrs and 6 hrs) timepoints were higher than comparable negative controls; however the differences were not statistically significant (Figure 5-16). Pooled population data

did not show pressure related increases, significant or otherwise, until at least 4 hrs after the pressure conditions (Fig. 5-19). This timecourse data reveals that the TUNEL intensity and the number of apoptotic cells steadily increases with increasing duration from the application of pressure, such that the last timepoint shows pressure induced apoptosis of statistical significance (Figs. 5-16 and 5-19). Differentiated PC12 neurons have been previously shown to undergo apoptosis upon withdrawal of growth factors (Michel, Vyas et al. 1995; Oberdoerster, Kamer et al. 1998). In our study all PC12 cells were maintained in growth factors at all times.

Interestingly therefore the undifferentiated neurons seem to have an early pressure induced apoptosis response while the differentiated PC12 neurons respond later. There are two possible explanations for this difference in timecourse. The variation could be due to the cell type, or it may relate to the proliferative state of B35 group cells versus the post-mitotic PC12 cells (Gunning, Landreth et al. 1981). The B35 group cells in this study were not cell cycle synchronised, and therefore were at all stages of the cell cycle, which may help explain the variable results at later timepoints. Perhaps the pressure conditions in this current study selectively affected a specific phase of the cell cycle early, with the remaining population less susceptible thereafter. In view of a consistently significant difference for the initial timepoint alone in the B35 group of undifferentiated cell lines, the neuronal effect may be temporally related to application of pressure if this is a factor in triggering apoptosis. Any effect then would be expected to be maximal closer to the time of the stimulus relative to a more remote period.

Studies on lymphoblast cultures have reported pressure induced apoptosis and necrosis to be accelerated in the S phase of the cell cycle (Takano, Takano et al. 1997). PC12 cells used in our study were induced to differentiate to a post-mitotic state. Having exited the cell cycle they may demonstrate a differing response to the

extracellular stimulus of elevated pressure. Post-mitotic PC12 neurons behave differently with other apoptotic stimuli, even when compared to their undifferentiated state (Lambeng, Michel et al. 1999). Other studies have shown undifferentiated (proliferative) cells to be more sensitive to an apoptotic stimulus than post-mitotic neurons, similar to our observations for the undifferentiated B35 group cells (Oberdoerster and Rabin 1999). Our finding of significant apoptosis induction in differentiated PC12 neurons at 24 hrs is also the same as found in reported work using the same cells (Oberdoerster, Kamer et al. 1998). Interestingly some of the cell lines we investigated appeared more sensitive to the pressure stimuli than others. As described NT2 neurons in particular showed very high levels of induced apoptosis, comparable to the maximal apoptosis of the positive control (Lockhart, Warner et al. 2002).

In summary the results presented in this chapter indicate that the experimental protocol we used was sensitive enough to detect apoptotic neurons. Results for apoptotic Annexin V and TUNEL assays showed increased levels of apoptosis in pressure treated cell lines. TUNEL labelling was consistently and significantly greater in undifferentiated B35, C17 and NT2 cell lines at the 2 hrs timepoint, and at the 24 hrs timepoint in the differentiated PC12 cell line. Our results also suggest that the induction of pressure induced apoptosis varies with the neuron's phase within the cell cycle. These findings have already been reported (Agar, Hill et al. 1999; Agar, Yip et al. 2000; Coroneo, Agar et al. 2000; Coroneo, Agar et al. 2001).

The next phase of our research made use of the developments in the bioassay and the analysis of pressure induced apoptosis. The properties of cell lines that enhanced the reliability of this model were combined with investigations into the target cell affected by glaucoma, the retinal ganglion cell. We therefore extended our studies to a RGC cell line. These studies are described in the following chapter.

Chapter Six

Study of Retinal Ganglion Cell Line

6

6.1 Introduction

The neuronal cell line work presented in Chapter 5 overcame the variability of primary cultures and allowed a repeatable bioassay system to be refined. However the question remained whether these results were applicable to the target neuron affected in glaucoma, namely the RGC. In order to study these cells in our pressure and bioassay system the ideal culture material would be RGCs alone. Primary retinal cultures containing RGCs achieve the desired neuronal component but lack the reproducibility of cell lines. One alternative has been to develop purified RGC cultures from primary cultures. However these are fraught with additional and often complex steps in preparation, and remain subject to the same variability and poor survival of mixed cultures (McCaffery, Bennett et al. 1982; Sarthy, Curtis et al. 1983).

These limitations could be overcome with a RGC cell line and several laboratories, including those experienced in purified RGC cultures, have emphasized the need for such a line (Barres, Silverstein et al. 1988; Takahashi, Cummins et al. 1991; Kerrigan, Zack et al. 1997). This was the impetus behind the development of a permanent and stable RGC cell line culture by Prof N Agarwal's team. Retinal cells were isolated from post-natal Sprague-Dawley rats to generate a mixed primary retinal culture. These cells were transformed with Ψ 2 E1A virus and single cell clones analyzed with the 'RGC-5' clone found to have many RGC characteristics (Krishnamoorthy, Agarwal et al. 2001).

This characterization included an antigenic profile with positive expression of Thy-1.1, the RGC specific marker used to identify these neurons in mixed retinal cultures. Other positive markers were Brn-3b, a RGC specific surface antigen and neuritin and

synaptophysin, neuronal cell antigens. The antigenic profile extended to neurotrophin receptors Trk-A, B and C, and neurotrophins 3, 4 and NGF (nerve growth factor). Importantly negative findings for non-RGC markers, such as for glial, amacrine, and horizontal cells were also confirmed (Krishnamoorthy, Agarwal et al. 2001). Other RGC features identified were morphology and sensitivity to glutamate toxicity and neurotrophin withdrawal (Aoun, Simpkins et al. 2003). Membrane currents in the RGC-5 cell line have also been characterised in our laboratory (Moorhouse, Li et al. 2004).

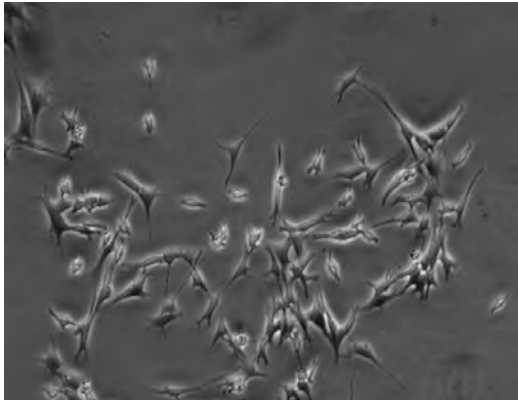
Experimental conditions for assessing pressure responses in RGC-5 cultures were expanded in the next series of studies reported in this chapter. The principle of selecting pressures relevant to IOPs seen in clinical settings was retained. In addition to the simulated conditions of acute glaucoma (100 mmHg as used in the studies reported in the earlier chapters) other pressure elevations were also considered. Chronic glaucoma clinically is associated with IOPs of around 30 mmHg (Cantor, Berlin et al. 2000). As with most disease states this is a guide only as individual patients will vary considerably, however in clinical practice it is widely accepted that 30 mmHg is an unsafe IOP. Indeed this pressure is usually the point to begin treatment even without definite evidence of RGC damage (Kass, Heuer et al. 2002; Shields 2004). Pressure settings analogous to 'normal' IOP were also studied. Conventionally a level of 15 mmHg has been considered a reasonable benchmark for an eye unaffected by glaucoma (Hollows and Graham 1966). In 'normal tension glaucoma' this pressure is associated with pathology, but is still believed to have a causal relationship (Zeitzi, Matthiessen et al. 2005). Thus the experimental pressure conditions selected for these studies on the RGC-5 cell line were (i) 100 mmHg analogous to acute glaucoma, (ii) 30 mmHg for chronic glaucoma and (iii) 15 mmHg representing normal IOP. Apoptosis was assayed as described in Chapter 2 using morphology and specific fluorescent markers.

6.2 Results: Pressure response

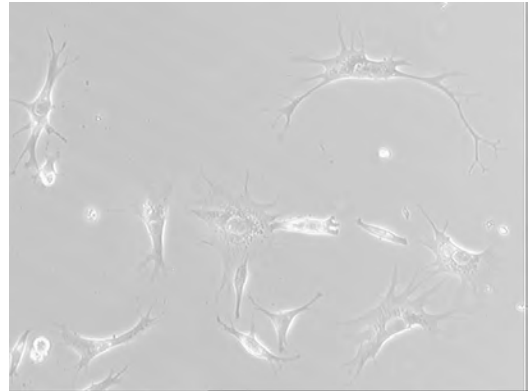
6.2.1 Morphological examination

Before commencing pressure studies the cultures of RGC-5 neurons were established in our laboratory at the University of New South Wales. Culture conditions were optimised according to protocols and personal communications from Prof Agarwal. Microscopy of live cultures confirmed morphology consistent with that described by the originators of the line. The cells exhibited axonal processes and dendritic proliferation (Fig. 6-1). Neurons were of homogenous appearance and repeat passages confirmed the maintenance of these features without alteration. Differentiated RGC-5 cells showed slightly enhanced neurite formation, and stable populations as expected in this post-mitotic state (Fig. 6-1B,D,E).

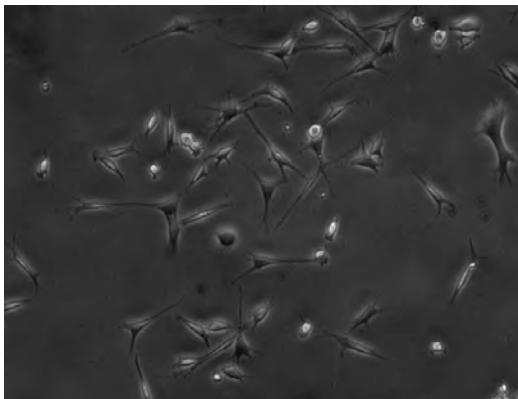
Examination of RGC-5 neurons subjected to various experimental conditions displayed characteristic features of apoptosis by visual inspection with light and confocal laser scanning microscopy. Necrosis was found not to be significant in all cultures by vital dye staining with PI and fluorescent microscope analysis. Morphological confirmation was obtained by inspection of randomly selected fields. Features including cell body and nuclear swelling, vacuolation and karyolysis that typify necrosis were similarly negligible. These findings were seen in both undifferentiated and differentiated RGC-5 cells.



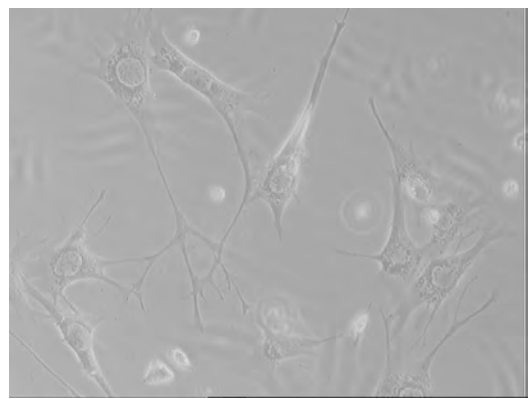
A. Undifferentiated RGC-5 cells (20x)



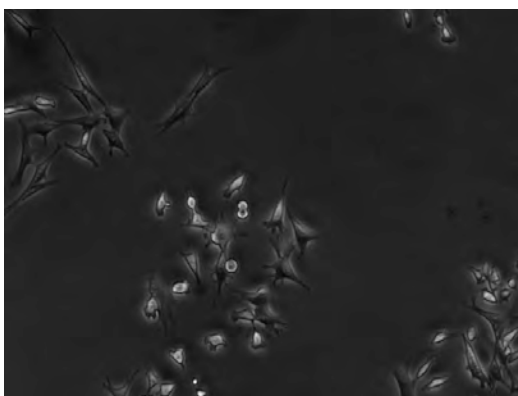
B. Differentiated RGC-5 cells (20x)



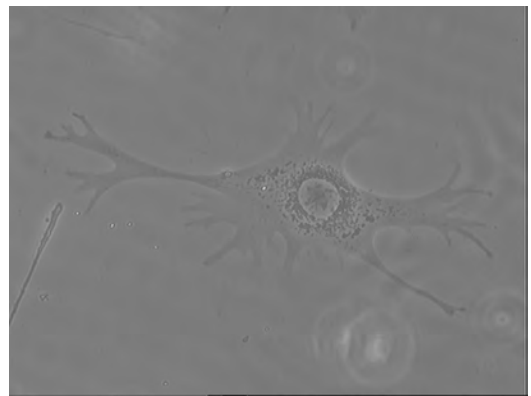
C. Undifferentiated RGC-5 cells (20x)



D. Differentiated RGC-5 cells (30x)



E. Undifferentiated RGC-5 cells (20x)



F. Differentiated RGC-5 cells (60x)

Figure 6-1 Morphology of undifferentiated & differentiated RGC-5 cells

Apoptotic neurons were identified in several stages of apoptosis with cell shrinkage, retraction of neuronal processes, chromatin condensation, apoptotic body formation and cell membrane blebbing. Figs. 6-2 to 6-3 show TUNEL stained RGC-5 neurons demonstrating some of these features, in particular the nuclear and cell shape morphology. Fig. 6-4 shows these changes in differentiated RGC-5 cells. Annexin V assays further highlight cell membrane changes, including bleb formation, as shown in Fig. 6-5. Laser scanning microscopy at different levels of the cell allowed surface bleb formation to be well visualized as seen in Fig. 6-5C.

The range of apoptosis stages was most readily seen in the pressure treated neurons, 30 mmHg (Fig. 6-2) and 100mmHg (Fig. 6-3 to 6-5), while more advanced apoptosis was evident in the corresponding positive control neurons. Qualitatively the proportion of apoptotic neurons was the clear majority in these positive control cultures. Fewer apoptotic neurons were seen in the normal pressure group (15 mmHg), and they were minimal in negative control cultures (Figs. 6-2 to 6-5).

Apoptotic morphology was correlated with fluorescent marker staining during this visual analysis. Concurrent imaging during LSC scanning demonstrated the presence of apoptotic changes in cells with FITC positive nuclei stained by TUNEL. Here hyperfluorescence of condensed chromatin could be detected within the nucleus (Fig. 6-2 to 6-4). Annexin V immunofluorescent staining confirmed the general cell body apoptotic changes and highlighted membrane morphology (Fig. 6-5). Cytoplasmic features were enhanced on PI sensor settings, showing process loss and pyknotic cell bodies. Spatial co-ordinates were recorded of imaged cells and higher resolution images on confocal laser scanning microscopy revealed more detailed features including apoptotic bodies and membrane blebs. The difference between pressure and control groups was subtle however, thus conclusions based on morphology alone were limited.

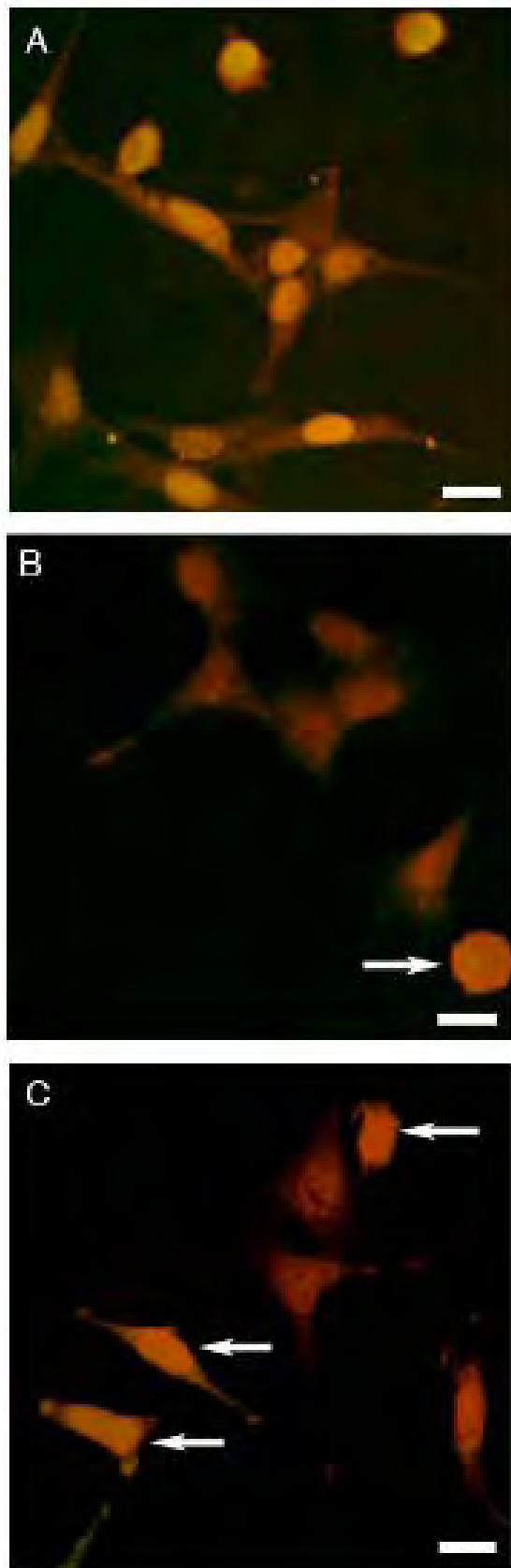


Figure 6-2 Morphology of RGC-5 cells: TUNEL assay (30 mmHg)

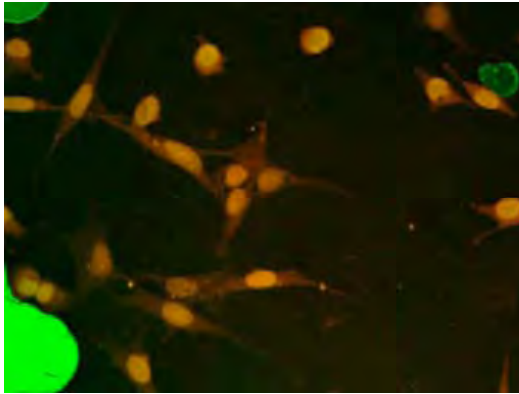
Figure 6-2 Legend: Morphology of RGC-5 cells: TUNEL assay (30 mmHg)

Representative confocal laser scanning microscope images of cultured undifferentiated RGC-5 neurons following various experimental conditions. Cells stained with TUNEL assay for DNA fragmentation show yellow-green nuclear fluorescence as a marker of apoptosis. Red counterstain is with Propidium Iodide. Scale Bar = 10 μ m.

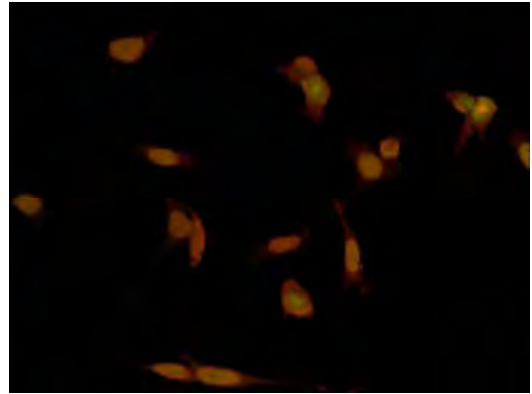
A. Positive control RGC-5 culture treated with ethanol to induce maximal apoptosis. The majority of cells show distinctive and strong nuclear TUNEL staining. Morphologically various stages of apoptosis are seen, with uppermost neurons demonstrating more advanced features of loss of processes and membrane blebbing.

B. Negative control neurons subject to identical conditions as experimental group in panel (C) but without elevation of pressure. Most cells show relatively normal morphology and no TUNEL positive nuclear staining. Single apoptotic cell (arrow) seen in this field displays nuclear and morphological features.

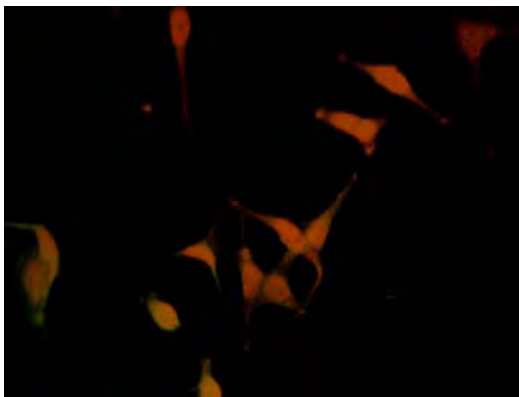
C. RGC-5 neurons exposed to elevated ambient hydrostatic pressure (30 mmHg). Level of apoptosis is less than in ethanol positive controls in panel (A). Some cells also demonstrate apoptotic morphology. However an increased proportion of cells with DNA fragmentation as detected by TUNEL assay fluorochrome (arrows) is seen in comparison to negative control group in panel (B).



A. RGC-5 positive control cells (20x)



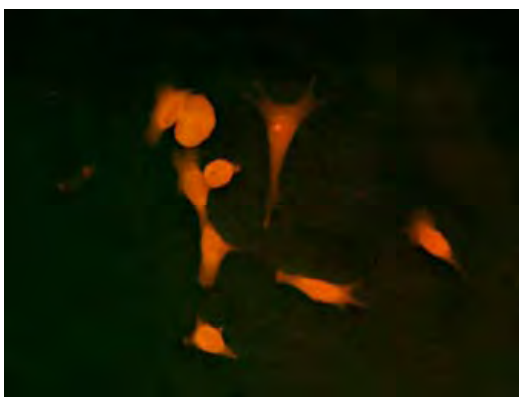
B. RGC-5 positive control cells (20x)



C. RGC-5 negative control cells (20x)



D. RGC-5 negative control cells (20x)



E. RGC-5 pressurised cells (30x)

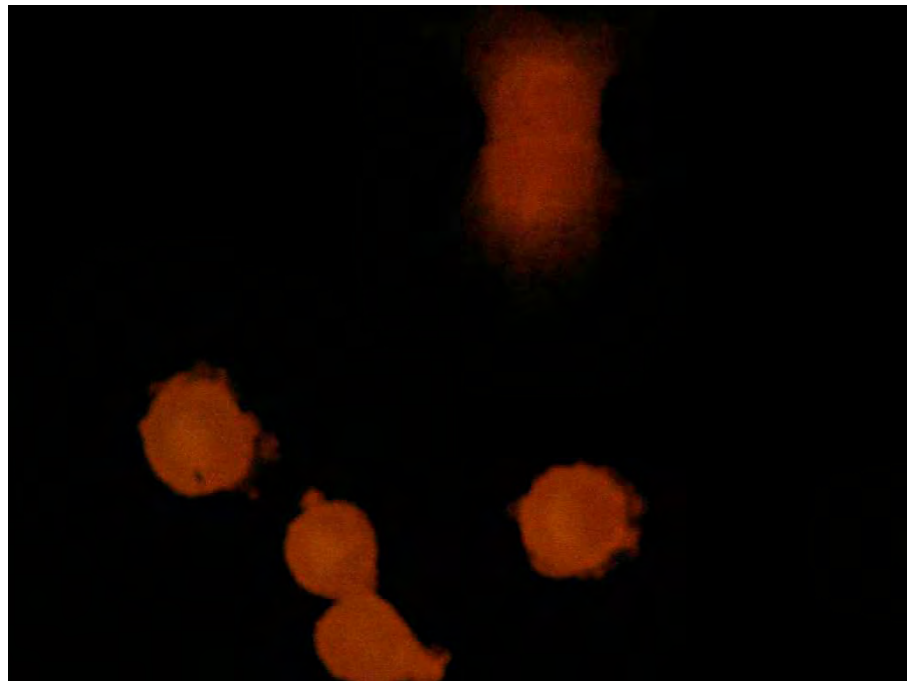


F. RGC-5 pressurised cells (30x)

Figure 6-3 Morphology of RGC-5 cells: TUNEL assay (100 mmHg)



A



B

Figure 6-4 Morphology of differentiated RGC-5 cells: TUNEL assay (100mmHg)

A. Positive control (ethanol treated) differentiated RGC-5 cells. Normal morphology seen in cells on right and top, with large soma and defined processes. Apoptotic morphology seen in most cells on left. (30x)

B. Detail of apoptotic cells in panel A. Apoptotic morphology apparent in lower cells. Note shrunken, pyknotic cell soma and prominent membrane blebs. Blebs are visible in various stages of evolution, from early budding to free membrane bound vesicles. (60x)

Figure 6-5 Legend: Morphology of RGC-5 cells: Annexin V assay (100 mmHg)

Representative confocal laser scanning microscope images of cultured undifferentiated RGC-5 neurons following negative control (A) and pressure experimental conditions (B & C). Cells stained with Annexin V assay for phosphatidylserine translocation to the external cell membrane. No significant PI staining was seen, and these images show FITC Annexin V label. Scale Bar = 10 μm .

A. Confocal laser scanning microscope slice taken at the level of the substrate demonstrating no staining of negative control cells. No apoptotic marker fluorescence was identified on the cells, hence morphology is most clearly seen at this level by contrasting with surrounding substrate stain. The RGC-5 neurons show normal morphology with dendritic processes in particular clearly seen (arrow).

B. Representative image of RGC-5 neurons exposed to elevated ambient hydrostatic pressure (100 mmHg). An apoptotic neuron is seen with intense Annexin V fluorescein staining in the upper part of the image (arrow). An unaffected cell is located adjacent to this, with very faint outlines barely visible due to the lack of apoptosis marker fluorescence. The inset magnifies the shrunken apoptotic cell above and consists of serial confocal sections which have been overlayed. This highlights the brightly fluorescent membrane with distinct bleb formation evident.

C. Single RGC-5 neuron subject to 100 mmHg pressure conditions. Confocal slices taken at a superficial (left image) and deeper substrate (right image) level. Surface membrane morphology, including bleb and vacuole formation, can be seen in each image as well as their relative locations by comparing the two images. General phosphatidylserine externalization is readily visible in the superficial (left) image, outlining the whole cell membrane, which also demonstrates various stages of process retraction as well as membrane blebbing (arrows).

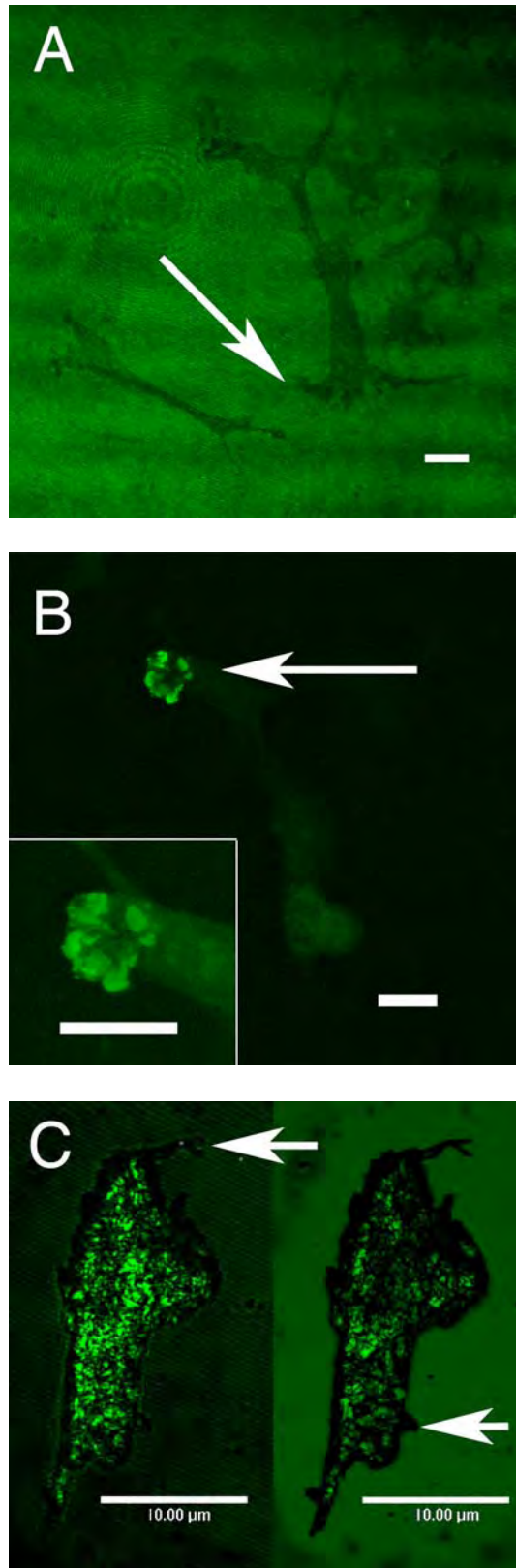


Figure 6-5 Morphology of RGC-5 cells: Annexin V assay (100 mmHg)

6.2.2 Quantitative analysis

Preliminary experiments on undifferentiated RGC-5 cultures supported our earlier observations on other undifferentiated 'B35 group' cell lines (Chapter 5) that the data obtained from late timepoints (4 hrs, 6 hrs or 24 hrs) were not reliable. Accordingly pressure conditions of 15, 30 and 100 mmHg were tested on undifferentiated RGC-5 neurons after 2 hrs of pressurisation. The results presented in Figs. 6-6 to 6-10 are the percentage of neurons that were apoptotic in all experimental runs for a given pressure group. Studies on differentiated RGC-5 neurons subjected to 100 mmHg also included extended timepoints of 24 hrs, similar to our previous work on differentiated PC12 neurons.

Studies were undertaken principally by TUNEL GI bioassay to correlate with the bulk of cell line data presented in Chapter 5. Annexin V was tested in limited pressure runs. Objective measurements of fluorescent apoptosis marker made by LSC were analyzed for the single cell population, and numerical data pooled for all experiments. The results demonstrate differences in intensity and population data between the assayed cell groups. We found high values for intensity parameters (GI, GMP) in the positive control (ethanol treated) cultures. The proportion of the total RGC-5 population positive for apoptosis was similarly high, in the order of 80%. This was comparable across all experimental groups. Results for these conditions (pooled average for all experiments) are shown in Figs. 6-6 to 6-10. This data correlated with the predominance of apoptotic features seen on morphology. Quantitative data thus suggest that the experiments were successful in identifying and distinguishing cells undergoing apoptosis, validating the detection protocols.

Background apoptosis was determined in the negative control cultures. Intensity and population analysis of these cell cultures showed significantly lower levels of apoptosis. Approximately 15-20% of neurons were apoptotic, and this was relatively consistent among various experiments. This contrasted markedly with the positive controls. These observations matched those made on visual inspections, and this data correlated with the predominance of apoptotic features seen on morphology.

Increased levels of apoptosis were found in the pressure group of RGC-5 cultures compared to the negative controls by both intensity and population TUNEL data. The levels of apoptosis in pressure groups were comparatively less than for positive controls, represented in Figs. 6-6 to 6-8 and 6-10.

The relative increase in apoptosis in neurons subjected to hydrostatic pressure elevation was greatest for the 100 mmHg 'high' pressure group. Pooled data for three experiments show that approximately 40% of RGC-5 neurons were identified as apoptotic (Fig. 6-6). The corresponding negative control, treated identically but for the application of pressure, had a significantly ($p < 0.0005$) lower proportion. Neurons exposed to 'low' pressure conditions of 30 mmHg for 2 hrs also had a statistically significantly ($p < 0.01$) greater apoptotic population (Fig. 6-7). In results from five experiments around 30% of neurons were positive for apoptosis, more than double their equivalent negative controls (~13%). The third experimental pressure group underwent pressures of 15 mmHg, analogous to 'normal' IOP (Fig. 6-8). Analysis of data from three experiments revealed higher levels (21%) of apoptosis than in negative controls however this difference was not found to be statistically significant. A consistently lower but similar level of background apoptosis in the negative controls of these three pressure groups is also evident from these figures (Figs. 6-6 to 6-8).

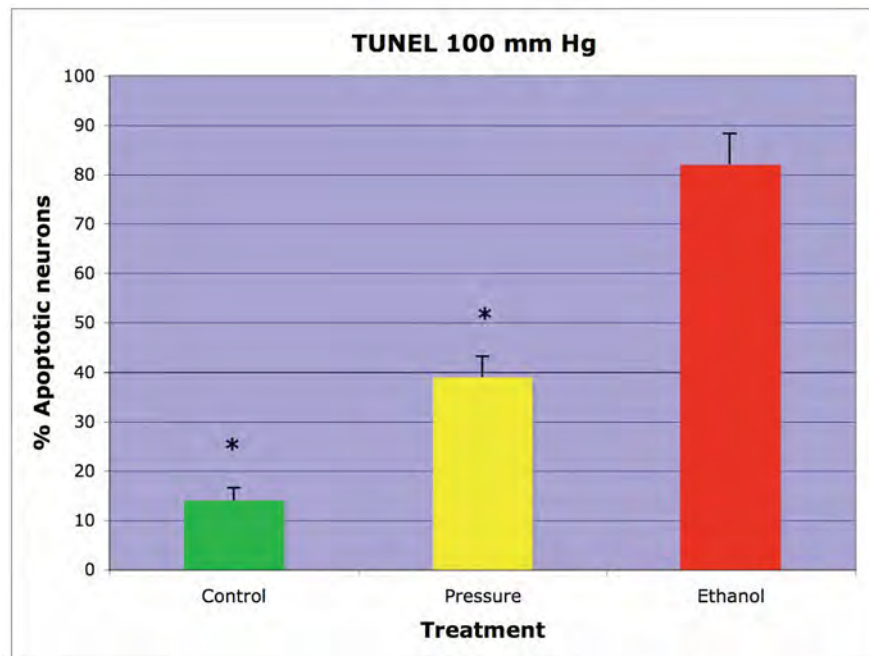


Figure 6-6 RGC-5: Quantitative analysis of TUNEL assay (% , 100 mmHg)

Graph of apoptosis data pooled for RGC-5 cultures subjected to experimental conditions of elevated hydrostatic pressure of 100 mmHg for 2 hrs. Data show the apoptotic proportion of the total neuronal population assayed for TUNEL staining and analysed by LSC, normalised to the 'Ethanol' (positive) control. Note very high levels of apoptosis in this positive control, reflecting maximal induced apoptosis. RGC-5 neurons subjected to 'Pressure' conditions showed greater levels of apoptosis compared to negative 'Control' group. This difference was highly significant ($p < 0.0005$, $n = 7$, mean \pm SEM).

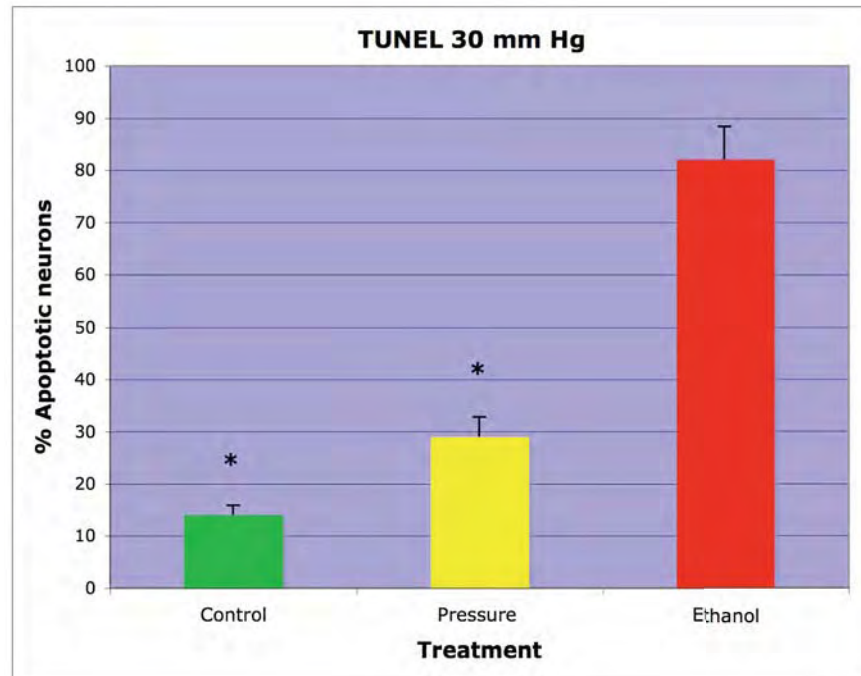


Figure 6-7 RGC-5: Quantitative analysis of TUNEL assay (% , 30 mmHg)

Graph of apoptosis data pooled for RGC-5 cultures subjected to experimental conditions of elevated hydrostatic pressure of 30 mmHg for 2 hrs. Data show the apoptotic proportion of the total neuronal population assayed for TUNEL staining and analysed by LSC, normalised to the 'Ethanol' (positive) control. Note that this positive control group shows very high levels of apoptosis. RGC-5 neurons subjected to 'Pressure' conditions showed greater levels of apoptosis compared to negative 'Control' group. This difference was statistically significant ($p < 0.01$, $n = 12$, mean \pm SEM).

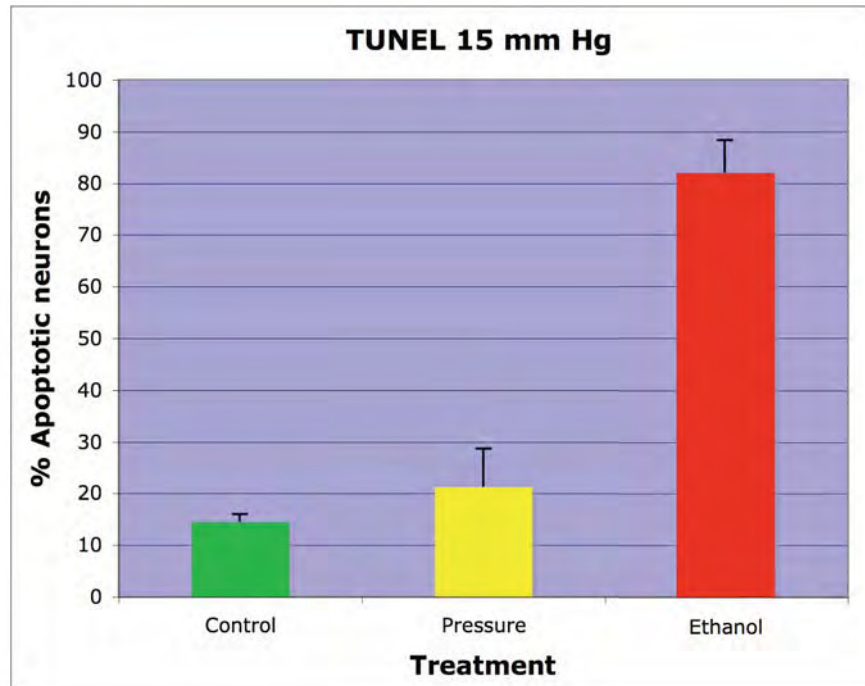


Figure 6-8 RGC-5: Quantitative analysis of TUNEL assay (% , 15 mmHg)

Graph of apoptosis data pooled for RGC-5 cultures subjected to experimental conditions of elevated hydrostatic pressure of 15 mmHg for 2 hrs. Data show the apoptotic proportion of the total neuronal population assayed for TUNEL staining and analysed by LSC, normalised to the 'Ethanol' (positive) control with high levels of apoptosis. RGC-5 neurons subjected to 'Pressure' conditions did not show significantly greater levels of apoptosis compared to negative 'Control' group. (n=7, mean \pm SEM).

RGC-5 neuron cultures were also assayed for the Annexin V immunofluorescent marker by live staining and subsequently analysed by LSC. As with the TUNEL data, these results were also normalised. This data for pressurisation of 100 mmHg for 2 hrs is graphed in Fig. 6-9. Data is normalised to the average ethanol positive control for the experiment. Cultures exposed to these pressure conditions also had a higher proportion of apoptotic cells compared to the negative control cultures. This was statistically significant ($p < 0.02$). The level of over 40% apoptosis observed by Annexin V is comparable to that obtained in TUNEL experiments (Fig. 6-6).

Differentiated RGC-5 neurons were treated to experimental pressure elevations of 100 mmHg for 2 hrs and assayed immediately after pressurisation (P2) and at 24 hrs (P24). Negative controls were likewise examined at these timepoints. Maximal apoptosis was again induced by the treatment of RGC-5 cultures with 5% ethanol. This data of TUNEL analysis for the apoptotic population is presented in Fig. 6-10, normalised to this average ethanol (E) positive control for the group. Levels of apoptosis were higher in the pressurised cultures than corresponding negative controls at both timepoints, however this was significant only at 24 hrs ($p < 0.02$).

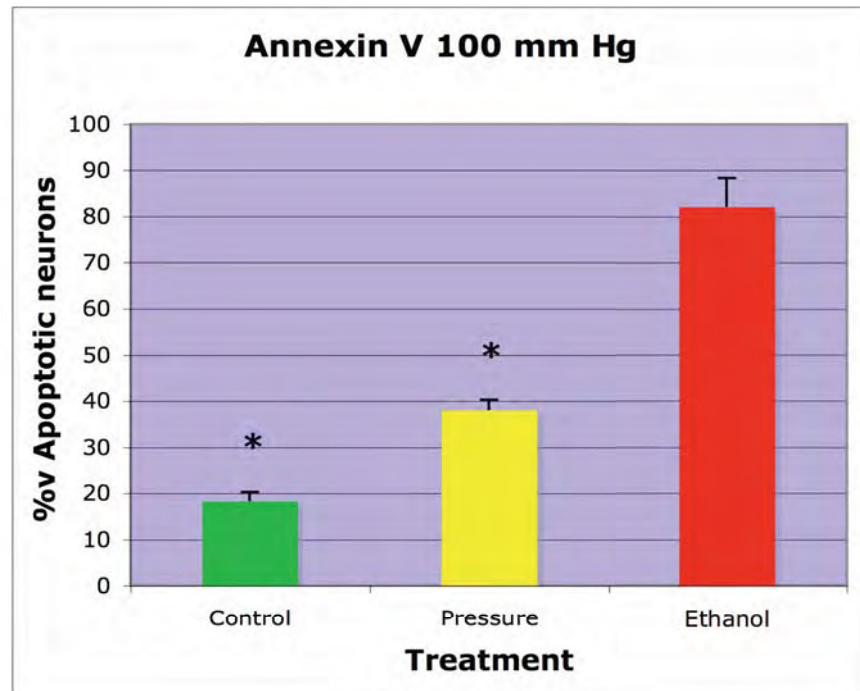


Figure 6-9 RGC-5: Quantitative analysis of Annexin V assay (% , 100 mmHg)

RGC-5 culture data for neurons exposed to elevated hydrostatic pressure of 100 mmHg and assayed live for the Annexin V early apoptosis marker at the 2 hrs timepoint. Results for experiments presented as the apoptotic proportion of the total cell population, normalised to the positive control. The apoptotic response was found to be similar to that observed in the TUNEL data (Figs. 6-5 to 6-7). A high level of apoptosis was detected in 'Ethanol' treated positive controls. Increased levels were found in 'Pressure' neurons relative to negative 'Controls'. This difference was statistically significant ($p < 0.02$, $n = 5$, mean \pm SEM).

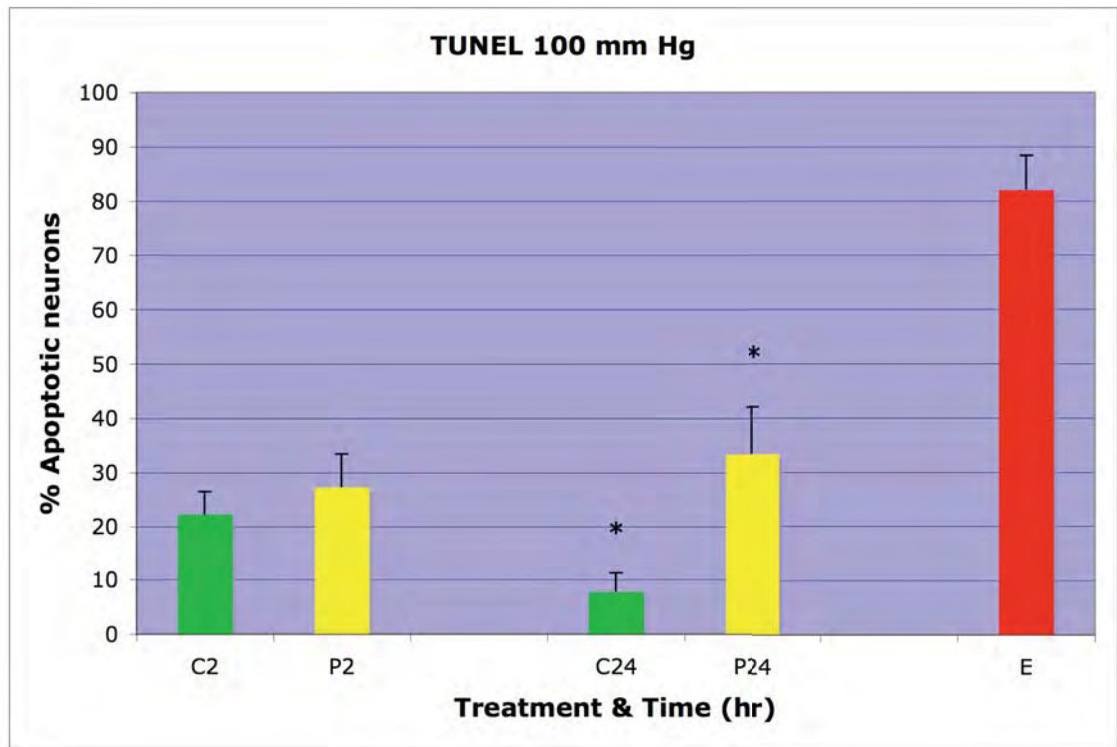


Figure 6-10 Differentiated RGC-5: Quantitative analysis of TUNEL assay-(%) timecourse (100 mmHg)

Graph of apoptosis data pooled for differentiated RGC-5 cultures subject to experimental conditions of elevated hydrostatic pressure of 100 mmHg, assayed at 2 hrs and 24 hrs. This data shows the apoptotic proportion of the total neuronal population assayed for TUNEL staining and analysed by LSC. Data is for three experiments and is normalised to the ethanol (E) positive control, reflecting maximal apoptosis. RGC-5 neurons subjected to pressure conditions (P) showed greater levels of apoptosis compared to negative control (C) group. This difference was significant only at the 24 hrs timepoint ($p < 0.02$, $n = 8$, mean \pm SEM).

6.3 Results: Activated caspase-3

In addition to the studies described so far, RGC-5 cultures in our model were also studied for an indicator of an intracellular biochemical pathway known to mediate apoptosis. The caspase cascade is one of the principal executors of the apoptotic program. Hence we assayed for the presence of the activated (or cleaved) form of the caspase-3 protein by immunofluorescent techniques. Undifferentiated RGC-5 cell line cultures were subjected to the normal experimental protocols and then assayed for the cleaved caspase-3 marker. In line with our other studies each experiment comprised three culture groups- a positive control to confirm apoptosis detection, a pressure group (subjected to 100 mmHg elevated ambient hydrostatic pressure for 2 hrs), and a negative control.

6.3.1 Morphological examination

Cleaved caspase-3 stained with FITC green fluorescence and a red PI dye provided a counterstain. Cells which were positive for cleaved caspase-3 staining displayed discrete pinpoint staining localised to the cytoplasm and cell membrane, which in areas coalesced to form accumulations of fluorescence (Figs. 6-11 low, 6-12 high magnification). Apoptotic morphology was also evident with pyknosis and blebbing. The three experimental groups showed differences in the frequency of cleaved caspase-3 positive RGC-5 neurons and apoptotic morphology. The ethanol treated positive controls showed a large majority of positive cells, negative control cultures had a small minority of these while the pressure group was intermediate in their frequency. This pattern mirrored that seen in both the TUNEL and Annexin V assays in RGC-5 cultures.

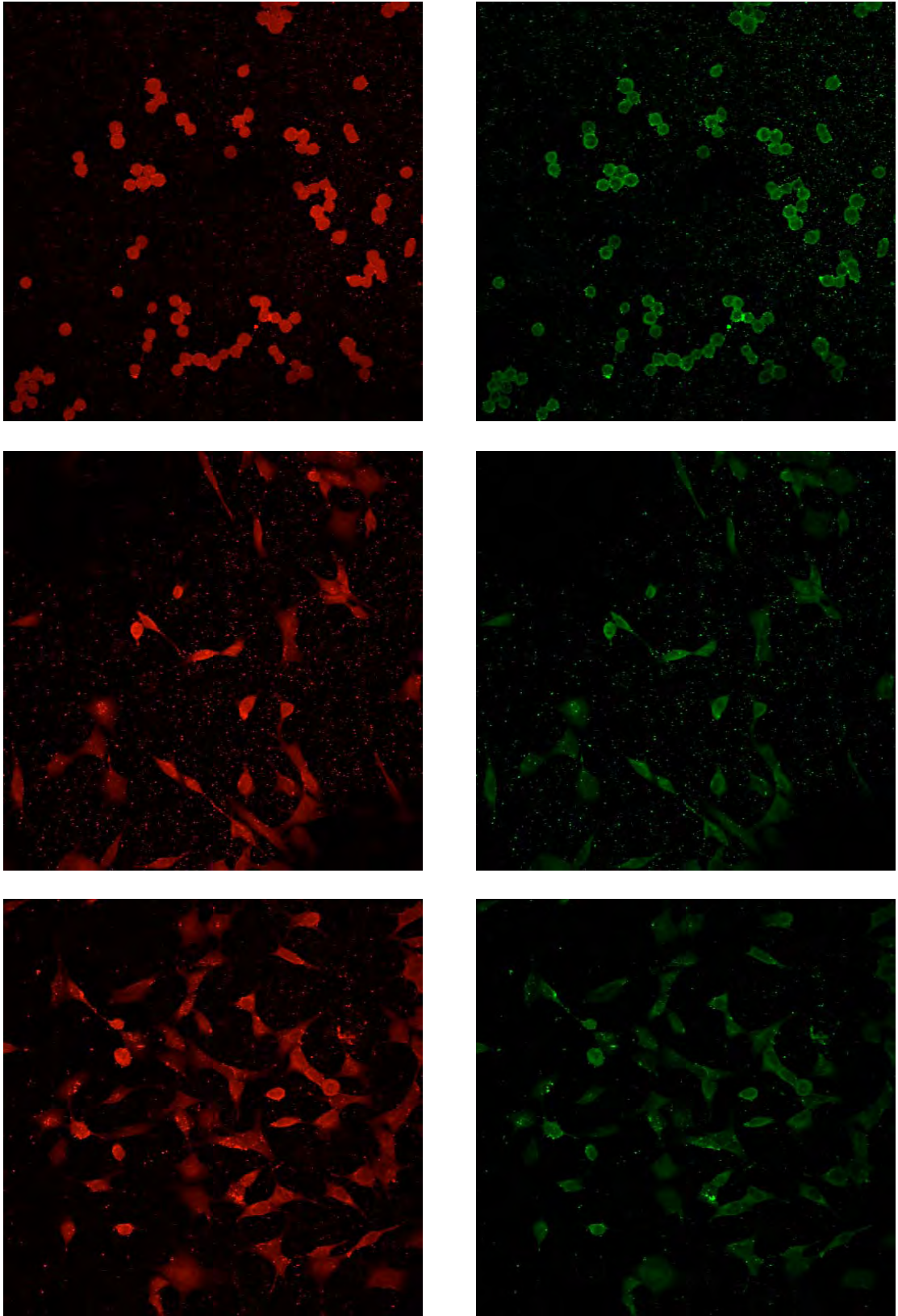


Figure 6-11 Morphology of RGC-5 cells: cleaved caspase-3 assay (Low power)

PI red staining (left panels) & corresponding cleaved Caspase-3 green staining (right panels). Top row: positive controls, Middle: negative controls, (Bottom) pressure (20x)

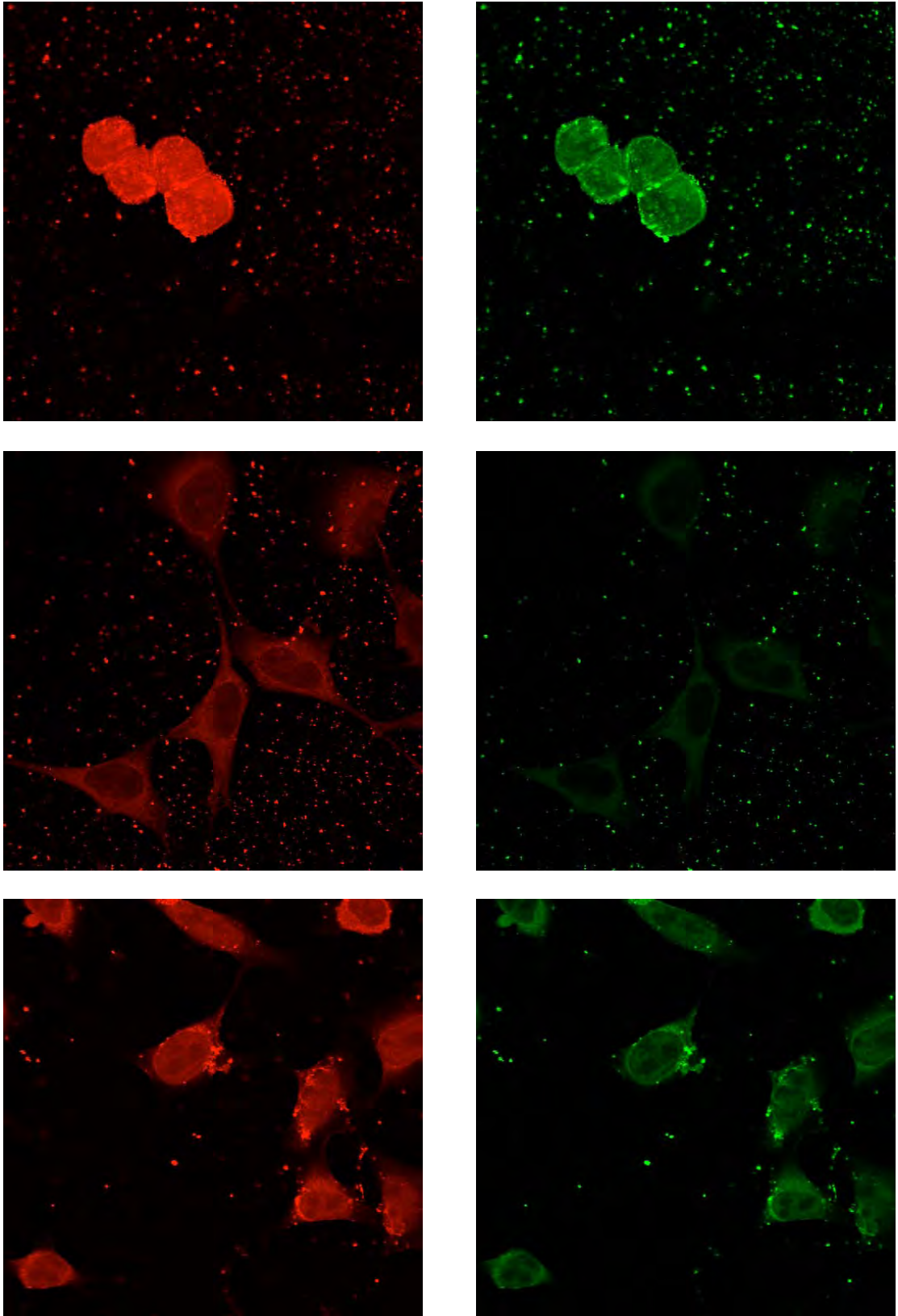


Figure 6-12 Morphology of RGC-5 cells: cleaved caspase-3 assay (High power)

PI red staining (left panels) & corresponding cleaved Caspase-3 green staining (right panels). Top row: positive controls, Middle: negative controls, Bottom: pressure (40x)

6.3.2 Quantitative analysis

Quantitative data on the level of marker staining of RGC-5 cultures assayed for cleaved caspase-3 was also obtained. The finer and more random nature of the marker fluorescence was found to be less amenable to LSC cytometry due to increased variability in laser scatter. Manual cell counts for the proportion of label positive cells were thus performed. These results are graphed in Fig. 6-13.

The percentage of RGC-5 neurons that were found to have caspase-3 activation was high in the cultures treated with the known apoptotic stimulus of ethanol. Around 75% of cells were seen to have positive labelling in this group of positive controls. Cell cultures that were not subject to any apoptotic inducers, the negative controls, did show some caspase-3 activity however at much lower levels (~10%). RGC-5 cultures exposed to ambient hydrostatic pressure elevation of 100 mmHg for 2 hrs, the pressure group, showed that over 30% cells had cleaved caspase-3 immunofluorescent labelling (Fig. 6-13). This was less than in the positive control cultures, but was significantly ($p < 0.01$) greater than the corresponding negative control RGC-5 cultures.

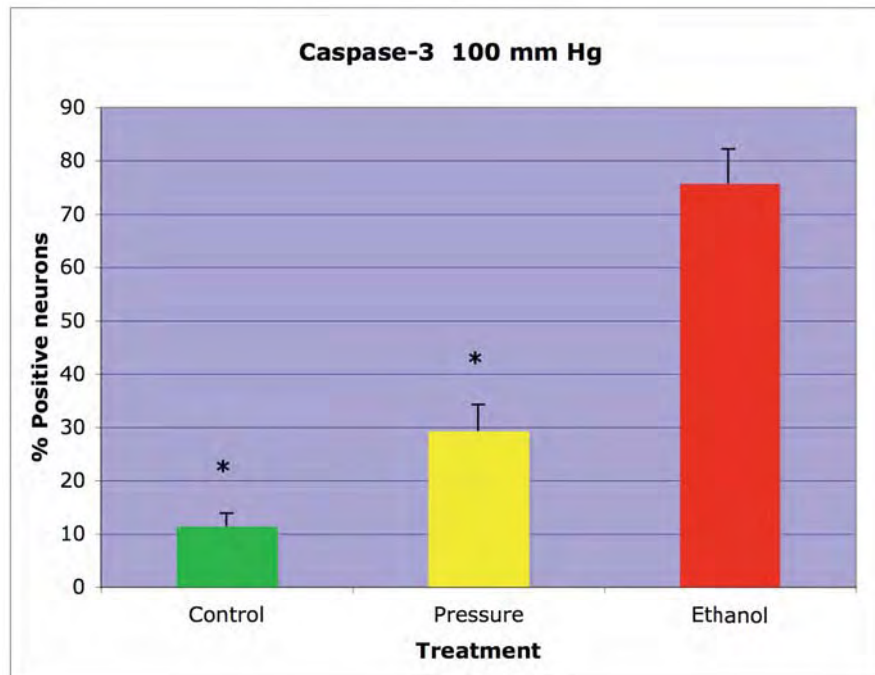


Figure 6-13 RGC-5: Quantitative analysis of cleaved caspase-3 assay (%) (100 mmHg)

Graph of apoptosis data for RGC-5 cultures subject to experimental conditions of elevated hydrostatic pressure to 100 mmHg for 2 hrs. The data show the proportion of the total neuronal population assayed for cleaved caspase-3 staining. Data is for three experiments and is normalised to the positive control. Note very high levels of caspase-3 activity in the positive control 'Ethanol' treatment reflecting maximal induced apoptosis. RGC-5 neurons subjected to 'Pressure' conditions showed significantly greater levels of cleaved caspase-3 compared to negative 'Control' group ($p < 0.01$, $n = 3$, mean \pm SEM).

6.4 Discussion

It is evident from the results presented that there was an increased level of apoptosis in RGC-5 neurons exposed to elevated hydrostatic pressure conditions relevant to acute and chronic glaucoma (Figs. 6-2 to 6-10). These results complement our earlier 'acute' pressure data in this model from primary retinal cultures (Chapter 4) and various neuronal cell lines (Chapter 5). We also found evidence to suggest that this apoptosis may be mediated by the caspase molecular cascade. Thus the RGC-5 line was demonstrated to be a useful tool for investigating RGC pathology in vitro. This has been substantiated by several reports in the literature (Aoun, Simpkins et al. 2003; Martin, Ola et al. 2004; Maher and Hanneken 2005; Shimazawa, Yamashima et al. 2005; Fan, Agarwal et al. 2005).

Studies were conducted on both undifferentiated and differentiated RGC-5 cell cultures. The ability to examine these two forms of the cell line allowed experiments to be designed that paralleled those presented in Chapter 5. That is, looking at the effect of hydrostatic pressure elevation on undifferentiated 'B35 group' cell lines as well as the differentiated PC12 cell line. Thus comparisons could be made between like cell types and results considered in this context. Differentiation also has intrinsic benefits that make this a useful procedure for interpreting neuronal cell responses to experimental stimuli, hence differentiating RGC-5 cells had significant advantages for this study.

Undifferentiated neurons have many characteristics of RGCs, but have notable differences too. Prime among these is the capacity of undifferentiated cells to proliferate. This was demonstrated in the B35 group cell lines where assays were increasingly variable at later timepoints after the pressure conditions (Chapter 5).

Results from RGC-5 cells were similarly reliable only for the earliest 2 hrs timepoint, when cell populations were still stable. Differentiation renders the cell post-mitotic and so the consistency of cell numbers over time enables longer durations for experiments. Further, this state is more analogous to that of RGCs *in vivo* where neurons are also post mitotic (Frassetto, Schlieve et al. 2006).

Differentiation also alters the morphology of these cells. Once the RGC-5 line was established in our facility the cellular appearance was assessed with live phase contrast light microscopy. Differentiated neurons shared the same basic structure but with greater neurite formation. These neurites have more extensive branching, at times displaying prolific dendritic trees, suggesting a higher level of development. This is seen in Fig. 6-1. Again the differentiated morphology is closer to that of RGCs and this can be seen by comparing the abovementioned figures with those taken of RGCs from primary rat retinal cultures in Chapter 4, especially Figs. 4-2 and 4-3. The morphology observed was consistent with that reported by the cell line's originators (Krishnamoorthy, Agarwal et al. 2001) as well as by other researchers since (Aoun, Simpkins et al. 2003; Boyd, Kriatchko et al. 2003).

There are other significant differences between the two forms of RGC-5 neurons. Recent characterisation of differentiated RGC-5 cells has revealed numerous neuronal properties distinct from their undifferentiated counterparts (Frassetto, Schlieve et al. 2006). Increased expression of RGC markers was found by immunofluorescent labeling and by Western immunoblot analysis. The upregulated markers included the highly RGC specific Thy1.1, NMDAR 1, and the dendritic microtubule-associated protein MAP-2. Electrophysiological properties of the cells were another aspect that changed with differentiation. Work done in our laboratory by fellow researchers found that large voltage-gated conductances and increased K^+ conductance were seen in differentiated

RGC-5 cells, as were the establishment of outward rectifying channels. These findings were short of the full complement of electrophysiological properties of *in vivo* cells, but compared to undifferentiated RGC-5 cells represents maturation toward a true RGC phenotype (Moorhouse, Li et al. 2004).

Our study used a differentiation protocol based on that developed by Prof Agarwal's team, involving serum starvation and subsequent treatment with succinyl concanavalin A (Krishnamoorthy, Agarwal et al. 2001). The only other method was reported recently where treatment with staurosporine induced differentiation of RGC-5 neurons (Frassetto, Schlieve et al. 2006). Interestingly both are associated with treatments that are pro-apoptotic. Serum deprivation is analogous to trophic factor withdrawal, a recognised apoptotic stimulus, and staurosporine in high concentrations has been used as a specific inducer of apoptosis. Apoptosis as a result of these protocols was also investigated by these researchers. Staurosporine at the levels used to induce differentiation was not found to trigger apoptosis, and no reduction in cell numbers seen. The sensitivity of differentiated cultures to serum withdrawal was actually seen to confirm the success of the process, as dependence on trophic factors are one of the most important characteristics of post-mitotic neurons (Krishnamoorthy, Agarwal et al. 2001). However RGC-5 cultures were serum starved for a limited period only (24 hrs), after which the standard serum supplemented culture media was reinstated. Further the cultures were maintained in this for several days prior to experimentation, so any apoptotic effect was negated. Our experience with this differentiation protocol confirmed this finding.

The assay we used incorporated a combination of both morphological and immunofluorescent features based on Annexin V and TUNEL labels and confirmed the observed cell death to be due to apoptosis. The detection of apoptosis in this study can

be complicated by several factors. RGC-5 cells may not show all the features of apoptosis examined if they were at differing stages of this multi-step process. Necrosis needs to be distinguished and excluded as a cause of cell death. Necrosis was assessed by vital PI dye exclusion as well as morphological characteristics (including cell swelling, membrane rupture and cell lysis (Wyllie, Kerr et al. 1980). Necrotic cells can also have strand breaks which could show TUNEL positivity, but they are an order of magnitude fewer and are randomly sized in contrast to the 180 bp multiples generated in apoptotic cells (Schmid, Krall et al. 1992). We found negligible levels of necrosis across all experiments. To maximise reliability, however, assessment of apoptosis should rely on more than one method, ideally based on different principles of detection (Darzynkiewicz, Bedner et al. 1998). Cell morphology remains the gold standard, and visual inspection of RGC-5 neurons was thus integral to our assays.

Other studies on this cell line have also looked at cell death by dye techniques. Assays of RGC-5 culture viability involved dye exclusion principles not unlike the use of PI in our work. In one study Hoechst 33342 dye was used in combination with PI to morphologically assess cell viability and apoptosis (Shimazawa, Yamashima et al. 2005). Other work has been concerned with cell viability in general rather than apoptosis specifically. The 'Live-Dead Assay' uses two dyes, calcein-acetomthoxyl ester which fluoresces green in living cells, and ethidium homodimer-1 which stains dead cells red (Dun, Mysona et al. 2006). In another study the uptake by living cells of neutral red dye was measured by using microarray measurements of the optical densities of extracted dye (Aoun, Simpkins et al. 2003). Microplate analysis has also been used with absorbance studies of RGC-5 cells after treatment with the 'MTT' (3-(4,5-dimethylthiazol-2-yl)-2,5-diphenyl tetrazolium bromide) assay for cell viability (Maher and Hanneken 2005).

Apoptosis as a unique form of cell death has been investigated in RGC-5 neurons using similar immunofluorescent techniques to those described in this thesis. The most established assay remains the TUNEL label which detects the nuclear fragmentation of apoptosis. This method was employed in the very first report on the development of this cell line (Krishnamoorthy, Agarwal et al. 2001). The assay confirmed the growth factor dependence of the differentiated RGC-5 cultures after serum starvation. Later research into apoptosis induction by specific biochemical stimuli has used TUNEL labelling (Martin, Ola et al. 2004). A TUNEL-like method also targeting nuclear changes is based on the YO-PRO-1 proprietary dye. This has been used in combination with PI counterstaining to determine apoptosis by flow cytometry in this cell line (Boyd, Kriatchko et al. 2003). Recently reported work using a similar model for pressure effects also relied on TUNEL immunofluorescence, assessing apoptosis by morphological changes (Kim, Lee et al. 2006).

In our study microscopy revealed many morphological features of apoptotic cells. As is the case with neurons undergoing this mode of cell death, the loss of processes was seen. Cell bodies were shrunken and condensed. Figs. 6-2 to 6-5 illustrate these changes in both TUNEL and Annexin V stained cells. Nuclear changes of positive labelling for DNA strand breaks and nuclear condensation were highlighted with the TUNEL assay (Figs. 6-2 to 6-4). Annexin V immunofluorescent staining for phosphatidyl externalisation clearly demonstrated alterations in membrane morphology including blebbing (Fig. 6-5).

These changes were similar to those observed in primary retinal cultures (Chapter 4) and particularly in the neuronal cell lines (Chapter 5). Also reproduced was the relative frequency of morphologically positive apoptotic cells in the different experimental groups. That is, maximal numbers and fluorescent marker staining intensity were seen

in the ethanol treated positive controls and least in the negative controls. RGC-5 cultures exposed to elevated pressure conditions displayed intermediate levels of apoptosis by morphological assessment. These findings are seen in Figs. 6-2 to 6-5.

The graded pressure elevations used in these studies were not found to have a similarly graded response in terms of morphology. However the general trend of apoptotic morphology varying with the experimental group described earlier was maintained. Thus positive controls showed more apoptosis than pressurised cultures, and the latter group displayed greater levels than comparable negative controls, for both marker intensity and the frequency of apoptotic morphology. However on visual inspection alone it was difficult to conclude that the findings in the 100 mmHg pressure group were very different to those from the 15 mmHg group, for example. The subjective nature of this form of analysis made such judgements difficult. Hence the role of cytometry was crucial for our studies.

The LSC was once again found to be useful in its ability to correlate microscopy with cytometry. As described in Chapter 5 in some detail, the relocation of RGC-5 neurons that appeared positive by marker staining for subsequent direct visual inspection was a unique attribute. A cell that was deemed apoptotic by automated cytometry was confirmed by independent morphological examination to indeed have apoptotic characteristics.

The combination here of these techniques should enhance the accuracy of apoptosis detection. The LSC's capacity to visualise adherent cells such as neurons for morphology enables subjective analysis, while automated cytometry minimises observer bias. Fluorescent marker intensity values for TUNEL assays reflect morphological apoptotic features and are a reliable indicator of apoptosis as measured by LSC (Li and Darzynkiewicz 1995; Darzynkiewicz and Bedner 2000). However fluorochrome

intensity can vary due to laser scatter and staining. Population analysis integrates intensity data which is gated and averaged at the outset, minimising the impact of such variations. Hence the increased reliance on this analytical method. The uniformly high level of apoptosis in the positive controls (> 80%), suggests the assay can reliably detect apoptotic RGC-5 neurons, and confirms the LSC as a uniquely useful tool for studying apoptosis (Martin-Reay, Kamensky et al. 1994; Kamensky, Burger et al. 1997; Bedner, Li et al. 1999).

The results from negative control cultures together with those in the pressure group indicate that the levels of background apoptosis were higher than expected. This may reflect specific and as yet undetermined features of this RGC-5 line. It should be noted that this is a transformed line, and may have altered apoptotic machinery and therefore behave differently to primary RGCs. As the cells were derived from the same RGC-5 populations and passage they should however be identical. This finding should then apply to all experimental groups equally, and data was consistent across the separate experimental runs.

One remarkable finding in this study was that the pressure induced apoptosis varied with the applied pressure. The greatest proportion of TUNEL and Annexin V positive cells was at 'high' hydrostatic pressure conditions of 100 mmHg, which at ~ 40% was almost 2.5 times the negative control level (Figs. 6-6 and 6-9). The results for these late and early apoptosis mechanisms were comparable for all experimental groups, with good correlation by morphology as well as quantitative analysis. These findings also compare favorably with work on other neuronal lines exposed to these pressure conditions in our model (Chapter 5, where B35, C17, NT2 and PC12 neuronal cell cultures had 2 to 3 times greater levels of apoptosis induced by pressure). 'Low' settings of 30 mmHg, analogous to clinical chronic glaucoma, induced ~30% higher apoptosis

than the corresponding negative control (Fig. 6-7). The data for the third experimental pressure group, with elevation to 15 mm Hg representing 'normal' IOP, revealed around 20% apoptosis (Fig. 6-8). Although this was greater than the comparable negative control (~15%) the difference was not statistically significant.

The study of differentiated RGC-5 neurons also found a pressure dependent increase in apoptosis with 'high' elevated pressure (Fig. 6-10). Interestingly these post-mitotic cells responded to the pressure stimulus with a much more delayed effect, unlike the undifferentiated cultures of RGC-5 and the other 'B35' group of undifferentiated neuronal cell lines studied in Chapter 5. In fact the response mirrored that seen in differentiated PC12 neurons (Figs. 5-16 to 5-19). This suggests that the pressure sensitivity of these cells is dependant on their post-mitotic nature, with an as yet undetermined role of the cell cycle in this induced apoptosis.

The increase in induced apoptosis does not appear to bear a linear relationship to pressure, with relatively consistent changes in apoptosis corresponding to much greater changes in applied pressure conditions. The reasons for this are unclear; it may relate to the specific apoptotic mechanism triggered or be a characteristic of the transformed RGC-5 cell line itself. The graded response is however interesting in terms of the selected pressures. The 'high' pressure is analogous to the most severe pressures seen in clinical acute glaucoma; the 'low' to chronic glaucoma and the lowest pressures approximate "normal" IOP. It should be added that RGC loss can occur in a subgroup of patients even at 15 mmHg. These levels correlate broadly with the observed disease severity nonetheless (Palmberg and Wiggs 1999).

The RGC-5 cell line has been studied with respect to other apoptotic stimuli relevant to ocular pathologies. These have focussed predominantly but not exclusively on glaucoma. The excitatory theory of glaucoma pathogenesis has received particular

attention, and this cell line has served as a useful in-vitro model for studying this biochemical concept. Glutamate toxicity in RGC-5 neurons was first noted by the originators of the line. Apoptosis was assessed in response to glutamate treatment of both undifferentiated and differentiated cell lines. This was seen to occur in both of these culture types, with significantly greater sensitivity to glutamate arising after differentiation (Krishnamoorthy, Agarwal et al. 2001). RGC-5 cells were shown to express functional glutamate NMDA receptors, the stimulation of which results in excitotoxic cell death. Differentiation with succinyl concanavalin A was thought to increase NMDA receptor expression (Aoun, Simpkins et al. 2003).

Further studies have also examined the effects of this neurotransmitter in RGC-5 cells (Fan, Agarwal et al. 2005; Shimazawa, Yamashima et al. 2005). Using undifferentiated cultures glutamate was shown to induce apoptosis that was inhibited by the NMDA receptor antagonist MK-801, suggesting excitotoxic cell death mediated by overstimulation of these receptors (Martin, Ola et al. 2004). Another study into undifferentiated RGC-5 cells demonstrated similar glutamate dependant apoptosis but found no such protective effect of MK-801. This suggested a mechanism independent of the NMDA receptor (Aoun, Simpkins et al. 2003). RGC-5 cells have also been found to undergo apoptosis by another excitotoxic agent, the amino acid homocysteine. Glutamate biochemistry is also related to the redox system of cells and oxidative stress believed to be another mechanism effecting excitotoxicity. Molecular systems regulating the exchange of glutamate with cysteine and thus levels of intracellular glutamate have been found in RGC-5 cells, and cell viability assessed in response to oxidative stressors (Dun, Mysona et al. 2006).

Oxidative stress has been examined as an inducer of apoptosis in RGC-5 neurons in its own right. This has relevance to other diseases where RGCs are lost and redox

derangements implicated, such as diabetic retinopathy (Barber, Antonetti et al. 2005). Treatment of neurons with the steroid dexamethasone promotes oxidative stress, and apoptosis arising from this stressor has been demonstrated in this cell line (Boyd, Kriatchko et al. 2003). Glutathione depletion, and hydrogen peroxide treatment are other means of simulating oxidative stress in RGC-5 neurons and have also been found to reduce cell viability (Maher and Hanneken 2005). Direct treatment of RGC-5 cultures with NO and reactive oxygen species produces similar outcomes (Dun, Mysona et al. 2006).

The lack of trophic factors due to axonal transport blockade and thus leading to the death of RGCs is central to the mechanical theory of glaucoma pathogenesis. This has been investigated in RGC-5 cells. Serum deprivation effectively removes growth factors from the cell environment, simulating this scenario *in vitro*. Apoptosis was found to be induced in cultures as a result, and as mentioned previously this feature of neurons was important in initial characterisation of the cell line (Krishnamoorthy, Agarwal et al. 2001). A similar technique has been employed in later studies and reduced cell viability confirmed (Boyd, Kriatchko et al. 2003).

Hydrostatic pressure is known to impact on various aspects of cellular anatomy and physiology, and much of this information has been derived from *in vitro* work. Morphological changes including altered cell shape, alignment, processes and redistribution of cytoskeletal components such as actin filaments have been demonstrated in human ocular cells- astrocytes, lamina cribrosa glia and trabecular meshwork cells (Kosnosky, Tripathi et al. 1995; Kobayashi, Pena et al. 1997; Wax, Tezel et al. 2000). Reported neuronal responses to hydrostatic pressure indicate electrophysiological changes (Southan and Wann 1996). Interestingly peripheral nerve sensory block in carpal tunnel syndrome occurs at pressures of between 30 and 50 mm

Hg (Gelberman, Szabo et al. 1983).

Apoptosis as a result of altered pressure conditions is increasingly relevant to a number of non-neurological diseases including hypertension and cardiac failure (Nishigaki, Minatoguchi et al. 1997; Bing 1994). Neuronal loss related to pressure is also a feature of neuropathies other than glaucoma. Apoptosis in cortical neurons has been found in high pressure neurological syndrome and cerebral trauma (Mennel, Stumm et al. 1997; Reyes, Lauritzen et al. 2000). In vitro work linking hydrostatic pressure directly with induced apoptosis has now been described in several cell types, including vascular endothelia and smooth muscle cells, lymphoblasts and leukemic cells (Galea, Armstrong et al. 1999; Takano, Takano et al. 1997; Take, Yamaguchi et al. 2001). However very little is known regarding neuronal apoptosis and hydrostatic pressure as an isolated and independent stimulus.

We first identified in vitro neuronal apoptosis directly induced by hydrostatic pressure in primary mixed retinal cultures and the B35 cell line (Agar, Hill et al. 1999). These initial findings have subsequently been expanded to multiple neuronal types (Agar, Yip et al. 2000; Coroneo, Agar et al. 2001). These results for RGC-5 cells have also been reported (Agar, Yip et al. 2000; Agar, Agarwal et al. 2001; Agar, Li et al. 2002; Agar, Li et al. 2006). A co-culture of primary rat RGCs and glial cells has been studied using a similar in vitro pressure chamber based model, and apoptosis demonstrated as a result (Tezel and Wax 2000). Here a single pressure of 50 mmHg for 6 hrs to 24 hrs was applied and the induced apoptosis was significantly greater than in the negative controls. Allowing for differences in cell type and the role of the glial cells, their data suggests outcomes similar to that of our present work.

We have demonstrated that pressure related apoptosis in RGC-5 neurons was associated with the activation of a key component of the caspase cascade. Cleaved

caspase-3 levels were found to be increased in response to the hydrostatic pressure stimulus of 100 mmHg (Figs. 6-13). These results paralleled those observed with TUNEL (Fig. 6-6) and Annexin V (Fig. 6-9) of equivalent RGC-5 experiments, with the proportions of positive neurons approximating the levels seen in the apoptosis assays.

This suggests that cleaved caspase-3 may play a role in the mechanism of RGC-5 pressure induced apoptosis. The caspase family of gene products are related to the interleukin 1 β -converting enzyme and have been implicated in the cascade of apoptosis in many types of cells (Yuan, Shaham et al. 1993; Nicholson, Ali et al. 1995; Martins, Kottke et al. 1997). They exist as inactive proenzymes that are processed into their active forms in response to an apoptotic stimulus. Activated caspases cleave each other's precursors into mature active enzymes by proteolytic cleavage, in a cascade similar to the activation of complement in blood clotting (Tezel and Wax 1999). There are about a dozen named caspases, but most pathways eventually induce caspase-3 activation as a common executioner of the proteolysis cascade (Fig. 1-9).

Caspase-3 contributes to apoptosis in several ways (Porter and Janicke 1999). Activated or cleaved caspase-3 catalyzes the polyADP ribosylation of various nuclear proteins resulting in the depletion of ATP. The cell thus loses its energy source and proceeds to cell death (Tewari, Quan et al. 1995). Caspase-3 also activates deoxyribonuclease that degrades DNA during apoptosis (Enari, Sakahira et al. 1998). Further consequences of caspase activation that are involved in apoptosis are the direct disassembly of cell structures, including nuclear lamina and the cytoskeleton, and the release of cytochrome c from mitochondria (Thornberry and Lazebnik 1998; Schuler, Bossy-Wetzel et al. 2000).

Other research in vitro corroborates the role of caspases in RGC apoptosis. Multiple stimuli have been reported to induce apoptosis via caspase activation. Glutamate

excitotoxicity, simulated hypoxia and specific triggers like heat shock protein 27 have all resulted in retinal cell death linked to cleaved caspase-3 (Tezel and Wax 1999). In vivo studies into RGC apoptosis in glaucoma have also implicated caspase activation. Elevated IOP was used to simulate retinal ischemia in a rat model and TUNEL defined apoptosis was demonstrated (Katai and Yoshimura 1999). Caspase-1 and caspase-3 expression was determined by immunofluorescence and by western blot. Caspase-3 was activated in the retinal neurons, including RGCs. Interestingly this study also reported caspase-1 activity in the photoreceptor layer, suggesting pressure sensitivity of this more distal visual component.

Similar findings have been made in studies of other neurons. Treatment with a caspase inhibitor has been reported to attenuate apoptosis in isolated sympathetic neurons (McCarthy, Rubin et al. 1997). A combination of hydrostatic and compressive forces as seen in traumatic brain injury has also been found to result in neuronal apoptosis associated with caspase-3 activation (Yakovlev, Knoblach et al. 1997). This apoptotic mechanism has also been found in PC12 cells. Apoptosis was induced by oxidative stress and caspase activity recorded in PC12 neuronal cultures (Troy, Stefanis et al. 1996). PC12 studies have also suggested that caspase-3 may be important in cell volume regulation and the development of cell shrinkage in apoptosis (Maeno, Ishizaki et al. 2000). We can extrapolate from this that caspase activation may be relevant to our observed apoptosis in the PC12 line (Chapter 5).

One study has looked at hydrostatic pressure as an independent stimulus for cell apoptosis, and suggested a role for caspase-3 (Take, Yamaguchi et al. 2001). Erythroleukemia cells in culture were subjected to high pressures of over 60 megapascals or 4.5×10^5 mmHg. Apoptosis was confirmed by nuclear morphology, gel electrophoresis of DNA fragmentation and flow cytometry. Caspase-3 activity was

found to increase in a pressure dependant manner. The induced apoptosis was partly reduced by the caspase-3 inhibitor acetyl-asp-glu-val-asp-aldehyde (Take, Yamaguchi et al. 2001).

Exactly how does the hydrostatic pressure stimulus induces apoptosis? Various mechanisms have been proposed, but the process remains poorly understood. Our results for an early (Annexin V) and a late apoptotic marker (TUNEL) correlated well with each other, suggesting a multifaceted process. The cleaved caspase-3 data also point to this casacade being involved in the apoptotic mechanism. Tezel's study on primary RGC cultures suggested that the apoptosis was mediated by TNF and NO, however these were derived from concurrent glial cultures and were hence not intrinsic to the RGCs (Tezel and Wax 2000). Intracellular signalling pathways have been implicated in other ocular cells, where adenyl cyclase activity and G protein alterations were detected (Wax, Tezel et al. 2000). Research into other pressure related effects have shown modified gene expression and protein synthesis, reflecting the central role of the cytoskeleton in transducing pressure stimuli (Haskin, Athanasiou et al. 1993). Actin stress fibre reorganisation has been reported to affect morphology in many cell types, and microtubule disruption shown to alter the function of Golgi apparatus (Mattana and Singhal 1995; Parkkinen, Lammi et al. 1995).

Clues to potential mechanisms of this pressure related apoptosis may be gained from RGC-5 studies into other aspects of glaucoma pathogenesis. Hypotheses tested include the excitotoxicity theory of glutamate toxicity and trophic factor withdrawal as proposed by the mechanical theory. As mentioned above, glutamate toxicity has been demonstrated in several studies to cause RGC-5 cell death, including by apoptosis (Krishnamoorthy, Agarwal et al. 2001; Martin, Ola et al. 2004; Shimazawa, Yamashima et al. 2005). NMDA receptor overstimulation with consequent rises in intracellular Ca^{++}

has been proposed as the mechanism. Supporting this idea has been the demonstration of these receptors on RGC-5 cells and the use of NMDA receptor antagonists to successfully block this effect in these neurons. However at least one study did not find these antagonists effective in reducing glutamate related cell loss and so the possibility of another mechanism independent of NMDA receptor activation remains (Aoun, Simpkins et al. 2003).

The cytokine interleukin-10 (IL-10) has been shown to regulate RGC-5 apoptosis in another model of oxidative stress. Here IL-10 receptor signaling through the Stat-3 pathway was suggested as acting against the induction of apoptosis (Boyd, Kriatchko et al. 2003). The synthesis of inflammatory cytokines such as TNF- α is known to be inhibited by IL-10. Levels of TNF- α in glaucoma patients have been found to be elevated in blood serum and in post-mortem retinae (Yang, Yang et al. 2001; Tezel, Li et al. 2001). Using a pressure chamber model similar to that used in our study Tezel and Wax (2000) found increased levels of TNF- α in cultured human glial cells. These findings suggest a possible role for this cytokine in RGC apoptosis from oxidative and perhaps even hydrostatic pressure stimuli.

The withdrawal of trophic factors as simulated by serum starvation induces apoptosis in RGC-5 cells. This was first demonstrated in differentiated cells and has also been seen in undifferentiated cultures (Krishnamoorthy, Agarwal et al. 2001; Boyd, Kriatchko et al. 2003; Shimazawa, Yamashima et al. 2005). Interestingly this is an effect also seen in the other differentiated cell line we studied, PC12. The mechanism of apoptosis induction in differentiated PC12 neurons is believed to be via a decrease in mitochondrial membrane potential (Wadia, Chalmers-Redman et al. 1998). One study has also linked trophic withdrawal to oxidative stress by showing an increase in the fluorescent intensity of a reactive oxygen species indicator (Shimazawa, Yamashima et

al. 2005). IL-10 is also implicated in RGC-5 cell loss from the withdrawal of trophic factors (Boyd, Kriatchko et al. 2003). RGC-5 cultures exposed to glutamate displayed a transient increase in the mRNA and protein of the growth factor BDNF (brain derived neurotrophic factor), proposed to be through activation of its receptor TrkB and a Ca^{++} dependant protein kinase (Fan, Agarwal et al. 2006). Taken together these studies show interrelationships between several potential mechanisms of apoptosis in RGC-5 neurons.

A recent study has reproduced our model system. Using a similar pressure chamber approach this research corroborated our findings of hydrostatic pressure induced apoptosis in the RGC-5 cell line. Following a pressure elevation of 100 mmHg for a period of hours, apoptosis in undifferentiated cells was detected by TUNEL (Kim, Lee et al. 2006). In this study changes were also seen in the expression and distribution of the enzyme glyceraldehyde-3-phosphate-dehydrogenase (GAPDH) as determined by gel electrophoresis. GAPDH is involved in metabolic energy production and in several subcellular processes including DNA replication and apoptosis. Increased expression, accumulation and translocalisation of GAPDH were seen in RGC-5 cells after the application of pressure. These were suggested as being involved with the apoptotic process. The mechanism was however undefined.

The electrophysiology of RGC-5 cells may provide other approaches to explaining the observed cell death. Differentiation with staurosporine has been shown to alter the electrical properties of the neurons in culture by the expression of outward rectifying ion channels, large voltage conductances and increased K^{+} conductance (Frassetto, Schlieve et al. 2006). A group collaborating with our research team has further investigated the channel properties of undifferentiated RGC-5 neurons by patch clamping studies. They demonstrated inwardly rectifying K^{+} currents and stretch

activated channels (Moorhouse, Li et al. 2004). Significantly these mechanosensitive channels were activated at pressures above 20 mm Hg. These pressures are of relevance to the common clinical scenario of primary open angle glaucoma. Although the channels have yet to be characterised fully, the prospect of TRAAK channels being involved is an intriguing possibility, as these also are mechanostimulated to open at around 30 mmHg (Maingret, Fosset et al. 1999).

In summary the results presented here provide strong evidence that elevated hydrostatic pressure induces apoptosis in RGC-5 neurons directly and thus extends our earlier findings on other neuronal cell lines and in primary retinal cultures. We propose a novel relationship linking pressure directly with apoptosis. The mechanisms that may mediate this response remain unknown and warrant further investigation, and perhaps could offer new avenues for therapeutic manipulation in baropathies like glaucoma.

Chapter Seven

General Discussion

7

Glaucoma is an important eye disease of considerable public health significance. It is believed to affect almost 70 million people around the world (Quigley 1996), and is the leading cause of irreversible blindness globally (Foster and Resnikoff 2005). In Australia there are over a quarter of a million patients, with estimates that a comparable number remain undiagnosed (Access-Economics 2004). The disease is characterised by the progressive loss of RGCs over time. The most frequent and important association is that of elevated IOP (Armaly, Krueger et al. 1980), and the only proven treatment for any type of glaucoma is to reduce this hydrostatic pressure within the eye (Rait 2000; Shields 2004). Induced increases in IOP in animal models have been shown to result in the loss of RGCs, confirming the relationship seen in clinical glaucoma (Nickells 1996). These studies have revealed the major mode of RGC loss to be via apoptosis, the genetically programmed form of cell death. This has also been validated in human glaucoma (Kerrigan, Zack et al. 1997). The molecular events that result in apoptosis can be initiated by a variety of stimuli (Nickells and Zack 1996).

Exactly how elevated IOP leads to the death of RGCs by apoptosis is the central question of glaucoma pathogenesis, and still remains unanswered. Theories of glaucoma pathogenesis include mechanodistortion of the optic nerve at its exit from the eyeball affecting RGC transport mechanisms, and compression of optic nerve head microvasculature compromising neuronal circulation (reviewed by Quigley, 1995). Toxicity of RGCs due to elevated levels of the neurotransmitter glutamate has also been implicated (Dreyer 1998). It has been reported that inhibition of retrograde axonal flow can only partly explain RGC loss post axotomy (Fagiolini et al., 1997). There is evidence from other studies that RGC loss may be mediated independently of these mechanisms (Radius 1981; Johansson 1983; Johansson 1988). Therefore, in addition to

the known components of glaucoma pathology, pressure may also have some direct effect on RGC apoptosis. Each theory however has limitations; there are inconsistencies and exceptions based on experimental and clinical evidence that continue to foster debate and the continuing search for pathogenic mechanisms. Current understanding is thus shifting toward a multifactorial causation, and cellular biology is at the forefront of the latest investigative approaches (Kuehn, Fingert et al. 2005; Casson 2006).

Pressure as a crucial physical component of the cellular milieu is known to have varied impacts upon cell function and survival (Somero 1991; Ashcroft 2000). Recent developments in the field of mechanotransduction suggest a paradigm in which cells are able to sense pressure changes directly and transduce this into changes in cell function. Pressure stimuli could thus be felt directly by a cell and possibly result in apoptosis (Ko and McCulloch 2000; Ingber 1997). Apoptosis of cells as the result of increased hydrostatic pressure has been studied in the context of cardiac, vascular and renal disease (Galea, Armstrong et al. 1999; Bing 1994; Mertens, Espenkott et al. 1998). Pressure as an isolated stimulus has been demonstrated to induce apoptosis in leukemia cells (Takano, Takano et al. 1997). Yet this physical variable remains one of the least understood in terms of disease pathogenesis, even in well known baropathies such as glaucoma. This is especially true at the cellular and subcellular level, leading one author to comment that "...for a major neurodegenerative disease, there are comparatively few studies into the cellular mechanisms which underlie glaucoma" (Vickers 1997).

The aim of the research reported in this thesis was thus to examine the direct response of neuronal cells to the stimulus of elevated hydrostatic pressure, looking specifically for apoptosis. To our knowledge such work had not been reported prior to undertaking this work. Our objective was therefore to further our understanding of the disease processes underlying pressure related conditions such as glaucoma.

To achieve this objective we developed an *in vitro* model so as to fulfill the inherent requirements of such a study, namely a device to apply and adjust hydrostatic pressure, a source of neuronal cells, and methods to measure their response to this pressure in terms of apoptosis. Our system was based on pressure chambers which allowed neuronal cell cultures to be subjected to elevated ambient hydrostatic pressure (Fig. 2-1). The pressure chamber is the most physiologically relevant *in vitro* model for consistently varying hydrostatic pressure at levels relevant to the pathogenesis of glaucoma. It is conceivable that increased ambient hydrostatic pressure of a defined incubation gas mix (5% CO₂ and air) on a liquid phase culture media could alter partial pressures of the vital gases O₂ and CO₂, and through dissolved CO₂ affect pH, affecting neuronal viability. We therefore tested our pressure chamber for such a potential gas effect on cell cultures. Our experiments showed no significant difference in pH, O₂ or CO₂ in cultures subjected to pressure of 100 mmHg for 2 hrs compared to controls (Figs. 3-1 to 3-3, Table 3-1). These results therefore assured us that the experimental protocol used in the current investigations did not significantly alter gas relationships of the neuronal cultures, and that any effects noted in cultured neurons were attributable primarily to the altered pressure conditions alone. Studies using similar pressure chamber designs with other cell types, showing a negligible impact on gas relationships of culture media, also support our conclusion (Kosnosky et al., 1995; Sumpio et al., 1994; Mattana and Singhal 1995; Qian et al., 1999).

For this research project the principal advantage of cell culture is the ability to precisely control the physical environment of cells free of systemic influences (Kevles and Geison 1995). We could thus isolate and study pressure as an independent experimental variable. The target cell in glaucoma is the RGC, however this is not easily grown in laboratory conditions (Kerrigan, Zack et al. 1997). Hence we obtained

primary cultures derived from the retinae of neonatal rat eyes. These mixed retinal cultures were shown to contain RGCs identified morphologically and by the use of specific immunofluorescent labels (Fig. 4-2). Our techniques were then successfully applied to retinal cultures of human fetal eyes.

This work with primary retinal cultures enabled us to develop a bioassay to examine pressure related neuronal apoptosis. The viability of the primary cultures however was found to vary considerably, as evidenced by the survival assays (Fig. 4-1). This together with the mixed nature of the cell population (ie. both neuronal and non-neuronal cell types) made the assessment of any pressure effect on neurons difficult.

Subsequent work thus focussed on cell lines. Cell lines are derived from primary culture cells that have been transformed into clonally identical cells capable of repeated propagation, and offers uniform and predictable characteristics of cells (Freshney 1994). Initially three cell lines were used: B35, C17 and NT2 (Figs. 5-1, 5-2). These lines may however not be post-mitotic and thus continue to proliferate. Indeed later timepoints in the bioassay of apoptotic markers were found to be less reliable, a finding we ascribed to population variation (Figs. 5-10, 5-14 and 5-15). To further investigate this issue a cell line capable of differentiation into a post-mitotic state, the PC12 line, was then studied (Fig. 5-3). Finally a recently developed RGC-5 cell line, in both undifferentiated and differentiated states, was included (Fig. 6-1). This enabled us to study the target cell of glaucoma for pressure induced apoptosis.

Apoptosis was first defined in terms of the appearance of affected cells, and morphology remains central to its detection (Kerr, Wyllie et al. 1972; Darzynkiewicz, Bedner et al. 1998). There are several features that characterise this mode of cell death. Neurons undergoing apoptosis show a loss of neurites and their cell bodies shrink. The nucleus also reduces in size and becomes condensed and pyknotic, and the cell

membrane displays characteristic blebbing (Wyllie, Kerr et al. 1980; Buja, Eigenbrodt et al. 1993; Nickells and Zack 1996). Immunofluorescent labelling with specific apoptotic markers for nuclear changes (TUNEL) or membrane changes (Annexin V) enhance many of these changes in neuronal appearance (van Engeland, Ramaekers et al. 1996; Castedo, Hirsch et al. 1996; Darzynkiewicz, Juan et al. 1997; Ecker and Steiner 2004).

Light microscopic examination of live cell cultures confirmed cell viability during the current experiments and allowed for ongoing assessment of cell growth and development. Fluorescent marker staining of fixed cells highlighted morphologic features by imaging with a laser scanning microscope. Characteristic features of the various cell types studied were evident from such morphological analysis.

Primary retinal cultures displayed a range of differing cell morphologies, with both glial and neuronal cells seen reflecting the mixed nature of the culture (Figs. 4-1, 4-2). Neurons displayed specific characteristics such as neurite formation, and it was also possible to differentiate populations of neurons by morphology that may represent retinal cell sub-types such as horizontal, amacrine and bipolar cells (Fig. 4-2). RGCs were identified by Thy 1.1 immunofluorescent marker staining, and showed characteristic large cell bodies and extensive neurite formation.

Cell line cultures on the other hand demonstrated relatively homogenous morphology that was preserved across all cultures of a specific cell line. These features confirmed the uniform and reproducible features which define this form of cell culture, ideal for the purposes of a bioassay. All types showed characteristic neurite formation. There were however variations between the different neuronal types studied, which were distinctive for a given cell line. Dendrites ranged from the broad processes in NT2 neurons (Fig. 5-2) to intermediate sized in B35 neurons, (Fig. 5-1) and the fine

processes of PC12 neurons (Fig. 5-3). Differentiation of the PC12 cell line gave rise to extensive branching neurite formation, with at times extensive neuronal networks seen (Fig. 5-3). A similar pattern was seen in the differentiated RGC-5 cell line. Undifferentiated neurons showed neurite formation which was relatively basic in comparison to the prolific dendrites of the differentiated RGC-5 cells (Fig. 6-1). This differentiated morphology resembled that of RGCs seen in our primary rat retinal cultures (Fig. 4-2). Features of necrosis (including swelling of cells with disruption of cell membranes) were negligible.

Morphologic evidence of apoptosis was identified in our bioassay in all cell cultures studied, both undifferentiated and differentiated. Apoptosis was most pronounced in the 'positive control' cultures treated with known stimuli of apoptosis (ethanol or DNase). Here the vast majority of cells were apoptotic and the degree of apoptosis was also more marked. By contrast 'negative control' cultures, (ie. not exposed to apoptotic stimuli or elevated pressure conditions) showed apoptosis only occasionally. Experimental 'pressure' cultures (those exposed to ambient hydrostatic pressure over and above atmospheric) were generally found to have levels of apoptosis intermediary between these two companion control groups. The relative degrees to which apoptosis was seen morphologically can be gauged by comparing the LM and LSM images of the three culture groups (Figs. 4-3, 5-4 to 5-9, 6-2 to 6-5).

Our assay techniques using morphology and apoptotic markers all indicated that cell death following experimental pressure conditions occurred by apoptosis. Apoptosis is an active and physiological mode of cell death characterised by a series of morphological and molecular events (Figs. 1-6, 1-7) which can be detected by a variety of techniques. It is increasingly apparent that no single method can be reliably used to identify apoptosis. Rather, the use of more than one technique, ideally based on

different detection principles, is best suited to distinguish apoptotic cells (Darzynkiewicz, 1998).

The approach used in this study combines morphology, molecular markers of nuclear fragmentation (TUNEL) and membrane alterations (Annexin V) to optimise apoptosis detection. Several factors may confound the observations made in this study. Cells could be at different stages of apoptosis and may not exhibit all the features (morphological or molecular) of this process. TUNEL positive nuclear strand breaks can be seen in necrotic cells, but they are randomly sized and an order of magnitude fewer, hence the staining is much less intense (Schmid, Krall et al. 1992). Annexin V in conjunction with PI can distinguish the two modes of cell death in live cells more accurately, but this is less reliable in the late stages of apoptosis (van Engeland, Ramaekers et al. 1996). Annexin V phosphatidyl translocation can also occur with necrotic cells, but PI vital dye staining confirmed this was not significant in our experiments. The combination here of multiple techniques should enhance the sensitivity of apoptosis detection and also improve its accuracy (Darzynkiewicz, Bedner et al. 1998). Since apoptotic morphology remains the gold standard of its detection, visual inspection of neurons remained integral to our bioassay.

This study also establishes the Laser Scanning Cytometer as a unique tool for the examination of apoptosis in neurons. The LSC is able to visualise adherent cells such as neurons using the integrated laser scanning microscope (Fig. 2-2). By storing vectored data in relation to each scanned cell, the fluorescent marker intensity- a quantitative result- can be confirmed by visual, and hence morphological examination. The LSC's automation minimises potential observer influence on data collection and analysis; the data can be normalised between separate pressure runs using a positive control (Fig. 2-3). Fluorescent marker intensity values for TUNEL and Annexin V assays have been

demonstrated to reflect morphological apoptotic features and are a reliable indicator of apoptosis as measured by LSC (Darzynkiewicz and Bedner 2000).

During the course of this work the techniques of quantitative analysis were refined as the LSC's capabilities of automated cytometry were explored. As the first group in our institution to use this technology (the only one of its kind in the country at that time) we had to develop our LSC detection protocols 'de novo'. Thus in our initial work this data for TUNEL and Annexin V markers of apoptosis enabled us to quantify marker staining intensity only (in primary retinal cultures and B35 cell line work). Subsequently however by using sophisticated software we were able to perform two-pass laser scans and achieve data that would represent not only the intensity of staining in cells, but also the number of these stained cells, thus giving us the percentage of apoptotic cells in the total cell population. Hence the data from the majority of our work (C17, NT2, PC12 and RGC-5) has been analysed and presented this way. The only exception to the LSC's utility was the cleaved caspase-3 assay, where the staining characteristics were too fine and scattered for reliable automated scanning.

Quantitative results for positive control cells which had been subjected to a known apoptotic stimulus (ie. 100 mmHg for 2 hrs) showed much greater labeling for both TUNEL and Annexin V in all cell cultures. The uniformly high level of apoptosis in the positive controls, by both marker intensity and apoptotic population (> 80%) suggests that the LSC can reliably detect apoptotic neurons (Figs. 4-5, 4-6, 5-10 to 5-19, 6-6 to 6-10). The quantitative results obtained by LSC correlated well with the morphological findings of more notable and higher proportions of apoptotic characteristics in these cultures. The validity of the experimental protocol to accurately detect apoptotic neurons was thus established.

The results for negative control cultures were notable for their low but consistent levels of background apoptosis in the absence of any specific experimental apoptotic stimuli. The extent of this apoptosis was higher than expected, and the reasons are unknown. Presumably they reflect specific and as yet undetermined features of the neuronal cultures. In primary cultures the mixed nature of the cells makes interpretation difficult. Cell lines having been derived from transformation of primary cells may have altered apoptotic mechanisms and thus behave differently to primary neurons and RGCs in particular. However all cell lines of a given type are by definition identical as they are derived from a single clonal population. It follows then that this level of background apoptosis would apply to all experimental groups equally, and indeed data was consistent for each cell line.

Data for undifferentiated cell line cultures (B35, C17, NT2 and undifferentiated RGC-5) showed that increased TUNEL labeling was statistically significant at the 2 hrs timepoint, i.e. after the application of pressure conditions for 2 hrs, (Figs. 5-10 to 5-12, 5-14 to 5-15, 6-6 to 6-8). Statistical analysis of the data from later timepoints was inconclusive. These results are not unexpected since such a pressure induced apoptotic response would be expected to be greatest closer to the time of induction of the pressure stimulus, compared to a later timepoint. Annexin V results were similar to the TUNEL data, i.e. greater apoptosis in pressure treated cells compared to negative controls (Figs. 5-13, 6-9). In contrast to these findings the results from differentiated PC12 and RGC-5 cells showed that the increase in apoptotic cells in the pressure group compared to the negative control group was significant only at the 24 hrs timepoint, and not at the earlier 2 hrs timepoint (Figs. 5-16 to 5-19, 6-10). Our previous work on retinal culture (with a mixed population of pre- and post-mitotic cells) had already shown this 'delayed' effect (Figs. 4-5, 4-6).

Thus we found that undifferentiated neurons appear to have a pressure induced apoptosis response at an earlier stage in contrast to differentiated neurons which have a delayed response. The explanations for this difference lie either in some intrinsic feature of the specific cells, or relate to the proliferative state of undifferentiated cells versus the post-mitotic differentiated cells. Undifferentiated cells are by definition at potentially all stages of the cell cycle, with no cell cycle synchronisation. Our pressure conditions may selectively affect cells at a specific phase of the cell cycle early, with the remaining population less susceptible thereafter. In fact there is a report in the literature on pressure induced apoptosis related to a particular phase of the cell cycle (Takano et al., 1997). This may help explain our variable results at later timepoints. Another factor is likely to relate to proliferation of the undifferentiated cell lines, so that the numbers of cells would be expected to increase with time. Later timepoints may thus have considerably different populations, which would vary even between individual wells. As this growth is often unpredictable and difficult to control for, comparisons between different experimental groups at later timepoints would be difficult.

By contrast the PC12 and RGC-5 cell lines were induced to differentiate to a post-mitotic state. The primary retinal culture neurons were similar post-mitotic. The extracellular stimulus of elevated pressure may cause a differing response in these neurons which have exited the cell cycle. It is known that post-mitotic neurons behave differently with other apoptotic stimuli, even when compared to their undifferentiated state (Lambeng, Michel et al. 1999; Oberdoerster and Rabin 1999). Other studies support our findings of undifferentiated cells to be more sensitive than post-mitotic neurons to an apoptotic stimulus. Differentiated PC12 neurons, for example, have been reported to have significant apoptosis induction only at 24 hrs (Oberdoerster, Kamer et al. 1998).

Pressure induced apoptosis in this study varied with the applied pressure. In undifferentiated RGC-5 cultures the greatest proportion of TUNEL and Annexin V positive cells (~40%) was at 'high' hydrostatic pressure conditions of 100 mmHg. This is about 2.5 times the negative control level (~15%) (Figs. 6-6, 6-9). These high levels were also found in our earlier experiments with other undifferentiated cell lines (Figs. 5-10 to 5-15). 'Low' settings of 30 mmHg induced ~30% (Fig. 6-7), and the 15 mmHg conditions ~20% apoptosis positive cells (Fig. 6-8). This latter data was still greater than the comparable negative control (~15%), although the difference was not statistically significant. The RGC-5 results for the late and early apoptosis markers were comparable for all experimental groups, with good correlation by morphology as well as quantitative analysis.

The findings into a graded pressure response in RGC-5 neurons were interesting in terms of the selected pressures. The 'high' pressure of 100 mmHg is analogous to that seen clinically in the most severe cases of acute glaucoma; the 'low' 30 mmHg represents chronic glaucoma and the 'lowest' pressures of 15 mmHg reflect 'normal' IOP. These three levels correlate broadly with the observed disease severity. These results showed that relatively consistent changes in apoptosis corresponded to much greater changes in applied pressure conditions, suggesting that an increase in induced apoptosis does not have a linear relationship with pressure. Two possible explanations may be provided for this. Firstly this may be a characteristic of the transformed RGC-5 cell line itself and secondly, the relationship may also relate to the specific apoptotic mechanism triggered. For example a channel dependant system may respond to physical stimuli in a non-linear fashion; mechanosensitive channels such as TRAAK, have been reported to open at hydrostatic pressures of 30 mmHg and could be involved (Maingret, Fosset et al. 1999).

Several aspects of cellular anatomy and physiology are affected by variations in hydrostatic pressure (Somero 1991). Interestingly similar elevations of pressure, between 30 to 50 mmHg, have induced peripheral nerve sensory block in carpal tunnel syndrome (Gelberman, Szabo et al. 1983). In the human eye morphological changes in cell shape, alignment and processes, and cytoskeletal actin redistribution have been demonstrated in astrocytes, lamina cribrosa glia and trabecular meshwork cells (Kosnosky, Tripathi et al. 1995; Wax, Tezel et al. 2000; Kobayashi, Pena et al. 1997). However very little is known regarding neuronal apoptosis and hydrostatic pressure as an isolated and independent stimulus. A study into neural cell cultures and physical stressors in relation to glaucoma found mechanical shear to induce apoptosis (Edwards et al., 1998). In comparison, extremely high hydrostatic pressure (non-physiological) can induce apoptosis and necrosis in human lymphoblasts (Takano et al., 1997). Our current study indicates that changes in hydrostatic pressure within physiological limits may also stimulate neural apoptosis. We believe that this is the first study of the effect on neurons of clinically relevant raised hydrostatic pressures alone, and to demonstrate that these pressure conditions result in neuronal apoptosis. In addition to the broad range of known factors that trigger apoptosis, we suggest pressure may also be included as a potential activator of apoptotic pathways in neurons.

Since our initial report showing *in vitro* neuronal apoptosis directly induced by hydrostatic pressure (Agar, Hill et al. 1999), another group used a similar pressure chamber based model and demonstrated apoptosis induced by pressures of 50 mmHg in a co-culture of primary rat RGCs and glial cells (Tezel and Wax 2000). Although the role of glial cells may be significant in that report, their data suggests similar outcomes to those we have demonstrated. A recent report on the response of RGC-5 cultures to elevated hydrostatic pressures has also corroborated our data (Kim, Lee et al. 2006).

Using equivalent stimuli of 100 mmHg in similar pressure chamber systems they found induced apoptosis by TUNEL assay.

How the hydrostatic pressure stimulus induces apoptosis in neurons is not clearly understood, though various mechanisms have been proposed. The cell cycle stage may be relevant, as suggested by our data and alluded to by other studies (Takano et al., 1997; Oberdoerster et al., 1999). Apoptosis in the neuronal study involving mechanical shear was associated with an increase in nitrous oxide (NO) production and G protein activation (Edwards et al., 1998). The results for an early (Annexin V) and a late apoptotic marker (TUNEL) correlated well with each other, suggesting a multifaceted process. Tumour necrosis factor (TNF) and NO mediated apoptosis were implicated in the study on primary RGC and glial co-cultures, however these were not intrinsic to the RGCs but derived from the glial cells (Tezel and Wax 2000). In other ocular cells adenylyl cyclase activity and G protein alterations were detected suggesting intracellular signalling pathways were involved (Wax, Tezel et al. 2000).

The caspase pathway is believed to be one of the main mediators of apoptosis. In glaucoma it has been postulated as being involved in RGC apoptosis from glutamate toxicity and ischemia (Katai and Yoshimura 1999; Tezel and Wax 2000). Our work showed that activation of one of the key caspase enzymes, detectable as cleavage of caspase-3, was enhanced by the application of pressure conditions identical to those that induced apoptosis. Morphological analysis confirmed the co-localisation of apoptotic features with cleaved caspase-3 labelling (Figs. 6-11, 6-12). The differing staining intensities and proportions of the cell population affected mirrored those found in comparable apoptosis assays. Quantitative analysis also confirmed these findings (Fig. 6-13). Thus the role of caspase-3 in apoptosis induced by hydrostatic pressure alone is evident from this data. These results are supported by a report suggesting caspase-3

activation is enhanced by increased hydrostatic pressure in a dose-dependant manner (Take, Yamaguchi et al. 2001).

Cellular responses to pressure other than apoptosis also provide clues to potential mechanisms. Cell cultures studied in pressure models similar to that used in this study reveal enhanced cell proliferation and modification of protein expression (Mattana and Singhal 1995). This suggests cytoskeletal proteins may be subject to modulation by ambient pressure, consistent with tension-rigidity models of cell structure where such proteins contribute to and may therefore mediate physical force transfers (Wang et al., 1993). Such a concept is supported by findings of morphological responses to pressure (Sumpio et al., 1994). If neuronal compression is significant in our work, it is unclear whether the stimulus is related to compression or decompression or the static period of elevated pressure. Further, we do not know how the rates and durations of these changes affect the neuronal response. Our study using this model dealt with a specific set of experimental variables, and has found an effect related to these pressure conditions. Future work may allow evaluation of the basic parameters involved in pressure induced apoptosis, such as the rate of change and response threshold of the pressure stimulus.

Apoptosis may be stimulated by a sensitivity of the cell membrane to pressure changes. How pressure alterations are detected, let alone the mechanism of conversion of this into intercellular responses, is yet to be resolved. Mechanisms that allow cells to sense pressure changes are the focus of widespread research in the emerging field of mechanotransduction (Ko and McCulloch 2000). Biomechanical modelling has emphasised the central role of pressure related stress in glaucomatous damage using structural principles at the cellular level (Bellezza, Hart et al. 2000; Burgoyne, Crawford Downs et al. 2005). Pressure has been found to cause changes in trans-membrane ion fluxes, currents and subsequent downstream processes such as neural transmission

(Southan and Wann 1996; Parmentier, Shrivastav et al. 1981). Membrane bound mechanosensitive ion channels are gaining importance as integral to normal cell physiology, and have been identified in astrocytes and found to be activated by just seconds of hydrostatic pressures of 45 mmHg (Islas, Pasantes-Morales et al. 1993; Hamill and McBride 1996). Calcium ion channels have been shown to be responsive to hydrostatic pressure in neuronal cell lines (Tarnok and Ulrich 2001). TRAAK is a novel two-pore mammalian K⁺ mechanosensitive channel that has been shown to be expressed in retinal tissues in both rat and human retina, with localisation to RGCs (Maingret, Fosset et al. 1999; Reyes, Lauritzen et al. 2000; Edward and Ueda 2001). Our laboratory has recently identified this channel in RGC-5 cells (Coroneo, Li et al. 2002; Kalapesi, Coroneo et al. 2005) and reviewed these channels in the context of glaucoma pathogenesis (Kalapesi, Tan et al. 2005; Tan, Kalapesi et al. 2006).

Mechanosensitive channels offer a novel alternative for explaining the mechanisms involved in pressure induced apoptosis. This hypothesis allows for intrinsic processes independent of other stimuli, and one which could be sensitive to pressure directly. The channels could play a role in the initiation of intracellular pathways that could ultimately lead to apoptosis by various known mechanisms, such as p53 or caspase activation, or modulation of Bax, gene expression (Nickells 1999). A graded response may be mediated by sub-populations of channels open at different levels of stimulation, or conversely by a graded response of the channel itself.

The possibility that pressure may be related to apoptosis is an interesting concept. At the cellular level there could be a greater sensitivity to this physical variable than previously thought. Since there appear to be a variety of cellular processes already shown to be modulated by pressure, it is not unreasonable to consider apoptosis also as an endpoint. This is relevant in a disease such as glaucoma where neuronal apoptosis is

somehow associated with an environment of altered pressure conditions. In addition to the known macroscopic anatomical, circulatory and excitotoxic pathophysiology of glaucoma, this concept suggests that RGCs may also be susceptible to elevated pressure at the cellular level. A neuronal response may thus be mediated by a more direct exposure to increased IOP. Indeed large neurons in the retina (RGCs), cerebellum (Purkinje), and spinal cord (motor neurons) appear to respond differently (usually more sensitive) to physiological stressors compared with smaller neurons (Gilman, Colton et al. 1986; McKinney, Willoughby et al. 1996; Southan and Wann 1996) .

In summary this study subjected neuronal cell lines to raised ambient hydrostatic pressures relevant to those found clinically in glaucoma, and found an increase in neuronal apoptosis under these conditions. Apoptosis was confirmed qualitatively by cell morphology analysis and quantitatively by two separate specific markers of apoptosis. Laser scanning cytometry also allowed correlation of morphology with marker staining, as well as quantitative analysis of these fluorescent labels. This apoptotic effect was initially noted for high pressures analogous to acute glaucoma in primary rat mixed retinal cultures and then extended to both undifferentiated and differentiated post-mitotic neuronal cell lines (Agar, Yip et al. 2000). We also found increased levels of apoptosis in undifferentiated and differentiated RGC-5 neurons exposed to elevated hydrostatic pressure conditions relevant to both acute and chronic glaucoma, but no effect at pressures analogous to ‘normal’ intraocular pressure. The proportion of apoptotic neurons was significantly higher compared to matched controls, and greater for 100 mmHg than 30 mmHg (Agar, Li et al. 2006). Finally we have demonstrated that RGC-5 neurons responded to experimental pressure conditions by increasing activation of Caspase-3. This suggests that this cellular pathway may play a role in the mechanism of observed pressure induced apoptosis. The RGC-5 line was

further shown to be a useful tool for investigating RGC pathology *in vitro*, and in experimental assays in particular.

This study was the first to demonstrate in a biological assay system that physiologically relevant levels of pressure may have an impact on neuronal survival. We suggest the possibility of a novel relationship linking pressure and neuronal apoptosis directly. It follows that conditions of elevated hydrostatic pressure, such as those found in glaucoma, may stimulate apoptosis by mechanisms other than those implicated in conventional pathogenesis theories. We would also propose that raised hydrostatic pressures associated with other neural diseases, or following trauma, could induce neuronal apoptosis. The specific mechanism of pressure activation of this apoptotic pathway is not known at present. The potential activation of an apoptotic pathway requires exploration to understand the conversion of this physical stimulus to a biological outcome. The role of Caspase-3 activation provides a useful starting point to further these investigations. Both molecular and genetic processes, such as signal transduction and analysis of protein and mRNA or DNA expression, can be studied using this bioassay. This system now allows us to further investigate a number of other variables including different neurons and the basic parameters of the pressure stimulus. We can also study pharmacological and genetic factors that may support neuronal survival following these pressure conditions. This could potentially then open up new therapeutic approaches, based on an enhanced understanding of the pathogenesis of this important blinding eye disease.

References

8

- Abu-Amero, K. K., J. Morales, et al. (2006). "Mitochondrial abnormalities in patients with primary open-angle glaucoma." Invest Ophthalmol Vis Sci **47**(6): 2533-41.
- Access-Economics (2004). Clear Insight. Melbourne, Centre for Eye Research Australia.
- Adachi, M., K. Takahashi, et al. (1996). "High intraocular pressure-induced ischemia and reperfusion injury in the optic nerve and retina in rats." Graefes Arch Clin Exp Ophthalmol **234**(7): 445-51.
- Adler, R. (1996). "Mechanisms of photoreceptor death in retinal degenerations. From the cell biology of the 1990s to the ophthalmology of the 21st century?" Arch Ophthalmol **114**(1): 79-83.
- Agar, A., N. J. Agarwal, et al. (2001). "Retinal Ganglion Cell line apoptosis in a hydrostatic pressure model." Invest Ophthal & Vis Sci **42**(4): S139 [ARVO Abstract].
- Agar, A., M. Hill, et al. (1999). "Pressure induced apoptosis in neurons." Invest Ophthalmol Vis Sci **40**(4): S265 [ARVO abstract].
- Agar, A., S. Li, et al. (2002). "In-vitro pressure induced apoptosis in RGC line shows graded response to simulated Acute, Chronic Glaucoma & normal pressure." Invest Ophthal Vis Sci **43**(4): S4060 [ARVO abstract].
- Agar, A., S. Li, et al. (2006). "Retinal ganglion cell line apoptosis induced by hydrostatic pressure." Brain Res **1086**(1): 191-200. (*see Appendices*)
- Agar, A., S. S. Yip, et al. (2000). "Pressure induced apoptosis in an RGC neuronal cell line." Invest Ophthal Vis Sci **41**(4): S4378 [ARVO abstract].
- Agar, A., S. S. Yip, et al. (2000). "Pressure related apoptosis in neuronal cell lines." J Neurosci Res **60**(4): 495-503. (*see Appendices*)
- Akaike, A., K. Adachi, et al. (1998). "[Techniques for evaluating neuronal death of the retina in vitro and in vivo]." Nippon Yakurigaku Zasshi **111**(2): 97-104.
- Allen, S. P., H. M. Liang, et al. (1996). "Elevated pressure stimulates protooncogene expression in isolated mesenteric arteries." Am J Physiol **271**(4 Pt 2): H1517-23.
- Aloyz, R. S., S. X. Bamji, et al. (1998). "p53 is essential for developmental neuron death as regulated by the TrkA and p75 neurotrophin receptors." J Cell Biol **143**(6): 1691-703.

- Anatomy, University of Melbourne (2006). "Anatomy- research labs: retina image." Retrieved Nov 2006, <http://www.anatomy.unimelb.edu.au/researchlabs/rees/images/retina.jpg>
- Anderson, D. R. (1977). "The management of elevated intraocular pressure with normal optic discs and visual fields. I. Therapeutic approach based on high risk factors." Surv Ophthalmol **21**(6): 479-89.
- Anderson, D. R. (1995). Glaucoma, its terminology and fundamental nature. Optic Nerve in Glaucoma. S. M. Drance and D. R. Anderson. Amsterdam, Kugler Publications bv: 1-14.
- Anderson, D. R. (1996). "Glaucoma, capillaries and pericytes. 1. Blood flow regulation." Ophthalmologica **210**(5): 257-62.
- Anderson, D. R. and A. Hendrickson (1974). "Effect of intraocular pressure on rapid axoplasmic transport in monkey optic nerve." Invest Ophthalmol **13**(10): 771-83.
- Anderson, D. R. and H. A. Quigley (1999). The Optic Nerve. Adler's Physiology of the Eye. W. Hart. St Louis, Mosby: 616-626.
- Aoun, P., J. W. Simpkins, et al. (2003). "Role of PPAR-gamma ligands in neuroprotection against glutamate-induced cytotoxicity in retinal ganglion cells." Invest Ophthalmol Vis Sci **44**(7): 2999-3004.
- Arend, O., N. Plange, et al. (2004). "Pathogenetic aspects of the glaucomatous optic neuropathy: fluorescein angiographic findings in patients with primary open angle glaucoma." Brain Res Bull **62**(6): 517-24.
- Arends, M. J., R. G. Morris, et al. (1990). "Apoptosis. The role of the endonuclease." Am J Pathol **136**(3): 593-608.
- Armaly, M. F., D. E. Krueger, et al. (1980). "Biostatistical analysis of the collaborative glaucoma study. I. Summary report of the risk factors for glaucomatous visual-field defects." Arch Ophthalmol **98**(12): 2163-71.
- Ashcroft, F. (2000). Life at the extremes. London, Harper Collins.
- Aung, T., L. P. Ang, et al. (2001). "Acute primary angle-closure: long-term intraocular pressure outcome in Asian eyes." Am J Ophthalmol **131**(1): 7-12.
- Barber, A. J., D. A. Antonetti, et al. (2005). "The Ins2Akita mouse as a model of early retinal complications in diabetes." Invest Ophthalmol Vis Sci **46**(6): 2210-8.
- Barbiero, G., L. Munaron, et al. (1995). "Role of mitogen-induced calcium influx in the control of the cell cycle in Balb-c 3T3 fibroblasts." Cell Calcium **18**(6): 542-56.
- Barres, B. A., B. E. Silverstein, et al. (1988). "Immunological, morphological and electrophysiological variation among retinal cells purified by panning." neuron **1**(9): 791-803.

- Bathija, R., N. Gupta, et al. (1998). "Changing definition of glaucoma." J Glaucoma **7**(3): 165-9.
- Beale, R. and N. N. Osborne (1982). "Localization of the Thy-1 antigen to the surface of rat retinal ganglion cells." Neurosci. Int., **4**: 587-596.
- Bedner, E., X. Li, et al. (1999). "Analysis of apoptosis by laser scanning cytometry." Cytometry **35**(3): 181-95.
- Bellezza, A. J., R. T. Hart, et al. (2000). "The optic nerve head as a biomechanical structure: initial finite element modeling." Invest Ophthalmol Vis Sci **41**(10): 2991-3000.
- Ben-Sasson, S. A., Y. Sherman, et al. (1995). "Identification of dying cells--in situ staining." Methods Cell Biol 1995;46:29-39.
- Berkelaar, M., D. B. Clarke, et al. (1994). "Axotomy results in delayed death and apoptosis of retinal ganglion cells in adult rats." J Neurosci **14**(7): 4368-74.
- Bhandari, A., D. P. Crabb, et al. (1997). "Effect of surgery on visual field progression in normal-tension glaucoma." Ophthalmology **104**(7): 1131-7.
- Bing, O. H. (1994). "Hypothesis: apoptosis may be a mechanism for the transition to heart failure with chronic pressure overload." J Mol Cell Cardiol **26**(8): 943-8.
- Blodi, F. C. (2000). Development of our Concept of Glaucoma. Glaucoma. L. Cantor. San Francisco, American Academy of Ophthalmology. **10**: 5-6.
- Boise, L. H., M. Gonzalez-Garcia, et al. (1993). "bcl-x, a bcl-2-related gene that functions as a dominant regulator of apoptotic cell death." Cell **74**(4): 597-608.
- Bonfanti, L., E. Strettoi, et al. (1996). "Protection of retinal ganglion cells from natural and axotomy-induced cell death in neonatal transgenic mice overexpressing bcl-2." J Neurosci **16**(13): 4186-94.
- Boyd, Z. S., A. Kriatchko, et al. (2003). "Interleukin-10 receptor signaling through STAT-3 regulates the apoptosis of retinal ganglion cells in response to stress." Invest Ophthalmol Vis Sci **44**(12): 5206-11.
- Bretscher, M. S. (1972). "Asymmetrical lipid bilayer structure for biological membranes." Nat New Biol **236**(61): 11-2.
- Brewer, G. J. (1995). "Serum-free B27/neurobasal medium supports differentiated growth of neurons from the striatum, substantia nigra, septum, cerebral cortex, cerebellum, and dentate gyrus." J Neurosci Res **42**(5): 674-83.
- Brewer, G. J., S. Deshmane, et al. (1998). "Precocious axons and improved survival of rat hippocampal neurons on lysine-alanine polymer substrates." J Neurosci Methods **85**(1): 13-20.

- Brewer, G. J., J. R. Torricelli, et al. (1993). "Optimized survival of hippocampal neurons in B27-supplemented Neurobasal, a new serum-free medium combination." J Neurosci Res **35**(5): 567-76.
- Broe, M. (1997). The role of the Actin cytoskeleton in the development of the retina. School of Anatomy. Sydney, University of New South Wales. [BSc honours thesis].
- Bron, A., R. Tripathi, et al. (1997). Wolff's Anatomy of the Eye and Orbit. London, Chapman & Hall.
- Brubaker, R. F. (1996). "Delayed functional loss in glaucoma. LII Edward Jackson Memorial Lecture." Am J Ophthalmol **121**(5): 473-83.
- Buchi, E. R. (1992). "Cell death in the rat retina after a pressure-induced ischaemia-reperfusion insult: an electron microscopic study. I. Ganglion cell layer and inner nuclear layer." Exp Eye Res **55**(4): 605-13.
- Buja, L. M., M. L. Eigenbrodt, et al. (1993). "Apoptosis and necrosis. Basic types and mechanisms of cell death." Arch Pathol Lab Med **117**(12): 1208-14.
- Burgoyne, C., J. Crawford Downs, et al. (2005). "The optic nerve head as a biochemical structure: a new paradigm for understanding the role of IOP-related stress and strain in the pathophysiology of glaucomatous optic nerve head damage." Progress in Retinal and Eye Research **25**: 39-75.
- Burke, W., L. J. Cottee, et al. (1986). "Selective degeneration of optic nerve fibres in the cat produced by a pressure block." J Physiol **376**: 461-76.
- Buus, D. R. and D. R. Anderson (1989). "Peripapillary crescents and halos in normal-tension glaucoma and ocular hypertension." Ophthalmology **96**(1): 16-9.
- Canadas, P., S. Wendling-Mansuy, et al. (2006). "Frequency response of a viscoelastic tensegrity model: Structural rearrangement contribution to cell dynamics." J Biomech Eng **128**(4): 487-95.
- Cantor, L., M. Berlin, et al. (2000). Glaucoma. San Francisco, American Academy of Ophthalmology.
- Caprioli, J. (1995). Pressure and Glaucoma. Optic Nerve in Glaucoma. S. J. Drance. Amsterdam, Kugler Publications bv: 151-157.
- Carmignoto, G., L. Maffei, et al. (1989). "Effect of NGF on the survival of rat retinal ganglion cells following optic nerve section." J Neurosci **9**(4): 1263-72.
- Casson, R. J. (2006). "Possible role of excitotoxicity in the pathogenesis of glaucoma." Clin Experiment Ophthalmol **34**(1): 54-63.
- Castedo, M., K. Ferri, et al. (2002). "Quantitation of mitochondrial alterations associated with apoptosis." J Immunol Methods **265**(1-2): 39-47.

- Castedo, M., T. Hirsch, et al. (1996). "Sequential acquisition of mitochondrial and plasma membrane alterations during early lymphocyte apoptosis." *J Immunol* **157**(2): 512-21.
- Castillo, B., Jr., M. del Cerro, et al. (1994). "Retinal ganglion cell survival is promoted by genetically modified astrocytes designed to secrete brain-derived neurotrophic factor (BDNF)." *Brain Res* **647**(1): 30-6.
- Chen, C. S. and D. E. Ingber (1999). "Tensegrity and mechanoregulation: from skeleton to cytoskeleton." *Osteoarthritis Cartilage* **7**(1): 81-94.
- Chinese and University of Hong Kong. (2006). "Apoptosis and necrosis image." Retrieved Nov 2006, from <http://ihome.cuhk.edu.hk/~b105122/image/0611.jpg>.
- Chiu, J. J., B. S. Wung, et al. (1999). "Nitric oxide regulates shear stress-induced early growth response-1. Expression via the extracellular signal-regulated kinase pathway in endothelial cells." *Circ Res* **85**(3): 238-46.
- Chung, H. S., A. Harris, et al. (1999). "Vascular aspects in the pathophysiology of glaucomatous optic neuropathy." *Surv Ophthalmol* **43** Suppl 1: S43-50.
- Cleveland, J. L. and J. N. Ihle (1995). "Contenders in FasL/TNF death signaling." *Cell* **81**(4): 479-82.
- Cohen, A. (1992). The Retina. *Adler's Physiology of the Eye*. W. Hart. St Louis, Mosby: 579-616.
- Cohen, A., G. M. Bray, et al. (1994). "Neurotrophin-4/5 (NT-4/5) increases adult rat retinal ganglion cell survival and neurite outgrowth in vitro." *J Neurobiol* **25**(8): 953-9.
- Coleman, D. J. and S. Trokel (1969). "Direct-recorded intraocular pressure variations in a human subject." *Arch Ophthalmol* **82**(5): 637-40.
- Colton, T. and F. Ederer (1980). "The distribution of intraocular pressures in the general population." *Surv Ophthalmol* **25**(3): 123-9.
- Compton, M. M. (1992). "A biochemical hallmark of apoptosis: internucleosomal degradation of the genome." *Cancer Metastasis Rev* **11**(2): 105-19.
- Condorelli, G., C. Morisco, et al. (1999). "Increased cardiomyocyte apoptosis and changes in proapoptotic and antiapoptotic genes bax and bcl-2 during left ventricular adaptations to chronic pressure overload in the rat." *Circulation* **99**(23): 3071-8.
- Congdon, N. G., H. A. Quigley, et al. (1996). "Screening techniques for angle-closure glaucoma in rural Taiwan." *Acta Ophthalmol Scand* **74**(2): 113-9.
- Cordeiro, M. F., L. Guo, et al. (2004). "Real-time imaging of single nerve cell apoptosis in retinal neurodegeneration." *Proc Natl Acad Sci U S A* **101**(36): 13352-6.

- Coroneo, M., A. Agar, et al. (2000). "Differentiated neuronal apoptosis following elevated hydrostatic pressure." Invest Ophthal Vis Sci **41**(4): S4379 [ARVO abstract].
- Coroneo, M., A. Agar, et al. (2001). "Pressure related apoptosis in human and neuronal cell lines." Invest Ophthal & Vis Sci **42**(4): S129 [ARVO Abstract].
- Coroneo, M., S. Li, et al. (2002). "The 2-pore K⁺ channel opener Arachidonic Acid induces apoptosis in RGC-5 & differentiated PC-12 neuronal cell lines." Invest Ophthal Vis Sci **43**(4): S750 [ARVO abstract].
- Craig, J. E., P. N. Baird, et al. (2001). "Evidence for genetic heterogeneity within eight glaucoma families, with the GLC1A Gln368STOP mutation being an important phenotypic modifier." Ophthalmology **108**(9): 1607-20.
- Crisanti, P., O. Laplace, et al. (2006). "The role of PKCzeta in NMDA-induced retinal ganglion cell death: prevention by aspirin." Apoptosis **11**(6): 983-91.
- Critchley, M. (1984). Butterworths Medical Dictionary London, Butterworths.
- Cuende, E., J. E. Ales-Martinez, et al. (1993). "Programmed cell death by bcl-2-dependent and independent mechanisms in B lymphoma cells." Embo J **12**(4): 1555-60.
- Dahlin, L. B., C. Nordborg, et al. (1987). "Morphologic changes in nerve cell bodies induced by experimental graded nerve compression." Exp Neurol **95**(3): 611-21.
- Dartsch, P. C. and H. Hammerle (1986). "Orientation response of arterial smooth muscle cells to mechanical stimulation." Eur J Cell Biol **41**(2): 339-46.
- Darzynkiewicz, Z. (1998). *In Situ* DNA Strand Break Labeling for Analysis of Apoptosis and Cell Proliferation by Flow and Laser Scanning Cytometry. Cell Biology: a laboratory handbook, Academic Press. **1**: 341-350.
- Darzynkiewicz, Z. (1995). "Apoptosis in antitumor strategies: modulation of cell cycle or differentiation." J Cell Biochem **58**(2): 151-9.
- Darzynkiewicz, Z. and E. Bedner (2000). "Analysis of apoptotic cells by flow and laser scanning cytometry." Methods Enzymol **322**:18-39.
- Darzynkiewicz, Z., E. Bedner, et al. (1998). "Critical aspects in the analysis of apoptosis and necrosis." Hum Cell **11**(1): 3-12.
- Darzynkiewicz, Z., G. Juan, et al. (1997). "Cytometry in cell necrobiology: analysis of apoptosis and accidental cell death (necrosis)." Cytometry **27**(1): 1-20.
- De, A., N. I. Boyadjieva, et al. (1994). "Cyclic AMP and ethanol interact to control apoptosis and differentiation in hypothalamic beta-endorphin neurons." J Biol Chem **269**(43): 26697-705.

- Dielemans, I., P. T. de Jong, et al. (1996). "Primary open-angle glaucoma, intraocular pressure, and diabetes mellitus in the general elderly population. The Rotterdam Study." Ophthalmology **103**(8): 1271-5.
- Dimasi, D. P., A. W. Hewitt, et al. (2005). "Lack of association of p53 polymorphisms and haplotypes in high and normal tension open angle glaucoma." J Med Genet **42**(9): e55.
- Doble, A. (1999). "The role of excitotoxicity in neurodegenerative disease: implications for therapy." Pharmacol Ther **81**(3): 163-221.
- Drance, S. M. (1973). "Glaucoma panel summary. The implications on the findings and suggestions for management of angle closure glaucoma in Northern communities." Can J Ophthalmol **8**(2): 278-9.
- Drance, S. M. (1995). Optic Nerve in Glaucoma. Amsterdam, Kugler Publications bv.
- Dreyer, E. B. (1998). "A proposed role for excitotoxicity in glaucoma." J Glaucoma **7**(1): 62-7.
- Dreyer, E. B., D. Zurakowski, et al. (1996). "Elevated glutamate levels in the vitreous body of humans and monkeys with glaucoma." Arch Ophthalmol **114**(3): 299-305.
- Duke-Elder, W. (1941). Anomalies of intraocular pressure. Textbook of Ophthalmology. W. Duke-Elder. St Louis, Mosby. **3**: 3280-3429.
- Dun, Y., B. Mysona, et al. (2006). "Expression of the cystine-glutamate exchanger (x(c) (-)) in retinal ganglion cells and regulation by nitric oxide and oxidative stress." Cell Tissue Res **324**(2): 189-202.
- Ecker, R. C. and G. E. Steiner (2004). "Microscopy-based multicolor tissue cytometry at the single-cell level." Cytometry A **59**(2): 182-90.
- Edward, D. P. and J. Ueda (2001). "Immunolocalisation of TRAAK- a mechanosensitive K⁺ channel in the human and rat retina." Invest Ophthalmol & Vis Sci **42**(4): 2032 [ARVO Abstract].
- Edwards, M. E., G. C. Y. Chiou, et al. (1998). "Biomechanical force mediated G-Protein activation and RGC Apoptosis." Investigative Ophthalmology & Visual Science **39**(4): s916 [ARVO Abstract].
- el-Asrar, A. M., P. H. Morse, et al. (1992). "MK-801 protects retinal neurons from hypoxia and the toxicity of glutamate and aspartate." Invest Ophthalmol Vis Sci **33**(12): 3463-8.
- Elinder, F., N. Akanda, et al. (2005). "Opening of plasma membrane voltage-dependent anion channels (VDAC) precedes caspase activation in neuronal apoptosis induced by toxic stimuli." Cell Death Differ **12**(8): 1134-40.

- Enari, M., H. Sakahira, et al. (1998). "A caspase-activated DNase that degrades DNA during apoptosis, and its inhibitor ICAD." Nature **391**(6662): 43-50.
- Ernest, J. T. and A. M. Potts (1971). "Pathophysiology of the distal portion of the optic nerve." Am J Ophthalmol **72**(2): 433-44.
- Fadok, V. A., D. R. Voelker, et al. (1992). "Exposure of phosphatidylserine on the surface of apoptotic lymphocytes triggers specific recognition and removal by macrophages." J Immunol **148**(7): 2207-16.
- Fagiolini, M., M. Caleo, et al. (1997). "Axonal transport blockade in the neonatal rat optic nerve induces limited retinal ganglion cell death." J Neurosci **17**(18): 7045-52.
- Fan, W., N. Agarwal, et al. (2006). "The role of CaMKII in BDNF-mediated neuroprotection of retinal ganglion cells (RGC-5)." Brain Res **1067**(1): 48-57.
- Fan, W., N. Agarwal, et al. (2005). "Retinal ganglion cell death and neuroprotection: Involvement of the CaMKIIalpha gene." Brain Res Mol Brain Res **139**(2): 306-16.
- Fantes, F. E. and D. R. Anderson (2000). Optic Nerve in Glaucoma, Current Medicine.
- Farber, J. L. (1982). "Biology of disease: membrane injury and calcium homeostasis in the pathogenesis of coagulative necrosis." Lab Invest **47**(2): 114-23.
- Finlay, D., G. Wilkinson, et al. (1996). "Retinal cultures." Methods Cell Biol **51**: 265-83.
- Flammer, J. and S. Orgul (1998). "Optic nerve blood-flow abnormalities in glaucoma." Prog Retin Eye Res **17**(2): 267-89.
- Flanagan, J. G. (1998). "Glaucoma update: epidemiology and new approaches to medical management." Ophthalmic Physiol Opt **18**(2): 126-32.
- Forrester, J. V., A. D. Dick, et al. (1996). The Eye: Basic Sciences in Practice. London, W.B. Saunders.
- Foster, A. and S. Resnikoff (2005). "The impact of Vision 2020 on global blindness." Eye **19**(10): 1133-5.
- Fraser, S. and R. Wormald (1999). Epidemiology of Glaucoma. Ophthalmology. M. Yanoff and J. Duker. St Louis, Mosby: 12.1.1-5.
- Frassetto, L. J., C. R. Schlieve, et al. (2006). "Kinase-dependent differentiation of a retinal ganglion cell precursor." Invest Ophthalmol Vis Sci **47**(1): 427-38.
- Freshney, I. (2001). "Application of cell cultures to toxicology." Cell Biol Toxicol **17**(4-5): 213-30.

- Freshney, R. I. (1994). Culture of Animal Cells: A Manual of Basic Technique. New York, Wiley-Liss.
- Frey, B., S. Franz, et al. (2004). "Hydrostatic pressure induced death of mammalian cells engages pathways related to apoptosis or necrosis." Cell Mol Biol (Noisy-le-grand) **50**(4): 459-67.
- Frick, K. D. and A. Foster (2003). "The magnitude and cost of global blindness: an increasing problem that can be alleviated." Am J Ophthalmol **135**(4): 471-6.
- Galea, J., J. Armstrong, et al. (1999). "Alterations in c-fos expression, cell proliferation and apoptosis in pressure distended human saphenous vein." Cardiovasc Res **44**(2): 436-48.
- Galli, C., S. Guizzardi, et al. (2005). "Life on the wire: on tensegrity and force balance in cells." Acta Biomed Ateneo Parmense **76**(1): 5-12.
- Garcia-Valenzuela, E., W. Gorczyca, et al. (1994). "Apoptosis in adult retinal ganglion cells after axotomy." J Neurobiol **25**(4): 431-8.
- Garcia-Valenzuela, E., S. Shareef, et al. (1995). "Programmed cell death of retinal ganglion cells during experimental glaucoma." Exp Eye Res **61**(1): 33-44.
- Gelberman, R. H., R. M. Szabo, et al. (1983). "Tissue pressure threshold for peripheral nerve viability." Clin Orthop(178): 285-91.
- Geyer, O., J. Almog, et al. (1995). "Nitric oxide synthase inhibitors protect rat retina against ischemic injury." FEBS Lett **374**(3): 399-402.
- Gilman, S. C., J. S. Colton, et al. (1987). "Effect of pressure on the release of radioactive glycine and gamma-aminobutyric acid from spinal cord synaptosomes." J Neurochem **49**(5): 1571-8.
- Gilman, S. C., J. S. Colton, et al. (1986). "Effects of high pressure on the release of excitatory amino acids by brain synaptosomes." Undersea Biomed Res **13**(4): 397-406.
- Gilman, S. C., K. K. Kumaroo, et al. (1986). "Effects of pressure on uptake and release of calcium by brain synaptosomes." J Appl Physiol **60**(4): 1446-50.
- Glaucoma-Australia (2006) "What is Glaucoma?" Retrieved Jun 2006, from <http://www.glaucoma.org.au/whatis.htm>
- Gong, J., F. Traganos, et al. (1994). "A selective procedure for DNA extraction from apoptotic cells applicable for gel electrophoresis and flow cytometry." Anal Biochem **218**(2): 314-9.
- Goodman, C. M., A. K. Steadman, et al. (2001). "Comparison of carpal canal pressure in paraplegic and nonparaplegic subjects: clinical implications." Plast Reconstr Surg **107**(6): 1464-71; discussion 1472.

- Gotoh, N., K. Kambara, et al. (2000). "Apoptosis in microvascular endothelial cells of perfused rabbit lungs with acute hydrostatic edema." J Appl Physiol **88**(2): 518-26.
- Greene, L. A., M. M. Sobeih, et al., Eds. (1991). Methodologies for the culture and experimental use of the PC12 rat pheochromocytoma cell line. Culturing nerve cells. Cambridge, M.A., MIT Press.
- Greene, L. A. and A. S. Tischler (1976). "Establishment of a noradrenergic clonal line of rat adrenal pheochromocytoma cells which respond to nerve growth factor." Proc Natl Acad Sci U S A **73**(7): 2424-8.
- Greene, L. A. and A. S. Tischler (1982). "PC12 pheochromocytoma cultures in neurobiological research." Adv Cellular Neurobiology **3**: 373-414.
- Guenther, E., S. Schmid, et al. (1994). "In vitro identification of retinal ganglion cells in culture without the need of dye labeling." J Neurosci Methods **51**(2): 177-81.
- Gunning, P. W., G. E. Landreth, et al. (1981). "Differential and synergistic actions of nerve growth factor and cyclic AMP in PC12 cells." J Cell Biol **89**(2): 240-5.
- Gunning, P. W., G. E. Landreth, et al. (1981). "Nerve growth factor-induced differentiation of PC12 cells: evaluation of changes in RNA and DNA metabolism." J Neurosci **1**(4): 368-79.
- Gupta, N. and Y. H. Yucel (2001). "Glaucoma and the brain." J Glaucoma **10**(5 Suppl 1): S28-9.
- Hall, A. C. and J. C. Ellory (1986). "Effects of high hydrostatic pressure on 'passive' monovalent cation transport in human red cells." J Membr Biol **94**(1): 1-17.
- Hamill, O. P. and D. W. McBride, Jr. (1996). "The pharmacology of mechanogated membrane ion channels." Pharmacol Rev **48**(2): 231-52.
- Harada, C., K. Nakamura, et al. (2006). "Role of apoptosis signal-regulating kinase 1 in stress-induced neural cell apoptosis in vivo." Am J Pathol **168**(1): 261-9.
- Hare, W. A., E. WoldeMussie, et al. (2004). "Efficacy and safety of memantine treatment for reduction of changes associated with experimental glaucoma in monkey, I: Functional measures." Invest Ophthalmol Vis Sci **45**(8): 2625-39.
- Harris, R. C., M. A. Haralson, et al. (1992). "Continuous stretch-relaxation in culture alters rat mesangial cell morphology, growth characteristics, and metabolic activity." Lab Invest **66**(5): 548-54.
- Hart, W. (1992). Intraocular pressure. Adler's Physiology of the Eye. W. Hart. St Louis, Mosby: 248-348.
- Haskin, C. L., K. A. Athanasiou, et al. (1993). "A heat-shock-like response with cytoskeletal disruption occurs following hydrostatic pressure in MG-63 osteosarcoma cells." Biochem Cell Biol **71**(7-8): 361-71.

- Hedges, T., D. Friedman, et al. (2000). Neuro-Ophthalmology. San Francisco, American Academy of Ophthalmology.
- Hegarty, P., R. W. Watson, et al. (2004). "Pressure effects on cellular systems: is there a link with benign prostatic hyperplasia?" Urology **64**(2): 195-200.
- Hegarty, P. K., R. W. Watson, et al. (2002). "Effects of cyclic stretch on prostatic cells in culture." J Urol **168**(5): 2291-5.
- Heinemann, S. H., F. Conti, et al. (1987). "Effects of hydrostatic pressure on membrane processes. Sodium channels, calcium channels, and exocytosis." J Gen Physiol **90**(6): 765-78.
- Helena, M. C., F. Baerveldt, et al. (1998). "Keratocyte apoptosis after corneal surgery." Invest Ophthalmol Vis Sci **39**(2): 276-83.
- Hernandez, M. R., J. D. Pena, et al. (2000). "Hydrostatic pressure stimulates synthesis of elastin in cultured optic nerve head astrocytes." Glia **32**(2): 122-36.
- Hewitt, A. W., J. E. Craig, et al. (2006). "Complex genetics of complex traits: the case of primary open-angle glaucoma." Clin Experiment Ophthalmol **34**(5): 472-84.
- Higginbotham, E. and D. Lee (1994). Management of Difficult Glaucoma: A Clinician's Guide. London, Blackwell Scientific.
- Higginbotham, E. J., M. O. Gordon, et al. (2004). "The Ocular Hypertension Treatment Study: topical medication delays or prevents primary open-angle glaucoma in African American individuals." Arch Ophthalmol **122**(6): 813-20.
- Hill, M. A. and P. Gunning (1995). The cell cytoskeleton's requirement for localized mRNA. Localized RNAs. H. Lipshitz. Austin, R.D. Landes Biomedical Publishers.
- Hill, M. A. and D. Walsh (1997). Heatshock Protein 27 and actin isoform distribution in 3T3 fibroblast cells following cytoskeletal reorganization. 5th Intl Fed Teratology Soc Scientific Conference, Sydney.
- Hitchings, R. (1999). Normal-tension glaucoma. Ophthalmology. M. Yanoff and J. Duker. St Louis, Mosby: 12.12.1-4.
- Hollander, H., F. Makarov, et al. (1995). "Evidence of constriction of optic nerve axons at the lamina cribrosa in the normotensive eye in humans and other mammals." Ophthalmic Res **27**(5): 296-309.
- Hollows, F. C. (1966). "The detection of chronic simple glaucoma; an analysis of methods." Pac Med Surg **74**(5): 283-7.
- Hollows, F. C. and P. A. Graham (1966). "Intra-ocular pressure, glaucoma, and glaucoma suspects in a defined population." Br J Ophthalmol **50**(10): 570-86.

- Holyoke, E. D. and F. H. Johnson (1951). "The influence of hydrostatic pressure and pH on the rate of lysis of *Micrococcus lysodeikticus* by lysozyme." Arch Biochem **31**(1): 41-8.
- Honkanen, R. A., S. Baruah, et al. (2003). "Vitreous amino acid concentrations in patients with glaucoma undergoing vitrectomy." Arch Ophthalmol **121**(2): 183-8.
- Honn, K. V., J. A. Singley, et al. (1975). "Fetal bovine serum: a multivariate standard." Proc Soc Exp Biol Med **149**(2): 344-7.
- Hsu, W. L. and R. D. Everett (2001). "Human neuron-committed teratocarcinoma NT2 cell line has abnormal ND10 structures and is poorly infected by herpes simplex virus type 1." J Virol **75**(8): 3819-31.
- Hu, D. N. and R. Ritch (1997). "Tissue culture of adult human retinal ganglion cells." J Glaucoma **6**(1): 37-43.
- Huber, K., N. Plange, et al. (2004). "Comparison of colour Doppler imaging and retinal scanning laser fluorescein angiography in healthy volunteers and normal pressure glaucoma patients." Acta Ophthalmol Scand **82**(4): 426-31.
- Ilschner, S. U. and P. Waring (1992). "Fragmentation of DNA in the retina of chicken embryos coincides with retinal ganglion cell death." Biochem Biophys Res Commun **183**(3): 1056-61.
- Ingber, D. E. (1997). "Tensegrity: the architectural basis of cellular mechanotransduction." Annu Rev Physiol **59**: 575-99.
- Isaacs, J. T. (1993). "Role of programmed cell death in carcinogenesis." Environ Health Perspect **101 Suppl 5**: 27-33.
- Islas, L., H. Pasantes-Morales, et al. (1993). "Characterization of stretch-activated ion channels in cultured astrocytes." Glia **8**(2): 87-96.
- Ives, C. L., S. G. Eskin, et al. (1986). "Mechanical effects on endothelial cell morphology: in vitro assessment." In Vitro Cell Dev Biol **22**(9): 500-7.
- Janssen, P., R. Naskar, et al. (1996). "Evidence for glaucoma-induced horizontal cell alterations in the human retina." Ger J Ophthalmol **5**(6): 378-85.
- Jay, J. L. and J. R. Murdoch (1993). "The rate of visual field loss in untreated primary open angle glaucoma." Br J Ophthalmol **77**(3): 176-8.
- Johansson, J. O. (1983). "Inhibition of retrograde axoplasmic transport in rat optic nerve by increased IOP in vitro." Invest Ophthalmol Vis Sci **24**(12): 1552-8.
- Johansson, J. O. (1988). "Inhibition and recovery of retrograde axoplasmic transport in rat optic nerve during and after elevated IOP in vivo." Exp Eye Res **46**(2): 223-7.

- Johnson, F. H. and G. G. Wright (1946). "Influence of Hydrostatic Pressure on the Denaturation of Staphylococcus Antitoxin at 65 degrees C." Proc Natl Acad Sci U S A **32**(2): 21-5.
- Juan, G. and Z. Darzynkiewicz (1998). *In situ* DNA strand break labeling for Analysis of Apoptosis and Cell Proliferation by Flow and Laser Scanning Cytometry. Cell Biology: A Laboratory Handbook, Academic Press. **1**: 341-350.
- Kalapesi, F., M. Coroneo, et al. (2005). "Human ganglion cells express the Alpha-2 adrenergic receptor: relevance to neuroprotection." Br J Ophth **89**(6): 758-63.
- Kalapesi, F., J. Tan, et al. (2005). "Stretch-activated channels: a mini review. Are stretch-activated channels an ocular barometer." Clin & Exp Ophth **33**(2): 210-217.
- Kamentsky, L. A., D. E. Burger, et al. (1997). "Slide-based laser scanning cytometry." Acta Cytol **41**(1): 123-43.
- Kanamori, A., M. Nakamura, et al. (2004). "Akt is activated via insulin/IGF-1 receptor in rat retina with episcleral vein cauterization." Brain Res **1022**(1-2): 195-204.
- Kanski, J. (2003). Clinical Ophthalmology. London, Butterworth Heinemann.
- Kaskel, D., H. Valenzuela, et al. (1976). "Enzymologic and histologic investigations in normal and pressure- ischemic retina of rabbits." Albrecht Von Graefes Arch Klin Exp Ophthalmol **200**(1): 71-8.
- Kasper, D. L. (2006). Harrison's Principles of Internal Medicine. New York, McGraw-Hill.
- Kass, M. A., D. K. Heuer, et al. (2002). "The Ocular Hypertension Treatment Study: a randomized trial determines that topical ocular hypotensive medication delays or prevents the onset of primary open-angle glaucoma." Arch Ophthalmol **120**(6): 701-13; discussion 829-30.
- Katai, N. and N. Yoshimura (1999). "Apoptotic retinal neuronal death by ischemia-reperfusion is executed by two distinct caspase family proteases." Invest Ophthalmol Vis Sci **40**(11): 2697-705.
- Katz, J., J. M. Tielsch, et al. (1995). "Automated perimetry detects visual field loss before manual Goldmann perimetry." Ophthalmology **102**(1): 21-6.
- Kerr, J. F., A. H. Wyllie, et al. (1972). "Apoptosis: a basic biological phenomenon with wide-ranging implications in tissue kinetics." Br J Cancer **26**(4): 239-57.
- Kerrigan, L. A., D. J. Zack, et al. (1997). "TUNEL-positive ganglion cells in human primary open-angle glaucoma." Arch Ophthalmol **115**(8): 1031-5.
- Kevles, D. J. and G. L. Geison (1995). "The experimental life sciences in the twentieth century." Osiris **10**: 97-121.

- Kim, C. I., S. H. Lee, et al. (2006). "Nuclear translocation and overexpression of GAPDH by the hyper-pressure in retinal ganglion cell." Biochem Biophys Res Commun **341**(4): 1237-43.
- Kim, H. S. and C. K. Park (2005). "Retinal ganglion cell death is delayed by activation of retinal intrinsic cell survival program." Brain Res **1057**(1-2): 17-28.
- Klein, B. E., R. Klein, et al. (1992). "Prevalence of glaucoma. The Beaver Dam Eye Study." Ophthalmology **99**(10): 1499-504.
- Ko, K. S. and C. A. McCulloch (2000). "Partners in protection: interdependence of cytoskeleton and plasma membrane in adaptations to applied forces." J Membr Biol **174**(2): 85-95.
- Kobayashi, S., J. D. O. Pena, et al. (1997). "Cultured astrocytes from human optic nerves respond to elevated hydrostatic pressure." Invest Ophthalm & Vis Sci **38**(4): 802 [ARVO Abstract].
- Kosnosky, W., B. J. Tripathi, et al. (1995). "An *in vitro* system for studying pressure effects on growth, morphology and biochemical aspects of trabecular meshwork cells." Invest. Ophthalmol. Vis. Sci., **36**(4): 8731.
- Krick, S., O. Platoshyn, et al. (2001). "Activation of K⁺ channels induces apoptosis in vascular smooth muscle cells." Am J Physiol Cell Physiol **280**(4): C970-9.
- Krishnamoorthy, R. R., P. Agarwal, et al. (2001). "Characterization of a transformed rat retinal ganglion cell line." Brain Res Mol Brain Res **86**(1-2): 1-12.
- Kuehn, M. H., J. H. Fingert, et al. (2005). "Retinal ganglion cell death in glaucoma: mechanisms and neuroprotective strategies." Ophthalmol Clin North Am **18**(3): 383-95, vi.
- Kuroiwa, S., N. Katai, et al. (1998). "Expression of cell cycle-related genes in dying cells in retinal ischemic injury." Invest Ophthalmol Vis Sci **39**(3): 610-7.
- Lam, T. T., E. Siew, et al. (1997). "Ameliorative effect of MK-801 on retinal ischemia." J Ocul Pharmacol Ther **13**(2): 129-37.
- Lambeng, N., P. P. Michel, et al. (1999). "Mechanisms of apoptosis in PC12 cells irreversibly differentiated with nerve growth factor and cyclic AMP." Brain Res **821**(1): 60-8.
- Landau, J. V. (1965). "High Hydrostatic Pressure Effects on Amoeba Proteus; Changes in Shape, Volume, and Surface Area." J Cell Biol **24**: 332-6.
- Landau, J. V. (1966). "Protein and nucleic acid synthesis in Escherichia coli: pressure and temperature effects." Science **153**(741): 1273-4.
- Landau, J. V. (1967). "Induction, transcription and translation in Escherichia coli: a hydrostatic pressure study." Biochim Biophys Acta **149**(2): 506-12.

- Landau, J. V. and J. H. McAlear (1961). "The micromorphology of FL and primary human amnion cells following exposure to high hydrostatic pressure." Cancer Res **21**: 812-4.
- Laquis, S., P. Chaudhary, et al. (1998). "The patterns of retinal ganglion cell death in hypertensive eyes." Brain Res **784**(1-2): 100-4.
- Lechardeur, D., M. Xu, et al. (2004). "Contrasting nuclear dynamics of the caspase-activated DNase (CAD) in dividing and apoptotic cells." J Cell Biol **167**(5): 851-62.
- Levin, L. A. (1999). "Direct and indirect approaches to neuroprotective therapy of glaucomatous optic neuropathy." Survey of Ophthalmology **43 Suppl 1**: S98-101.
- Levin, L. A. (2005). "Neuroprotection and regeneration in glaucoma." Ophthalmology Clinics of North America **18**(4): 585-96.
- Levin, L. A. and L. K. Gordon (2002). "Retinal ganglion cell disorders: types and treatments." Prog Retin Eye Res **21**(5): 465-84.
- Levin, L. A. and A. Louhab (1996). "Apoptosis of retinal ganglion cells in anterior ischemic optic neuropathy." Arch Ophthalmol **114**(4): 488-91.
- Levkovitch-Verbin, H., R. Dardik, et al. (2006). "Experimental glaucoma and optic nerve transection induce simultaneous upregulation of proapoptotic and prosurvival genes." Invest Ophthalmol Vis Sci **47**(6): 2491-7.
- Levkovitch-Verbin, H., M. Kaley-Landoy, et al. (2006). "Minocycline delays death of retinal ganglion cells in experimental glaucoma and after optic nerve transection." Arch Ophthalmol **124**(4): 520-6.
- Levkovitch-Verbin, H., H. A. Quigley, et al. (2003). "A model to study differences between primary and secondary degeneration of retinal ganglion cells in rats by partial optic nerve transection." Invest Ophthalmol Vis Sci **44**(8): 3388-93.
- Levy, N. S. and C. K. Adams (1975). "Slow axonal protein transport and visual function following retinal and optic nerve ischemia." Invest Ophthalmol **14**(2): 91-7.
- Li, W. C., J. R. Kuszak, et al. (1995). "Lens epithelial cell apoptosis appears to be a common cellular basis for non-congenital cataract development in humans and animals." J Cell Biol **130**(1): 169-81.
- Li, X. and Z. Darzynkiewicz (1995). "Labelling DNA strand breaks with BrdUTP. Detection of apoptosis and cell proliferation." Cell Prolif **28**(11): 571-9.
- Li, X., M. R. Melamed, et al. (1996). "Detection of apoptosis and DNA replication by differential labeling of DNA strand breaks with fluorochromes of different color." Exp Cell Res **222**(1): 28-37.

- Li, Y., C. L. Schlamp, et al. (1999). "Experimental induction of retinal ganglion cell death in adult mice." Invest Ophthalmol Vis Sci **40**(5): 1004-8.
- Linette, G. P. and S. J. Korsmeyer (1994). "Differentiation and cell death: lessons from the immune system." Curr Opin Cell Biol **6**(6): 809-15.
- Lockhart, E. M., D. S. Warner, et al. (2002). "Allopregnanolone attenuates N-methyl-D-aspartate-induced excitotoxicity and apoptosis in the human NT2 cell line in culture." Neurosci Lett **328**(1): 33-6.
- Maeno, E., Y. Ishizaki, et al. (2000). "Normotonic cell shrinkage because of disordered volume regulation is an early prerequisite to apoptosis." Proc Natl Acad Sci U S A **97**(17): 9487-92.
- Maher, P. and A. Hanneken (2005). "Flavonoids protect retinal ganglion cells from oxidative stress-induced death." Invest Ophthalmol Vis Sci **46**(12): 4796-803.
- Maher, P. and A. Hanneken (2005). "The molecular basis of oxidative stress-induced cell death in an immortalized retinal ganglion cell line." Invest Ophthalmol Vis Sci **46**(2): 749-57.
- Maingret, F., M. Fosset, et al. (1999). "TRAAK is a mammalian neuronal mechano-gated K⁺ channel." J Biol Chem **274**(3): 1381-7.
- Maingret, F., A. J. Patel, et al. (1999). "Mechano- or acid stimulation, two interactive modes of activation of the TREK-1 potassium channel." J Biol Chem **274**(38): 26691-6.
- Majno, G. and I. Joris (1995). "Apoptosis, oncosis, and necrosis. An overview of cell death." Am J Pathol **146**(1): 3-15.
- Manas, P. and B. M. Mackey (2004). "Morphological and physiological changes induced by high hydrostatic pressure in exponential- and stationary-phase cells of *Escherichia coli*: relationship with cell death." Appl Environ Microbiol **70**(3): 1545-54.
- Mantzioris, N. (2006) "The history of the meaning of the word Glaucoma." Glaucoma Australia Retrieved Feb 2006 from <http://www.glaucoma.org.au/History.pdf>
- Martin, P. M., M. S. Ola, et al. (2004). "The sigma receptor ligand (+)-pentazocine prevents apoptotic retinal ganglion cell death induced in vitro by homocysteine and glutamate." Brain Res Mol Brain Res **123**(1-2): 66-75.
- Martin-Reay, D. G., L. A. Kametsky, et al. (1994). "Evaluation of a new slide-based laser scanning cytometer for DNA analysis of tumors. Comparison with flow cytometry and image analysis." Am J Clin Pathol **102**(4): 432-8.
- Martins, L. M., T. Kottke, et al. (1997). "Activation of multiple interleukin-1beta converting enzyme homologues in cytosol and nuclei of HL-60 cells during etoposide-induced apoptosis." J Biol Chem **272**(11): 7421-30.

- Matsugi, T., Q. Chen, et al. (1997). "Contractile responses of cultured bovine retinal pericytes to angiotensin II." Arch Ophthalmol **115**(10): 1281-5.
- Matsuo, T. (2000). "Basal nitric oxide production is enhanced by hydraulic pressure in cultured human trabecular cells." Br J Ophthalmol **84**(6): 631-5.
- Matsuo, T., H. Uchida, et al. (1996). "Bovine and porcine trabecular cells produce prostaglandin F2 alpha in response to cyclic mechanical stretching." Jpn J Ophthalmol **40**(3): 289-96.
- Mattana, J. and P. C. Singhal (1995). "Applied pressure modulates mesangial cell proliferation and matrix synthesis." Am J Hypertens **8**(11): 1112-20.
- McCaffery, C. A., M. R. Bennett, et al. (1982). "The survival of neonatal rat retinal ganglion cells in vitro is enhanced in the presence of appropriate parts of the brain." Exp Brain Res **48**(3): 377-86.
- McCarthy, M. J., L. L. Rubin, et al. (1997). "Involvement of caspases in sympathetic neuron apoptosis." J Cell Sci **110**(18): 2165-73.
- McGehee Harvey, A. (1975). "Johns Hopkins--the birthplace of tissue culture: the story of Ross G. Harrison, Warren H. Lewis and George O. Gey." Johns Hopkins Med J **136**(3): 142-9.
- McHugh, P. and M. Turina (2006). "Apoptosis and necrosis: a review for surgeons." Surg Infect (Larchmt) **7**(1): 53-68.
- McKinney, J. S., K. A. Willoughby, et al. (1996). "Stretch-induced injury of cultured neuronal, glial, and endothelial cells. Effect of polyethylene glycol-conjugated superoxide dismutase." Stroke **27**(5): 934-40.
- McMahon, G. and J. V. Landau (1983). "Effect of hydrostatic pressure on translational fidelity." Biochim Biophys Acta **739**(2): 244-8.
- Mennel, H. D., G. Stumm, et al. (1997). "Early morphological findings in experimental high pressure neurological syndrome." Exp Toxicol Pathol **49**(6): 425-32.
- Mertens, P. R., V. Espenkott, et al. (1998). "Pressure oscillation regulates human mesangial cell growth and collagen synthesis." Hypertension **32**(5): 945-52.
- Meyer-Franke, A., M. R. Kaplan, et al. (1995). "Characterisation of the Signalling Interactions that promote the Signalling Survival and Growth of developing Retinal Ganglion Cells in Culture." Neuron **15**: 805-819.
- Michel, P. P., S. Vyas, et al. (1995). "Synergistic differentiation by chronic exposure to cyclic AMP and nerve growth factor renders rat pheochromocytoma PC12 cells totally dependent upon trophic support for survival." Eur J Neurosci **7**(2): 251-60.

- Migdal, C., W. Gregory, et al. (1994). "Long-term functional outcome after early surgery compared with laser and medicine in open-angle glaucoma." Ophthalmology **101**(10): 1651-6; discussion 1657.
- Mills, J. C., S. Wang, et al. (1995). "Use of cultured neurons and neuronal cell lines to study morphological, biochemical, and molecular changes occurring in cell death." Methods Cell Biol **46**: 217-42.
- Minckler, D. S. (1986). "Correlations between anatomic features and axonal transport in primate optic nerve head." Trans Am Ophthalmol Soc **84**: 429-52.
- Minckler, D. S., A. H. Bunt, et al. (1977). "Orthograde and retrograde axoplasmic transport during acute ocular hypertension in the monkey." Invest Ophthalmol Vis Sci **16**(5): 426-41.
- Mitchell, P., W. Smith, et al. (1996). "Prevalence of open-angle glaucoma in Australia. The Blue Mountains Eye Study." Ophthalmology **103**(10): 1661-9.
- Mizushima, T., S. Tsutsumi, et al. (1999). "Suppression of ethanol-induced apoptotic DNA fragmentation by geranylgeranylacetone in cultured guinea pig gastric mucosal cells." Dig Dis Sci **44**(3): 510-4.
- Moorhouse, A. J., S. Li, et al. (2004). "A patch-clamp investigation of membrane currents in a novel mammalian retinal ganglion cell line." Brain Res **1003**(1-2): 205-8.
- Morgan, J. E., H. Uchida, et al. (2000). "Retinal ganglion cell death in experimental glaucoma." Br J Ophthalmol **84**(3): 303-10.
- Morgan, W. H. (1995). "Glaucoma: is there light at the end of the tunnel?" Med J Aust **163**(6): 286-7.
- Morris, C. E. (1990). "Mechanosensitive ion channels." J Membr Biol **113**(2): 93-107.
- Morrison, J. (1995). The Microanatomy of the Optic Nerve. Optic Nerve in Glaucoma. S. M. Drance. Amsterdam, Kugler Publications bv: 57-78.
- Morrison, J. and I. Pollack (2003). Glaucoma: Science and Practice. New York, Thieme.
- Mukesh, B. N., C. A. McCarty, et al. (2002). "Five-year incidence of open-angle glaucoma: the visual impairment project." Ophthalmology **109**(6): 1047-51.
- Naito, M., K. Nagashima, et al. (1997). "Phosphatidylserine externalization is a downstream event of interleukin-1 beta-converting enzyme family protease activation during apoptosis." Blood **89**(6): 2060-6.
- NEI. (2006) NEI Health Information Retrieved Nov, 2006 from <http://www.nei.nih.gov/health/glaucoma/glaucbeforesurg.gif>

- Nichol, K. A., A. W. Everett, et al. (1994). "Retinal ganglion cell survival in vitro maintained by a chondroitin sulfate proteoglycan from the superior colliculus carrying the HNK-1 epitope." J Neurosci Res **37**(5): 623-32.
- Nichol, K. A., M. W. Schulz, et al. (1995). "Nitric oxide-mediated death of cultured neonatal retinal ganglion cells: neuroprotective properties of glutamate and chondroitin sulfate proteoglycan." Brain Res **697**(1-2): 1-16.
- Nicholson, D. W. (2000). "From bench to clinic with apoptosis-based therapeutic agents." Nature **407**(6805): 810-6.
- Nicholson, D. W. (2001). "Apoptosis. Baiting death inhibitors." Nature **410**(6824): 33-4.
- Nicholson, D. W., A. Ali, et al. (1995). "Identification and inhibition of the ICE/CED-3 protease necessary for mammalian apoptosis." Nature **376**(6535): 37-43.
- Nickells, R. W. (1996). "Retinal ganglion cell death in glaucoma: the how, the why, and the maybe." J Glaucoma **5**(5): 345-56.
- Nickells, R. W. (1999). "Apoptosis of retinal ganglion cells in glaucoma: an update of the molecular pathways involved in cell death." Surv Ophthalmol **43**(Suppl 1): S151-61.
- Nickells, R. W. and D. J. Zack (1996). "Apoptosis in ocular disease: a molecular overview." Ophthalmic Genet **17**(4): 145-65.
- Nishigaki, K., S. Minatoguchi, et al. (1997). "Plasma Fas ligand, an inducer of apoptosis, and plasma soluble Fas, an inhibitor of apoptosis, in patients with chronic congestive heart failure." J Am Coll Cardiol **29**(6): 1214-20.
- Nork, T. M. (2000). "Acquired color vision loss and a possible mechanism of ganglion cell death in glaucoma." Trans Am Ophthalmol Soc **98**: 331-63.
- Nork, T. M., G. L. Poulsen, et al. (1997). "p53 regulates apoptosis in human retinoblastoma." Arch Ophthalmol **115**(2): 213-9.
- Nork, T. M., J. N. Ver Hoeve, et al. (2000). "Swelling and loss of photoreceptors in chronic human and experimental glaucomas." Arch Ophthalmol **118**(2): 235-45.
- Oberdoerster, J., A. R. Kamer, et al. (1998). "Differential effect of ethanol on PC12 cell death." J Pharmacol Exp Ther **287**(1): 359-65.
- Oberdoerster, J. and R. A. Rabin (1999). "NGF-differentiated and undifferentiated PC12 cells vary in induction of apoptosis by ethanol." Life Sci **64**(23): PL 267-72.
- Odberg, T. (1993). "Visual field prognosis in early glaucoma. A long-term clinical follow-up." Acta Ophthalmol (Copenh) **71**(6): 721-6.

- Oishi, Y., Y. Uezono, et al. (1998). "Transmural compression-induced proliferation and DNA synthesis through activation of a tyrosine kinase pathway in rat astrocytoma RCR-1 cells." Brain Res **781**(1-2): 159-66.
- Oka, T., Y. Tamada, et al. (2006). "Presence of calpain-induced proteolysis in retinal degeneration and dysfunction in a rat model of acute ocular hypertension." J Neurosci Res **83**(7): 1342-51.
- Okada, Y., T. Matsuo, et al. (1998). "Bovine trabecular cells produce TIMP-1 and MMP-2 in response to mechanical stretching." Jpn J Ophthalmol **42**(2): 90-4.
- Okisaka, S., A. Murakami, et al. (1997). "Apoptosis in retinal ganglion cell decrease in human glaucomatous eyes." Jpn J Ophthalmol **41**(2): 84-8.
- Olney, J. W. and L. G. Sharpe (1969). "Brain lesions in an infant rhesus monkey treated with monosodium glutamate." Science **166**(903): 386-8.
- Oltvai, Z. N. and S. J. Korsmeyer (1994). "Checkpoints of dueling dimers foil death wishes." Cell **79**(2): 189-92.
- Osborne, N. N., M. Ugarte, et al. (1999). "Neuroprotection in relation to retinal ischemia and relevance to glaucoma." Surv Ophthalmol **43** Suppl 1: S102-28.
- Osborne, N. N., J. P. Wood, et al. (1999). "Ganglion cell death in glaucoma: what do we really know?" Br J Ophthalmol **83**(8): 980-6.
- Otori, Y., J. Y. Wei, et al. (1998). "Neurotoxic effects of low doses of glutamate on purified rat retinal ganglion cells." Invest Ophthalmol Vis Sci **39**(6): 972-81.
- Palmberg, P. and J. Wiggs (1999). Mechanisms of Glaucoma. Ophthalmology. M. Yanoff and J. Duker. St Louis, Mosby: 12.3.1-8.
- Parkkinen, J. J., J. Ikonen, et al. (1993). "Effects of cyclic hydrostatic pressure on proteoglycan synthesis in cultured chondrocytes and articular cartilage explants." Arch Biochem Biophys **300**(1): 458-65.
- Parkkinen, J. J., M. J. Lammi, et al. (1995). "Influence of short-term hydrostatic pressure on organization of stress fibers in cultured chondrocytes." J Orthop Res **13**(4): 495-502.
- Parmentier, J. L., B. B. Shrivastav, et al. (1981). "Hydrostatic pressure reduces synaptic efficiency by inhibiting transmitter release." Undersea Biomed Res **8**(3): 175-83.
- Patel, A. J., E. Honore, et al. (1998). "A mammalian two pore domain mechano-gated S-like K⁺ channel." Embo J **17**(15): 4283-90.
- Pease, M. E., S. J. McKinnon, et al. (2000). "Obstructed axonal transport of BDNF and its receptor TrkB in experimental glaucoma." Invest Ophthalmol Vis Sci **41**(3): 764-74.

- Pedut-Kloizman, T. and J. Schuman (1999). Disc analysis. Ophthalmology. M. Yanoff and J. Duker. St Louis, Mosby: 12.7.1-6.
- Pena, J. D., O. Agapova, et al. (2001). "Increased elastin expression in astrocytes of the lamina cribrosa in response to elevated intraocular pressure." Invest Ophthalmol Vis Sci **42**(10): 2303-14.
- Pena, J. D., P. A. Mello, et al. (2000). "Synthesis of elastic microfibrillar components fibrillin-1 and fibrillin-2 by human optic nerve head astrocytes in situ and in vitro." Exp Eye Res **70**(5): 589-601.
- Perry, V. H., Z. Henderson, et al. (1983). "Postnatal Changes in Retinal Ganglion Cell and Optic Axon Populations in the Pigmented Rat." The Journal of Comparative Neurology **219**: 356-368.
- Picaud, S., D. Hicks, et al. (1998). "Adult human retinal neurons in culture: Physiology of horizontal cells." Invest Ophthalmol Vis Sci **39**(13): 2637-48.
- Plange, N., M. Kaup, et al. (2004). "Fluorescein filling defects and quantitative morphologic analysis of the optic nerve head in glaucoma." Arch Ophthalmol **122**(2): 195-201.
- Plitz-Seymour, J. and R. Walker (1999). When to treat Glaucoma. Ophthalmology. M. Yanoff and J. Duker. St Louis, Mosby: 12.22.1-4.
- Popp, R., J. Hoyer, et al. (1993). "Mechanosensitive nonselective cation channels in the antiluminal membrane of cerebral capillaries (blood-brain barrier)." Exs **66**: 101-5.
- Porter, A. G. and R. U. Janicke (1999). "Emerging roles of caspase-3 in apoptosis." Cell Death Differ **6**(2): 99-104.
- Prunte, C., S. Orgul, et al. (1998). "Abnormalities of microcirculation in glaucoma: facts and hints." Curr Opin Ophthalmol **9**(2): 50-5.
- Qian, Y., B. J. Tripathi, et al. (1999). "Short-term elevation of hydrostatic pressure reduces TGF-beta 2 secretion and has no effect on the level of fibronectin in trabecular cells." Invest Ophthalmol Vis Sci **40**: S668 [ARVO Abstract].
- Quigley, H. A. (1995). Connective tissue of the Optic Nerve in Glaucoma. Optic Nerve in Glaucoma. S. M. Drance and D. R. Anderson. Amsterdam, Kugler Publications by.
- Quigley, H. A. (1995). "Ganglion cell death in glaucoma: pathology recapitulates ontogeny." Aust N Z J Ophthalmol **23**(2): 85-91.
- Quigley, H. A. (1996). "Number of people with glaucoma worldwide." Br J Ophthalmol **80**(5): 389-93.

- Quigley, H. A. (1999). "Neuronal death in glaucoma." Prog Retin Eye Res **18**(1): 39-57.
- Quigley, H. A. and E. M. Addicks (1980). "Chronic experimental glaucoma in primates. II. Effect of extended intraocular pressure elevation on optic nerve head and axonal transport." Invest Ophthalmol Vis Sci **19**(2): 137-52.
- Quigley, H. A. and E. M. Addicks (1981). "Regional differences in the structure of the lamina cribrosa and their relation to glaucomatous optic nerve damage." Arch Ophthalmol **99**(1): 137-43.
- Quigley, H. A. and D. R. Anderson (1977). "Distribution of axonal transport blockade by acute intraocular pressure elevation in the primate optic nerve head." Invest Ophthalmol Vis Sci **16**(7): 640-4.
- Quigley, H. A. and A. T. Broman (2006). "The number of people with glaucoma worldwide in 2010 and 2020." Br J Ophthalmol **90**(3): 262-7.
- Quigley, H. A., R. W. Flower, et al. (1980). "The mechanism of optic nerve damage in experimental acute intraocular pressure elevation." Invest Ophthalmol Vis Sci **19**(5): 505-17.
- Quigley, H. A. and W. R. Green (1979). "The histology of human glaucoma cupping and optic nerve damage: clinicopathologic correlation in 21 eyes." Ophthalmology **86**(10): 1803-30.
- Quigley, H. A., R. M. Hohman, et al. (1984). "Blood vessels of the glaucomatous optic disc in experimental primate and human eyes." Invest Ophthalmol Vis Sci **25**(8): 918-31.
- Quigley, H. A., R. M. Hohman, et al. (1985). "Optic nerve head blood flow in chronic experimental glaucoma." Arch Ophthalmol **103**(7): 956-62.
- Quigley, H. A., R. W. Nickells, et al. (1995). "Retinal ganglion cell death in experimental glaucoma and after axotomy occurs by apoptosis." Invest Ophthalmol Vis Sci **36**(5): 774-86.
- Radius, R. L. (1981). "Rapid axonal transport in primate optic nerve." Arch Ophthalmol **99**(Apr): 650-4.
- Radius, R. L. (1982). "Axonal transport interruption and anatomy at the lamina cribrosa." Arch Ophthalmol **100**(Oct): 1661-4.
- Rait, J. J. (2000). "An evidence-based approach to glaucoma therapy." Clin Exp Optom **83**(3): 111-112.
- Raju, T. R., M. S. Rao, et al. (1994). "Retinal ganglion cell survival and neurite regeneration in vitro after cell death period are dependent upon target derived trophic factor and retinal glial factor(s)." Brain Res **664**(1-2): 247-51.

- Ressiniotis, T., P. G. Griffiths, et al. (2005). "A polymorphism at codon 31 of gene p21 is not associated with primary open angle glaucoma in Caucasians." BMC Ophthalmol **5**(1): 5.
- Reyes, R., I. Lauritzen, et al. (2000). "Immunolocalization of the arachidonic acid and mechanosensitive baseline traak potassium channel in the nervous system." Neuroscience **95**(3): 893-901.
- Rhee, D. J. (2003). Glaucoma. New York, McGraw-Hill.
- Rosenberg, L. and T. Krupin (1999). Primary Open-Angle Glaucoma. Ophthalmology. M. Yanoff and J. Duker. St Louis, Mosby: 12.11.1-6.
- Rudzinski, M., T. P. Wong, et al. (2004). "Changes in retinal expression of neurotrophins and neurotrophin receptors induced by ocular hypertension." J Neurobiol **58**(3): 341-54.
- Runnerstam, M., F. Bao, et al. (2001). "A new model for diffuse brain injury by rotational acceleration: II. Effects on extracellular glutamate, intracranial pressure, and neuronal apoptosis." J Neurotrauma **18**(3): 259-73.
- Sackin, H. (1995). "Mechanosensitive channels." Annu Rev Physiol **57**: 333-53.
- Sakurai, T., K. Itoh, et al. (2005). "Low temperature protects mammalian cells from apoptosis initiated by various stimuli in vitro." Exp Cell Res **309**(2): 264-72.
- Sarthy, P. V., B. M. Curtis, et al. (1983). "Retrograde labeling, enrichment, and characterization of retinal ganglion cells from the neonatal rat." J Neurosci **3**(12): 2532-44.
- Schaeffer, W. I. (1979). "Proposed usage of animal tissue culture terms (revised 1978). Usage of vertebrate cell, tissue and organ culture terminology." In Vitro **15**(9): 649-53.
- Scheck, A. C. and J. V. Landau (1982). "The effect of high hydrostatic pressure on eukaryotic protein synthesis." Biochim Biophys Acta **698**(2): 149-57.
- Schlessinger, J. and A. Ullrich (1992). "Growth factor signaling by receptor tyrosine kinases." Neuron **9**(3): 383-91.
- Schmid, I., W. J. Krall, et al. (1992). "Dead cell discrimination with 7-actinomycin D in combination with dual color immunofluorescence in single laser flow cytometry." Cytometry **13**(2): 204-8.
- Schubert, D. (1974). "Induced differentiation of clonal rat nerve and glial cells." Neurobiology **4**(6): 376-87.
- Schubert, D., S. Heinemann, et al. (1974). "Clonal cell lines from the rat central nervous system." Nature **249**(454): 224-7.

- Schuler, M., E. Bossy-Wetzler, et al. (2000). "p53 induces apoptosis by caspase activation through mitochondrial cytochrome c release." *J Biol Chem* **275**(10): 7337-42.
- Schutte, B., R. Nuydens, et al. (1998). "Annexin V binding assay as a tool to measure apoptosis in differentiated neuronal cells." *J Neurosci Methods* **86**(1): 63-9.
- Schwarz, J. R. and J. V. Landau (1972). "Inhibition of cell-free protein synthesis by hydrostatic pressure." *J Bacteriol* **112**(3): 1222-7.
- Searle, J., J. F. Kerr, et al. (1982). "Necrosis and apoptosis: distinct modes of cell death with fundamentally different significance." *Pathol Annu* **17 Pt 2**: 229-59.
- Seigel, G. M. and M. F. Notter (1992). "Lectin-induced differentiation of transformed neuroretinal cells in vitro." *Exp Cell Res* **199**(2): 240-7.
- Seko, Y., H. Fujikura, et al. (1999). "Induction of vascular endothelial growth factor after application of mechanical stress to retinal pigment epithelium of the rat in vitro." *Invest Ophthalmol Vis Sci* **40**(13): 3287-91.
- Selles-Navarro, I., M. P. Villegas-Perez, et al. (1996). "Retinal ganglion cell death after different transient periods of pressure-induced ischemia and survival intervals. A quantitative in vivo study." *Invest Ophthalmol Vis Sci* **37**(10): 2002-14.
- Shareef, S. R., E. Garcia-Valenzuela, et al. (1995). "Chronic ocular hypertension following episcleral venous occlusion in rats." *Exp Eye Res* **61**(3): 379-82.
- Sheedlo, H. J. and J. E. Turner (1996). "Effects of retinal pigment epithelial cell-secreted factors on neonatal rat retinal explant progenitor cells." *J Neurosci Res* **44**(6): 519-31.
- Shields, M. (2004). *Textbook of Glaucoma*. Baltimore, Williams & Wilkins.
- Shimazawa, M., T. Yamashima, et al. (2005). "Neuroprotective effects of minocycline against in vitro and in vivo retinal ganglion cell damage." *Brain Res* **1053**(1-2): 185-94.
- Shiokawa, D., T. Kobayashi, et al. (2002). "Involvement of DNase gamma in apoptosis associated with myogenic differentiation of C2C12 cells." *J Biol Chem* **277**(34): 31031-7.
- Sievers, J., B. Hausmann, et al. (1987). "Fibroblast growth factors promote the survival of adult rat retinal ganglion cells after transection of the optic nerve." *Neurosci Lett* **76**(2): 157-62.
- Silveira, L. C., M. Russelakis-Carneiro, et al. (1994). "The ganglion cell response to optic nerve injury in the cat: differential responses revealed by neurofibrillar staining." *J Neurocytol* **23**(2): 75-86.

- Skerry, T. M., L. Bitensky, et al. (1988). "Loading-related reorientation of bone proteoglycan in vivo. Strain memory in bone tissue?" J Orthop Res **6**(4): 547-51.
- Smith, M. and J. Doyle (1999). Clinical Examination of Glaucoma. Ophthalmology. M. Yanoff and J. Duker. St Louis, Mosby: 12.4.1-12.
- Smith, R. L., S. F. Rusk, et al. (1996). "In vitro stimulation of articular chondrocyte mRNA and extracellular matrix synthesis by hydrostatic pressure." J Orthop Res **14**(1): 53-60.
- Somero, G. N. (1991). Hydrostatic pressure and adaptation to the deep sea. Environmental and Metabolic Animal Physiology. C. L. Prosser. New York, Wiley Liss: 167-204.
- Somjen, D., I. Binderman, et al. (1980). "Bone remodelling induced by physical stress is prostaglandin E2 mediated." Biochim Biophys Acta **627**(1): 91-100.
- Sommer, A. (1989). "Intraocular pressure and glaucoma." Am J Ophthalmol **107**(2): 186-8.
- Sommer, A., J. M. Tielsch, et al. (1991). "Relationship between intraocular pressure and primary open angle glaucoma among white and black Americans. The Baltimore Eye Survey." Arch Ophthalmol **109**(8): 1090-5.
- Sossi, N. and D. R. Anderson (1983). "Blockage of axonal transport in optic nerve induced by elevation of intraocular pressure. Effect of arterial hypertension induced by angiotensin I." Arch Ophthalmol **101**(1): 94-7.
- Southan, A. P. and K. T. Wann (1996). "Effects of high helium pressure on intracellular and field potential responses in the CA1 region of the in vitro rat hippocampus." Eur J Neurosci **8**(12): 2571-81.
- Spaeth, G. (1995). Diagnosis of Glaucoma, Searchlight series. Glaucoma Service Foundation to Prevent Blindness, Wills Eye Hospital Retrieved July 2006 from: <http://www.willsglaucoma.org/searchlight/vol4no1.html>
- Spalton, D. J., R. A. Hitchings, et al. (2005). Atlas of Clinical Ophthalmology. Philadelphia, Mosby.
- Spector, A., G. M. Wang, et al. (1995). "A brief photochemically induced oxidative insult causes irreversible lens damage and cataract. I. Transparency and epithelial cell layer." Exp Eye Res **60**(5): 471-81.
- Sperber, G. O. and A. Bill (1985). "Blood flow and glucose consumption in the optic nerve, retina and brain: effects of high intraocular pressure." Exp Eye Res **41**(5): 639-53.
- Stamenovic, D., S. M. Mijailovich, et al. (2003). "Experimental tests of the cellular tensegrity hypothesis." Biorheology **40**(1-3): 221-5.

- Standley, P. R., T. J. Obards, et al. (1999). "Cyclic stretch regulates autocrine IGF-I in vascular smooth muscle cells: implications in vascular hyperplasia." Am J Physiol **276**(4 Pt 1): E697-705.
- Strehler, B. L. and F. H. Johnson (1954). "The Temperature-Pressure-Inhibitor Relations of Bacterial Luminescence in Vitro." Proc Natl Acad Sci U S A **40**(7): 606-17.
- Sucher, N. J., S. A. Lipton, et al. (1997). "Molecular basis of glutamate toxicity in retinal ganglion cells." Vision Res **37**(24): 3483-93.
- Sumpio, B. E., M. D. Widmann, et al. (1994). "Increased ambient pressure stimulates proliferation and morphologic changes in cultured endothelial cells." J Cell Physiol **158**(1): 133-9.
- Takahashi, K., T. T. Lam, et al. (1992). "Protective effects of flunarizine on ischemic injury in the rat retina." Arch Ophthalmol **110**(6): 862-70.
- Takahashi, N., D. Cummins, et al. (1991). "Rat retinal ganglion cells in culture." Exp Eye Res **53**(5): 565-72.
- Takami, H., A. Inoue, et al. (1997). "Microbial flora in the deepest sea mud of the Mariana Trench." FEMS Microbiol Lett **152**(2): 279-85.
- Takano, K. J., T. Takano, et al. (1997). "Pressure-induced apoptosis in human lymphoblasts." Exp Cell Res **235**(1): 155-60.
- Take, J., T. Yamaguchi, et al. (2001). "Caspase activation in high-pressure--induced apoptosis of murine erythroleukemia cells." Jpn J Physiol **51**(2): 193-9.
- Tamm, E. R., P. Russell, et al. (1999). "Modulation of myocilin/TIGR expression in human trabecular meshwork." Invest Ophthalmol Vis Sci **40**(11): 2577-82.
- Tan, J., F. Kalapesi, et al. (2006). "Mechanosensitivity and the eye: cells coping with the pressure." Br J Ophth **90**: 383-388.
- Tang, S., Y. Toda, et al. (2003). "The association between Japanese primary open-angle glaucoma and normal tension glaucoma patients and the optineurin gene." Hum Genet **113**(3): 276-9.
- Tarnok, A. and H. Ulrich (2001). "Characterization of pressure-induced calcium response in neuronal cell lines." Cytometry **43**(3): 175-81.
- Tatton, N. A., G. Tezel, et al. (2001). "In situ detection of apoptosis in normal pressure glaucoma. a preliminary examination." Surv Ophthalmol **45**(Suppl 3): S268-72; discussion S273-6.
- Teiger, E., V. D. Than, et al. (1996). "Apoptosis in pressure overload-induced heart hypertrophy in the rat." J Clin Invest **97**(12): 2891-7.

- Terracio, L., B. Miller, et al. (1988). "Effects of cyclic mechanical stimulation of the cellular components of the heart: in vitro." In Vitro Cell Dev Biol **24**(1): 53-8.
- Tewari, M., L. T. Quan, et al. (1995). "Yama/ CPP32 beta, a mammalian homolog of CED-3, is a CrmA-inhibitable protease that cleaves the death substrate poly(ADP-ribose) polymerase." Cell **81**(5): 801-9.
- Tezel, G., L. Y. Li, et al. (2001). "TNF-alpha and TNF-alpha receptor-1 in the retina of normal and glaucomatous eyes." Invest Ophthalmol Vis Sci **42**(8): 1787-94.
- Tezel, G. and M. B. Wax (1999). "Inhibition of caspase activity in retinal cell apoptosis induced by various stimuli in vitro." Invest Ophthalmol Vis Sci **40**(11): 2660-7.
- Tezel, G. and M. B. Wax (2000). "Increased production of tumor necrosis factor-alpha by glial cells exposed to simulated ischemia or elevated hydrostatic pressure induces apoptosis in cocultured retinal ganglion cells." J Neurosci **20**(23): 8693-700.
- Tezel, G. and M. B. Wax (2000). "The mechanisms of hsp27 antibody-mediated apoptosis in retinal neuronal cells." J Neurosci **20**(10): 3552-62.
- Thornberry, N. A. and Y. Lazebnik (1998). "Caspases: enemies within." Science **281**(5381): 1312-6.
- Thylefors, B., A. D. Negrel, et al. (1995). "Global data on blindness." Bull World Health Organ **73**(1): 115-21.
- Tielsch, J. M., A. Sommer, et al. (1991). "Racial variations in the prevalence of primary open-angle glaucoma. The Baltimore Eye Survey." Jama **266**(3): 369-74.
- Travis, G. H. (1998). "Mechanisms of cell death in the inherited retinal degenerations." Am J Hum Genet **62**(3): 503-8.
- Troy, C. M., L. Stefanis, et al. (1996). "The contrasting roles of ICE family proteases and interleukin-1beta in apoptosis induced by trophic factor withdrawal and by copper/zinc superoxide dismutase down-regulation." Proc Natl Acad Sci U S A **93**(11): 5635-40.
- Tuulonen, A., J. Koponen, et al. (1989). "Laser trabeculoplasty versus medication treatment as primary therapy for glaucoma." Acta Ophthalmol (Copenh) **67**(3): 275-80.
- Urban, J. P. (1994). "The chondrocyte: a cell under pressure." Br J Rheumatol **33**(10): 901-8.
- Uusitalo, R. J. and A. Palkama (1989). "Long-term evaluation of timolol." Acta Ophthalmol (Copenh) **67**(5): 573-81.
- van Engeland, M., L. J. Nieland, et al. (1998). "Annexin V-affinity assay: a review on an apoptosis detection system based on phosphatidylserine exposure." Cytometry **31**(1): 1-9.

- van Engeland, M., F. C. Ramaekers, et al. (1996). "A novel assay to measure loss of plasma membrane asymmetry during apoptosis of adherent cells in culture." Cytometry **24**(2): 131-9.
- Vandenburgh, H. H., S. Hatfaludy, et al. (1989). "Skeletal muscle growth is stimulated by intermittent stretch-relaxation in tissue culture." Am J Physiol **256**(3 Pt 1): C674-82.
- Vaughan, D., T. Asbury, et al. (1992). General Ophthalmology. East Norwalk, Connecticut, Appleton & Lange.
- Vaux, D. L. and A. Strasser (1996). "The molecular biology of apoptosis." Proc Natl Acad Sci U S A **93**(6): 2239-44.
- Vickers, J. C. (1997). "The cellular mechanism underlying neuronal degeneration in glaucoma: parallels with Alzheimer's disease." Aust N Z J Ophthalmol **25**(2): 105-9.
- Vorwerk, C. K., S. A. Lipton, et al. (1996). "Chronic low-dose glutamate is toxic to retinal ganglion cells. Toxicity blocked by memantine." Invest Ophthalmol Vis Sci **37**(8): 1618-24.
- Wadia, J. S., R. M. Chalmers-Redman, et al. (1998). "Mitochondrial membrane potential and nuclear changes in apoptosis caused by serum and nerve growth factor withdrawal: time course and modification by (-)-deprenyl." J Neurosci **18**(3): 932-47.
- Wainer, B. H., J. Kwon, et al. (1997). "Neural plasticity as studied in neuronal cell lines." Adv Neurol **72**: 133-42.
- Walsh, T. (1996). Visual fields: Examination & Interpretation. Ophthalmology Monographs. T. Walsh. San Francisco, American Academy of Ophthalmology.
- Wamsley, S., B. T. Gabelt, et al. (2005). "Vitreous glutamate concentration and axon loss in monkeys with experimental glaucoma." Arch Ophthalmol **123**(1): 64-70.
- Wang, I. K., S. Y. Lin-Shiau, et al. (2000). "Induction of apoptosis by lovastatin through activation of caspase-3 and DNase II in leukaemia HL-60 cells." Pharmacol Toxicol **86**(2): 83-91.
- Wang, N., K. Naruse, et al. (2001). "Mechanical behavior in living cells consistent with the tensegrity model." Proc Natl Acad Sci U S A **98**(14): 7765-70.
- Wax, M. B., G. Tezel, et al. (2000). "Responses of different cell lines from ocular tissues to elevated hydrostatic pressure." Br J Ophthalmol **84**(4): 423-8.
- Weiner, A., D. J. Ripkin, et al. (1998). "Foveal dysfunction and central visual field loss in glaucoma." Arch Ophthalmol **116**(9): 1169-74.
- Weinreb, R. N. (2001). "Neuroprotection--possibilities in perspective." Surv Ophthalmol **45**(Suppl 3): S241-2.

- Weinstein, D. E., M. L. Shelanski, et al. (1990). "C17, a retrovirally immortalized neuronal cell line, inhibits the proliferation of astrocytes and astrocytoma cells by a contact-mediated mechanism." Glia **3**(2): 130-9.
- Wendling, S., P. CaNadas, et al. (2002). "Interrelations between elastic energy and strain in a tensegrity model: contribution to the analysis of the mechanical response in living cells." Comput Methods Biomech Biomed Engin **5**(1): 1-6.
- Werner, E. (1999). Visual Field Perimetry testing in Glaucoma. Ophthalmology. M. Yanoff and J. Duker. St Louis, Mosby: 12.5.1-12.
- WHO (2004). Vision 2020: The Right to Sight, the Global Initiative for the Elimination of Avoidable Blindness. . WHO Fact Sheets. Geneva, World Health Organisation.
- Williams, R. S. (1999). "Apoptosis and heart failure." N Engl J Med **341**(10): 759-60.
- Wilson, S. E. (1999). "Stimulus-specific and cell type-specific cascades: emerging principles relating to control of apoptosis in the eye." Exp Eye Res **69**(3): 255-66.
- Wilson, S. E. and W. J. Kim (1998). "Keratocyte apoptosis: implications on corneal wound healing, tissue organization, and disease." Invest Ophthalmol Vis Sci **39**(2): 220-6.
- Wolf, S., O. Arend, et al. (1995). "Retinal hemodynamics in patients with chronic open-angle glaucoma." Ger J Ophthalmol **4**(5): 279-82.
- Wong, E. Y., J. E. Keeffe, et al. (2004). "Detection of undiagnosed glaucoma by eye health professionals." Ophthalmology **111**(8): 1508-14.
- Wormald, R. P., E. Basauri, et al. (1994). "The African Caribbean Eye Survey: risk factors for glaucoma in a sample of African Caribbean people living in London." Eye **8 (Pt 3)**: 315-20.
- Wright, M., P. Jobanputra, et al. (1996). "Effects of intermittent pressure-induced strain on the electrophysiology of cultured human chondrocytes: evidence for the presence of stretch-activated membrane ion channels." Clin Sci (Lond) **90**(1): 61-71.
- Wynanski, T., H. Desatnik, et al. (1995). "Comparison of ganglion cell loss and cone loss in experimental glaucoma." Am J Ophthalmol **120**(2): 184-9.
- Wyllie, A. H. (1992). "Apoptosis and the regulation of cell numbers in normal and neoplastic tissues: an overview." Cancer Metastasis Rev **11**(2): 95-103.
- Wyllie, A. H., M. J. Arends, et al. (1992). "The apoptosis endonuclease and its regulation." Semin Immunol **4**(6): 389-97.
- Wyllie, A. H., J. F. Kerr, et al. (1980). "Cell death: the significance of apoptosis." Int Rev Cytol **68**: 251-306.

- Yakovlev, A. G., S. M. Knoblach, et al. (1997). "Activation of CPP32-like caspases contributes to neuronal apoptosis and neurological dysfunction after traumatic brain injury." J Neurosci **17**(19): 7415-24.
- Yang, J., P. Yang, et al. (2001). "Induction of HLA-DR expression in human lamina cribrosa astrocytes by cytokines and simulated ischemia." Invest Ophthalmol Vis Sci **42**(2): 365-71.
- Yang, J. L., A. H. Neufeld, et al. (1993). "Collagen type I mRNA levels in cultured human lamina cribrosa cells: effects of elevated hydrostatic pressure." Exp Eye Res **56**(5): 567-74.
- Yau, P. (2006) "Apoptosis." Science Creative Quarterly Retrieved Nov 2006 from <http://ihome.cuhk.edu.hk/~b105122/image/0611.jpg>
- Yayanos, A. A., A. S. Dietz, et al. (1981). "Obligately barophilic bacterium from the Mariana trench." Proc Natl Acad Sci U S A **78**(8): 5212-5.
- Yin, D. X. and R. T. Schimke (1996). "Inhibition of apoptosis by overexpressing Bcl-2 enhances gene amplification by a mechanism independent of aphidicolin pretreatment." Proc Natl Acad Sci U S A **93**(8): 3394-8.
- Yoles, E., S. Muller, et al. (1997). "NMDA-receptor antagonist protects neurons from secondary degeneration after partial optic nerve crush." J Neurotrauma **14**(9): 665-75.
- Yoles, E., L. A. Wheeler, et al. (1999). "Alpha2-adrenoreceptor agonists are neuroprotective in a rat model of optic nerve degeneration." Invest Ophthalmol Vis Sci **40**(1): 65-73.
- Young, A. P., P. W. Gunning, et al. (1983). "The nerve growth factor induced differentiation of a pheochromocytoma PC12 cell line." Birth Defects Orig Artic Ser **19**(4): 33-46.
- Younkin, D. P., C. M. Tang, et al. (1993). "Inducible expression of neuronal glutamate receptor channels in the NT2 human cell line." Proc Natl Acad Sci U S A **90**(6): 2174-8.
- Yuan, J., S. Shaham, et al. (1993). "The C. elegans cell death gene ced-3 encodes a protein similar to mammalian interleukin-1 beta-converting enzyme." Cell **75**(4): 641-52.
- Yucel, Y. H., Q. Zhang, et al. (2001). "Atrophy of relay neurons in magno- and parvocellular layers in the lateral geniculate nucleus in experimental glaucoma." Invest Ophthalmol Vis Sci **42**(13): 3216-22.
- Zeitz, O., E. T. Matthiessen, et al. (2005). "Effects of glaucoma drugs on ocular hemodynamics in normal tension glaucoma: a randomized trial comparing bimatoprost and latanoprost with dorzolamide [ISRCTN18873428]." BMC Ophthalmol **5**(1): 6.

- Zhao, S. and C. J. Barnstable (1996). "Differential effects of bFGF on development of the rat retina." Brain Res **723**(1-2): 169-76.
- Zhou, X., F. Li, et al. (2005). "Involvement of inflammation, degradation, and apoptosis in a mouse model of glaucoma." J Biol Chem **280**(35): 31240-8.
- Zimmerman, A. M., J. V. Landau, et al. (1957). "Cell division: a pressure-temperature analysis of the effects of sulfhydryl reagents on the cortical plasmagel structure and furrowing strength of dividing eggs (*Arbacia* and *Chaetopterus*)." J Cell Physiol **49**(3): 395-435.
- Zobell, C. E. and R. Y. Morita (1957). "Barophilic bacteria in some deep sea sediments." J Bacteriol **73**(4): 563-8.
- Zobell, C. E. and C. H. Oppenheimer (1950). "Some effects of hydrostatic pressure on multiplication and morphology of marine bacteria." J Bacteriol **60**(6): 771-81.

Appendices

Pressure Related Apoptosis in Neuronal Cell Lines

Ashish Agar,^{1,2} Sonia S. Yip,¹ Mark A. Hill,^{1*} and Minas T. Coroneo²

¹Cell Biology Lab, School of Anatomy, University of New South Wales, Sydney, Australia

²Department of Ophthalmology, Prince of Wales Hospital, University of New South Wales, Sydney, Australia

Pressure is a crucial component of the cellular environment, and can lead to pathology if it varies beyond its normal range. The increased intra-ocular pressures in acute glaucoma are associated with the loss of neurons by apoptosis. Little is known regarding the interaction between pressure and apoptosis at the level of the cell. The model developed in this study examines the effects of elevated ambient hydrostatic pressure directly upon cultured neuronal lines. Conditions were selected to be within physiological limits: 100 mmHg over and above atmospheric pressure for a period of 2 hr, as seen clinically in acute glaucoma. This system can be used to investigate pressure relatively independently of other variables. Neuronal cell line cultures (B35 and PC12) were subjected to pressure conditions in specially designed pressure chambers. Controls were treated identically, except for the application of pressure, and positive controls were treated with a known apoptotic stimulus. Apoptosis was detected by cell morphology changes and by 2 specific apoptotic markers: TUNEL (Terminal transferase dUTP Nick-End Labeling) and Annexin V. These fluorescent markers were detected and quantified by automated Laser Scanning Cytometry. All techniques showed that increased pressure was associated with a greater level of apoptosis compared to equivalent controls. Our results suggest that pressure alone may act as a stimulus for apoptosis in neuronal cell cultures. This raises the possibility of a more direct relationship at the cellular level between pressure and neuronal loss. *J. Neurosci. Res.* 60:495–503, 2000.

© 2000 Wiley-Liss, Inc.

Key words: hydrostatic pressure; pressure chamber; glaucoma; neuronal culture; apoptosis; laser scanning cytometer

Pressure is a fundamental physical quantity, being a determinant of both the integrity and function of cells including neurons. Disorders of this relationship, such as when pressures vary beyond physiological limits, can thus lead to disease states. In the ocular disease glaucoma, for example, the most frequent and important association is that of raised intraocular pressure (IOP), either acute or chronic (Armaly et al., 1980). This disease is characterized by the progressive loss of Retinal Ganglion Cells (RGCs).

Induced increases in IOP in animal models have been shown to result in the loss of RGCs, confirming the relationship seen in clinical glaucoma (Nickells, 1996). These studies have revealed the major mode of RGC loss to be via apoptosis, the genetically programmed form of cell death. Recently this has also been validated in human glaucoma (Kerrigan et al., 1997). The molecular events that result in apoptosis can be initiated by a variety of stimuli (Nickells, 1996).

This mechanism, whereby an increase in IOP triggers events that damage and then destroy RGCs, remains to be fully explained. Theories of glaucoma pathogenesis include mechanodistortion of the optic nerve at its exit from the eyeball affecting RGC transport mechanisms, and compression of optic nerve head microvasculature compromising neuronal circulation (reviewed by Quigley, 1995). It has been reported that inhibition of retrograde axonal flow can only partly explain RGC loss post axotomy (Fagiolini et al., 1997). There is evidence from other studies that RGC loss may be mediated independently of these mechanisms (Radtius 1981; Johansson 1983, 1988). Therefore, in addition to the known components of glaucoma pathology, pressure may also have some direct effect on RGC apoptosis.

Of the few published studies that have applied increased physiological levels of hydrostatic pressure alone to cells in vitro, none have used neurons. In-vitro cultures of other cell types have been placed in pressure chambers (Kosnosky et al., 1995), and neurons have been subjected to pressure conditions in vivo in animal models (Weber et al., 1998). Apoptosis has been induced in cultured neuroblastoma cells, but in response to mechanical shear (Edwards et al., 1998). A large range of sometimes non-physiological pressures have been applied to cell cultures. Human lymphoblasts have been subjected to pressures ≈7000 mmHg, far in excess of those seen in disease states

Abbreviations: GI, green integral; GMP, green max pixel; IOP, intra ocular pressure; LSC, laser scanning cytometer; PI, propidium iodide; RGC, retinal ganglion cell; TUNEL, terminal transferase dUTP nick-end labeling.

Contract grant sponsor: Allergan Australia.

*Correspondence to: Dr. M.A. Hill, Cell Biology Lab, School of Anatomy, University of New South Wales, Sydney NSW 2052, Australia.

E-mail: m.hill@unsw.edu.au

Received 4 October 1999; Revised 1 February 2000; Accepted 2 February 2000

including glaucoma (Takano, et al., 1997). Significantly, this experiment has demonstrated that pressure can be an independent stimulus for inducing apoptosis.

This current study investigates the effect of elevated hydrostatic pressure *in vitro* on neuronal cell lines. The experimental parameters were selected to simulate the known clinical scenario of acute glaucoma. Our initial research, presented here, investigated a single pressure elevation and duration at physiological levels, relevant to intra-ocular pressures seen in this disease. Cultures of neuronal cell lines were exposed to an increased ambient hydrostatic pressure of 100 mmHg for 2 hr. The cells were then assessed for apoptosis morphologically and by means of specific fluorescent markers of apoptosis.

MATERIALS AND METHODS

Cell Culture

Cell cultures were generated using the neuroblastoma cell line B35, derived from the rat central nervous system (Schubert 1974). Cells were grown in Dulbecco's modified Eagle medium (DMEM, Gibco) supplemented with 10% heat inactivated fetal calf serum (Gibco) and 1% penicillin/streptomycin.

As B35 cells are not post-mitotic and continue to proliferate, we have also used a second neuronal cell line PC12 (Greene and Tischler, 1976). These cells were differentiated *in vitro* to produce neurons that had exited the cell cycle (Michel et al., 1995). Undifferentiated PC12 cultures were maintained in DMEM with 5% fetal calf serum and 10% heat inactivated horse serum (Gibco). PC12 cultures were cultured in DMEM with 1% heat inactivated horse serum supplemented with 1 mM di-butyl cAMP (Sigma) and 50 ng/mL NGF (kindly provided by Prof. I. Hendry) for 3 days to induce differentiation.

Neurons were plated ($10,000/\text{cm}^2$) onto poly-L-lysine coated glass coverslips in 24-well culture dishes. Neuronal cultures were grown in 250 μL of growth media per well, and incubated at 37°C in 5% CO_2 and air.

Pressure System

Specialised pressure chambers were designed based upon a simple model described previously for use with cell cultures (Sumpio et al., 1994; Kosnosky et al., 1995; Mattana et al., 1996). Briefly, a Perspex and glass chamber was constructed with gas inlet and flow valves incorporated for connection to a low-pressure regulator (BOC Gases). The chamber could be pressurized with a 5% CO_2 and air gas mix to a constant hydrostatic pressure ranging from 0–200 mmHg. Pressure levels were monitored continuously by mercury column barometer, with atmospheric pressure (760 mmHg) calibrated to 0 mmHg. Compression and decompression to 100 mmHg (over and above atmospheric pressure) was attained over 30 sec. The apparatus was equilibrated and maintained within an electronically controlled CO_2 incubator at 37°C (Nuair NU4500E).

The possibility that increased hydrostatic pressure could alter gas exchange was assessed. Culture growth medium was sampled in pressure and control cultures before and immediately after the 2 hr pressurization, and at subsequent timepoints. Measurements for pH, pCO_2 and pO_2 analysis were done by stat gas analyzer (Radiometer ABL 725).

Experimental Protocol

Experimental neuronal culture dishes were placed within the pressure chamber and the gas mix was then pressurized to subject the cells to conditions of 100 mmHg for 2 hr, simulating conditions analogous to acute glaucoma. After this period of pressure elevation cultures were restored to atmospheric pressure and the culture dishes removed from the chamber and incubated for a further 24 hr. Control neuronal culture dishes were treated identically, being placed within the pressure chamber but without the application of pressure. At serial timepoints of 2, 6 and 20 or 24 hr after initiation of pressure, duplicate coverslips were removed for analysis. These were fixed for DNA fragmentation assays and morphological examination, or stained live for the Annexin V assay before fixation. Cell fixation used in all experiments was 4% w/v paraformaldehyde in phosphate buffered saline pH 7.5 for 10 min.

A maximum apoptosis control for the B35 cell line was established in each experiment by treatment with ethanol (Fig. 1A), a known stimulator of apoptosis (De et al., 1994; Oberdoerster et al., 1998; Mizushima et al., 1999). This enabled validation in each experiment of the various apoptosis detection methods. Initial studies using a range of culture timepoints established maximal inducible apoptosis with 5% ethanol treatment after 2 hr (data not shown). These cultures were used in both apoptosis marker assays (TUNEL and Annexin V) as a positive 'maximum cell death' control for each experiment. Ethanol treatment of differentiated PC12 neurons led to excessive cell loss by detachment. In PC12 experiments a fixed control culture was treated with DNase (Promega) for 25 min at room temperature to elicit maximal TUNEL signal. Using this data results were normalized to the cell line's maximal apoptosis control within each experiment, allowing comparison between the experiments.

Apoptosis Detection

Morphologically apoptosis is characterized by progressive condensation of the cytoplasm and nucleus, followed by fragmentation and phagocytosis by other cells (Majno and Joris, 1995). In neurons there is also seen a withdrawal of cell processes and a "blebbing" or "budding" of the cell membrane. Neurons were examined by phase contrast microscopy for these features of apoptosis and to allow identification of necrotic cells.

TUNEL is a well-established assay for the detection of apoptosis. Endonuclease activation in the nucleus cleaves DNA into segments that can be labeled by terminal transferase dUTP nick-end labeling (Ben-Sasson et al., 1995). After fixation adherent cells on the coverslips were assayed for TUNEL using direct binding fluorescein-conjugated dUTP (green fluorochrome), with propidium iodide (PI) providing the red counterstain, as described by the *in situ* detection kit (Promega). Mounted coverslips were then analyzed by fluorescent microscopy and laser scanning cytometry.

To complement the detection of later nuclear changes associated with apoptosis measured by TUNEL, a relatively early marker of apoptosis was also studied. Annexin V detects one of the earliest molecular events in apoptosis, the translocation of phosphatidyl-serine to the outer leaflet of the cell membrane (van Engeland et al., 1996). The staining procedure was carried out on live cells using a direct binding Annexin V-FITC conjugate, ac-

according to the protocol supplied with the detection kit (Zymed). Counterstaining live cells with PI enables necrotic cells to be distinguished by the dye exclusion principle. Cells were then analyzed by fluorescent microscopy and laser scanning cytometry, with or without fixation and mounting of the coverslip.

Analysis

Morphological assessment was carried out using an Olympus IX-70 phase contrast microscope with NIH Image (version 1.61) software. Visualization of Annexin V and TUNEL apoptosis markers was performed with a confocal Laser Scanning

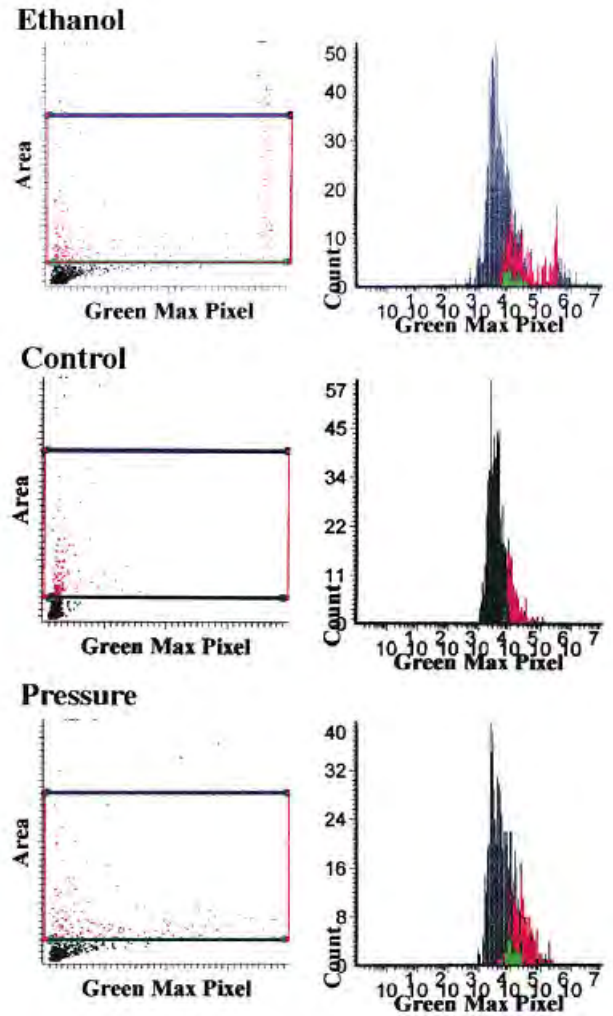
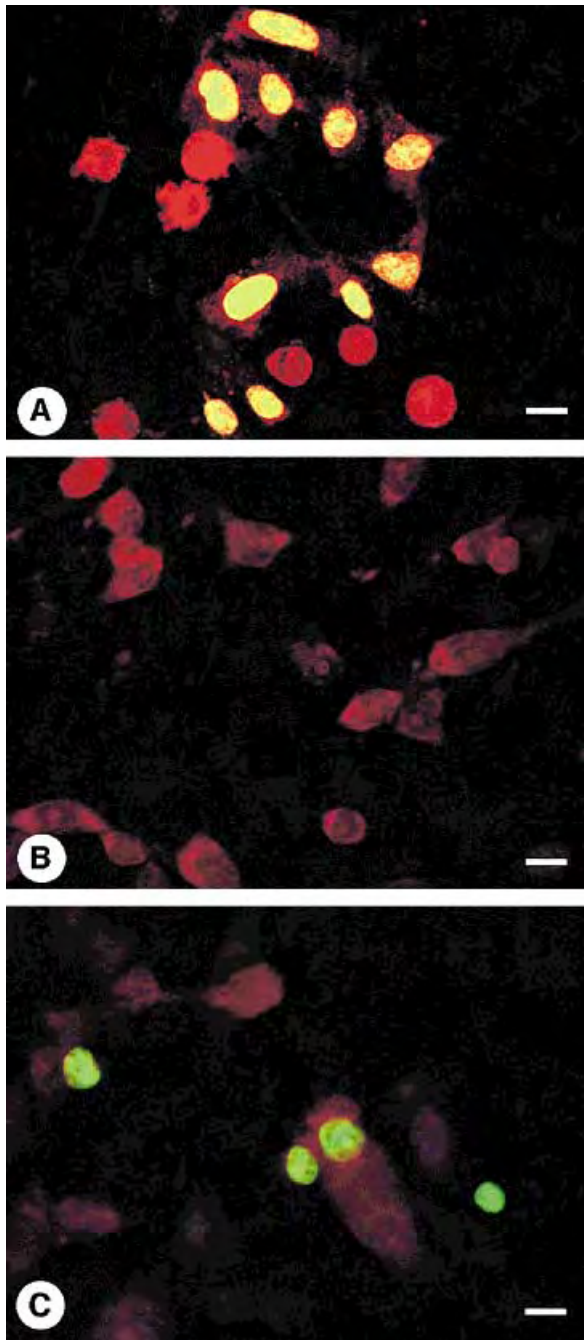


Figure 2. (Legend on following page.)

←
 Fig. 1. (A) Ethanol (positive control) neurons. Immunofluorescent images of cultured B35 neurons treated with 5% ethanol for 2 hr, a known stimulus of apoptosis. Cells stained with TUNEL assay for DNA fragmentation (green). Counterstain with propidium iodide (red). Ethanol treatment gave maximal fluorochrome signal strength, with intense green and red signals appearing as yellow. Neurons show high level of apoptosis, with strongly positive nuclei for TUNEL marker, and chromatin condensation also evident in some nuclei. Remainder of cells in late stage apoptosis show morphological features of shrunken cell body, loss of processes and membrane blebs. Scale bar = 10 μm. (B) Control neurons. B35 neural cell line maintained in pressure chamber apparatus for 2 hr but not subject to increased pressure conditions. TUNEL assay and propidium iodide staining. Neurons show generally normal morphology and little or no nuclear staining for DNA fragmentation. Note centrally located cell showing weakly TUNEL positive nucleus. (C) Neurons subject to pressure conditions. B35 neural cell line after 2 hr of elevated ambient hydrostatic pressure (first timepoint). Cells assayed with TUNEL (green) and counterstained with propidium iodide (red). Neurons show increased level of DNA fragmentation and some chromatin condensation as detected by fluorescent label compared to controls (B).

Microscope (Olympus GB200). Quantitative determination of these fluorochromes, as well as concurrent morphological inspection, was made possible using the relatively new technique of laser scanning cytometry (laser scanning cytometer, or LSC, Compucyte, USA) that allows automated analysis of adherent fluorescently labeled cells. Recently the LSC has been demonstrated to be an accurate tool for the detection of apoptosis using both markers employed in this study (Schutte et al., 1998; Darzynkiewicz et al., 1998).

Fluorescein isothiocyanate or FITC is the hapten label in both Annexin and TUNEL assays. The LSC Argon laser was set to 488 nm and appropriate sensors selected for the FITC fluorochrome, to detect and measure this green fluorescent marker, (note red PI intensity not measured). FITC label intensity is measured and cell values determined for two parameters. Green max pixel (GMP) or fluorescence peak reflects the highest value within a cell. Hyperchromicity of DNA in condensed chromatin of apoptotic cells can be recognized by high GMP values with the nuclear TUNEL assay. Membrane bound Annexin V label also gives high readings for apoptotic cells, as other cells do not stain or do so at a significantly lower intensity. The sum of the signal value for all pixels over threshold for a scanned cell is given as the green integral (GI). This measure of total fluorescence is similarly indicative of the degree of labeling (Darzynkiewicz et al., 1998). The spatial X-Y coordinates of each scanned cell are recorded, so an individual neuron can be relocated after initial LSC measurement for visual microscopy. As the resolution of the LSC image is limited, these features are visualized at greater detail via a co-mounted fluorescent microscope. The position is recorded and the image then captured digitally using the confocal laser scanning microscope. The LSC determines the size of all scanned objects by the number of pixels over threshold, or the 'fluorescent area.' Visual inspection of cells during scanning allowed exclusion of debris and cell clumps on the basis of size. Appropriate area limits were then set to select or gate the target group of single cells, seen within the colored rectangular region in the data scattergrams (Fig. 2).

A total of seven experiments were undertaken with the B35 cells and 3 with the PC12 cell line. Neurons on the coverslips were scanned in each of four equal sized quadrants. At each timepoint in each experiment 4 sets of LSC measurements were made, one per quadrant. Data were collected for both GMP and GI parameters as well as fluorescent area for each cell. Absolute measured values were

Fig. 2. (Figure appears on preceding page.) Typical quantitative TUNEL data from LSC analysis of B35 cultures after ethanol, control or pressure treatment. Single scan for green dUTP-FITC fluorochrome, shown as displayed by LSC software. Scattergrams (**left column**) show green max pixel (peak TUNEL label intensity of cell) plotted against area (fluorescent area of scanned cell). Boxed area in graph includes only single cells (**red**), and excludes cell clumps and debris (**black**). Scattergram data reflected in adjacent histogram (**right column**; note arbitrary 'Count' scale is set by LSC software). Colors correspond to scattergram with red region lying within selected box. High apoptosis in ethanol treated culture shown by high fluorescent signal (red peak shifted right). Corresponding scattergram also shows strongly fluorescent cells at right within boxed region. This pattern is seen in pressure treated cells but not control cells.

TABLE I. Measurement of pH, pCO₂ and pO₂ Initially and Following 2 hr With or Without Pressure Application

Treatment	Control	Control	Pressure
Time (hr)	0	2	2
pH	7.63 ± 0.02	7.67 ± 0.04	7.66 ± 0.04
pCO ₂ (mmHg)	27.8 ± 0.4	26.1 ± 1.0	25.6 ± 0.4
pO ₂ (mmHg)	164 ± 1.4	168.5 ± 2.8	168.5 ± 3.8

Statistical analysis (Student's paired *t*-test) of these results showed no significant variation in the readings of pH, pCO₂ or pO₂ following the experimental procedure (2 hr values) for control or pressure groups, compared to initial or 'atmospheric' measurements ($P > 0.1$ to $P > 0.5$, $n = 6$). Further, after the experimental conditions of 100 mmHg for 2 hr, the results show no significant difference in pCO₂, pO₂ or pH between the pressure and control neuronal cultures ($P > 0.5$, $n = 6$).

recorded by the LSC and data analyzed as the average for the gated single cell population. Normalized data of pooled results were generated by comparison of individual absolute measurements with the averaged positive control (maximal apoptosis) value for that experiment. Data could thus be expressed as a ratio of the positive control. The quantitative data are presented as the mean ± standard error (SE). Analysis of variance was determined using Student's paired *t*-test.

RESULTS

Pressure System

Conditions of raised pressure of 100 mmHg were attained for 2 hr with a variance of ±2 mmHg on continuous monitoring. Taking into account the 0.25 ml of culture media per well, experimental pressure conditions were thus maintained with a variability of approximately ±2.25 mmHg, or ±2.25%, for the duration of the experiment. Stat gas analysis was undertaken on samples of well culture media before the experimental procedure ('atmospheric' or 0 hr), immediately after pressure conditions of 100 mmHg for 2 hr (Table I) and at later timepoints (data not shown). Analyses for the later timepoints were similar to the initial 0 hr findings, with control and pressure groups not differing significantly. Statistical analysis (Student's paired *t*-test) of pressure and control values for pH, pCO₂ or pO₂ before (0 hr) and after 2 hr showed no significant differences ($P > 0.1$ to $P > 0.5$ respectively, $n = 6$). Furthermore, after the experimental conditions of 100 mmHg for 2 hr, the results showed no significant difference in pCO₂, pO₂ or pH between the pressure and control neuronal cultures ($P > 0.5$, $n = 6$).

Morphological Apoptosis Detection

Apoptosis was confirmed by phase contrast microscopy and fluorescent microscopy (Fig. 1). These findings were applicable to both B35 and PC12 neuronal cell lines, with few subjective differences. Morphological analysis revealed several characteristics of apoptosis including: shrunken cell size, plasma membrane blebbing, loss of processes, and nuclear condensation. This combination of advanced apoptosis features was most pronounced in the positive ethanol-treated neurons (Fig. 1A). A greater range

of apoptotic morphological features was seen in the control (Fig. 1B) and pressure cells (Fig. 1C), with affected neurons displaying some but not all of these features. Therefore, using this criteria alone, it would be difficult to quantify apoptosis in these cultures. Qualitatively, there were fewer cells showing apoptotic morphological features in control than pressure conditions.

Staining of live cells with Annexin V and PI counterstain confirmed necrosis as not being significant in the studied populations by PI dye exclusion. Morphological examination of randomly selected fields looked for necrotic features such as: swelling of both soma and nucleus, plasma membrane rupture, vacuolation or karyolysis. These were uncommon in all experimental groups. Neurons in various stages of apoptosis showed features including loss of processes, shrunken cell body, membrane blebbing and condensed nuclei.

Confocal fluorescent microscopy allowed concomitant examination of both morphology and fluorochrome molecular marker. This generally confirmed the association of visual features of apoptosis with positive labeling (Fig. 1) in individual cells. In a large population of cells staining variability may be a factor, as would the presence of a range of apoptotic stages.

Quantitative Apoptosis Detection

Quantitative analysis by LSC revealed detectable differences in fluorescent label intensity among the experimental cell groups (Fig. 2). The ethanol treated positive controls recorded significantly higher values across all experiments. This was true for both parameters GMP and GI. Positively staining cells as determined by the LSC were also examined for morphology. Visualization confirmed the presence of characteristics of apoptosis such as condensed cells, nuclei and process retraction, as well as the high FITC-marker staining in these cells. The technique was therefore able to identify and distinguish cells positive for the apoptosis markers.

Data for all groups is the mean measurement value for the scanned population of single cells. GI data for TUNEL staining on a single B35 run are presented normalized against the ethanol treated positive control (Fig. 3). This illustrates the relative staining intensity of the respective neuronal cell groups. Neurons subjected to conditions of 100 mmHg pressure for 2 hr had higher levels of apoptotic marker compared to negative control neurons. This was significant at the 2 hr timepoint ($P < 0.005$, $n = 4$). B35 data was pooled for all TUNEL experiments and normalized as previously described (Fig. 4). Neurons subjected to pressure conditions showed increased apoptotic marker intensity compared to controls. This result was significant at the 2 hr timepoint for both parameters GMP ($P < 0.05$, $n = 24$) and especially GI ($P = 0.005$, $n = 24$). Later timepoints showed a similar trend but with greater variability, such that no significant differences were found at 6 hr or 20 hr. Quantitative data for a single B35 run using Annexin V showed experimental neurons subjected to pressure conditions had greater values for Annexin V staining compared with negative controls (Fig. 5). By contrast with the TUNEL data, this effect was interestingly more marked with time (20 hr, $P < 0.05$, $n = 4$). The

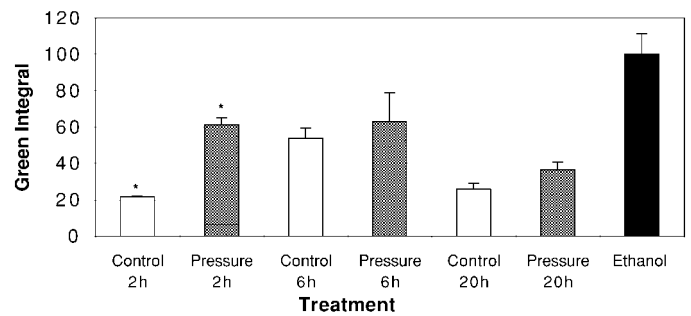


Fig. 3. LSC data for TUNEL apoptosis marker over time for B35 neurons after control, pressure and ethanol (positive control) treatment. Green integral LSC fluorescent values from single experimental run normalized to average positive control for that run (5% ethanol treatment for 2 hr to generate maximum detected apoptosis). Greater TUNEL labeling of neurons subjected to pressure conditions in comparison to control neurons significant at 2 hr ($P < 0.005$, $n = 4$, Control bars = ± 1 SE). Note that pressure measurements are always higher than the controls at the equivalent time period, though there are variations of these values with time after treatment.

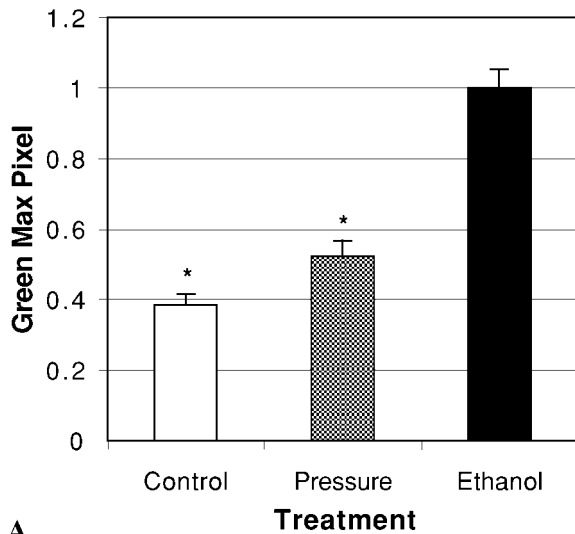
intensity levels were also increased at the later timepoints, for both pressure and negative control neurons. Positive control data was similarly greater than in other groups.

PC12 differentiated neurons had increased cell surface areas, compared with rounded undifferentiated PC12 cells, and expressed neurites. Results for differentiated PC12 neurons show a similar pattern of increased apoptosis after elevated pressure. Figure 6 shows GI TUNEL data for a single PC12 run normalized against the maximal apoptosis control of DNase treatment. Apoptosis marker intensities for neurons subjected to pressure conditions were higher than comparable controls at all timepoints, with significance at 24 hr ($P < 0.05$, $n = 4$). Pooled TUNEL data for all PC12 experiments was also normalized to positive DNase control (Fig. 7). In these post-mitotic neurons the effect was statistically significant at 24 hr. GI and GMP data showed greater levels of apoptosis marker intensity for pressure treated neurons compared to controls (significance $P < 0.05$, $n = 11$).

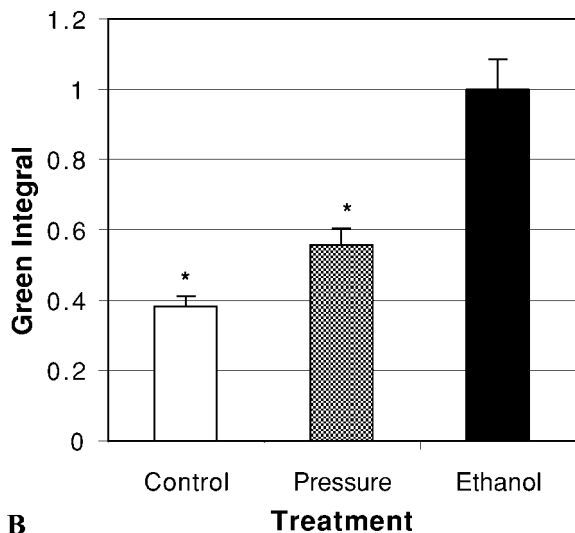
DISCUSSION

This study subjected neuronal cell lines to raised pressures and durations similar to those found in acute glaucoma, and found an increase in neuronal apoptosis under these conditions. This effect was noted in both proliferative B35 cells and in differentiated post-mitotic PC12 neurons. Apoptosis was confirmed qualitatively by cell morphology analysis and quantitatively by two separate specific markers of apoptosis. Laser scanning cytometry also allowed quantitative analysis of the fluorescent labels. These results support earlier findings using this experimental model and bioassay (Agar et al., 1999).

Increased ambient hydrostatic pressure of a defined incubation gas mix (5% CO₂ and air) on a liquid phase culture media could alter partial pressures of the vital gases O₂ and CO₂, and through dissolved CO₂ on pH, poten-



A



B

Fig. 4. Apoptosis in B35 neurons after 2 hr as measured by TUNEL using the LSC. An increase in apoptosis in neuronal cultures subjected to elevated pressure relative to control neurons is shown for both measures of quantitative fluorescence green integral (A) and green max pixel (B). Data is the mean of 7 separate experiments, normalized to average value for positive (ethanol) control. Significance of differences for green integral: $P = 0.005$ and green max pixel: $P < 0.05$, ($n = 24$, Scale bars = ± 1 SE).

tially affecting neuronal viability. Our experiments showed no significant difference in pH or the vital gases in cultures subjected to pressure compared to controls. It therefore seems that the experimental protocol did not significantly alter gas relationships of the neuronal cultures. With other parameters constant, this suggests any effects noted in cultured neurons were attributable primarily to the altered pressure conditions. Our findings agree with studies using similar pressure chamber designs with other cell types showing a negligible impact on gas relationships of culture media (Sumpio et al., 1994; Kosnosky et al.,

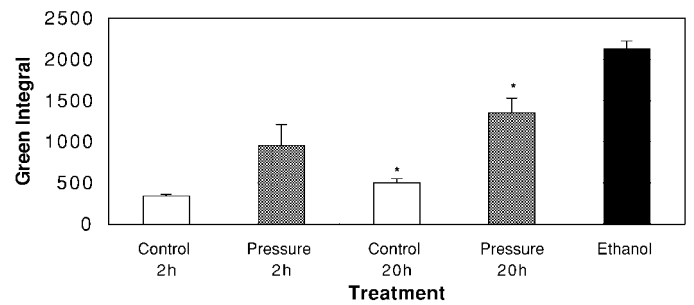


Fig. 5. Annexin V apoptosis assay of B35 neuronal cultures over time after ethanol, pressure and control treatments. Findings for single experimental run show increased apoptosis for both early (2 hr) and late (20 hr) timepoints in neurons subjected to pressure conditions compared to controls. Positive control for maximal apoptosis induction for experiment was 5% ethanol treatment for 2 hr. Differences significant at 20 hr ($P < 0.05$, Scale bars = ± 1 SE). Quantitative LSC data displayed for green integral (averaged label fluorescence for cell) absolute values for single experiment of 4 measurements.

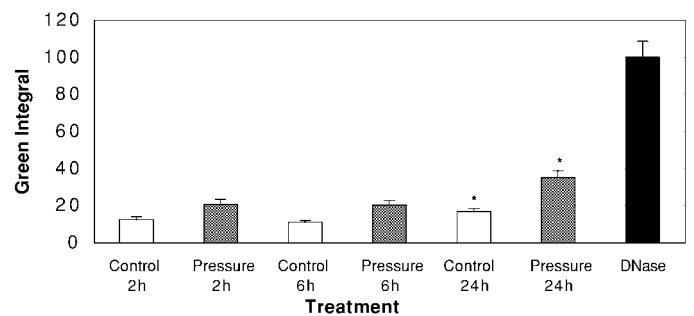


Fig. 6. Apoptosis in differentiated PC12 neurons after control, pressure and DNase treatment. LSC TUNEL data for single experimental run normalized to average positive control for that run (DNase treatment for 25 min to generate maximum detected apoptosis). Greater apoptosis marker labeling of neurons subjected to pressure conditions in comparison to control neurons significant at 24 hr ($P < 0.05$, $n = 4$, Scale bars = ± 1 SE). TUNEL values for pressure treated neurons are always higher than equivalent controls, with the difference increasingly apparent with time after treatment.

1995; Mattana and Singhal 1995; Qian et al., 1999). Relatively small variations of pH, pCO_2 and O_2 have been noted but were not considered to have affected viability in endothelial cells (Sumpio et al., 1994). Other studies on mesangial cells found small but statistically significant changes in pCO_2 and pH, but none in pO_2 . A series of experiments were then run with culture media adjusted to various pH levels to assess the impact of this effect on cell viability, with no significant effect found (Mattana and Singhal, 1995).

Our assay techniques using morphology and apoptotic markers all indicated that cell death after experimental pressure conditions occurred by apoptosis. Apoptosis is an active and physiological mode of cell death characterized by a series of morphological and molecular events, that can be detected by a variety of techniques. It is increasingly

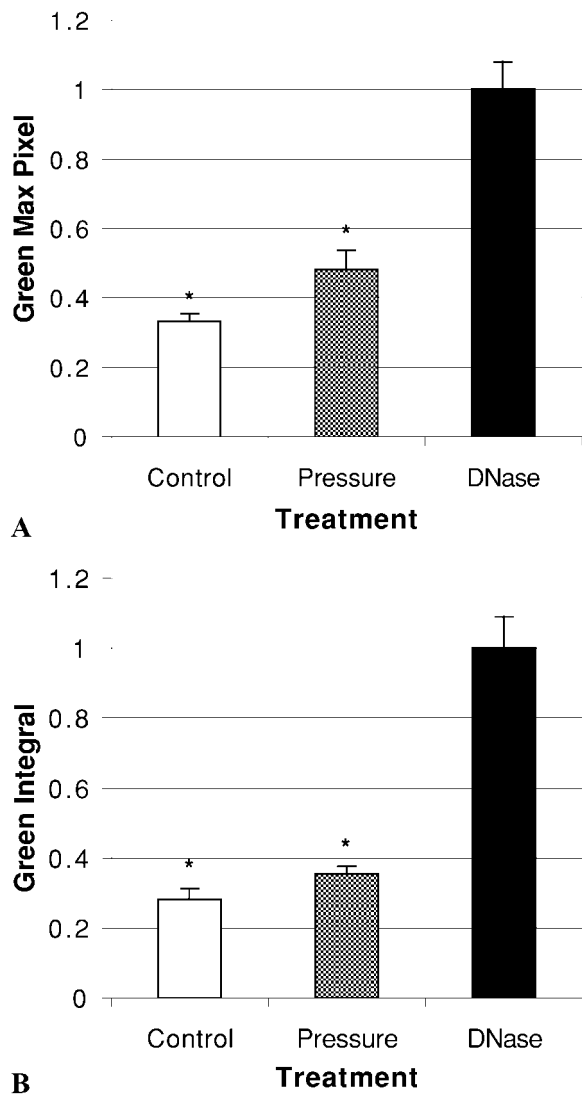


Fig. 7. Increased apoptosis in differentiated PC12 neurons 24 hr after treatment with elevated pressure, compared to controls. Quantitative analysis of TUNEL as measured by LSC. Both measures of fluorescence, green integral (**A**) and green max pixel (**B**), show significance differences $P < 0.05$, ($n = 11$, Scale bars = ± 1 SE). Data is the mean of 3 separate experiments, normalized to average value for positive (DNase) control.

apparent that no single method can be reliably used to identify apoptosis. Rather, the use of more than one technique, ideally based on different detection principles, is likely to distinguish apoptotic cells (Darzynkiewicz et al., 1998). The approach used in this study combines morphology, molecular markers of nuclear fragmentation (TUNEL) and membrane alterations (Annexin V) to optimize apoptosis detection. Several factors may confound the observations made in this study. Cells could be at different stages of apoptosis and may not exhibit all the features (morphological or molecular) of this process. TUNEL may also stain necrotic cells, though relatively

infrequently. Annexin V in conjunction with PI can distinguish the two modes of cell death in live cells more accurately, but this is less reliable in the late stages of apoptosis. The combination here of multiple techniques should enhance the sensitivity of apoptosis detection and also improve its accuracy.

This study also establishes the Laser Scanning Cytometer as an efficient bioassay tool for apoptosis in neurons. The LSCs automation minimizes potential observer influence on data collection and analysis; data can be normalized between separate pressure runs using a positive control; and storing of vectored data in relation to each scanned cell allows results to be confirmed by visual, and hence morphological, analysis. Results for positive control cells subjected to a known stimulus show much greater labeling for TUNEL (ethanol and DNase stimuli) and Annexin V (ethanol). Combined with morphological findings, they suggest the experimental protocol was able to detect apoptotic neurons. We detected a background level of apoptosis occurring in control B35 and PC12 neurons. It would be expected that this would apply to all experimental groups equally, as the cells used are from the same populations and identical.

Data for B35 cultures showed increased TUNEL labeling was statistically significant at the 2 hr timepoint, i.e., after application of pressure conditions. Later results were more varied and not conclusive after further statistical analysis. In view of a consistently significant difference for the initial timepoint alone, the neuronal effect may be temporally related to application of pressure if this is a factor in triggering apoptosis. Any effect then, if present, would be expected to be maximal closer to the time of the stimulus relative to a more remote period. Our early work with the Annexin V assay confirms similar results to the TUNEL data with greater apoptosis in pressure treated cells compared to controls. Differentiated PC12 neurons subject to pressure treatment were also found to have increased apoptosis labeling compared to controls, significant 24 hr after the initiation of pressure treatment. Differentiated PC12 neurons have been previously shown to undergo apoptosis upon withdrawal of growth factors (Michel et al., 1995; Oberdoerster et al., 1998, 1999). In our current study all PC12 cells were maintained in growth factors at all times.

Interestingly the B35 neurons seem to have an early pressure induced apoptosis response whereas the PC12 neurons respond later. At this point we suggest there may be two possibilities to help explain this difference in timecourse. The variation could be due to the cell type, or more likely may relate to the proliferative state of B35 cells versus the post-mitotic PC12 cells. The B35 cells in this study were not cell cycle synchronized, and therefore at all stages of the cell cycle, that may help explain the variable results at later timepoints. Perhaps the pressure conditions in this current study selectively affected a specific phase of the cell cycle early, with the remaining population less susceptible thereafter. Studies on lymphoblast cultures have reported pressure induced apoptosis and necrosis to be accelerated in the S phase of the cell

cycle (Takano et al., 1997). PC12 cells, on the other hand, were induced to differentiate to a post-mitotic state. Having exited the cell cycle they may demonstrate a differing response to the extracellular stimulus of elevated pressure. Post-mitotic PC12 neurons behave differently with other apoptotic stimuli, even when compared to their undifferentiated state. Other studies have shown undifferentiated (proliferative) cells to be more sensitive to an apoptotic stimulus, as we found for the B35 cells, than post-mitotic neurons (Oberdoerster et al., 1999). Our finding of significant apoptosis induction in differentiated PC12 neurons at the later timepoint (24 hr) is also the same as found in this other study using the same cells (Oberdoerster et al., 1999).

Apoptotic stimuli are varied and include internal and external activators, trophic factor deprivation and cellular damage. Physical stimuli can also induce apoptosis. Irradiation with UV light, for example, mediates apoptotic nuclear strand cleavage (Buja et al., 1993). We know little, however, about pressure acts as an apoptotic stimulus. In vivo research into heart failure has found pressure overload to induce apoptosis in animals (Teiger et al., 1996) and humans (Olivetti et al., 1996). A study into neural cell cultures and physical stressors in relation to glaucoma found mechanical shear to induce apoptosis (Edwards et al., 1998). In comparison, extremely high hydrostatic pressure (non-physiological) can induce apoptosis and necrosis in human lymphoblasts (Takano et al., 1997). Our current study indicates physiological changes in hydrostatic pressure may also stimulate neural apoptosis. We believe this is the first study of the effect on neurons of clinically relevant raised hydrostatic pressures alone, and to demonstrate apoptosis related to these pressure conditions. In addition to the broad range of known triggers for apoptosis, we suggest pressure may also be included as potential activators of apoptotic pathways.

The mechanisms that may mediate such a stimulus remain unclear. The cell cycle stage may be relevant, as suggested by our data and alluded to by other studies (Takano et al., 1997; Oberdoerster et al., 1999). Apoptosis in the neuronal study involving mechanical shear was associated with an increase in NO production and G protein activation (Edwards et al., 1998). Cellular responses to pressure other than apoptosis also provide clues to potential mechanisms. Cell cultures subject to similar pressure models to that used in this study reveal enhanced cell proliferation and modification of protein expression (Mattana and Singhal, 1995). This suggests cytoskeletal proteins may be subject to modulation by ambient pressure, consistent with tension-rigidity models of cell structure where such proteins contribute to and may therefore mediate physical force transfers (Wang et al., 1993). Such a concept is supported by findings of morphological responses to pressure (Sumpio et al., 1994). If neuronal compression is significant in our work, it is unclear whether the stimulus is related to compression or decompression or the static period of elevated pressure. Further, we do not know how the rates and durations of these changes affect the neuronal response. This first study using our model dealt with a specific set of experimental variables, and has found an effect related to these pressure conditions. Subsequent work will

allow evaluation of the basic parameters involved in pressure induced apoptosis, such as the rate of change and response threshold of the pressure stimulus.

Apoptosis may be stimulated by a sensitivity of the cell membrane to pressure changes. How pressure alterations are detected, let alone the mechanism of conversion of this into intercellular responses, is yet to be resolved. Hydrostatic pressure has been shown to influence transmembrane ion fluxes (Goldinger et al., 1980) and membrane receptor and protein activity, including the crucial Na-K-ATPase pump (Somero 1991). Pressure has been found to decrease spinal cord transmitter release (Gilman et al., 1987) and affect Ca^{2+} currents in chromaffin cells (Heinemann et al., 1987). Neuronal electrophysiological activity can also vary with pressure. Depression of near threshold orthodromic responses has been postulated to be due to a direct effect of high pressures on the conductance of specific K^{+} channels (Southan and Wann, 1996).

The possibility that pressure may be related to apoptosis is an interesting concept. At the cellular level there could be a greater sensitivity to this physical variable than previously thought. Because there seem to be a variety of cellular processes already shown to be modulated by pressure, it is not unreasonable to also consider apoptosis as an endpoint. This is of relevance in a disease such as glaucoma where neuronal apoptosis is somehow associated with an environment of altered pressure conditions. In addition to the known macroscopic anatomical and circulatory pathophysiology of glaucoma, this concept suggests retinal ganglion cells may be susceptible to elevated pressure at the cellular level. A neuronal response may be mediated by a more direct exposure to elevated pressure. Indeed large neurons, in the retina (RGC), cerebellum (Purkinje), and spinal cord (motor neurons) all seem to respond differently (usually more sensitive) to physiological stressors compared with smaller neurons.

We have shown a pressure stimulus to have an effect on apoptosis in more than one cell line, and in proliferating as well as post-mitotic neurons. The differentiated PC12 neurons have exited the cell cycle, as is the case in vivo for retinal neurons, including RGCs. Future work on the response of primary cultures to pressure would help broaden the relevance to disease processes. The potential activation of an apoptotic pathway also requires exploration to understand the conversion of this physical stimulus to a biological outcome. Both molecular and genetic processes, such as signal transduction and analysis of protein and mRNA or DNA expression, can be studied using this bioassay.

This study is the first to demonstrate in a biological assay system that physiologically relevant levels of pressure may have an impact on neuronal survival. This also suggests that conditions of elevated hydrostatic pressure, such as those found in acute glaucoma, may stimulate apoptosis. We would also suggest the possibility that raised hydrostatic pressures associated with other neural diseases, or after trauma, could induce neuronal apoptosis. The specific mechanism of pressure activation of this apoptotic pathway is not known at present. This system now allows

us to further investigate a number of other variables including different neurons and the basic parameters of the pressure stimulus. We can also study pharmacological and genetic factors that may support neuronal survival after these pressure conditions.

ACKNOWLEDGMENTS

The authors wish to thank Dr. Stephanie Watson (Dept. Ophthalmology, Prince of Wales Hospital) for invaluable guidance in developing this model system; Prof. R. Frost (Dept. Mechanical Engineering, University of New South Wales) for assistance in designing the pressure chambers; Prof. M. Perry and Amanda Marsh (Dept. Physiology, University of New South Wales) for help in assessing our system; Ms. Moya Seeto (Cell Biology Lab) for extensive technical assistance; and Mr. Rob Wadley (Cellular Analysis Facility, University of New South Wales) for generous support with the Laser Scanning Cytometer. This study was supported in part by a discretionary general grant from Allergan Australia.

REFERENCES

- Agar A, Hill M, Coroneo MT. 1999. Pressure induced apoptosis in neurons [ARVO Abstract]. *Invest Ophthalmol Vis Sci* 40:S265.
- Armaly MF, Krueger DE, Maunder L, Becker B, Hetherington J, Jr., Kolker AE, Levene RZ, Maumenee AE, Pollack IP, Shaffer RN. 1980. Biostatistical analysis of the collaborative glaucoma study. I. Summary report of the risk factors for glaucomatous visual-field defects. *Arch Ophthalmol* 98:2163–2171.
- Ben-Sasson SA, Sherman Y, Gavrieli Y. 1995. Identification of dying cells—in situ staining *Methods Cell Biol* 46:29–39.
- Buja LM, Eigenbrodt ML, Eigenbrodt EH. 1993. Apoptosis and necrosis. Basic types and mechanisms of cell death. *Arch Pathol Lab Med* 117:1208–1214.
- Darzynkiewicz Z, Bedner E, Traganos F, Murakami T. 1998. Critical aspects in the analysis of apoptosis and necrosis. *Hum Cell* 11:3–12.
- De A, Boyadjieva NI, Pastorcic M, Reddy BV, Sarkar DK. 1994. Cyclic AMP and ethanol interact to control apoptosis and differentiation in hypothalamic beta-endorphin neurons. *J Biol Chem* 269:26697–26705.
- Edwards ME, Chiou GCY, Good TA. 1998. Biomechanical force mediated G-protein activation and RGC apoptosis [ARVO Abstract]. *Invest Ophthalmol Vis Sci* 39:S916.
- Fagiolini M, Caleo M, Strettoi E, Maffei L. 1997. Axonal transport blockade in the neonatal rat optic nerve induces limited retinal ganglion cell death. *J Neurosci* 17:7045–7052.
- Gilman SC, Colton JS, Dutka AJ. 1987. Effect of pressure on the release of radioactive glycine and gamma-aminobutyric acid from spinal cord synaptosomes. *J Neurochem* 49:1571–1578.
- Goldinger JM, Kang BS, Choo YE, Paganelli CV, Hong SK. 1980. Effect of hydrostatic pressure on ion transport and metabolism in human erythrocytes. *J Appl Physiol* 49:224–231.
- Greene LA, Tischler AS. 1976. Establishment of a noradrenergic clonal line of rat adrenal pheochromocytoma cells which respond to nerve growth factor. *Proc Natl Acad Sci USA* 73:2424–2428.
- Heinemann SH, Conti F, Stuhmer W, Neher E. 1987. Effects of hydrostatic pressure on membrane processes. Sodium channels, calcium channels, and exocytosis. *J Gen Physiol* 90:765–778.
- Johansson JO. 1983. Inhibition of retrograde axoplasmic transport in rat optic nerve by increased IOP in vitro. *Invest Ophthalmol Vis Sci* 24:1552–1558.
- Johansson JO. 1988. Inhibition and recovery of retrograde axoplasmic transport in rat optic nerve during and after elevated IOP in vivo. *Exp Eye Res* 46:223–227.
- Kerrigan LA, Zack DJ, Quigley HA, Smith SD, Pease ME. 1997. TUNEL-positive ganglion cells in human primary open-angle glaucoma. *Arch Ophthalmol* 115:1031–1035.
- Kosnosky W, Tripathi BJ, Tripathi RC. 1995. An in vitro system for studying pressure effects on growth, morphology and biochemical aspects of trabecular meshwork cells. *Invest Ophthalmol Vis Sci* 36:8731.
- Majno G, Joris I. 1995. Apoptosis, oncosis, and necrosis. An overview of cell death. *Am J Pathol* 146:3–15.
- Mattana J, Sankaran RT, Singhal PC. 1996. Increased applied pressure enhances the uptake of IgG complexes by macrophages. *Pathobiology* 64:40–45.
- Mattana J, Singhal PC. 1995. Applied pressure modulates mesangial cell proliferation and matrix synthesis. *Am J Hypertens* 8:1112–1120.
- Michel PP, Vyas S, Agid Y. 1995. Synergistic differentiation by chronic exposure to cyclic AMP and nerve growth factor renders rat pheochromocytoma PC12 cells totally dependent upon trophic support for survival. *Eur J Neurosci* 7:251–260.
- Mizushima T, Tsutsumi S, Rokutan K, Tsuchiya T. 1999. Suppression of ethanol-induced apoptotic DNA fragmentation by geranylgeranylacetone in cultured guinea pig gastric mucosal cells. *Dig Dis Sci* 44:510–514.
- Nickells RW. 1996. Retinal ganglion cell death in glaucoma: the how, the why, and the maybe. *J Glaucoma* 5:345–356.
- Oberdoerster J, Kamer AR, Rabin RA. 1998. Differential effect of ethanol on PC12 cell death. *J Pharmacol Exp Ther* 287:359–365.
- Oberdoerster J, Rabin RA. 1999. NGF-differentiated and undifferentiated PC12 cells vary in induction of apoptosis by ethanol. *Life Sci* 64:PL267–272.
- Olivetti G, Quaini F, Sala R, Lagrasta C, Corradi D, Bonacina E, Gambert SR, Cigola E, Anversa P. 1996. Acute myocardial infarction in humans is associated with activation of programmed myocyte cell death in the surviving portion of the heart. *J Mol Cell Cardiol* 28:2005–2016.
- Qian Y, Tripathi BJ, Tripathi RC. 1999. Short-term elevation of hydrostatic pressure reduces TGF-beta 2 secretion and has no effect on the level of fibronectin in trabecular cells [ARVO Abstract]. *Invest Ophthalmol Vis Sci* 40:S668.
- Quigley HA. 1995. Ganglion cell death in glaucoma: pathology recapitulates ontogeny. *Aust N Z J Ophthalmol*. 23:85–91.
- Radius RL. 1981. Rapid axonal transport in primate optic nerve. *Arch Ophthalmol* 99:650–654.
- Schubert D. 1974. Induced differentiation of clonal rat nerve and glial cells. *Neurobiology* 4:376–387.
- Schutte B, Nuydens R, Geerts H, Ramaekers F. 1998. Annexin V binding assay as a tool to measure apoptosis in differentiated neuronal cells. *J Neurosci Methods* 86:63–69.
- Somero GN. 1991. Hydrostatic pressure and adaptation to the deep sea. New York: Wiley-Liss 167–204.
- Southan AP, Wann KT. 1996. Effects of high helium pressure on intracellular and field potential responses in the CA1 region of the in vitro rat hippocampus. *Eur J Neurosci* 8:2571–2581.
- Sumpio BE, Widmann MD, Ricotta J, Awolesi MA, Watase M. 1994. Increased ambient pressure stimulates proliferation and morphologic changes in cultured endothelial cells. *J Cell Physiol* 158:133–139.
- Takano KJ, Takano T, Yamanouchi Y, Satou T. 1997. Pressure-induced apoptosis in human lymphoblasts. *Exp Cell Res* 235:155–160.
- Teiger E, Than VD, Richard L, Wisnewsky C, Tea BS, Gaboury L, Tremblay J, Schwartz K, Hamet P. 1996. Apoptosis in pressure overload-induced heart hypertrophy in the rat. *J Clin Invest* 97:2891–2897.
- van Engeland M, Ramaekers FC, Schutte B, Reutelingsperger CP. 1996. A novel assay to measure loss of plasma membrane asymmetry during apoptosis of adherent cells in culture. *Cytometry* 24:131–139.
- Wang N, Butler JP, Ingber DE. 1993. Mechanotransduction across the cell surface and through the cytoskeleton. *Science* 260:1124–1127.
- Weber AJ, Kaufman PL, Hubbard WC. 1998. Morphology of single ganglion cells in the glaucomatous primate retina. *Invest Ophthalmol Vis Sci*. 39:2304–2320.

available at www.sciencedirect.comwww.elsevier.com/locate/brainres

**BRAIN
RESEARCH**

Research Report
Retinal ganglion cell line apoptosis induced by hydrostatic pressure
Ashish Agar^{a,b}, Shaojuan Li^a, Neeraj Agarwal^c, Minas T. Coroneo^b, Mark A. Hill^{a,*}
^aCell Biology Laboratory, School of Anatomy, University of New South Wales, Sydney, NSW, Australia^bDepartment of Ophthalmology, Prince of Wales Hospital, University of New South Wales, Sydney, NSW, Australia^cDepartment of Cell Biology and Genetics, University of North Texas Health Sciences Center, Fort Worth, TX 76107, USA

ARTICLE INFO
Article history:

Accepted 13 February 2006

Available online 25 April 2006

Keywords:

Pressure chamber

Glaucoma

Neuronal cell line

Laser scanning cytometer

Abbreviations:

IOP, intra-ocular pressure

LSC, laser scanning cytometer

RGC, retinal ganglion cell

TUNEL, Terminal transferase dUTP

Nick-End Labeling

ABSTRACT

Cellular responses to changes in pressure are implicated in numerous disease processes. In glaucoma apoptosis of retinal ganglion cells (RGCs) is associated with elevated intra-ocular pressure, however, the exact cellular mechanisms remain unclear. We have previously shown that pressure can induce apoptosis in B35 and PC12 neuronal cell lines, using an in vitro model for pressure elevation. A novel RGC line allows us to study the effects of pressure on retinal neurons. 'RGC-5' cultures were subjected to elevated ambient hydrostatic pressure conditions in our model. Experimental pressure conditions were 100mm Hg and 30mm Hg, representing acute (high) and chronic (lower-pressure) glaucoma, and 15mm Hg for normal intra-ocular pressure, set above atmospheric pressure for 2h. Negative controls were treated identically except for the application of pressure, while positive controls were generated by treatment with a known apoptotic stimulus. Apoptosis was determined by a combination of cell morphology and specific TUNEL and Annexin V fluorescent markers. These were assessed simultaneously by laser scanning cytometry (LSC), which also enabled quantitative marker analysis. RGC-5 neurons showed a significantly increased proportion of apoptotic cells compared with controls; maximal at 100mm Hg, moderate at 30mm Hg and not statistically significant at 15mm Hg. This graded response, proportionate to the level of pressure elevation, is representative of the severity of analogous clinical settings (acute, chronic glaucoma and normal). These results complement earlier findings of pressure-induced apoptosis in other neuronal cultures. They suggest the possibility of novel mechanisms of pressure-related mechanotransduction and cell death, relevant to the pathogenesis of diseases such as glaucoma.

© 2006 Elsevier B.V. All rights reserved.

1. Introduction

A crucial component of the cell's environment is pressure, which can have a major impact on cell function and viability. This is evident in pathologies that are linked to changes in the pressure states of biological systems. In the eye, elevated pressure is associated with the optic neuropathy glaucoma

and leads to the death of RGC neurons. This intra-ocular pressure (IOP), which can be raised acutely or chronically, is the single most important association of this potentially blinding disease (Armaly et al., 1980). Yet this physical variable remains one of the least understood in terms of disease pathogenesis, even in well-known conditions such as glaucoma. This is especially true at the cellular and subcellular level.

* Corresponding author. Fax: +61 2 9385 8016.

E-mail address: m.hill@unsw.edu.au (M.A. Hill).

The loss of RGCs in glaucoma is believed to occur by apoptosis. This autonomous form of cell death has distinct morphological features, involves a programmed series of molecular events genetically controlled by the affected cell, and can be triggered by various stimuli (Wyllie et al., 1980). Apoptosis of RGCs in glaucoma has been demonstrated in vivo in several animal models and in humans (Garcia-Valenzuela et al., 1995; Tatton et al., 2001). The mechanisms of cell death in glaucoma, and in particular how elevated IOP leads to RGC apoptosis, are yet to be fully elucidated (Nickells, 1999; Osborne et al., 1999). Significant contributors are known to be mechanical compression at the optic nerve head inhibiting axonal transport and/or producing ischemia (Quigley, 1999). However, research has shown that neuronal loss may be autonomous of these factors (Johansson, 1988; Fagiolini et al., 1997; Radius, 1982). Current understanding views glaucoma pathogenesis as multifactorial, in line with many disease processes (Osborne et al., 1999). The RGC may also be susceptible to pressure by other means, including more direct effects or damage at the cell body (Levin, 2001; Caprioli, 1995).

We have shown previously for the first time that neurons may undergo apoptosis in direct response to increased pressures at clinically relevant levels (Agar et al., 1999). Cell cultures were subjected to elevated hydrostatic pressures in an in vitro system based on established pressure chamber models (Kosnosky et al., 1995; Mattana and Singhal, 1995). Pressure conditions of 100mm Hg were selected, analogous to levels seen in acute glaucoma. The neuronal lines studied, B35, PC12, C17 and NT2, however were not retinal neurons (Agar et al., 2000; Coroneo et al., 2001). To date, in vitro research on RGCs has relied on primary cultures. In addition, to the labor-intensive procedures involved and the rapid drop-off in viable RGCs, there is by nature significant variability between individual cultures (Barres et al., 1988; Takahashi et al., 1991). This poor reproducibility limits their use for assay-based models in particular.

The recent development of the RGC-5 neuronal line has overcome many of these hurdles. Derived from primary rat retinal cultures, this is a stable, permanently transformed RGC line, which has the potential to facilitate in vitro studies into RGC biology. Characterisation of these cells included: morphology, antigen markers such as RGC specific Thy-1 and neuronal markers, sensitivity to serum and neurotrophin withdrawal and sensitivity to glutamate excitotoxicity (Krishnamoorthy et al., 2001). Our group has also characterised membrane currents in the RGC-5 cell line (Moorhouse et al., 2004). The usefulness of this novel cell line has been demonstrated by research into several molecular triggers of apoptosis implicated in glaucoma. This work identified in vitro RGC-5 apoptosis mediated by interleukin-10, homocysteine and glutamate (Aoun et al., 2003; Boyd et al., 2003; Martin et al., 2004).

This study investigates the response of RGC-5 neurons to raised hydrostatic pressure with respect to apoptosis, extending the initial studies previously presented to the relevant ocular neuron and to a range of pressures. Experimental pressure conditions were selected to be relevant to intra-ocular pressures seen in clinical settings, with levels of 100mm Hg analogous to acute glaucoma, 30mm Hg for chronic glaucoma and 15mm Hg for the so-called 'normal' IOP. Apoptosis was assayed using a combination of morphology and specific fluorescent marker (TUNEL and Annexin V). These were

assessed concurrently by means of laser scanning cytometry (LSC, CompuCyte, Cambridge, MA), a microscope-based cytofluorometer. The LSC combines imaging analysis of adherent labelled neurons with the automated fluorochrome analysis once the domain of flow cytometry and has been shown to be uniquely suited to the analysis of apoptosis (Darzynkiewicz and Bedner, 2000).

2. Results

2.1. Morphological

RGC-5 neurons displayed characteristic features of apoptosis by visual inspection with phase contrast, fluorescent and confocal laser scanning microscopy. Necrosis was found not to be significant in all experimental cultures by vital dye staining with PI and fluorescent microscope analysis (data not shown). Morphological confirmation was obtained by inspection of randomly selected fields. Features including cell body and nuclear swelling, vacuolation and karyolysis that typify necrosis (Wyllie et al., 1980) were similarly negligible.

Apoptotic neurons were identified in several stages of apoptosis with cell shrinkage, retraction of neuronal processes, chromatin condensation, apoptotic body formation and cell membrane blebbing. Annexin V assays highlight cell membrane changes, including bleb formation, as shown in Fig. 1. Laser scanning microscopy at different levels of the cell allowed surface bleb formation to be well visualised as seen in Fig. 1C. Fig. 2 shows TUNEL-stained RGC-5 neurons demonstrating some of these features, in particular, the nuclear and cell shape morphology. The range of apoptosis stages was most readily seen in the pressure-treated neurons (30 and 100mm Hg), while more advanced apoptosis was especially evident in the positive control neurons that had been ethanol-treated (Fig. 2). Qualitatively, the proportion of apoptotic neurons was the clear majority in these positive control cultures. There were fewer apoptotic neurons in the normal pressure group (15mm Hg), and they were minimal in negative control cultures. The difference between pressure and control groups was subtle, however, hence conclusions on the basis of morphology alone were limited.

Positive morphology was correlated with fluorescent marker staining during this visual analysis. Concurrent imaging during LSC scanning demonstrated the presence of apoptotic changes in cells with green fluorescein positive nuclei. For example hyperfluorescence of condensed chromatin could be detected within the nucleus, and cytoplasmic features were enhanced on PI sensor settings. Spatial coordinates were recorded of imaged cells, and higher resolution images on confocal laser scanning microscopy revealed more detailed features including apoptotic bodies and membrane blebs.

2.2. Quantitative

Objective measurements of fluorescent apoptosis marker made by LSC were analyzed for the single cell population (see Fig. 3 for representative LSC data plot), and numerical data were pooled for all experiments. The results demonstrate differences in intensity and population data between the

assayed cell groups. We found high values for intensity parameters (GI, GMP) in the positive ethanol-treated control cultures. The proportion of the total RGC-5 population positive for apoptosis was similarly high, in the order of 80%. This was comparable across all experimental groups. Results for these conditions are shown as the pooled average for all experimental runs and hence were normalised for the study as a whole (Figs. 4, 5). These data correlated with the predominance of apoptotic features seen on morphology. Quantitative data thus suggest that the experiments were successful in

identifying and distinguishing cells undergoing apoptosis, validating the detection protocols.

Background apoptosis was determined in the negative control RGC-5 cultures. Intensity and population analysis showed significantly lower levels of apoptosis. Approximately 15–20% of neurons were apoptotic, and this was relatively consistent among experiments. This contrasted markedly with the positive controls and matched observations made on visual inspections.

Increased levels of apoptosis were found in the pressure group of RGC-5 cultures compared to the negative controls, by both intensity and population LSC TUNEL data. These levels were comparatively less than for corresponding positive controls. Qualitative morphological interpretations were also in general agreement with these findings. Data represented in Figs. 4 and 5 show pooled measurements averaged for each experimental pressure group. The relative increase in apoptosis in neurons subject to hydrostatic pressure elevation was greatest for the 100mm Hg 'high' pressure group, with approximately 40% of RGC-5 identified as apoptotic by TUNEL assay and a similar result by Annexin staining (Figs. 4, 5). The corresponding negative control, treated identically but for the application of pressure, had a significantly lower proportion ($P = 0.0009$, $n = 7$). Neurons exposed to 'low' pressure conditions of 30mm Hg for 2h also had a statistically significant difference in the apoptotic population (Fig. 4B). Here, 29% of neurons were positive for apoptosis, greater than their equivalent negative controls ($P = 0.0002$, $n = 12$). The third experimental pressure group underwent pressures of 15mm Hg, analogous to 'normal' IOP (Fig. 4C). Analysis revealed

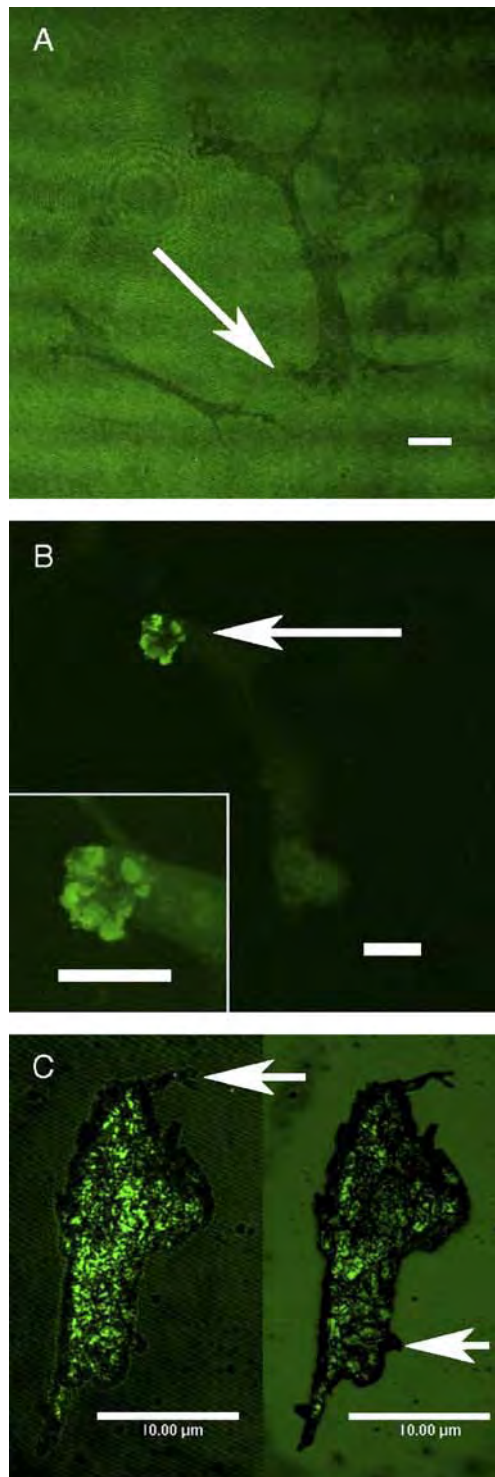


Fig. 1 – Morphological analysis by Annexin V assay. Confocal laser scanning microscope images of cultured RGC-5 neurons at control or pressure (100 mm Hg) experimental conditions. Cells stained with Annexin V assay for phosphatidylserine translocation to the external cell membrane. No significant PI staining was seen, and these images show FITC Annexin V label. Scale bar = 10 μ m. (A) Confocal slice taken at the level of the substrate demonstrating negative staining of control cells. No apoptotic marker fluorescence was identified on the cells, hence morphology is most clearly seen at this level by contrasting with surrounding substrate stain. The RGC-5 neurons show normal morphology with dendritic processes in particular clearly seen (arrow). (B) RGC-5 neurons exposed to pressure conditions, an apoptotic neuron (arrow) is shown with intense Annexin V fluorescein. An unaffected cell (no Annexin staining) is located at the lower right of the image. Inset shows detail of apoptotic neuron, shrunken with blebbed membrane. (C) RGC-5 neuron subject to pressure conditions, showing details of early apoptotic cell morphology. Confocal cell slices taken at a superficial (left image) and deeper substrate (right image) level. Surface membrane morphology, including bleb and vacuole formation, can be seen in each image as well as their relative locations by comparing the two images. Phosphatidylserine externalisation is readily visible in the superficial (left) image, outlining the whole cell membrane, which also demonstrates various stages of process retraction as well as membrane blebbing (arrows).

higher levels of apoptosis than in negative controls, at 21%, but this was of poor statistical significance ($P = 0.08$, $n = 7$).

3. Discussion

This research found increased levels of apoptosis in RGC-5 neurons exposed to elevated hydrostatic pressure conditions relevant to acute and chronic glaucoma. The proportion of

apoptotic neurons was significantly higher compared to matched controls, and greater for 100mm Hg than 30mm Hg. Pressures analogous to 'normal' IOP of 15mm Hg showed some increase in apoptosis, but this was not statistically significant. These results complement data from other neuronal lines studied in this model at 'acute' pressures (Agar et al., 2000; Coroneo et al., 2001). The RGC-5 line was further shown to be a useful tool for investigating RGC pathology in vitro, and in experimental assays in particular (Aoun et al., 2003; Boyd et al., 2003; Martin et al., 2004).

The assay used a combination of morphological and immunofluorescent features and confirmed observed cell death to be due to apoptosis. The detection of apoptosis in this assay can be complicated by several factors. RGC-5 cells may not show all the features of apoptosis examined if they were at differing stages of this multi-step process. Necrotic cells can also have strand breaks which could show TUNEL positivity, but they are an order of magnitude fewer and are randomly sized in contrast to the 180bp multiples generated in apoptotic cells (Schmid et al., 1992). Annexin V phosphatidyl translocation can also occur with necrotic cells, but PI vital dye staining confirmed that this was not significant. To maximise reliability, assessment of apoptosis should rely on more than one method, ideally based on different principles of detection (Darzynkiewicz et al., 1998).

The LSC's capacity to visualise adherent cells such as neurons for morphology enables subjective analysis, while automated cytometry minimises observer bias. Fluorescent marker intensity values for TUNEL assays reflect morphological apoptotic features and are a reliable indicator of apoptosis as measured by LSC (Darzynkiewicz et al., 1998). However, fluorochrome intensity can vary due to laser scatter and staining. Population analysis integrates intensity data which are gated and averaged at the outset, minimising the

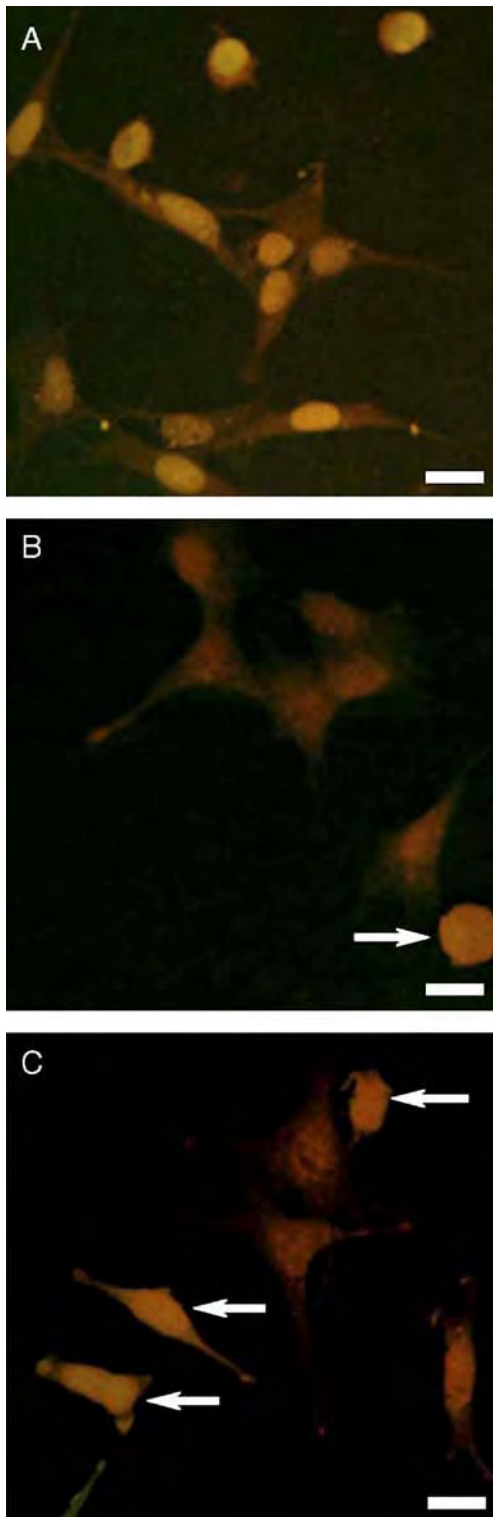


Fig. 2 – Morphological analysis by TUNEL assay. Representative confocal laser scanning microscope images of cultured RGC-5 neurons following various experimental conditions. Cells stained with TUNEL assay for DNA fragmentation show yellow–green nuclear fluorescence as a marker of apoptosis. Red counterstain is with propidium iodide. Scale bar = 10 μm . (A) Positive control RGC-5 culture treated with ethanol to induce maximal apoptosis. The majority of cells show distinctive and strong nuclear TUNEL staining. Morphologically various stages of apoptosis are seen, with uppermost neurons demonstrating more advanced features of loss of processes and membrane blebbing. (B) Negative control neurons subject to identical conditions as experimental group but without elevation of pressure. Most cells show relatively normal morphology and no TUNEL positive nuclear staining. Single apoptotic cell (arrow) seen in this field displays nuclear and morphological features. (C) RGC-5 neurons exposed to elevated ambient hydrostatic pressure (30mm Hg). Level of apoptosis is less than in ethanol positive controls in panel (A). Some cells also demonstrate apoptotic morphology. However, an increased proportion of cells with DNA fragmentation as detected by TUNEL assay fluorochrome (arrows) is seen in comparison to negative control group in panel (B).

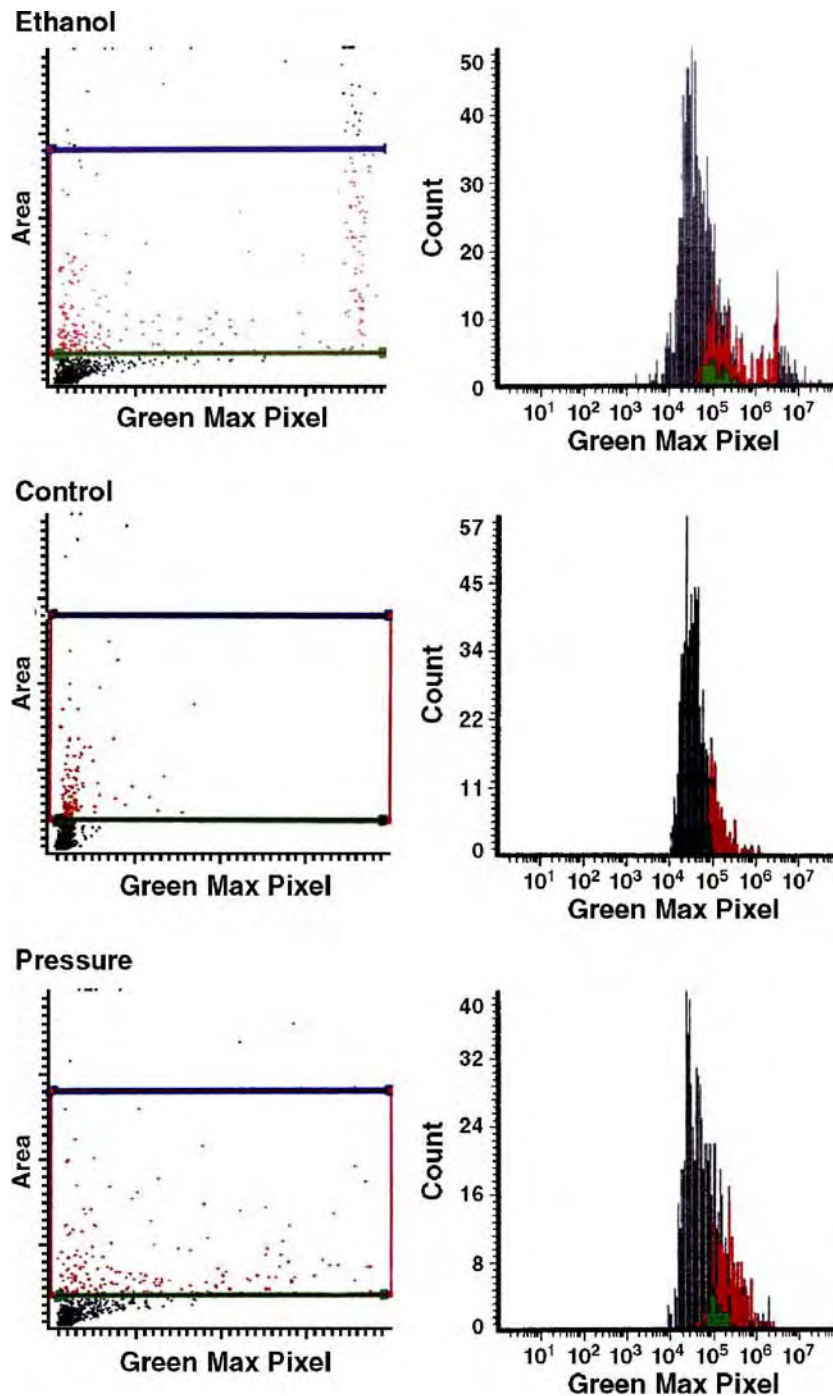


Fig. 3 – Laser scanning cytometer quantitative analysis. Laser scanning cytometer (LSC) quantitative analysis of cultured neuronal RGC-5 cells, labelled by TUNEL fluorescent apoptosis marker. Representative data for single scan. Dot-plot graphs show individual neuronal values for the peak fluorescence of a scanned cell (Green Max Pixel), and cell fluorescent area. The 'Area' combined with visualisation of scanned cells is used for selection of a single cell population (rectangular window within graph). Histograms show cell counts of corresponding graph. Note very high levels of apoptosis in ethanol-treated neurons, and high values in neurons subject to pressure, compared to control neurons, reflected in corresponding population distributions.

impact of such variations. The uniformly high level of apoptosis in the positive controls (>80%) suggests that the assay can reliably detect apoptotic RGC-5 neurons and confirms the LSC as a uniquely useful tool for studying apoptosis (Darzynkiewicz and Bedner, 2000).

Data showed background levels of apoptosis in all experimental conditions, as indicated by the negative control group. These results were higher than expected, which may reflect specific and as yet undetermined features of this RGC-5 line. It should be noted that this is a transformed line and may have

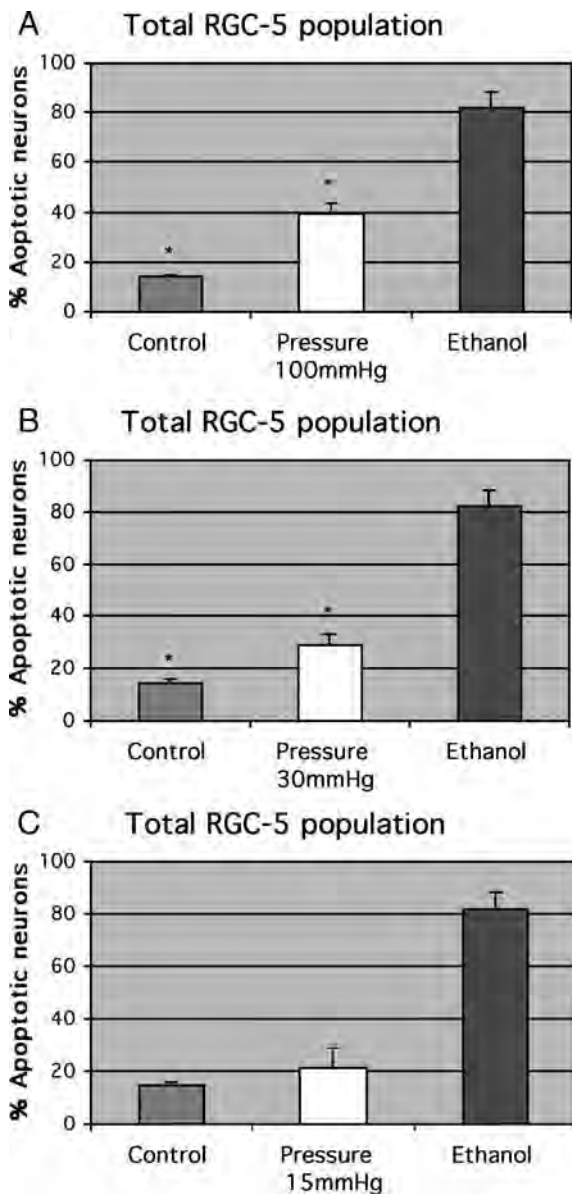


Fig. 4 – Quantitative analysis of TUNEL assay. Graph of apoptosis data pooled for RGC-5 cultures subject to experimental pressure conditions. Bars show apoptotic proportion of total neuronal population, assayed for TUNEL staining and quantified by analysis of LSC data. Note very high levels in ‘Ethanol’ group, reflecting nature of positive control treatment. Negative ‘Control’ group displayed low levels of apoptosis. Analysis of *P* values by Student’s paired *t* test, with asterisks representing statistically significant difference between pressure group and negative controls. (A) Cultures subjected to conditions of hydrostatic pressure elevation levels of 100mm Hg demonstrated significantly greater proportions of apoptosis compared to controls ($n = 7, P = 0.0002$). (B) RGC-5 neurons in the 30mm Hg pressure group also experienced increased levels of apoptosis. Absolute values were less dramatic than for high pressure, but still of statistical significance ($n = 12, P = 0.009$). (C) Experimental level of 15 mm Hg chosen to represent intra-ocular pressure within normal range of clinical values. RGC-5 cultures undergoing this minimal pressure elevation did not demonstrate any statistically significantly increased level of apoptosis ($n = 7, P = 0.08$).

altered apoptotic machinery and therefore behave differently to primary RGCs. As the cells were derived from the same RGC-5 populations and passage, they should however be identical. This finding should then apply to all experimental groups equally, and data were consistent across the separate experimental runs.

Pressure-induced apoptosis in this study varied with the applied pressure. The greatest proportion of TUNEL and Annexin V positive cells was at ‘high’ hydrostatic pressure conditions of 100mm Hg, which at ~40% was almost 2.5 times the negative control level. The results for these late and early apoptosis mechanisms were comparable for all experimental groups, with good correlation by morphology as well as quantitative analysis. These findings also compare favorably with work on other neuronal lines exposed to these pressure conditions in our model. B35, PC12, NT2 and C17 neuronal cell cultures had 2 to 3 times greater levels of apoptosis induced by pressure (Agar et al., 2000; Coroneo et al., 2001). ‘Low’ settings of 30mm Hg induced ~30%, the 15mm Hg experiments ~20% apoptosis positive cells respectively. This was still greater than the comparable negative control ~15%, although the difference was not statistically significant.

The increase in induced apoptosis does not appear to bear a linear relationship to pressure, with relatively consistent changes in apoptosis corresponding to much greater changes in applied pressure conditions. The reasons for this are unclear; it may relate to the specific apoptotic mechanism triggered or be a characteristic of the transformed RGC-5 cell line itself. The graded response is however interesting in terms of the selected pressures. The ‘high’ pressure is analogous to pressures seen in clinical acute glaucoma; the ‘low’ to chronic glaucoma and the lowest pressures used approximate ‘normal’

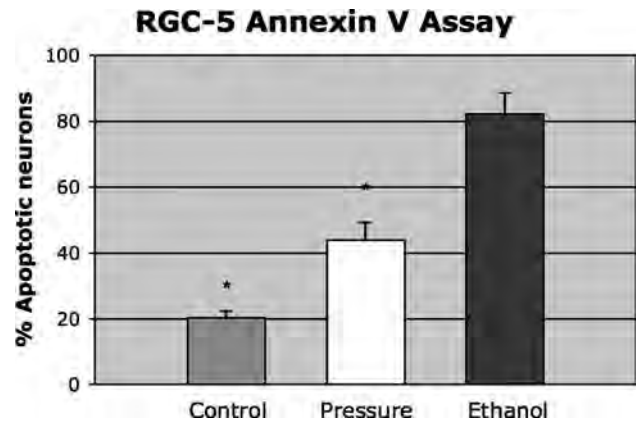


Fig. 5 – Quantitative analysis of Annexin V assay. RGC-5 culture data for neurons exposed to elevated hydrostatic pressure of 100mm Hg and assayed live for the Annexin V early apoptosis marker. Results are from quantitative analysis and represented as the apoptotic proportion of the total cell population. The apoptotic response was found to be similar to that observed in the TUNEL data in Fig. 4, with increased levels in pressurised neurons relative to negative controls and an equally high level of apoptosis detected in positive controls. Analysis of *P* values by Student’s paired *t* test, with asterisks representing statistically significant difference between pressure group and negative controls ($n = 5, P = 0.01$).

IOP. It should be added that RGC loss can occur in a subgroup of patients even at 15 mm Hg. These levels correlate broadly with the observed disease severity nonetheless.

Hydrostatic pressure is known to have an impact on various aspects of cellular anatomy and physiology. Morphological changes in cell shape, alignment and processes and cytoskeletal actin redistribution have been demonstrated in human ocular cells—astrocytes, lamina cribrosa glia and trabecular meshwork cells (Kosnosky et al., 1995; Wax et al., 2000; Kobayashi et al., 1997). Interestingly, peripheral nerve sensory block in carpal tunnel syndrome occurs at pressures of between 30 and 50 mm Hg (Gelberman et al., 1983). Apoptosis in cortical neurons has been found in vivo in research into high pressure neurological syndrome and cerebral trauma (Mennel et al., 1997; Runnerstam et al., 2001). In vitro work linking hydrostatic pressure directly with induced apoptosis has been described in vascular endothelial and smooth muscle cells, lymphoblasts and leukemia cells (Galea et al., 1999; Takano et al., 1997; Take et al., 2001).

However, very little is known regarding neuronal apoptosis and hydrostatic pressure as an isolated and independent stimulus. Since we first identified in vitro neuronal apoptosis directly induced by hydrostatic pressure, other researchers have used a similar pressure-chamber-based model and demonstrated apoptosis induced by pressures of 50 mm Hg in a co-culture of primary rat RGCs and glial cells (Tezel and Wax, 2000). Allowing for differences in cell type and the role of the glial cells, these data suggest similar outcomes to those we have demonstrated.

How the hydrostatic pressure stimulus induces apoptosis in RGC-5 neurons is uncertain. Various mechanisms have been proposed, but the process is not clearly understood. The results for an early (Annexin V) and a late apoptotic marker (TUNEL) correlated well with each other, suggesting a multifaceted process. The study on primary RGC cultures suggested TNF- and nitric-oxide-mediated apoptosis, however, these were derived from concurrent glial cultures and were hence not intrinsic to the RGCs (Tezel and Wax, 2000). Intracellular signalling pathways have been implicated in other ocular cells, where adenyl cyclase activity and G protein alterations were detected (Wax et al., 2000). Research into other pressure-related effects has shown modified gene expression and protein synthesis, reflecting the central role of the cytoskeleton in transducing pressure stimuli (Haskin et al., 1993).

Mechanisms that allow cells to sense pressure changes are also still largely unknown but are the focus of widespread research in the emerging field of mechanotransduction (Ko and McCulloch, 2000). Biomechanical modelling has emphasised the central role of pressure-related stress in glaucomatous damage using structural principles at the cellular level (Burgoyne et al., 2005). Pressure has been found to cause changes in trans-membrane ion fluxes, currents and subsequent downstream processes such as neural transmission (Southan and Wann, 1996; Parmentier et al., 1981). Membrane-bound mechanosensitive ion channels are gaining importance as integral to normal cell physiology and have been identified in astrocytes and found to be activated by just seconds of hydrostatic pressures of 45 mm Hg (Hamill and McBride, 1996; Islas et al., 1993). TRAAK is a novel two-pore mammalian K⁺ mechanosensitive channel that has been shown to be expressed in retinal tissues in both rat and human retina,

with localisation to RGCs (Maingret et al., 1999; Reyes et al., 2000; Edward and Ueda, 2001). We have reviewed these channels in the context of glaucoma pathogenesis (Kalapesi et al., 2005b; Tan et al., 2006) and recently have also identified this channel in RGC-5 cells (Coroneo et al., 2002; Kalapesi et al., 2005a).

Mechanosensitive channels offer an interesting alternative for explaining the mechanisms involved in pressure-induced apoptosis. This hypothesis allows for intrinsic processes independent of other stimuli, and one which could be sensitive to pressure directly. The channels could play a role in the initiation of intracellular pathways that could ultimately lead to apoptosis by various known mechanisms, such as p53 or caspase activation, or modulation of Bax, gene expression (Nickells, 1999). A graded response may be mediated by sub-populations of channels open at different levels of stimulation, or conversely by a graded response of the channel itself.

We have found that RGC-5 cells responded to elevated hydrostatic pressures directly and that an apoptotic process was induced. This effect was pressure-dependent and extends earlier findings on other neuronal cell lines. The mechanisms that may mediate this response are unknown and warrant further investigation and could offer new avenues for therapeutic manipulation. We suggest the possibility of a novel relationship linking pressure and apoptosis directly that may complement known factors in the pathogenesis of glaucoma and other pressure-related diseases.

4. Experimental procedures

4.1. Cell culture

The RGC-5 cell line was developed specifically to establish a permanent rat retinal ganglion cell culture. Retinal cells were isolated from post-natal Sprague–Dawley rats to generate a mixed primary retinal culture. These cells were then transformed with Ψ 2 E1A virus and single cell clones analyzed. The 'RGC-5' line was found to have numerous characteristics of retinal ganglion cells. The antigenic profile included positive expression of Thy-1, an RGC-specific surface antigen, and another ganglion cell marker, Brn-3b. Negative findings for non-RGC markers, such as for glial, amacrine and horizontal cells, were also confirmed. Other RGC features identified were morphology and sensitivity to glutamate toxicity and neurotrophin withdrawal (Krishnamoorthy et al., 2001).

RGC-5 cell cultures were grown in Dulbecco's Modified Eagle Medium (DMEM, Gibco Cat #23700-040) supplemented with 10% heat inactivated fetal bovine serum (Gibco Cat #26140-079) and 100 U/ml of penicillin and 100 μ g/ml of streptomycin. RGC-5 neurons were plated (10,000/cm²) onto poly-L-lysine-coated glass coverslips in 24-well culture dishes. Cultures were grown in 250 μ L of growth media per well and incubated at 37 °C in 5% CO₂ and air.

4.2. Pressure system

Several in vitro laboratory systems to study the response of cell cultures to increased pressure have been developed. Pressure chambers have been used extensively for some

years. We designed specialised pressure chambers based upon an established model incorporating a perspex and glass chamber with gas inlet and flow valves for connection to a low-pressure regulator (BOC Gases).

A mercury column barometer with atmospheric pressure (760mm Hg) calibrated to 0mm Hg continuously monitored pressure levels. The desired gas mix can be pressurised to a constant ambient hydrostatic pressure ranging from 0 to 200mm Hg (over and above atmospheric pressure) maintaining target pressures for the experimental durations with a variance of $\pm 2.25\%$ (Agar et al., 2000). Compression and decompression were attained over 30 s.

We used a gas mix identical to the cultures' incubating mix, namely 5% CO₂ and air. No significant impact on gas relationships in culture media as a result of pressurisation has been reported in this model (Mattana and Singhal, 1995; Sumpio et al., 1994). Our apparatus has also been assessed to exclude this confounder and demonstrated no 'gas effect', including at the highest pressure conditions used (Agar et al., 2000). The system apparatus was equilibrated and maintained within an electronically controlled CO₂ incubator at 37°C (Nuair NU4500E).

4.3. Experimental protocol

Each experiment comprised 3 culture groups: a positive control to confirm apoptosis detection, a pressure group subjected to experimental conditions of increased pressure and a negative control. For each experimental run, RGC-5 cultures were from the same plating, and experiments were conducted on the 3 groups simultaneously.

4.3.1. Positive group

Apoptosis controls were established by treatment with a known stimulator of apoptosis, 5% ethanol (Oberdoerster et al., 1998). Treatment for an equivalent time (2h) produced maximal inducible apoptosis from initial studies (data not shown). This allowed our apoptosis detection techniques, including morphology and TUNEL and Annexin V assays, to be validated within each experiment.

4.3.2. Pressure group

RGC-5 culture dishes were placed within the pressure chamber, and the incubating gas mix was pressurised. The cells were exposed to conditions of elevated ambient hydrostatic pressure, over and above atmospheric, for a period of 2h. This duration was selected based on our earlier work, including with other cell lines, which showed that this time point produced the most consistent and reproducible data (Agar et al., 2000; Coroneo et al., 2001). Experiments were carried out at 15, 30 and 100mm Hg, simulating conditions of 'normal' IOP, low-pressure chronic and high-pressure acute glaucoma respectively. The pressure conditions were then restored to atmospheric, and the culture dishes removed from the chamber for immediate analysis, representing the 2h time point.

All experiments used duplicate coverslips which enhanced reliability while still allowing immunofluorescence to be conducted without delay. As the time points needed to be synchronised simultaneously across all culture groups, the technical practicalities of immediately staining multiple coverslips limited the number of coverslips to duplicates. A

total of five experiments were conducted at 30mm Hg and three each at 100 and 15mm Hg respectively for the TUNEL assay. Three further experiments at 100mm Hg were carried out for Annexin V staining.

4.3.3. Control group

Negative experimental controls were included with cells treated identically to the pressure group with the culture dishes placed within pressure chambers at the same time for the same period of 2h. However, the gas mix was not pressurised, so these RGC-5 neurons were not subjected to elevated pressure conditions.

Following the experimental conditions of 2h pressurisation, the coverslips were removed immediately for analysis. Cells were stained live or fixed for examination by treatment with 4% w/v paraformaldehyde in phosphate-buffered saline pH 7.5 for 10min, and coverslips then mounted for further analysis.

4.4. Apoptosis detection

A combination of classical morphological changes along with immunocytochemistry of DNA changes was used to detect apoptosis. Apoptotic morphology includes cytoplasm and nuclear condensation, cell membrane blebbing and withdrawal of neuronal processes. RGC-5 neurons were visualised initially by phase contrast microscopy with a Olympus IX-70 light microscope and NIH Image (ver 1.61) software. Subsequent imaging was by fluorescent microscopy after staining, using an Olympus GB200 laser scanning confocal microscope or the LSC microscope.

Apoptosis is also characterised by endonuclease activation leading to DNA fragmentation into segments that can be labelled by immunofluorescent markers. This apoptosis detection was done by the established 'TUNEL' assay (Terminal transferase dUTP Nick-End Labeling) (Gold et al., 1994). We chose a direct binding fluorescein-conjugated dUTP as the green fluorochrome with a red propidium iodide (PI) counterstain using a commercially available in situ apoptosis detection kit (Promega G3250). The staining procedure followed the kit protocol. Briefly, it involved pretreatment with Triton-X 0.2% followed by equilibration buffer and then incubation with dUTP nucleotide label and Terminal transferase (TdT). Coverslips were then washed with sodium citrate buffer a before PI staining.

The nuclear changes identified by TUNEL assays are a relatively late marker of apoptosis. To further characterise the cell death, an early signal of apoptosis which acts by an independent mechanism was also selected. The externalisation of phosphatidylserine residues to the outer cell membrane is one of the first processes in apoptosis and can be detected by the Annexin V phospholipid binding protein (Zymed, 33-1200) (van Engeland et al., 1998). The staining is carried out on live cells by pre-treatment with phosphate-buffered saline, incubation in binding buffer and application of Annexin V-FITC, buffer wash and PI staining. Similar imaging and laser analysis procedures were applicable to both TUNEL and Annexin assays as both use a fluorescein-conjugated fluorochrome with a PI counterstain.

Morphological assessment comprised of light fluorescent microscopy. Quantitative immunofluorescent marker assessment was done by LSC. The LSC also allowed concurrent

assessment of both morphology and objective marker data, due to its ability to visualise scanned cells with the co-mounted fluorescent microscope. This was done both in real time as the laser scan is performed (a LSC image via the 'Scan data' feature) and later for additional image analysis once the slide has been scanned. The latter was made possible by the LSC recording of the spatial x–y coordinates of each cell, so an individual neuron can be relocated (via the 'compusort' feature) for visualisation in greater detail by the integrated fluorescent microscope (Darzynkiewicz et al., 1998). LSC image capture properties were limited, thus higher resolution images of selected neurons were taken on the confocal laser scanning microscope.

4.5. Quantitative marker analysis

Cytometric parameters of the fluorescent apoptosis markers were measured by the LSC. These included intensity of the fluorescent signal, its distribution and overall characteristics such as size and area of the scanned cell. RGC-5 neurons on the coverslips were scanned in each of four equal sized quadrants. For each scan, a population of predominantly single neurons was selected for analysis, with aggregations of no more than 3 to 5 cells accepted. The 'fluorescent area' of a cell was determined by the LSC, and on the basis of size, debris and large cell clumps (>5 cells) were excluded by visual microscopy during scanning. Representative LSC data scattergrams in Fig. 3 show that the single cell population within the coloured rectangular region was selected, by setting appropriate area limits and thus gating for fluorescent area.

The fluorochrome label in the TUNEL assay was Fluorescein isothiocyanate or FITC green with a red PI counterstain. The LSC Argon laser was set to 488nm, with sensors set to wavelengths of 530nm for FITC and 600nm for PI measurements. FITC label intensity was measured, and values were determined for two cell parameters. Green Max Pixel (GMP) is the fluorescence peak reflecting the highest value within a cell. It correlates well with DNA hyperchromicity in the condensed chromatin of apoptotic cells. Green Integral (GI) is a measure of total cell fluorescence and also reflects the degree of TUNEL labeling (Darzynkiewicz et al., 1998).

Cells were visualised during scanning to validate the predominantly single cell population and marker staining. TUNEL positive neurons with FITC positive nuclei were identified and appropriate LSC sensor settings derived to optimise their detection, in corroboration with intensity (GI, GMP) values. PI sensors were similarly optimised to detect all neurons and select for the desired cell population. Absolute measured intensity values were analyzed as the average for the gated population. Data generated were also used to determine the proportion of the total selected cell population that was TUNEL positive. Variance was statistically analyzed using Student's paired t test, and the quantitative data are presented as the mean \pm standard error of measurement.

Acknowledgments

We would like to thank Robert Wadley of the Cellular Analysis Facility, University of New South Wales, for invaluable

assistance in LSC scanning and Paul Halasz of the Histology and Microscopy Unit for assistance in confocal imaging. Research was aided by a grant from the Ophthalmic Research Institute of Australia, and in part by a general discretionary grant from Allergan Australia.

REFERENCES

- Agar, A., Hill, M., Coroneo, M.T., 1999. Pressure induced apoptosis in neurons [ARVO Abstract]. *Invest. Ophthalmol. Visual Sci.* 40, S265.
- Agar, A., Yip, S.S., Hill, M.A., Coroneo, M.T., 2000. Pressure related apoptosis in neuronal cell lines. *J. Neurosci. Res.* 60, 495–503.
- Aoun, P., Simpkins, J.W., Agarwal, N., 2003. Role of PPAR-gamma ligands in neuroprotection against glutamate-induced cytotoxicity in retinal ganglion cells. *Invest. Ophthalmol. Visual Sci.* 44, 2999–3004.
- Armaly, M.F., Krueger, D.E., Maunder, L., Becker, B., Hetherington Jr., J., Kolker, A.E., Levene, R.Z., Maumenee, A.E., Pollack, I.P., Shaffer, R.N., 1980. Biostatistical analysis of the collaborative glaucoma study: I. Summary report of the risk factors for glaucomatous visual-field defects. *Arch. Ophthalmol.* 98, 2163–2171.
- Barres, B.A., Silverstein, B.E., Corey, D.P., Chun, L.L., 1988. Immunological, morphological and electrophysiological variation among retinal cells purified by panning. *Neuron* 1, 791–803.
- Boyd, Z.S., Kriatchko, A., Yang, J., Agarwal, N., Wax, M.B., Patil, R.V., 2003. Interleukin-10 receptor signaling through STAT-3 regulates the apoptosis of retinal ganglion cells in response to stress. *Invest. Ophthalmol. Visual Sci.* 44, 5206–5211.
- Burgoyne, C., Crawford Downs, J., Belleza, A., Francis Suh, J.-K., Hart, R., 2005. The optic nerve head as a biochemical structure: a new paradigm for understanding the role of IOP-related stress and strain in the pathophysiology of glaucomatous optic nerve head damage. *Prog. Ret. Eye Res.* 25, 39–73.
- Caprioli, J., 1995. Pressure and glaucoma. In: Drance, S.J. (Ed.), *Optic Nerve in Glaucoma*. Kugler, New York, pp. 151–157.
- Coroneo, M., Agar, A., Hill, M., 2001. Pressure related apoptosis in human and neuronal cell lines. *Invest. Ophthalmol. Visual Sci.* 42, S129.
- Coroneo, M., Li, S., Agar, A., Hill, M., 2002. The 2-pore K⁺ channel opener arachidonic acid induces apoptosis in RGC-5 and differentiated PC-12 neuronal cell lines. *Invest. Ophthalmol. Visual Sci.* 43, S750.
- Darzynkiewicz, Z., Bedner, E., 2000. Analysis of apoptotic cells by flow and laser scanning cytometry. *Methods Enzymol.* 322, 18–39.
- Darzynkiewicz, Z., Bedner, E., Traganos, F., Murakami, T., 1998. Critical aspects in the analysis of apoptosis and necrosis. *Hum. Cell* 11, 3–12.
- Edward, D.P., Ueda, J., 2001. Immunolocalisation of TRAAK—a mechanosensitive K⁺ channel in the human and rat retina. *Invest. Ophthalmol. Visual Sci.* 42, 2032.
- Fagiolini, M., Caleo, M., Strettoi, E., Maffei, L., 1997. Axonal transport blockade in the neonatal rat optic nerve induces limited retinal ganglion cell death. *J. Neurosci.* 17, 7045–7052.
- Galea, J., Armstrong, J., Francis, S.E., Cooper, G., Crossman, D.C., Holt, C.M., 1999. Alterations in c-fos expression, cell proliferation and apoptosis in pressure distended human saphenous vein. *Cardiovasc. Res.* 44, 436–448.
- Garcia-Valenzuela, E., Shareef, S., Walsh, J., Sharma, S.C., 1995. Programmed cell death of retinal ganglion cells during experimental glaucoma. *Exp. Eye Res.* 61, 33–44.

- Gelberman, R.H., Szabo, R.M., Williamson, R.V., Hargens, A.R., Yaru, N.C., Minter-Convery, M.A., 1983. Tissue pressure threshold for peripheral nerve viability. *Clin. Orthop.* 285–291.
- Gold, R., Schmied, M., Giegerich, G., Breitschopf, H., Hartung, H.P., Toyka, K.V., Lassmann, H., 1994. Differentiation between cellular apoptosis and necrosis by the combined use of in situ tailing and nick translation techniques. *Lab. Invest.* 71, 219–225.
- Hamill, O.P., McBride Jr., D.W., 1996. The pharmacology of mechanogated membrane ion channels. *Pharmacol. Rev.* 48, 231–252.
- Haskin, C.L., Athanasiou, K.A., Klebe, R., Cameron, I.L., 1993. A heat-shock-like response with cytoskeletal disruption occurs following hydrostatic pressure in MG-63 osteosarcoma cells. *Biochem. Cell Biol.* 71, 361–371.
- Islas, L., Pasantes-Morales, H., Sanchez, J.A., 1993. Characterization of stretch-activated ion channels in cultured astrocytes. *Glia* 8, 87–96.
- Johansson, J.O., 1988. Inhibition and recovery of retrograde axoplasmic transport in rat optic nerve during and after elevated IOP in vivo. *Exp. Eye Res.* 46, 223–227.
- Kalapesi, F., Coroneo, M., Hill, M.A., 2005a. Human ganglion cells express the Alpha-2 adrenergic receptor: relevance to neuroprotection. *Br. J. Ophthalmol.* 89, 758–763.
- Kalapesi, F., Tan, J., Coroneo, M., 2005b. Stretch-activated channels: a mini review. Are stretch-activated channels an ocular barometer. *Clin. Exp. Ophthalmol.* 33, 210–217.
- Ko, K.S., McCulloch, C.A., 2000. Partners in protection: interdependence of cytoskeleton and plasma membrane in adaptations to applied forces. *J. Membr. Biol.* 174, 85–95.
- Kobayashi, S., Pena, J.D.O., Hernandez, M.R., 1997. Cultured astrocytes from human optic nerves respond to elevated hydrostatic pressure. *Invest. Ophthalmol. Visual Sci.* 38, 802.
- Kosnosky, W., Tripathi, B.J., Tripathi, R.C., 1995. An in vitro system for studying pressure effects on growth, morphology and biochemical aspects of trabecular meshwork cells. *Invest. Ophthalmol. Visual Sci.* 36, 8731.
- Krishnamoorthy, R.R., Agarwal, P., Prasanna, G., Vopat, K., Lambert, W., Sheedlo, H.J., Pang, I.H., Shade, D., Wordinger, R.J., Yorio, T., Clark, A.F., Agarwal, N., 2001. Characterization of a transformed rat retinal ganglion cell line. *Brain Res. Mol. Brain Res.* 86, 1–12.
- Levin, L.A., 2001. Relevance of the site of injury of glaucoma to neuroprotective strategies. *Surv. Ophthalmol.* 45, S243–S249 (discussion S273–6).
- Maingret, F., Fosset, M., Lesage, F., Lazdunski, M., Honore, E., 1999. TRAAK is a mammalian neuronal mechano-gated K⁺ channel. *J. Biol. Chem.* 274, 1381–1387.
- Martin, P.M., Ola, M.S., Agarwal, N., Ganapathy, V., Smith, S.B., 2004. The sigma receptor ligand (+)-pentazocine prevents apoptotic retinal ganglion cell death induced in vitro by homocysteine and glutamate. *Brain Res. Mol. Brain Res.* 123, 66–75.
- Mattana, J., Singhal, P.C., 1995. Applied pressure modulates mesangial cell proliferation and matrix synthesis. *Am. J. Hypertens.* 8, 1112–1120.
- Mennel, H.D., Stumm, G., Wenzel, J., 1997. Early morphological findings in experimental high pressure neurological syndrome. *Exp. Toxicol. Pathol.* 49, 425–432.
- Moorhouse, A.J., Li, S., Vickery, R.M., Hill, M.A., Morley, J.W., 2004. A patch-clamp investigation of membrane currents in a novel mammalian retinal ganglion cell line. *Brain Res.* 1003, 205–208.
- Nickells, R.W., 1999. Apoptosis of retinal ganglion cells in glaucoma: an update of the molecular pathways involved in cell death. *Surv. Ophthalmol.* 43, S151–S161.
- Oberdoerster, J., Kamer, A.R., Rabin, R.A., 1998. Differential effect of ethanol on PC12 cell death. *J. Pharmacol. Exp. Ther.* 287, 359–365.
- Osborne, N.N., Wood, J.P., Chidlow, G., Bae, J.H., Melena, J., Nash, M.S., 1999. Ganglion cell death in glaucoma: what do we really know? *Br. J. Ophthalmol.* 83, 980–986.
- Parmentier, J.L., Shrivastav, B.B., Bennett, P.B., 1981. Hydrostatic pressure reduces synaptic efficiency by inhibiting transmitter release. *Undersea Biomed. Res.* 8, 175–183.
- Quigley, H.A., 1999. Neuronal death in glaucoma. *Prog. Retin. Eye Res.* 18, 39–57.
- Radius, R.L., 1982. Axonal transport interruption and anatomy at the lamina cribrosa. *Arch. Ophthalmol.* 100, 1661–1664.
- Reyes, R., Lauritzen, I., Lesage, F., Ettaiche, M., Fosset, M., Lazdunski, M., 2000. Immunolocalization of the arachidonic acid and mechanosensitive baseline traak potassium channel in the nervous system. *Neuroscience* 95, 893–901.
- Runnerstam, M., Bao, F., Huang, Y., Shi, J., Gutierrez, E., Hamberger, A., Hansson, H.A., Viano, D., Haglid, K., 2001. A new model for diffuse brain injury by rotational acceleration: II. Effects on extracellular glutamate, intracranial pressure, and neuronal apoptosis. *J. Neurotrauma* 18, 259–273.
- Schmid, I., Krall, W.J., Uittenbogaart, C.H., Braun, J., Giorgi, J.V., 1992. Dead cell discrimination with 7-amino-actinomycin D in combination with dual color immunofluorescence in single laser flow cytometry. *Cytometry* 13, 204–208.
- Southan, A.P., Wann, K.T., 1996. Effects of high helium pressure on intracellular and field potential responses in the CA1 region of the in vitro rat hippocampus. *Eur. J. Neurosci.* 8, 2571–2581.
- Sumpio, B.E., Widmann, M.D., Ricotta, J., Awolesi, M.A., Watase, M., 1994. Increased ambient pressure stimulates proliferation and morphologic changes in cultured endothelial cells. *J. Cell. Physiol.* 158, 133–139.
- Takahashi, N., Cummins, D., Caprioli, J., 1991. Rat retinal ganglion cells in culture. *Exp. Eye Res.* 53, 565–572.
- Takano, K.J., Takano, T., Yamanouchi, Y., Satou, T., 1997. Pressure-induced apoptosis in human lymphoblasts. *Exp. Cell Res.* 235, 155–160.
- Take, J., Yamaguchi, T., Mine, N., Terada, S., 2001. Caspase activation in high-pressure-induced apoptosis of murine erythroleukemia cells. *Jpn. J. Physiol.* 51, 193–199.
- Tan, J., Kalapesi, F., Coroneo, M., 2006. Mechanosensitivity and the eye: cells coping with the pressure. *Br. J. Ophthalmol.* 90, 383–388.
- Tatton, N.A., Tezel, G., Insolia, S.A., Nandor, S.A., Edward, P.D., Wax, M.B., 2001. In situ detection of apoptosis in normal pressure glaucoma. A preliminary examination. *Surv. Ophthalmol.* 45, S268–S272 (discussion S273–6).
- Tezel, G., Wax, M.B., 2000. Increased production of tumor necrosis factor-alpha by glial cells exposed to simulated ischemia or elevated hydrostatic pressure induces apoptosis in cocultured retinal ganglion cells. *J. Neurosci.* 20, 8693–8700.
- van Engeland, M., Nieland, L.J., Ramaekers, F.C., Schutte, B., Reutelingsperger, C.P., 1998. Annexin V-affinity assay: a review on an apoptosis detection system based on phosphatidylserine exposure. *Cytometry* 31, 1–9.
- Wax, M.B., Tezel, G., Kobayashi, S., Hernandez, M.R., 2000. Responses of different cell lines from ocular tissues to elevated hydrostatic pressure. *Br. J. Ophthalmol.* 84, 423–428.
- Wyllie, A.H., Kerr, J.F., Currie, A.R., 1980. Cell death: the significance of apoptosis. *Int. Rev. Cytol.* 68, 251–306.